THE MECHANICAL BEHAVIOUR OF CHEMICALLY-TREATED PVC GEOSYNTHETIC MEMBRANES

Qifeng Yu
May, 2005

Department of Civil Engineering and Applied Mechanics
McGill University, Montreal

Thesis submitted to the Faculty of Graduate Studies and Research in partial fulfillment of the requirements of the degree of
Doctor of Philosophy

Your file Votre référence
ISBN: 978-0-494-21717-7
Our file Notre référence
ISBN: 978-0-494-21717-7

ABSTRACTS

Geosynthetics that are usually made of Poly(vinyl) Chloride (PVC) are used as components of engineered barriers in landfill applications. As a component of an engineered barrier scheme, it is used to mitigate the migration of hazardous and toxic mixtures of chemicals that can diffuse through the clay layer in the engineered barrier. The integrity of the geosynthetic layers that are in frequent contact with these chemicals is therefore of interest to the overall waste containment strategy. This thesis conducts a coordinated investigation that will allow the characterization of the deformability properties of geosynthetic materials, subjected to various levels of exposure to ethanol. Chemical alteration can take place by modifications to the fillers or plasticizers that contribute to both strength and ductility of the geosynthetics. The uniaxial tests conducted on a chemically-treated PVC geosynthetics, exposed to ethanol, point to the reduction in flexibility or embrittlement of the material. The results of the experiments conducted in connection with this research program indicate that, in its natural condition, the PVC geosynthetic is capable of undergoing moderately large strains, the constitutive behaviour of which can be modelled through the phenomenological hyperelastic theories by appealing to a strain energy function of the Mooney-Rivlin form. Unlike natural rubber at moderately large strains, which is virtually void of irreversible phenomena and strain-rate effects, the PVC geosynthetic exhibits a strong rate-dependency and irreversible effects; furthermore, the irreversible strains themselves can be within the realm of moderately large strains. The chemically-treated PVC geosynthetic, however, displays a dominant yield behaviour after chemical exposure: the material completely loses its large-strain deformability characteristics after prolonged chemical exposure. X-ray fluorescence techniques point to the loss of the plasticizer as a governing process in the alteration in the mechanical properties of the PVC geosynthetic. It is shown that the basic constitutive responses adopted for the description of the untreated PVC geosynthetic involving large strain hyperelastic behaviour, strain-rate effects and moderately large irreversible plastic strains, can also be used to characterize the constitutive behaviour of the treated PVC geosynthetic. The constitutive model development presented then addresses the incorporation of the loss of elasticity and the

development of a distinct yield point in the stress-strain response of the chemically-treated PVC geosynthetic.

In general, the constitutive model development for both the untreated and chemically-treated PVC results in correlations of satisfactory quality that permits the use of the models in the study of boundary value problems involving the indentation of PVC geosynthetic membranes. It serves as a useful method for calibrating the constitutive responses of the PVC geosynthetic determined from conventional uniaxial testing and provides a useful assessment of the out-of-plane deformability of PVC geosynthetic as a result of the loss of flexibility due to chemical exposure. The success of reasonable predictions of the experimental response by computational modelling then allows a further simulation of the situations that involve localized loading of PVC geosynthetics during either placement and construction or during the operation of the landfill, particularly in situations susceptible to chemical exposure.

RÉSUMÉ

Les géosynthétiques qui sont habituellement faits de chlorure de polyvinyle (PVC) sont employés comme composants de barrières ouvragées dans des applications de sites d'enfouissement. En tant que composant d'un arrangement de barrières ouvragées, il est employé pour atténuer la migration des mélanges dangereux et toxiques des produits chimiques qui peuvent se diffuse à dans la couche d'argile de la barrière machinée. L'intégrité des couches de géosynthétiques qui sont en contact fréquent avec ces produits chimiques est donc d'intérêt primordiale dans la stratégie globale de retenue. Cette thèse conduit une recherche coordonnée qui permettra de caractériser les propriétés de déformabilité des matériaux géosynthétiques, soumis à divers niveaux de contact chimique. Le changement chimique peut avoir lieu lors de modifications du remplisseurs ou der plastiques qui contribuent à la résistance en traction et à la ductilité des géosynthétiques. Des essais uniaxiaux effectués sur un géosynthétique de PVC chimiquement traité, exposé à un produit chimique commun tel que l'éthanol, démontrent la réduction de la flexibilité ou la fragilisation du matériel. Les résultats des expériences entreprises en liaison avec ce programme de recherche indiquent que, dans son état normal, le géosynthétiques de PVC est capable de subir des déformations modérément grandes, dont la loi de comportement peut être modélisée par des modèles hyperélastiques phénoménologiques en faisant appelle à une fonction d'énergie de déformation de la forme de Mooney-Rivlin. À la différence du caoutchouc naturel aux déformations modérément grandes, qui est pratiquement vide de phénomènes irréversibles et des effets taux de déformations, les géosynthétiques de PVC démontrent une dépendance à la vitesse de déformation et des effets irréversibles; en outre, les contraintes irréversibles elles-mêmes peuvent être dans le domaine des contraintes modérément grandes. Les géosynthétiques de PVC chimiquement traités presente, cependant, une limite de resistance élastique après une exposition chimique: le matériel perd complètement déformabilité aux grandes déformation après une exposition chimique prolongée. Les techniques d'analyse par fluorescence des X rayons démontrent la perte du plastique comme un processus gouvernant le changement des propriétés mécaniques du géosynthétique de PVC. La modélisation du comportement mécanique adoptées pour

la description des géosynthétiques non traités impliquant des comportement hyperélastiques aux grandes déformations, une dépendance à la vitesse de déformation et des déformation plastiques irréversibles, peuvent également être employées pour caractériser la loi de comportement du géosynthétique de PVC traité. Le développement du modèle de comportement mécanique alors présenté adresse l'incorporation de la perte d'élasticité et le développement d'une limite élastique distincte pour la réponse de contrainte-tension du géosynthétique de PVC chimiquement traité.

En général, le modélisation du comportement mecanique pour les géosynthétiques de PVC non traités et chimiquement traités a donné les corrélations de la qualité satisfaisante qui permettent l'utilisation des modèles dans l'étude des problèmes aux conditions aux limites impliquant l'impression des membranes géosynthétique de PVC. Il sert de méthode utile à la calibration les réponses du comportement mecanique du géosynthétiques de PVC détermine à partir de l'essai uniaxial conventionnel. Le modéle fournit aussi une apersu utile de la déformabilité hors-plan du géosynthétique de PVC en raison de la perte de flexibilité due à l'exposition chimique. Le succès de la prévision raisonnable des résultats expérimentaux par modélisation informatique permet alors d'autres simulations de situations qui comportent le chargement localisé de géosynthétiques de PVC pendant le placement et la construction ou pendant l'opération du remblai, en particulier les cas susceptibles à l'exposition chimique.

ACKNOWLEDGEMENTS

The author wishes to express his great gratitude to his supervisor, Professor A.P.S. Selvadurai, *William Scott Professor*, Department of Civil Engineering and Applied Mechanics, McGill University, for suggesting the research topic, his extensive guidance and support. His extensive corrections to this thesis and the research papers resulting from the work are gratefully appreciated. My time spent here at McGill University with him will always be a cherished memory.

The access to the use of the ABAQUS code was provided through the kind support of Professor J. Nemes, Department of Mechanical Engineering, McGill University.

The author would like to thank a number of people who assisted the research program in a number of ways. Mr. M. Przykorski, research technician in the Department of Civil Engineering and Applied Mechanics, McGill University, provided useful assistance and advice regarding connections of the various electrical transducers. Mr. J. Bartczak, research technician, Department of Civil Engineering and Applied Mechanics, McGill University and Mr. S. Kecani, research technician, Department of Physics, McGill University, helped the machining of the uniaxial testing gripper and other testing equipment. The X-ray fluorescence analysis was conducted at the Geochemical Laboratories, Department of Earth and Planetary Sciences, McGill University. The assistance of Professor T. Ahmedali and Ms. G. Keating is acknowledged. The assistance of Mr. T. Pike of Cadence Automatisation in configuring the Parker Automated linear electro-mechanical actuator and membrane indentation test is appreciated. Thanks further go to Mr. T. Micozzi, Laboratory superintendent, Machine Tool Laboratory, Department of Mechanical Engineering, McGill University, for providing the Surface Measurement Machine for measuring the roughness of a brass plate.

The author would particularly like to thank the graduate student and research assistance group in the geomechanics laboratory for their helpful comments and assistance; these include Mr. W. Dong, Mr. A. Glowacki, and Mr. P.A. Selvadurai. Dr. W.D. Cook, Department of Civil Engineering and Applied Mechanics, McGill University, provided

assistance in aspects related to setting up the computer system in the geomechanics computational laboratory.

The research described in the thesis was supported by the *Max Planck Research Prize* in the *Engineering Sciences* and by an *NSERC-Discovery Grant* awarded to Professor A.P.S. Selvadurai.

Finally, but not last, the author wishes to thank his family, relatives and friends for their prolonged understanding, support and encouragement during the course of this work.

TABLE OF CONTENTS

LIST OF TABLES

LIST OF FIGURES

LIST OF SYMBOLS AND ABBREVIATIONS

σ_0	Normal stress	$\mathbf{X}$ (X_A)	Coordinates of a material particle in its original configuration
ε_0	Normal strain	$\mathbf{x}$ (x_i)	Coordinates of a material particle in its deformed configuration
l_0, l	Initial and current gauge lengths of a uniaxial sample	$\mathbf{F}$	Deformation gradient tensor
C	Chemical concentration in the interior of the PVC membrane	$\mathbf{F}^e$, $\mathbf{F}^u$	Elastic and irreversible deformation gradient tensors
D	Diffusion coefficient	$\mathbf{B}(g_{ij})$	Strain measurement tensor
H	The thickness of the PVC geoynthtic membrane	$\mathbf{T}(T_{ij})$	Cauchy stress tensor
t_{90}	The time required to sature 90% of the central plane of a PVC membrane	$\mathbf{T}_A$, $\mathbf{T}_B$	Cauchy stress tensor for models A, B
W	Strain energy function	$\mathbf{L}$, $\mathbf{L}^u$	Total and irreversible deformation-rate tensors
W^e, W^u	Strain energy function responsible for the elastic and irreversible parts of the deformation	$\mathbf{D}$, $\mathbf{D}^u$	Total and irreversible strain-rate tensors
C_1, C_2	Elastic parameters for strain energy function of a Mooney-Rivlin form	$\mathbf{I}(\delta_{ij})$	Unit tensor
α_n, μ_n	Elastic parameters for strain energy function of an Ogden's form	$\mathbf{v}_1$, $\mathbf{v}_2$	Tangential vector during slip
I_i	The i^{th} strain invariant	$\mathbf{t}$	Surface tractions
I_i^e, I_i^u	The i^{th} elastic and irreversible strain invariants	$\mathbf{f}$	Body force vector
p	Arbitrary scalar pressure	LLDPE	Linear low density polyethylene
λ_i	Principal stretch i	MLDPE	Medium linear density polyethylene

$\tilde{\mu}$	linear elastic shear modulus
λ_m	limiting extensibility of a polymeric material
λ_{chain}	The current chain length
$\dot{\gamma}_0$	Generalized strain rate
C_1', C_2'	Modified elastic parameters for strain energy function of Mooney-Rivlin type
κ_1, κ_2	Rate-dependencies for the elastic parameters C_1', C_2'
E_1', E_2'	Elastic parameters for inextensible cord A
E_y	Post-yield hardening modulus
$\dot{\gamma}_c$	Rate-independent threshold strain-rate
$\dot{\gamma}_c^v$	Rate-independent viscous strain-rate
$\dot{\zeta}$	Visco-plastic strain-rate
s	Viscous sensitivity to rate-effects
τ_B	Scalar form of the effective stress for model B
q	Static yield stress
ζ_y	Yield strain of the chemically-treated PVC geosynthetic
α	Material parameter that account for combined stretch
φ	Relative shear displacement

HDPE	High density polyethylene
PP	Polypropylene
PVC	Poly(vinyl) Chloride
BOD	Biological oxygen demand
COD	Chemical oxygen demand
DAA	Di-'alphanyl' adipate
DAP	Diallyl phthalate
DAS	Di-'alphanyl' sebacate
DBP	Dibutyl phthalate
DHP	Dihexyl phthalate
DIDP	Di-isodecyl phthalate
DINP	Di-i-nonylphthatlate
DIOA	Di-iso-ictyl adipate
DIOP	Di-iso-octyl phthalate
DIOS	Di-iso-octyl sebacate
DIOZ	Di-iso-octyl azelate
DNP	Dinonyl phthalate

F_n, F_s	Normal and shear forces at the contact surface
u	Friction coefficient
A	Initial contact area
ϕ	Diameter of the indentation specimen
P	Indentation load
Δ	Indentation displacement
Δ_{max}	Maximum indentation displacement
Ω	Distance to the center of the membrane during asymmetric indentation
ζ_1, ζ_2	The first and second slip component
k_s	Elastic slip stiffness
$\bar{s}_{crit}$	Maximum elastic slip

DOA	Dioctyl adipate
DOP	Dioctyl (2-ethylhexyl) phthalate
DOS	Dioctyl sebacate
DTDP	Ditridecyl phthalate
PPA	Polypropylene adipate
PPS	Polypropylene sebacate
TPU	Thermoplastic polyurethane
TTP	Tritolyl phosphate
TXP	Trixylyl phosphate
A, V	Surface and volume ratio between time $t + dt$ and t
$R_{O/Cl}$	Weight fraction between the oxygen and chlorine elements inside a sample

LIST OF PUBLICATIONS RESULTING FROM THE RESEARCH

Journal Publications

	Journal impact factor (@Journal Citation report ® 2004)
Yu, Q. and Selvadurai, A.P.S. (2005) Mechanical behaviour of a plasticized PVC subjected to ethanol exposure, *Polymer Degradation and Stability*, **Vol. 89**, pp. 109-124.	1.685
Selvadurai, A.P.S. and **Yu, Q.** (2005) Constitutive modelling of a polymeric material subjected to chemical exposure, *International Journal of Plasticity* (in press)	3.819
Selvadurai, A.P.S. and **Yu, Q.** (2005) Indentation on a chemically-treated polymeric membrane, *CMES- Computer Modeling in Engineering & Sciences*, **Vol. 9**, pp. 85-110.	2.210
Selvadurai, A.P.S. and **Yu, Q.** (2005) On the indentation on a polymeric membrane, *Proceedings of Royal Society Series A: Mathematical, Physical and Engineering Sciences* (accepted)	1.326

Conference Publications

Yu, Q. and Selvadurai, A.P.S. (2003) Mechanical Behaviour of Geosynthetics, *Canadian Society for Civil Engineering 31st Annual Conference Moncton, New Brunswick, Canada, June 4-7, 2003*, paper GCJ-368.

Yu, Q. and Selvadurai, A.P.S. (2005) On the mechanics of a chemically treated geosynthetic, *The 11st International Conference of IACMAG, June 19-24, 2005, Turin, Italy*.(G. Barla and M. Barla Eds.) Pátron Editore, Bologna, Vol. 2, pp. 403-410.

Publications Extra to Thesis

	Journal impact factor (@Journal Citation report ® 2004)
Selvadurai, A.P.S. and **Yu, Q.** (2005) A Computational Perspective of a Discontinuity in a Geomaterial, *Computers and Geotechnics*, **Vol. 32**, pp. 92-106.	0.397

Conference publications

Selvadurai, A.P.S., **Yu, Q.** and El-Hindy, E. (2002) Transfer of Shear Loads at a Fracture: Influence of Profile, Contact Friction and Separation of Compatible Surfaces, *Annual Conference of the Canadian Society of Civil Engineering, Montreal, Quebec, Canada*, paper GE022.

CHAPTER 1
APPLICATION OF THE PVC GEOSYNTHETIC IN LANDFILL

1.1 Introduction of the PVC geosynthetic in landfill

Landfills form the major mode of disposal of large volumes of urban waste. Out of 300 million tons of solid waste per year generated in the US, 75% of the solid waste is placed in landfill (Qian et al., 2002). In Canada, 73% of solid waste is reported landfilled in 1997 (Glenda, 1997). In the province of Québec, Canada, this updated figure amounts to 83% (Recyc-Québec, 2002). The constituents of toxic materials and other forms of contaminants vary with the types of waste materials that accumulate throughout the life of the landfill. Ideally, it is desirable that the contents of the landfill be dry, a condition that would greatly minimize the problems associated with landfill design. This is, however, an unrealistic expectation, since, during the operation of a landfill site, the waste comes into contact with rainfall and other fluids that may be present in the stored waste at the time of its placement. With time, the fluids within the landfill will gravitate to the base of the stored waste. This fluid is usually referred to as *leachate* and contains a complex mixture of chemicals and other hazardous materials that pose a threat to human health and the environment. It is therefore important to provide landfill barriers that will eliminate the migration of the leachate to the natural groundwater regime. Most recent designs of landfill characterize it as a structure with a composite liner, leachate collection and removal system, gas collection and a control system, and finally a cover (see Figure 1.1). The liner system is placed at the bottom and sides of a landfill. It acts as a barrier against the advective and diffusive transport of the leachate. The conventional approach to the provision of engineered barriers for the leachate is two-fold: the first is to ensure that the leachates are trapped through a barrier system and the second is to collect the leachate so that it can be subjected to further treatment in the form of other neutralization,

incineration or encapsulation. A leachate collection and removal system with pipelines is used to collect the leachate and to prevent the buildup of a leachate head on the liner. The collected waste can be transferred by sanitary sewer to a wastewater treatment plant or disposed of *in situ*. In order to minimize the amount of water infiltrating into the landfill after closure, a final cover system is usually adopted, which can consist of a geosynthetic liner covered by a layer of topsoil. The topsoil is used to protect the geosynthetic liner from UV degradation and as a vegetative support layer. Also, in order to prevent the damage of geosynthetic liner from sharp objectives, a protection layer, such as a geotextile with high permeability, can be used. A drainage layer with high permeability added above the geosynthetic liner is intended to facilitate lateral drainage. During decomposition of the organic waste, gases such as methane (CH_4) and carbon dioxide (CO_2) can accumulate to a dangerous level, which is often sufficient to induce the inflation of the top cover system (Figure 1.2). Modern landfill sites, therefore, provide a gas collection and control system. The collected gas can either be used to produce energy or flared under controlled conditions.

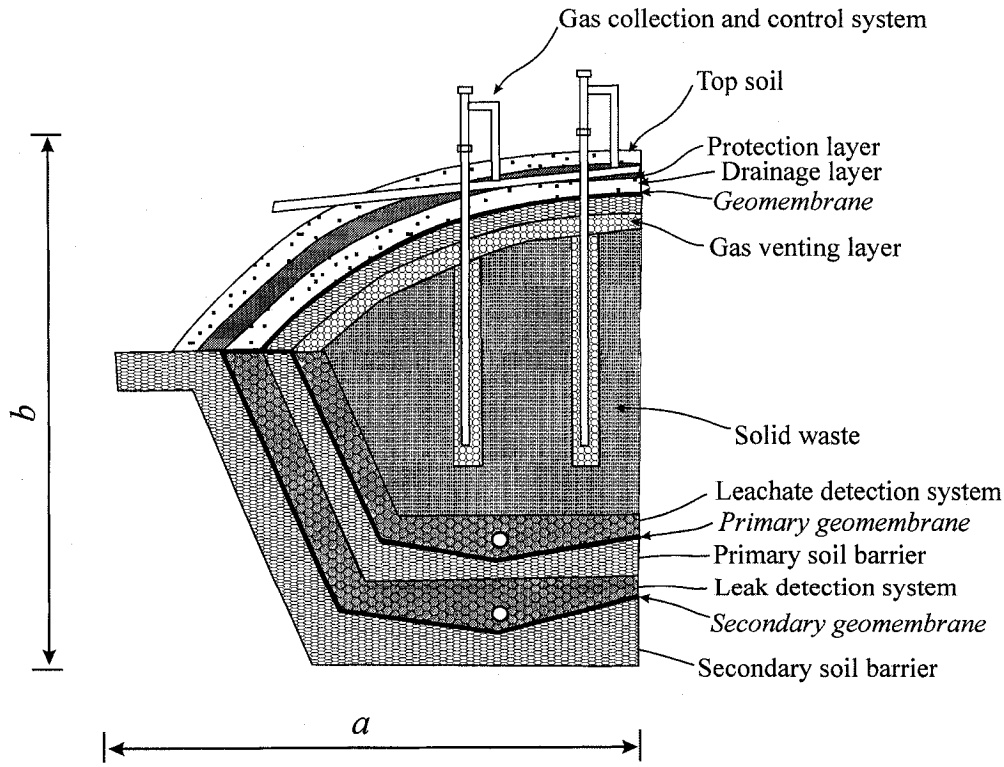

Figure 1.1 Schematic diagram of a municipal solid waste landfill (a: at a typical scale of $100m$~$300m$; *b:* at a typical scale of $20m$~$100m$) (after Qian et al., 2002)

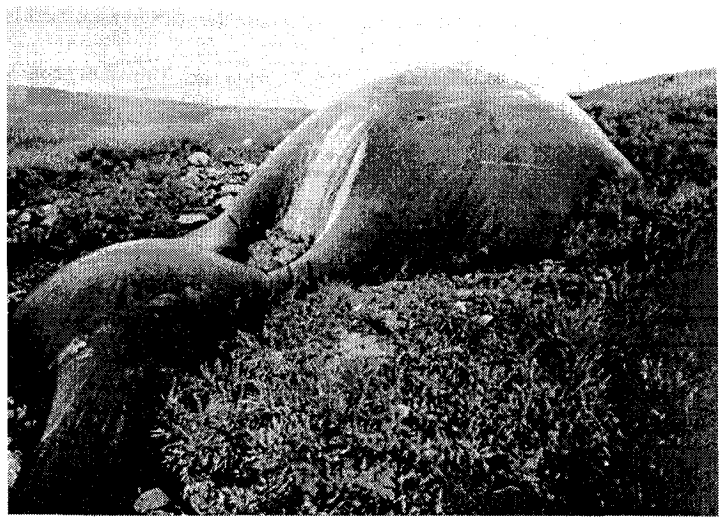

Figure 1.2 Localized inflation of a PVC membrane by gas pressure accumulated inside a landfill with restraint to inflation provided by topsoil coverage (after Koerner, 1994)

The liner system that is currently in use at the base of the landfill adopts a multi-barrier system that consists of alternate layers of geotextiles, compacted clay and other geosynthetics (Figures 1.1 and 1.3). The technology associated with the design of engineered barrier systems for landfills is regulated by agencies such as the Canadian Ministry of the Environment and the United States Environmental Protection Agency (US EPA). The clay barriers comprise the most important component of the liner system, used with the intention of minimizing the migration of leachate through the barrier system. A typical compacted clay liner has a porosity of 0.40 and a corresponding hydraulic conductivity of less than or equal to $10^{-7} cm/sec$ (Qian, et al., 2002). The clay liner, however, can only be subjected to a maximum volumetric strain of 4% (Daniel and Wu, 1993), which can cause serious problems in cases of shrinkage due to dry desiccation or action of freezing and thawing. According to LaGatta et al. (1997), the failure strain of a compacted clay ranges from 0.1% to 4%, therefore its ability to resist differential settlement is also limited. Benson et al. (1995) and Chamberlain et al. (1995) reported that there can be an increase of one-order of magnitude or more in the hydraulic conductivity after a single free-thaw cycle and an increase of one- to three-orders of magnitude after three to five freeze-thaw cycles. All these effects significantly reduce the

buffering capacity of the clay liner when it is used alone. The geosynthetic liner that rests on the top of the clay liner and acts in a composite fashion is intended to further mitigate the migration of the hazardous and toxic mixtures of chemicals as they diffuse through the clay layer. The design guidelines for geosynthetics are given in a number of texts including volumes by Koerner (1994) and Holtz et al. (1997). The primary geosynthetic liner, typically a layer of geomembrane and other protective geosynthetic arrangements, is designed as the main barrier. By definition, a *geomembrane* or a *geosynthetic membrane* is a very low permeable synthetic membrane liner or barrier used with any geotechnical engineering related material to control fluid migration in a geoenvironmental project, geotechnical structure, or system (ASTM 4833). A PVC geomembrane at a thickness of $1.5mm$ typically has a hydraulic conductivity of less than $5\times10^{-9} cm/sec$, which is two orders lower than that of a clay liner. The leakage through the primary liner can be further retained by a secondary geosynthetic liner and collected through lateral drainage layers that form the leachate detection system. The function of the geotextile layer (with a minimum permeability of $10^{-2} cm/sec$) is to provide this lateral drainage and to further protect the geomembrane from sharp objects that are frequently contained in the soil or waste layer. A layer of geonet consisting of braided parallel sets of synthetic ribs is also commonly used to reinforce the liner system and provide further lateral drainage. The geosynthetic liner referred to in Figure 1.3 showes a barrier that collects the majority of the landfill leachate. Those inorganic chemicals that succeed in penetrating the geosynthetic liner are further contained by the provision of the clay liner. The success of using a multi-barrier system in containing landfill leachate has been demonstrated in certain actual landfill applications. Giardino and Guglielmetti (1997) reported significantly lower flows collected through the leachate detection system in a landfill during its 13-*year* service period by using the multi-barrier system. The application of a multi-layer composite liner has also been proposed to contain low-level radioactive waste and uranium mill tailings that require a service life of 300 to 500 *years* due to radioactive decay of the waste (Kane and Widmayer, 1989).

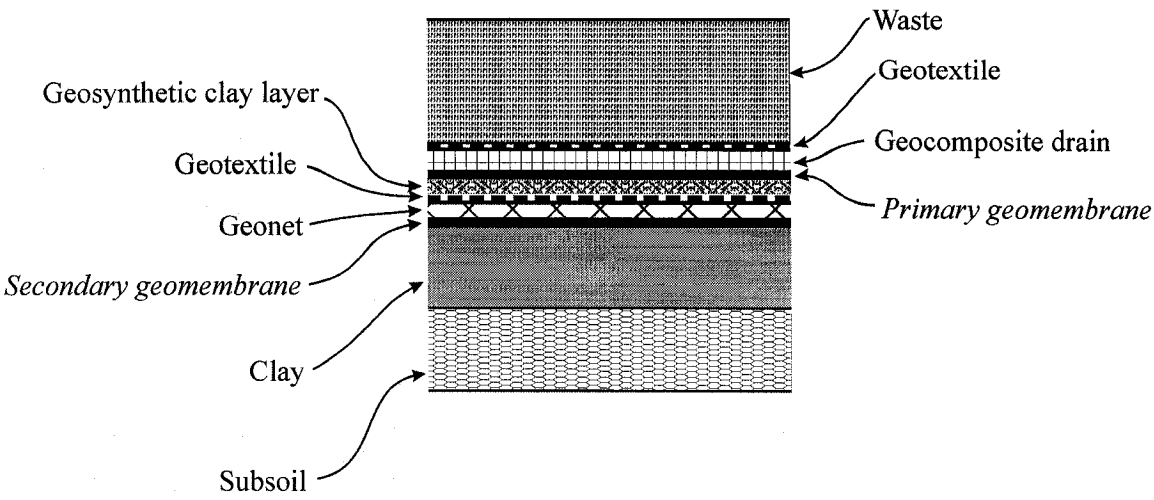

Figure 1.3 Double composite liners (after Koerner, 1994)

While the term *geosynthetic* generally refers to the entire synthetic component used in the multi-layer liner system (Koerner, 1994), this thesis focuses attention on the behaviour and chemical compatibility of the PVC *geomembrane* in contact with ethanol. Various polymers have been used to manufacture such geosynthetics including semi-crystalline thermoplastics such as LLDPE (linear low density polyethylene), MLDPE (medium linear density polyethylene), HDPE (high density polyethylene), fPP (flexible polypropylene), thermoplastics such as PVC (polyvinyl chloride), thermoplastic elastomer such as CSPE (chlorosulfonated polyethylene), and most recently, a bituminous geomembrane (Qian et al., 2002). A PVC geosynthetic, however, is claimed to possess several superior properties for serving as a landfill barrier (PVC Geomembrane Institute, 1999). Firstly, by considering the flexibility of a PVC geosynthetic membrane, it is more likely to withstand differential settlement without damage (Giroud and Soderman, 1995). Other geosynthetics, such as an HDPE geosynthetic, typically exhibit a yield point in its stress-strain behaviour that occurs at approximately 12% strain. PVC geosynthetics, however, do not exhibit a noticeable yield point and can experience large strain deformations at room temperature. In situations where strains caused by differential settlement can exceed 20 percent (Smith et al., 1994), large strain deformability of a PVC geosynthetic is regarded as an advantage. The second consideration is the easy maneuverability of the PVC geosynthetic membrane during installation, which results in fewer wrinkles post-installation and better interaction with the subgrade. Thirdly, due to

its flexibility, it presents better properties at low temperature (Giroud and Soderman, 1995). Lastly, PVC geosynthetic membrane rolls are factory seamed, which can produce larger panels and greatly reduces the number of problematic field welded seams.

1.2 Objectives and scope of the thesis

The longevity of the containment provided by PVC geosynthetics, however, can be influenced by chemical, mechanical and other environmental factors, including degradation due to ultraviolet radiation, oxidation and biological action. The integrity of the PVC geosynthetic layers is therefore of interest to the overall containment strategy. The scope of this thesis mainly focuses on the *embrittlement* phenomenon caused by the chemical process. The term *embrittlement*, which generally refers to the loss of the flexibility of the material, is represented by the alteration in the mechanical behaviour of the PVC geosynthetic used in this research. It is favorable that the chemical compatibility of the PVC geosynthetic can be studied during its exposure to a mixture of chemicals that is similar to landfill leachate. These chemicals, however, can be highly toxic and need special caution and equipment to deal with. In this research, it is proposed to adopt a commonplace non-toxic chemical, such as ethanol, to investigate the chemical compatibility of the PVC geosynthetic. Ethanol has been shown to be abundant in landfill leachates (USEPA, 1988) and is non-toxic. Previous preliminary experimental investigations (Haedrich, 1995; Contamin and Debeauvais, 1998) conducted on a PVC geosynthetic, point to a significant loss of desirable properties such as elasticity during exposure to acetone and ethanol, respectively. Following these preliminary investigations, the research reported in this thesis is a coordinated effort to examine the influence of the exposure of a PVC geosynthetic to ethanol, in terms of alteration in the deformability characteristics of the membrane material. The research starts with a series of experimental studies conducted on uniaxial samples. The PVC geomembranes inside a landfill, however, experience bi-axial loading states and can be subjected to very large deformations ($>10\%$) as a result of localized inflation, puncture by the sharp objects contained in soil layer or even localized differential settlement (see Figure 1.2). To provide a possibility to predict the performance of the PVC geosynthetic membranes subjected to any arbitary deformation, a constitutive model is developed for the

description of the behaviour of both the untreated and chemically-treated materials through a series of uniaxial tests and special tests that induce inhomogeous straining. The constitutive models that consider the large strain deformation, irreversible behaviour and strain-rate effects of the PVC geosynthetic are incorporated in the highly documented and validated Finite Element code ABAQUS/Standard. As an example of the PVC geosynthetic membrane subjected to any arbitary localized loading cases, the influence of the chemical exposure on the loss of flexibility of the PVC geosynthetic is further accessed by conducting transverse loading of edge supported membranes by indentation. To help a thorough understanding of this subject, the following sections provide a comprehensive review regarding the research on the durability of a PVC geosynthetic in a typical landfill environment.

1.3 Waste properties and leachate characterizations

Research on the chemical compatibility of the PVC geosynthetic commences with a primary knowledge of waste properties inside the landfill. Qian et al. (2002) proposed the following classified categories of waste type in a typical Municipal Solid Waste (MSW) landfill: (i) paper products, (ii) glass, (iii) metal, (iv) plastics, (v) rubber and leather, (vi) textiles, (vii) wood, (viii) food wastes, (ix) yard trimming, and (x) miscellaneous inorganic wastes. Due to the accumulated nature of the municipal waste, densities of the waste vary throughout its depth. Earth Technology (1988) reported the field evaluation of the unit weight performed at the Puente Hills landfill near Los Angeles, CA; the interpreted unit weight varied from $3.3kN/m^3$ at the surface to $12.8kN/m^3$ at a depth greater than $60m$. Also, MSW typically presents a high porosity, which varies from 0.40 to 0.67 depending on the compaction and composition of the waste (Qian, et al., 2002). Correspondingly, MSW can contain up to 30% moisture with a high range of hydraulic conductivity from $1.0\times10^{-3}cm/sec$ to $4.0\times10^{-2}cm/sec$ (Landva and Clark, 1990), similar to those associated with clean sand and gravel. The large values of porosity, moisture and hydraulic conductivity provide a medium that is susceptible to leachate movement.

Landfill leachate is generated by excess rainwater percolating through the waste layers in landfill. Its production will decrease significantly after the placement of the final cover (Loehr and Haikola, 2003). A combination of physical, chemical and microbial processes associated with waste decomposition transfers the pollutants from waste material to the leachate. Among all the types of solid waste, low-resistant polymers, such as food waste and animal waste is readily degradable; metals are corrodible to varying degrees; highly resistance polymers, such as paper and wood are only slowly biodegradable; and many inorganic items such as glass, rubble and ashes are almost non-degradable (Landva and Clark, 1990). Based on the published reports that study landfills at an age younger than 40 *years*, Christensen and Kjeldsen (1995) have identified four stages in the decomposition of solid waste: (i) an initial aerobic phase, (ii) an anaerobic phase, (iii) an initial methanogenic phase, and (iv) a stable methanogenic phase. In stage (i), aerobic decomposition of waste occurs rapidly in the presence of moisture and oxygen in the void spaces of the freshly buried refuse, resulting in production of CO_2 and possibly resulting in an increase in waste temperature. Most water at this stage comes from the release of the moisture during compaction as well as penetration of precipitation through the buried refuse. This phase lasts only a few days (Kjeldsen et al., 2002) and continues until available oxygen is depleted. In stage (ii), the waste become anaerobic, which supports fermentation reactions. Cellulose and hemicellulose biodegradation is carried out by three groups of bacteria: (a) hydrolytic and fermentative bacteria hydrolyze polymers and ferment the resulting monosaccharide to carboxylic acids and alcohols; (b) these acids and alcohols can be further converted by acetogenic bacteria to acetate, hydrogen and carbon dioxide; (c) the methanogens can further help the conversion of end product of the acetogenic reaction to methane and carbon dioxide (Zehnder et al., 1982). Typical characteristics of stage (ii) leachates are acidic pH levels (typically 5 to 6, Qian et al., 2002); and highest BOD (biological oxygen demand) and COD (chemical oxygen demand) concentrations in the leachate will be measured in this phase (Barlaz and Ham, 1993). At the onset of stage (iii), the initial methanogenic phase, occurs when measurable quantities of methane are produced. During this phase, the acids that have accumulated in phase (ii) are converted to methane and carbon dioxide by methanogenic bacteria with substantial methane production (Barlaz et al., 1989). The COD and BOD concentrations

begin to decrease and the pH value increases as acids are consumed. The landfill gas starts to form, usually as a mixture of carbon dioxide and methane. The last phase of landfill leachate that has been monitored within the time frame of landfill existence is a stable methanogenic phase, in which the methane production rate will reach its maximum and start to decrease as carboxylic acids decrease to their stabilized conditions. The pH value continues to its steady-state condition. A low BOD/COD ratio at this stage suggests a leachate with a low concentration of volatile fatty acids and relatively higher amount of humic and fulvic-like compounds. Since both phase (iii) and phase (iv) contribute to the activities of methanogenic bacteria, McBean et al. (1995) combined them into a single phase. A further detailed account of short-term and long-term characteristics of the leachate resulting from the waste decomposition in landfill was reviewed recently by Kjeldsen et al. (2002).

Due to the sequential nature of biochemical reactions in a MSW landfill, the leachate originating from a single location is highly variable over time. Likewise, the leachate is also inhomogeneous in space within the landfill. Young landfill typically contains leachate high in biodegradable organics. Older landfill contains much more complex chemicals. Kjeldsen et al. (2002), adopting the definition of leachate as a water-based liquid given by Christensen et al. (1994), classified four major groups of leachate, such as dissolved organic matter [qualified as TOC (Total Organic Carbon), volatile fatty acids and more refractory compounds such as fulvic-like and humic-like compounds], inorganic macrocomponents (Ca^{2+}, Fe^{2+}, Mg^{2+}, Mn^{2+}, Na^{+}, K^{+}, NH_4^{+}, Cl^{-}, SO_4^{2-} and HCO^{3-}), heavy metals (Cd^{2+}, Cu^{2+}, Pb^{2+}, Ni^{2+}, Zn^{2+}, Cr^{3+}), and xenobiotic organic compounds (originating from household or industrial chemicals including aromatic hydrocarbons, phenols, chlorinated aliphatics, pesticides and plasticizers). The average concentrations of heavy metals are fairly low due to the high sorption capacity of soils and organic matter (Bozkurt et al., 1999), which are even lower than the U.S. Drinking Water Standard and at present is not a major concern. The chemical characteristic of a leachate can also be altered by releasing its components to the surrounding environment. Due to leaching there is generally a decreasing trend of inorganic macrocomponents and heavy metals in landfill. Ammonia is released from

waste mainly by decomposition of proteins; the only mechanism for its change is due to leaching, which therefore has been identified as the most significant component of leachate over the a long term (Burton and Watson-Claik, 1998). The most frequently found xenobiotic organic compounds are the monoaromatic hydrocarbons (benzene, toluene, ethylbenzene, and xylenes) and halogenated hydrocarbons such as tetrachloroethane and trichloroethane; these pollutants are also the main groups to have negative effects in the aquatic environment. Other compounds, such as borate, sulfide, arsenate, selenate, barium, lithium, mercury and cobalt may be found. However, since these compounds are generally in low concentrations, they are only of secondary concern. USEPA (1988) documents the chemical characteristics of the leachate produced by municipal waste landfills (see Table 1.1).

In theory, after the occurrence of the methanogenic phase, the waste will continue to decompose until no more degradation occurs and the landfill becomes fully anaerobic. In the long term, however, Christensen and Kjeldsen (1995) and Bozkurt et al. (2000) proposed that the rate of oxygen diffusion into the landfill might exceed the rate of oxygen depletion due to microbial activities; thus, in their opinion, the anaerobic landfill is hypothesized to become an aerobic ecosystem in long term. They further concluded that heavy metals would not increase within the time frame of a thousand years in the presence of oxygen. Data on dissolved organic carbon and inorganic macrocomponents, from Kjeldsen and Christensen (2001), show a slow decreasing trend with time and their model showed that most xenobiotic organic compounds will be released in a few decades due to the diffusion, leaching, sorption and degradation processes. Frascari et al. (2004) reported leachate quality of a monitored landfill in Italy after occurrence of the methanogenic conditions for 10 *years*. The values of alkali pH and conductivity remained constant during the 10-*year* monitoring period.

Table 1.1 Municipal landfill leachate data (USEPA, 1988)

Indicator parameters	Leachate concentration (*ppm*)		Indicator parameters	Leachate concentration (*ppm*)	
	Minimum	Maximum		Minimum	Maximum
Alkalinity	470	57,850	Iron	0.22	2,280
Ammonia	0.39	1,200	Phosphorous	0.29	117.18
Biological oxygen demand	7	29,200	Potassium	17.8	1,175
Calcium	95.5	2,100	Sulfate	8	1,400
Chemical oxygen demand	42	50,450	Sodium	12	2,574
Chloride	31	5,475	Total dissolved solids	390	31,800
Fluoride	0.11	302	Total suspended solids	23	17,800
			Total organic carbon	20	14,500
Inorganic compound					
Aluminum	0.01	5.8	Cyanide	0.004	0.3
Antimony	0.0015	47	Lead	0.005	1.6
Arsenic	0.0002	0.982	Manganese	0.03	79
Barium	0.08	5	Magnesium	74	927
Beryllium	0.001	0.01	Mercury	0.0001	0.0098
Cadmium	0.0007	0.15	Nickel	0.02	2.227
Chromium (total)	0.0005	1.9	Vanadium	0.009	0.029
Cobalt	0.04	0.13	Zinc	0.03	350
Copper	0.003	2.8			
Organic compounds					
Acetone	8	11,000	Diethyl phthalate	3	330
Acrolein	270	270	2,4-Dimethyphenol	10	28
Benzene	4	1,080	Dimethyl phthalate	30	55
Bromomethane	170	170	Endrin	0.04	50
Butanol	10,000	10,000	***Ethanol***	23,000	23,000
1-Butanol	320	360	Ethyl acetate	42	130
2-Butanone	110	27,000	Ethylbenzene	6	4,900
Cardon tetrachloride	6	397.5	Bis(2-ethylhexyl) phthalate	16	750
Chlorobenzene	1	685	2-Hexanone (methyl butyl ketone)	6	690
Chloroethane	11.1	860	Isophorone	4	16,000
Bis(2-chloroethoxy) methane	18	25	Lindane	0.017	0.023
2-Chloroethyl vinyl ether	2	1,100	4-Methyl-2-pentanone	10	710
Chloroform	7.27	1,300	Methylene chloride	2	220,000
Chloromethane	170	400	Naphthalene	2	202
Bis(chloromethyl) ether	250	250	Nitrobenzene	4	120
2-Chloronaphthalene	46	46	4-Nitrophenol	17	17
p-Cresol	45.2	5,100	Pentachlorophenol	3	470
2,4-D	7.4	220	Phenol	7.3	28,000
4,4'-DDT	0.042	0.22	1-Propanol	11,000	11,000
Dibromomethane	5	5	2-Propanol	94	26,000
Di-n-butyl phthalate	12	150	Tetrachloroethylene	2	620
1,2-Dichlorobenzene	3	21.9	Tetrahydrofuran	18	1,300
1,4-Dichlorobenzene	1	52.1	Toluene	5.55	18,000
Dichlorodifluoromethane	10.3	450	Toxaphene	1	1
1,1-Dichloroethane	4	44,000	Trichloroethylene	1	1,300
1,2-Dichloroethane	1	11,000	Vinyl chloride	8	61
Cis-1,2-Dichloroethylene	190	470	Xylenes	32	310
Trans-1,2-Dichloroethylene	2	4,800			
1,2-Dichloropropane	0.03	500			
1,3-Dichloropropane	18	30			

Rowe (1995) reported a case study of the leachate contained at the Keele Valley Landfill near Toronto, Canada. The landfill had been developed since 1983 and was still in operation without cover at the time of reporting. Data were collected regularly on a yearly basis up to 10 *years*. In general, the concentration of chloride, BOD and COD kept increasing with oscillation in certain years (see Figure 1.4a). The content of BOD and COD reached over 10,000 mg/l in some years. About 10% changes in pH value in an acidic characteristic were observed. Barone et al. (1997) further reported other waste properties in this landfill including variations of the waste height, leachate head and temperature at the base over an extend monitor period of 12 *years*. The waste thickness stabilized after the first three-*years* of operation. The leachate head was kept stable at about $1m$ in the first 8 *years*, but significantly increased in the last four years up to $4.5m$ (see Figure 1.4b). The increase in the leachate head resulted from the injected groundwater to facilitate circulation.

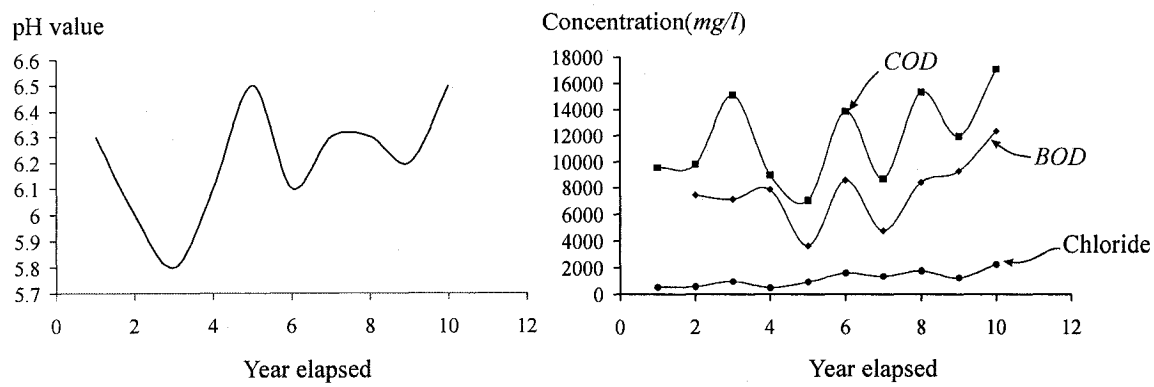

(a) Leachate characteristics (after Rowe, 1995)

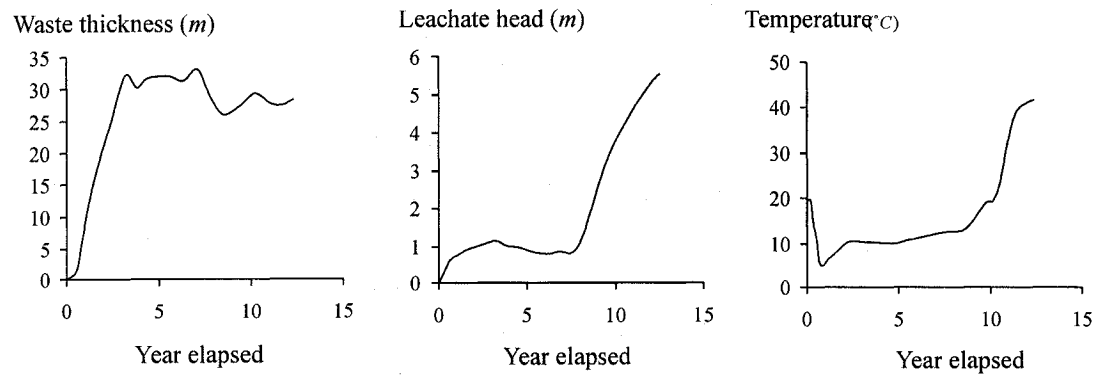

(b) Landfill conditions (after Barone et al., 1997)

Figure 1.4 Leachate characteristics and landfill conditions in first 12-*year* operation period of Keele Valley Landfill, ON, Canada (after Rowe, 1995; Barone et al., 1997)

In general, high toxicity is observed in leachate from landfills receiving MSW (Cameron and Koch, 1980; Schrab et al., 1993). The major potential environmental impact results from its contamination of groundwater and surface water. Christensen et al. (2001) stated the oxygen depletion as the major potential effect of release of leachate to surface water, which changes fauna and flora in the stream bottom. Clement and Merlin (1995) concluded that ammonia is the most probable factor contributing to the observed toxicity; alkalinity is not directly toxic to species, but enhances ammonia toxicity. The concentration of chloride, copper or zinc may also be of major importance to aquatic toxicity (Assmuth and Penttilae, 1995). Toxicity of xenobiotic organic compounds is less well documented, complicated by the fact that its toxicity is chronic (Schrab et al., 1993). The toxicity of leachate also poses high potential risks to human health. Risk calculations by Schrab et al. (1993) indicated that MSW leachates might present a cancer risk. Genotoxic effects were detected by Christoph et al. (1996), who ranked the toxicity of several fluids: landfill leachate, effluents from pulp and paper production, wastewater and contaminated groundwater. Fortunately, the concentration of the leachate components can decay in the long term due to natural degradation and leaching; and the toxicity of the leachate can also reduce with time. Cameron and Koch (1980) found that 5-*year* aging led to an 80-fold decrease in toxicity toward rainbow trout. A decision on the decay in the toxicity of a leachate, however, is not conclusive and requires further research. A case study of the effects of releasing leachate to underground water was performed by Loizidou and Kapetanios (1993), with results covering a distance up to 3*km* from the landfill showing an obvious influence of the leachate on the water quality. High conductivity and hardness values were measured from the underground water close to the landfill; this underground water was assessed as unsuitable for drinking and irrigation. The contamination, however, decreases with increasing distance from landfill. But even at 1*km* away from the landfill, the water was still considered to be unsuitable for drinking and irrigation.

In contrast to a MSW landfill, a hazardous waste landfill is probably aerobic, which would aid in the biological degradation of the waste contents (Haxo and Haxo, 1989). The problem of gas and waste consolidation might be less severe since there is usually less fermentation content. Pavelka et al. (1993) pointed out that, since concentration of an

organic constituent in landfill leachate corresponded to its solubility, co-disposal landfills (containing industrial and municipal solid waste and some hazardous waste) could have lower leachate concentrations than a purely hazardous waste one. However, Clement et al. (1996), after bioassay test on several species, found that toxic impacts were species-specific and that the most toxic leachate was that originating from landfills with co-disposed hazardous industrial waste. Schrab et al. (1993) estimated that the risk from co-disposal and industrial solid waste landfills was comparable to that of a MSW leachate.

In summary, the landfill leachate contains a complex mixture of chemicals, the components of which can be highly toxic and vary with time. Correspondingly, the contact conditions between the leachate and the geosynthetic liner can therefore be highly complex and variable with time.

1.4 PVC polymer and PVC geosynthetic

The chemical compatibility of PVC geosynthetic will be influenced by the chemical composition and chemical stability of the material itself. The study of its chemical composition begins with the raw resin of the geosynthetic, the PVC polymer. Issues such as its structure and the technique of its polymerization will be essential to correctly understand the properties of the PVC geosynthetic that is unique from other geosynthetics. An essentially a polymeric material, the PVC polymer has a molecule formula of $(CH_2 \cdot CHCl)_n$, where n is the number of the repeating unit. Its monomer, vinyl chloride, was first discovered by Justus von Liebig in 1835; PVC is now the cheapest and most widely used plastic for different applications, including items in everyday use such as containers and furniture, electrical isolators and automobile interior panels, and products for civil engineering applications such as floors and pipes, and of course, geosynthetics. The monomer, vinyl chloride, has a boiling point of $-13.9^{\circ}C$ and is then gaseous at normal atmospheric pressure (Matthews, 1996). Matthews (1996) also pointed out that vinyl chloride, however, had been found to be carcinogenic.

The current predominant production of vinyl chloride is from ethylene, which is a petroleum product. The ethylene is first converted to ethylene dichloride by the addition of chloride and then pyrolysed to obtain vinyl chloride and hydrogen chloride

$$CH_2 : CH_2 + Cl_2 = CH_2Cl \cdot CH_2Cl$$
$$CH_2Cl \cdot CH_2Cl \rightarrow CH_2 : CHCl + HCl$$

After the polymerization of vinyl chloride, the material of polyvinyl chloride (PVC) is obtained. PVC polymer is a high molecular thermoplastic polymer that is not cross-linked. For commercial PVC polymer, the average number of vinyl chloride repeating units ranges from about 500 to 1500, corresponding to a theoretical molecular weight between 31,000 to 94,000 (Titow, 1986). The process is achieved by a free radical mechanism, usually activated by added peroxide or a free radical initiator (Endo, 2002). Most production of PVC polymer is achieved by the method of emulsion polymerization, in which the monomer is distributed as a relatively stable dispersion in water and the resultant product is a stable suspension or latex of very small polymer particles in the water. The dispersion of the monomer in the aqueous phase is achieved by agitation with a dissolved emulsifying agent, producing the geosynthetic raw resin (Lauwers, 1994). PVC polymer, by polymerization, has a mainly 'head-to-tail' chain structure, in which a chlorine atom is situated on each alternative carbon atom in the polymer chains, as first demonstrated by Marvel et al. (1939):

$$-CH_2 \cdot CHCl \cdot CH_2 \cdot CHCl \cdot CH_2 \cdot CHCl -$$

The sequential arrangement of repeating units with substituent chloride group forms the stereoregularity of the polymer, which consists of three primary possibilities (Figure 1.5): (a) the isotactic sequence with the same configuration of chloride constituent along the polymer backbone; (b) syndiotactic sequence with chlorine configuration arranged in an alternative manner; (c) and atactic sequence dominated in a random or irregular arrangement of chloride substituent (Billmeyer, 1971; Nass and Heiberger, 1985). Polymerization defects, such as chain branching (5-10%) and 'head-to-head' structures also exist concurrently at the same time.

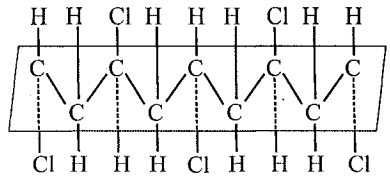

(a) Isotactic configuration

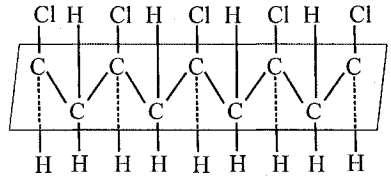

(b) Syndiotactic configuration

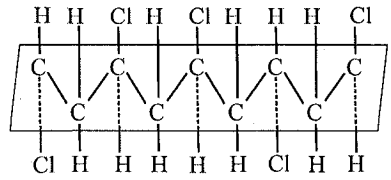

(c) Atactic configuration

Figure 1.5 Three types of stereoregularity of a PVC polymer (after Matthews, 1996)

The complex morphology of a PVC polymer has been studied by several researchers (Hattori et al., 1972; Faulkner, 1975; Wenig, 1978; Endo, 2002). Sections of PVC grains ($100\mu m - 150\mu m$), examined by electron microscopy, consist of primary particles of about $1\mu m$ in size and agglomerates of these. In the earliest stage of polymerization, the polymer coagulates to form aggregates of about 50 molecules, and by the time conversion has reached 2 percent, particles of $0.1\times10^{-6}m$ to $0.2\times10^{-6}m$, called domain, comprising of about 1000 of these aggregates, have been formed. By 10% conversion, domain grows to form the primary particle, which then coalesces further to form the agglomerate. Subsequent polymerization further results in the growth of size and distribution of PVC grain particle. The spatial packing of agglomerates determines the degree of porosity in the final product. The type of PVC morphology with mostly grain particles greater than $150\mu m$, has a porous structure that allows a ready absorption of plasticizer. The other type, with substantially spherical grains averaging size of $100\mu m$, has low or zero porosity that is specifically intended for unplasticized compositions. Two typical types of morphology are shown in Figure 1.6. The influence of the morphology of the PVC

structure will be reflected in other important physical properties, such as surface area, which largely determines the solvent absorption capacity and bulk density of a finished product.

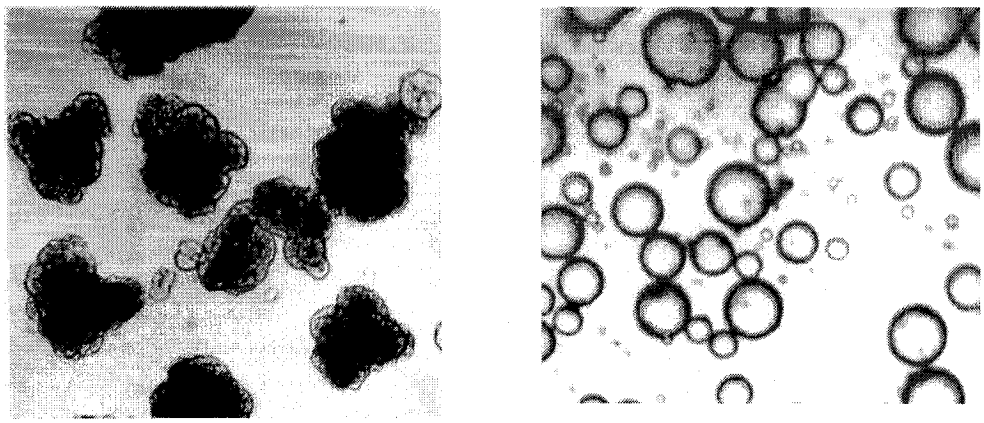

(a) Porous type (b) Non-porous type

Figure 1.6 Morphology of commercial PVC resins suspended in Di-iso-octyl phthalte (DIOP) (approximately $\times 90$) (after Matthews, 1996)

The PVC polymer has a glass transition temperature T_g above room temperature (Brandrup et al., 1999). The glass transition temperature of PVC varies with the polymerization method, but falls within the range of 60 to $80^{\circ}C$, well above other common plastics such as polyethylene ($-110^{\circ}C$) and polypropylene ($-18^{\circ}C$). At high temperatures above T_g, the PVC material comes in the form of a liquid; the highly viscous flow involves entire molecules slipping with respect to each other. At temperatures below T_g, PVC exists in a solid form, which presents a randomly unordered, *amorphous*, structure, which is inherently hard and brittle at room temperature (Nass and Heiberger, 1985). Its mechanical response is moderately rate-dependent. The stress-strain curves of a PVC polymer at various strain-rates are shown in Figure 1.7. As can be seen, a six orders of magnitude difference in the strain-rate leads to roughly doubling the peak stress and a large reduction in the breaking strain. The properties of PVC polymers are very dependent on the resin as well as other ingredients from which it is derived. The most important raw resin parameters are its molecular weight and the

molecular weight distribution. In a given formulation, increasing molecular weight leads to an increase in the melt viscosity at a particular temperature (Matthews, 1996).

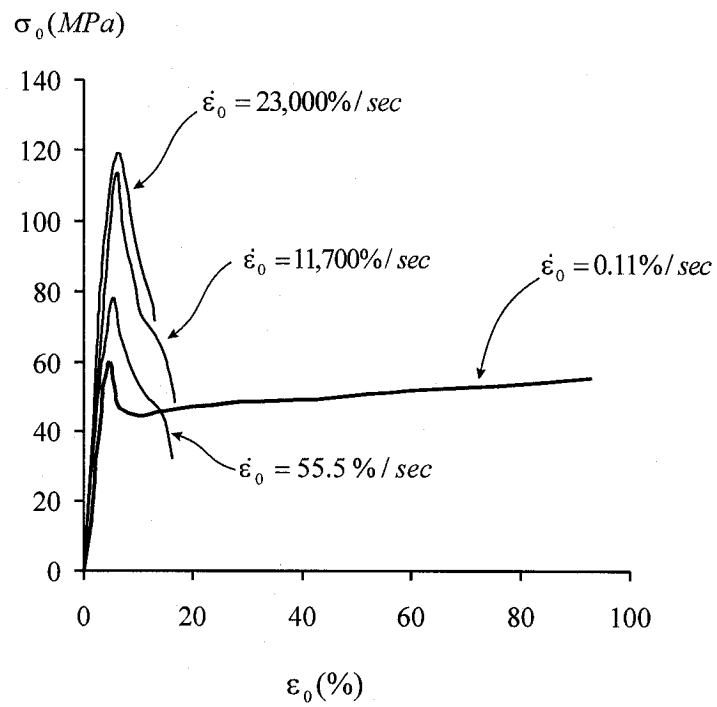

Figure 1.7 The stress-strain curves of a PVC polymer at various strain-rates (after Pezzin et al, 1972)

Commercially used PVC also presents about 10% crystallinity (Gilbert, 1994; Flores et al., 1994). The increase in the crystallinity is related to an increase in the syndiotactic sequence in the PVC polymer, which is typically $54\% - 56\%$ for commercial PVC (Carrega, 1977; Flores et al., 1994). The existence of crystals can be detected by X-ray measurement and presents as a nodular and lamellar structure (Blundell, 1979; Bort et al., 1968). This relatively low level of order has, however, a surprising effect on the properties of the final product. The most significant change is the glass transition temperature (T_g) of the PVC material. Gilbert (1994) claimed that T_g increased by about $20^{\circ}C$ for PVC at 20% crystallinity compared to conventional commercial PVC polymers. Young's modulus and tensile strength is expected to be slightly higher with the presence of low crystallinity, but the impact properties will be reduced (Manson, et al., 1972; Gilbert, 1994). High crystalline material can fail almost in a brittle fashion prior to occurrence of yielding. The main advantage of the presence of crystals, however, lies in

the reduction of the potential of solubility resulting in better chemical compatibility (Gray and Gilbert, 1975). Okuno et al. (1993) monitored a 2% reduction in the diffusion coefficient of water vapor through PVC polymer with an increase in crystallinity from 10% to 25% at $40^{\circ}C$.

The use of PVC as a geosynthetic membrane had its roots in North America in the 1930's, when the U.S. Bureau of Reclamation used it as a canal liner. A complete chemical formulation of a PVC geosynthetic is usually composed of the PVC resin itself along with several other additives, such as plasticizer, fillers, carbon black and lubricant. Plasticizers are generally added to increase the flexibility of an otherwise brittle material. Fillers, such as natural calcium carbonates and china clay are used to reduce cost and increase functional properties, such as impact resistance. Fillers of alumina can be added to reduce flammability. Lubricants, such as lead or calcium, can be added to ease the flow of polymer molecules relative to each other and to reduce adhesion between the hot plastic material and the metallic processing equipment. In this thesis, the term *PVC polymer* or *PVC resin* is used to refer to the material matrix or the material that contains no additives. The PVC resin itself is present in a colorless form; most of the commercial unplasticized or plasticized PVC, however, is colored by the addition of colorants or pigments, such as carbon black and titanium dioxide. Biocides are additives that provide protection against mold, mildew, fungi and bacterial growths. Thermal stabilizers are added to minimize thermal decomposition during processing and applications. Other stabilizers, such as UV stabilizers, can also be added to increase its resistance to ultra-violet degradation; pigments, including carbon black and titanium dioxide (PVC Geomembrane Institute, 1994), can also act as UV stabilizers. In order to distinguish from the material that contains no additives, the term *PVC material* or *PVC geosynthetic* in this thesis refers to the material that contains a complete production formulation of its compositions, including both PVC resin and additives.

The manufacturing of the PVC geosynthetic after selection of the PVC formulation can be broadly classified into three major stages: mixing, compounding and shaping. Mixing is defined as any physical process in which the various components of a formula are blended together. Compounding involves reactions between components of the formula

on a molecular scale with the formation of the continuous PVC matrix. Shaping generally refers to all the other processes used to produce the final shape of the product. The object of all these manufacturing stages is to achieve a finished product in as homogeneous a state as possible. A detailed account of the integration of these manufacturing stages is given by Penn et al. (1971). The process of producing PVC geosynthetic sheets of various width and thickness is called a *calendering method* (Koerner, 1994). In this method, the PVC formulation of the polymer resin and additives are mixed in a batch or a continuous mixer; this is then heated to initiate the reaction between components. The mixture is next conveyed into a roll mill, where it is further blended and masticated. Now, in a form of a continuous mass, it passes through a set of counter-rotating heated rollers, called a calender (see Figure 1.8), to form the final sheet. Each nip or roller can be adjusted to give a desired thickness of geosynthetic sheet. Continuous flexible sheets in a thickness range of $0.04mm - 0.8mm$ can be produced by the calendering method. When thicker sheets are produced, there is possibility of inadequate and non-uniform heating and air entrapment. Sometimes, a layer of open weave fabric, called scrim, can be used between individual sheets as reinforcement (see Figure 1.9). The finished PVC geosynthetic therefore can possibly exhibit anisotropic behaviour due to the forming operations of calendering; however, in such operations, there is ordinarily an opportunity for a considerable amount of the orientation to relax before the structure is frozen, so that only a small amount of anisotropy will sometimes be observed (Alfrey et al., 1949a). As an example, a complete formulation of PVC geosynthetic membrane by Canadian Tower Inc. (Diebel, 2002) is given in Table 1.2. Besides the additives discussed previously for PVC material, biocides are added for precaution against biological attack.

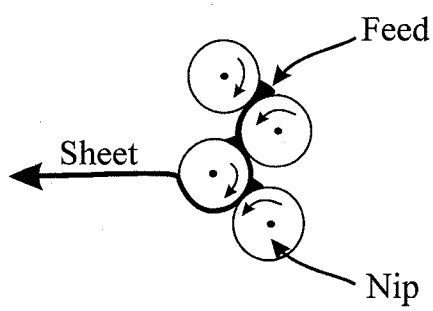

Figure 1.8 Calender bowl arrangement (after Matthews, 1996)

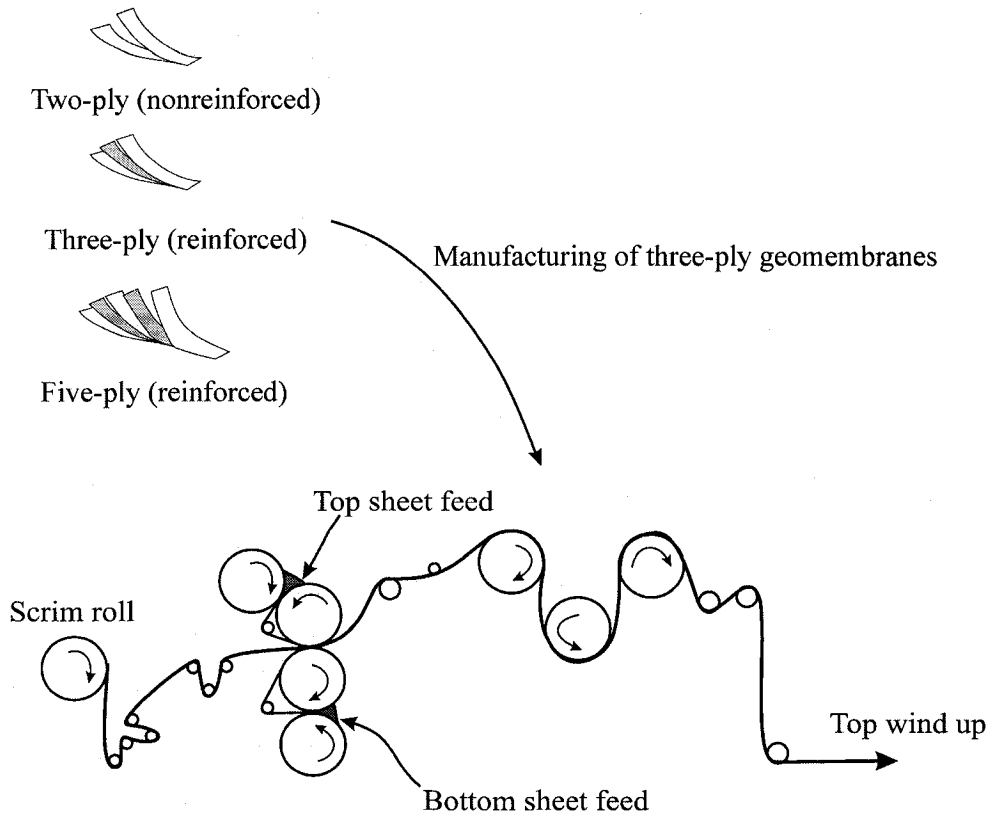

Figure 1.9 Manufacturing method for producing multi-ply geosynthetic (after Collette, 1994)

Table 1.2 A PVC formulation for PVC geosynthetic (after Diebel, 2002)

PVC resin	50-70%
Plasticizer (phthalate monomers)	25-35%
Stablizer/lubricant	1-3%
Pigments (aiding UV stability)	1-5%
Miscellaneous (Biocides, fire retardant)	0-3%
Filler	0-10%

1.5 PVC plasticization

Among all the additives used for PVC materials, plasticizer comprises the most important component. Plasticizer, generally a clear, organic liquid, is added to the PVC formulation to obtain a flexible film to enhance both processability and serviceability of the end

product. Generally, PVC material is plasticized with 20*phr*-70*phr* (parts per hundred parts of resin) of plasticizer (Nass and Heiberger, 1985), which roughly amounts to 30% to 35% plasticizers by weight. There is extensive literature on the subject of plasticization in general (Bruins, 1965; Sears and Darby, 1982; Wilson, 1995). The activity of plasticizer in the PVC matrix is, however, quite complex (Matthews, 1996). One favorite theory, which can be used as a guideline for obtaining compatibility between the plasticizer and the PVC resin, considers the interaction between plasticizer and PVC molecular backbone. As has already been discussed, PVC polymer has largely a head-to-tail arrangement of vinyl chloride units. The highly electro-negative nature of chloride leads to dipoles among the polymer molecules, resulting in high concentrations of secondary valency forces, which in turn results in the reduction of flexibility in the individual molecules and subsequently accounts for the rigidity of the material. Plasticizers have molecules with polar or polarisable groups, which has been visualized as a capacity to bond with the polymer dipoles; and the non-polar parts act as shields between polymer dipoles, which results in less overall cohesion (Aiken et al., 1947; Matthews, 1996). Consequently, a thermal barrier that restricts plasticizer molecules to diffuse between polymer molecules is required to overcome (Neilson et al., 1950). In practice, according to the compatibility between the PVC resin and plasticizing material, three broad classes of plasticizer exist (Sarvetnick, 1969; Matthews, 1996). The most important plasticizers, known as primary plasticizer, are those that are completely compatible with a PVC resin over the whole range of practical compositions and conditions. Secondary plasticizers are only compatible over a limited range of concentrations. This range, however, can be extended by the presence of primary plasticizers. The main purpose of the primary plasticizer is for end use, while a secondary plasticizer is used to ease processing. The third type of plasticizer, called plasticizer extenders, is generally incompatible on its own, but can become compatible over a limited range of concentrations by the addition of a primary plasticizer. Several important types of plasticizers are categorized in Table 1.3.

Table 1.3 Major plasticizers of the three classes (after Matthews, 1996)

Primary plasticizers	Secondary plasticizers	Extenders
Dibutyl phthalate (DBP)	Dioctyl adipate (DOA)	Chlorinated paraffins
Dioctyl (i.e. 2-ethylhexyl) phthalate (DOP)	Di-iso-ictyl adipate (DIOA)	Mineral oil extracts
Di-iso-octyl phthalate (DIOP)	Di-'alphanyl' adipate (DAA)	
Diallyl phthalate (DAP)	Dioctyl sebacate (DOS)	
Dionony phthalate (DNP)	Di-iso-octyl sebacate (DIOS)	
Di-isodecyl phthalate (DIDP)	Di-'alphanyl' sebacate (DAS)	
Ditridecyl phthalate (DTDP)	Di-iso-octyl azelate (DIOZ)	
Tritolyl phosphate (TTP)	Polypropylene adipate (PPA)	
Trixylyl phosphate (TXP)	Polypropylene sebacate (PPS)	

It is found that, as the concentration of plasticizer increases, there are corresponding alterations in the physical and mechanical behaviour of an otherwise brittle PVC polymer. The addition of plasticizers lowers T_g, the glass transition temperature, of rigid PVC, making it more flexible (Sarvetnick, 1969; Elicegui et al., 1997; Dubault et al., 2003). As the plasticizer content increases, there is usually an increase in toughness and a decrease in the Young's modulus and tensile strength. Elicegui et al. (1997) observed that plasticization of PVC lead to changes in the volumetric and elastic properties; suppression of the glass transition temperature tended to decrease the stiffness, but increased the thermal expansion coefficient and Poisson's ratio. At high levels of plasticization, Elicegui et al. (1997) argued that the material is essentially incompressible and that in cases involving only physical mixture of the plasticizer and PVC resin, the structure of the PVC polymer was unaltered. On occasions, however, nucleophilic substitution of atoms from the plasticizer for chloride atom occurred, altering the structure of the PVC polymer. Correspondingly, the properties of the PVC material got altered as a result of the structural change to the PVC resin. The spectroscopic evidence by Dubault et al. (2003) pointed out that the depression of the glass transition temperature of the PVC material was actually attributed to the interaction between the plasticizer and the PVC chain backbone, which further causes alterations in the mechanical behaviour of the material, such as plastic behaviour and yielding behaviour, defined as the mechanical energy prior to yielding. A study of the alteration in the stress-strain behaviour of the

PVC material induced by the addition of plasticizers was presented by Pita et al. (2002). Figure 1.10a shows the stress-strain curves of PVC materials with different amounts of di-2-ethylhexyl phthalate (DOP) plasticizer (in *phr*) obtained by Pita et al. (2002), while Figure 1.10b shows the results for PVC materials with the plasticizer of polyester-based thermoplastic polyurethane (TPU). A monotonic relation between stress and strain is observed for the PVC with a high plasticizer content. When the plasticizer content is lowered, however, a distinct yield-type stress-strain behaviour is observed. The precise mechanical properties of other types of plasticized PVC will depend on the nature and amounts of plasticizers. Typical variations in Young's modulus at 100% extension, tensile strength and failure strain with concentration of various plasticizers are presented in Figure 1.11. A general trend of reduction in Young's modulus and tensile strength, and an increase in failure strain are observed. While the addition of plasticizer is favored in terms of its modification of an otherwise brittle material, the possibility of the loss of plasticizer from a PVC material due to an environmental loading, such as chemical exposure, can present a mechanism for changing the performance of the material. Such a possibility will be discussed in subsequent sections.

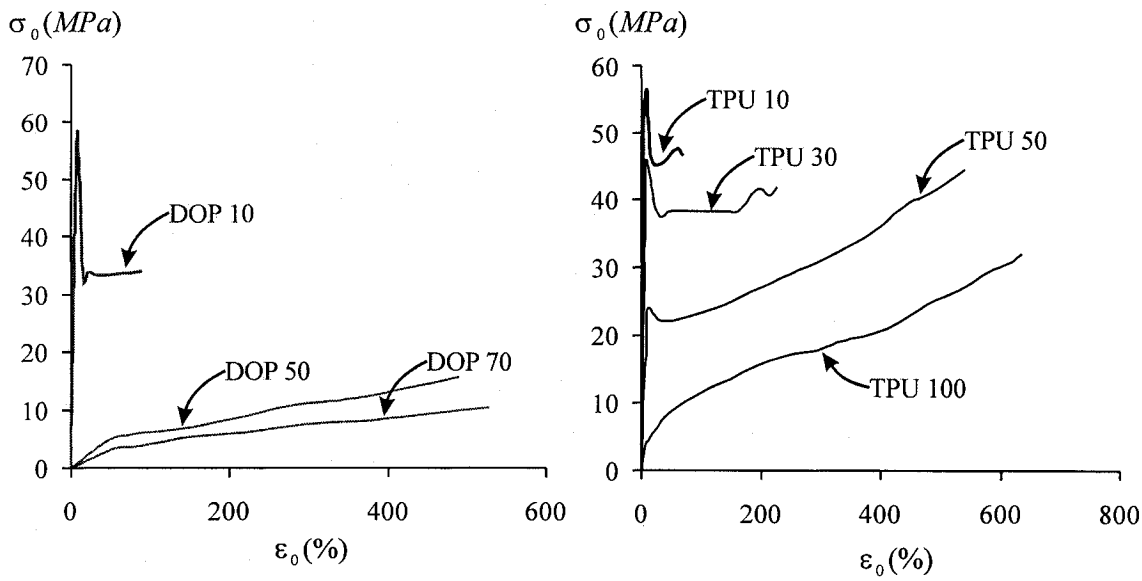

(a) Plasticized with DOP (in *phr*)

(b) Plasticized with TPU (in *phr*)

Figure 1.10 Stress-strain curves of the plasticized PVC material (after Pita et al., 2002)

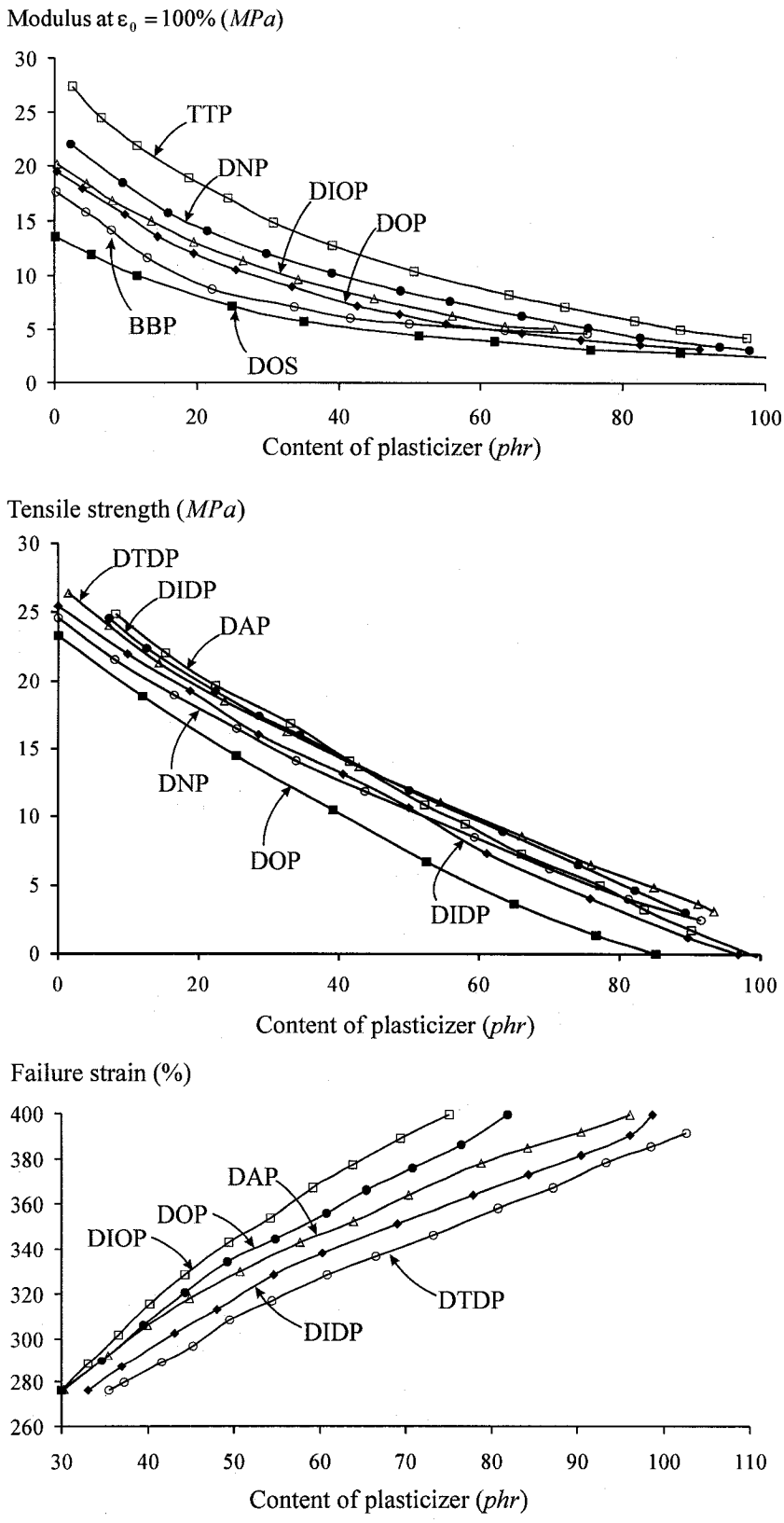

Figure 1.11 Mechanical behaviour of PVC material plasticized with different plasticizers (after Matthews, 1996)

The amount of free volume within the PVC geosynthetic can also be altered by the presence of plasticizer. Borek and Oscoba (1996) found a linear monotonic function between mean free volume radii and concentration of DOP plasticizer in the PVC material. The presence of the free volume increases the diffusion of a solid or a liquid inside a PVC material, which partially contributes to a more permeable property of a PVC geosynthetic compared to other types of geosynthetics. In practical situations, where a chemical permeate presents a potential threat to the integrity of the material structure, the alteration in the permeability should be a major concern to the chemical compatibility of the PVC material.

Crystallinity will be reduced in a plasticized PVC geosynthetic (Manson et al., 1972); this will further increase its susceptibility to chemical penetration. Shtarkman et al. (1972) reported a reduction in crystallinity from 11% to 4% as plasticizer concentration increased from 0% to 60%. Aiken et al. (1947) and Alfrey et al. (1949a) demonstrated that the existence of the crystallites cannot be eliminated due to the presence of plasticizer; in a stretched sample, the crystallites formed an oriented structure and the widely distributed small crystallites of the "fringed micelle" type acted as a linkage between amorphous networks. Later work by Taylor and Tobolsky (1964) confirmed that the addition of a plasticizer did not substantially alter the microcrystalline structure. The average crystallite size was actually unchanged by the presence of a plasticizer (Shtarkman et al., 1972).

The phenomenon of anti-plasticization, i.e. the embrittlement of the PVC material at low levels of plasticizers has also been noted (Jackson and Caldwell, 1967; Kinjo and Nakagawa, 1973; Gilbert, 1994). Gibbons et al. (1997) and Gibbons and Kusy (1998) studied the percentage of the alteration of the mechanical behaviour of a PVC material plasticized with nine different plasticizers; all results indicated an increase in strength, elastic modulus and toughness due to the effect of anti-plasticization. During the initial addition of the plasticizer, the maximum elastic modulus of PVC material occurred at a plasticizer content between 10%-15%. Guerreto (1989) attributed this phenomenon of anti-plasticization to the presence of crystallinity, while Kim et al. (1987) considered this a result of the reduction of free volume. Although the phenomenon of anti-plasticization

is well known, it is not a major concern for the scope of this thesis, since most PVC geosynthetics are produced at higher plasticizer concentrations which do not favour for the occurrence of such a phenomenon.

1.6 Durability of the geosynthetic in a landfill environment

In the previous sections, the topic of the durability of the PVC geosynthetic was addressed in relation to the composition and molecular structure of the material. The property of durability depends on the quality of the geosynthetic itself including the nature of reactivity of the polymer, and the purity of the finished product after a manufacturing process. In this section, the issue of the durability of the PVC material will be discussed from the aspect of its interaction with the surrounding environment as a geosynthetic liner over the life of a landfill. The main strategy is for the PVC geosynthetic to maintain its service requirement until the leachate fully reduces its potential threat. As discussed in Section 1.2, the time-scale suitable for such decomposition, however, can be several hundred years (Kjeldsen and Christensen, 2001). It would be appropriate to state that these geosynthetics are perhaps being used without a clear knowledge of their long-term behaviour; its degradation potential has been largely studied in connection with the barrier design (Koerner, 1990; Koerner et al., 1990). A detailed clarification of the reaction mechanism of the degradation of PVC material was provided by Bacaloglu and Fisch (1995). In their study, the issue of durability of the PVC material arose from three processes: the loss of the additives within the polymer matrix, the alteration in its chemical composition and polymeric chain scission within the polymer structure. Polymeric chain scission represents the chemical alteration of the polymer molecule backbone, which directly affects the integrity, and subsequently induces the failure of the material. While loss of protective additives may alter the properties of the material in some cases, it does not change the integrity of the polymer structure. A review of potential exposure conditions in landfill and other containment applications has been provided by Haxo and Haxo (1989). The longevity of the containment provided by PVC geosynthetics can be influenced by chemical, mechanical and other environmental factors such as ultraviolet radiation, oxidation and biological action (Cazzuffi et al., 1995). All these factors that influence the degradation can be

accelerated by elevated temperatures, such as might occur as a result of the exothermic decomposition of the organic waste. It should also be borne in mind that environmental conditions in a landfill are highly heterogeneous. For the multi-layer composite liner (referred to Figure 1.1), the primary liner will likely experience higher temperatures and chemical concentrations close to the leachate and waste, while the secondary geosynthetic liner will be subjected to environments closer to the groundwater; therefore the service life and the requirements of the primary and secondary geosynthetic liner may be different (Rowe, 1998). In the subsequent sections, the basic principles of several types of degradation process of a PVC material will be discussed along with the associated consequences on the durability of PVC geosynthetics in a landfill service.

1.6.1 Chemical compatibility of a PVC geosynthetic

A PVC polymer is essentially inert to many chemicals such as organic liquids, organic acids and aliphatic hydrocarbons. However, it can be softened, dissolved or degraded by a limited number of organic liquids including nitrobenzene, ketones and tetrahydrofuran. The presence of a plasticizer increases the susceptibility of the PVC material to degradation by surrounding media. The possibility of direct exposure of the plasticized PVC material to the liquid leachate or other chemicals that may be present is therefore of major concern to the engineering use of the PVC geosynthetic. A general account of the activity of PVC polymer with various chemicals was discussed by Matthews (1996). The methods for conducting chemical compatibility tests with geosynthetics were reviewed by Cassidy et al. (1991).

Oxygen and ozone do not appear to be attached to a PVC polymer at room temperature, but severe oxidizing agents do cause some breakdown of the molecular chain. Concentrated solutions of oxidizing agents, such as potassium permanganate, attack the PVC polymer superficially. Ozone degradation is a potential problem if the PVC polymer presents unsaturated groups. Ozone usually has no access to the geosynthetic in the interior of a landfill; however, it has the potential to damage exposed parts. In the presence of free radical and unsaturated groups, oxidation occurs, resulting in hydroperoxides and peroxides with resultant chain scission (Matthews, 1996). An

exposed geosynthetic or those covered by unsaturated soil can possibly be susceptible to oxidation. In contrast, for landfill base liners, the available free oxygen will be extremely limited due to the biodegradation in the waste, which significantly reduces the oxygen content (Rowe and Sangam, 2002). Since the PVC polymer is produced without crosslinking, the possibilities for PVC geosynthetic to present unsaturated group and free radicals, and therefore the susceptibility to attack by oxidation, are lower compared to other cross-linked polymer such as HDPE. It should be borne in mind, however, that the attack by oxidation on a plasticizer is always possible (Decoste, 1968).

Chlorides, which are frequently encountered in landfill leachate (see Table 1.1; USEPA, 1988), have little effect on PVC polymers; bromides and fluorides, however, readily attack PVC even at room temperature. An abundance of bromide and fluoride in MSW landfill leachate is seldom reported. In the cases of industrial or hazardous waste landfill that specifically releases such chemicals, the durability of the PVC geosynthetic needs to be examined.

PVC polymer is also resistant to most acids and aqueous alkalis with the exception of sulphuric acid at concentrations above 90% and nitric acid at concentrations above 50% (Matthews, 1996). The ages of acidics and alkali in leachate vary with the age of the landfill. Young landfill typically contains a leachate with an acidic characteristic, while older landfill contains leachate with a pH value larger than 7. At temperatures greater than $60^{\circ}C$, however, the diffusion of the chemicals into the interior of the PVC polymer is enhanced and therefore the possibility of an attack by normal acids and alkali is increased (Matthews, 1996). Bishop et al. (2000) observed that the creep behaviour of PVC polymer under a high external tensile stress of $40MPa$ can be elevated at the presence of an alkali; PH values of 13.5 pose the most severe condition. For a geosynthetic that services the base of a landfill experiencing large vertical stresses, the degradation due to either acidic or aqueous alkali leachate can be of concern in the long-term, particularly when the temperature within the landfill is elevated.

When compared to PVC geosynthetics that serve as a top cover system, the long-term chemical compatibility of PVC geosynthetics used at the base of a landfill as an

engineering barrier will be more influenced by its ability to resist the penetration of chemicals in an aqueous solution. Solvent liquids, which might induce the swelling of the material, are known to permeate the geosynthetic at a molecular level by the process of sorption and diffusion (Haxo et al., 1984; Haxo, 1990). The process of migration of a chemical inside a polymeric geosynthetic material involves three key steps (Park and Nibras, 1993; Prasad et al., 1994): (i) *absorption*: which involves the removal of a chemical from the surrounding media and its dispersion on or into the material. (when a contact between a geosynthetic and a liquid reaches equilibrium, the concentration of a chemical in the geosynthetic and that in the outer media will be a factor ratio, called the partition coefficient) (ii) *diffusion*: indicating the migration of chemical into the geosynthetic; (iii) *desorption*: which is a reverse process to the sorption process and involves the return of the chemical back to the ambient media (Sangam and Rowe, 2001). The ability of the chemical to migrate inside the PVC material in step (ii) is frequently characterized by the *diffusion coefficient* of the chemical. Mueller et al. (1998) found that the diffusion coefficient was considerably smaller for contaminants at low concentration in an aqueous solution than that for pure chemicals. Also the presence of the crystalline zones can add barriers to chemical migration (Gray and Gilbert, 1975; Gilbert and Mulla, 1983). In the literature, there is little data about the diffusion coefficients of leachate chemicals through a PVC geosynthetic. Data on diffusion coefficients of the other type of geosynthetic are available. Aminabhavi and Naik (1999) measured the diffusion coefficients of several organic liquids commonly encountered in landfill leachate through PP and HDPE geosynthetics. The results, obtained by measuring the weight change during the sorption/desorption test at $25^{\circ}C$, indicated a diffusion coefficient of the order of $10^{-11} m^2 / sec$ and a sensitivity of the organic chemicals inside the geosynthetic to the temperature of the environment. Corresponding values for PVC geosynthetics are expected to be slightly larger, since the presence of plasticizer tends to increase the free volume of the material, easing the migration of chemical contaminants (Matthews, 1996). Diffusion coefficients of various organic solvents at the order of $10^{-12} m^2 / sec$ were obtained by Sangam and Rowe (2001) in permeation/diffusion experiments, monitoring the concentration change in two compartments divided by a HDPE geosynthetic. The value obtained is comparable to the diffusion coefficient of water through a PVC

geosynthetic obtained by Giroud and Bonaparte (1989). The available diffusion coefficients, therefore, are questionable and may be sensitive to the measurement technique. For design of the PVC geosynthetic, caution should be exercised when using a laboratory diffusion data; larger estimates of diffusion coefficients need to be taken from a conservative point of view. The main consequence of the absorption of the organic chemicals by a polymeric material is the *swelling* of the material exhibiting a volumetric increase. The material softens as a result of swelling (Treloar, 1975; Haxo et al., 1985a). The phenomenon of swelling is reversible to some extent when desorption occurs (Rowe and Sangam, 2002). Aminabhavi and Naik (1999) noticed a 0.3% volumetric swelling of a HDPE geosynthetic due to the absorption of certain organic liquids such as benzene and toluene. The swelling reaches its maximum when the solubility parameter of the PVC polymer matches that of the contacting liquid (Haxo et al., 1985a). The phenomenon of swelling also increases the segmental mobility of a polymer, hence enhancing the migration properties of additives within the geosynthetic and accounts for the subsequent accelerated degradation process (Sangam, 2001). In cases where softening due to swelling occurs in combination with the thermal effects, it may significantly reduce the load carrying capacity of the material and potentially cause excessive deformation of the liner system and protective layers, particularly when decomposition or settlement of the underlying layer is pronounced. The softening behaviour of a chemically-treated PVC geosynthetic will be examined in a chapter of this thesis.

In the literature, the chemical compatibility between the landfill leachate and PVC geosynthetic is rarely quantitatively characterized. Instead, a general guideline by the supplier is provided for geosynthetics applications. Table 1.4 gives an example of the descriptive assessment of the compatibility between a PVC geosynthetic and several chemical contaminants (released by the website of Groupe Solmax Inc.,). The chemical compatibility is classified into two categories: satisfactory (S) and unsatisfactory (NS); the satisfactory classification are recommended for use. Based on these descriptive judgments, a PVC geosynthetic has good resistance to most inorganic compounds such as dilute acids and salts, and it is also unaffected by the presence of heavy metals. However, it has poor compatibility with many organic chemicals.

Table 1.4 Chemical compatibility of a PVC geosynthetic (after Groupe Solmax Inc.)

PVC CHEMICAL RESISTANCE					
Acetic Acid 10%	S	Gasoline	NS	Sodium Hydroxide 25%	S
Acetone	NS	Hydrochloric Acid	S	Sodium Hypochlorite 12%	S
Ammonium Hydroxide 25%	S	Hydrogen Sulfide	S	Sodium Sulfate	S
Ammonium Nitrate	S	Hydrogen Peroxide	S	Sulfuric Acid 20%	S
Aqua Regia	S	Methyl Alcohol	S	Sulfuric Acid 94%	NS
Benzene	NS	M.E.K.	NS	Tetrahydrofuran	NS
Brine Solutions	S	Nitric Acid 10%	S	Toluene	NS
Calcium Chloride	S	Nitric Acid Conc.	NS	Trichloroethylene	NS
Diesel	NS	Petroleum Oil	NS	Turpentine	S
Ethylene Glycol	S	Potassium Acetate	S	Urea 30%	S
Ethyl Alcohol	S	Sea Water	S	Zinc Chloride	S
Fertilizer	S	Soap Solutions	S		
S : Satisfactory; NS: Not Satisfactory					

Limited data concerning long-term performance of a HDPE geosynthetic and leachate is also available in the literature. Rowe et al. (2003) reported the condition of a HDPE geosynthetic after a 14-*year* service as a leachate lagoon liner without cover protection. Significant loss of additives, such as antioxidants, was observed for parts of the geosynthetic frequently in contact with the leachate. The aging process was also found to be accompanied by large amounts of crystallization, which reduces the diffusive capacity of some solvent solutions up to three times. For parts of the geosynthetic that were exposed to sunlight without exposure to leachate, the degradation process was more severe. Number of cracks were observed, indicating a severe attack by UV radiation.

1.6.2 Other types of degradation of a PVC geosynthetic

The degradation of a PVC geosynthetic by environmental factors such as UV radiation, thermal effects and biological actions is not the focus of this thesis. Knowledge of these degradation processes, however, further highlights the governing factors contributing to the chemical degradation of the PVC geosynthetic.

The UV degradation of a PVC polymer is induced by irradiation with ultra-violet or visible light. It can manifest itself by main-chain breakage in the molecular backbone and therefore alters the integrity of the polymer structure. Khalifa et al. (1979) exposed PVC films with various stabilizers to a laboratory light source for 8 *days*; most specimens

exhibited a 10% to 13% loss in tensile strength and a 4% to 7% reduction in critical elongation; correspondingly, there was up to 53% reduction in the PVC molecular weight, indicating severe molecular main-chain breakage. The extraction of protective additives essentially contributes to a progressive increase in embrittlement of the geosynthetic (Doyle and Baker, 1989). Hollande and Laurent (1997) reported that the plasticizer could also take part in the process of photo-degradation because it too decomposed itself after UV exposure. The presence of moisture and UV light can have a synergistic effect on the geosynthetic durability. The term *weathering* refers to a repeated attack of the PVC geosynthetic by moisture change and UV light radiation. Natural weathering tests conducted by Doyle and Baker (1989) indicated an increase in the hardness of a 0.75-*mm* PVC geosynthetic after a 28-*month* exposure. Martinez et al. (1996) reported a consistent reduction in the tensile strength and failure strain of PVC films with different plasticizers during a 9-*month* period of natural weathering; the reduction in tensile strength indicated a possible main-chain breakage during weathering. These authors further claimed that it was the photodegradation that mainly contributed to the change in the mechanical behaviour of the PVC geosynthetic rather than the moisture effects. Jakubowicz et al. (1999) reported a continued reduction in the impact resistance capacity of the PVC material during laboratory weathering. During natural weathering, the impact resistance capacity of the material kept decreasing up to 20% during the first 7 *years*, but then remained stable for the next 5 *years*. For geosynthetics servicing as a landfill cover, UV degradation is crucial for those parts exposed to natural weathering without soil coverage. These parts are in repeated contact with UV light, moisture, oxygen and thermal effects; therefore the phenomenon of material *embrittlement*, and therefore reduction in service life, can be expected. For a geosynthetic serviced in the interior of the landfill, the issue of UV degradation and weathering is of less concern.

All geosynthetic components in a landfill, however, have the possibility of experiencing physical aging. The term "physical aging" is used to describe the property changes that occur at room temperature but which do not involve any irreversible chemical change. When T_g is above room temperature, physical aging arises from changes in free volume (Struik, 1978). Dorrestijn et al. (1981) proposed that there was a uniform distribution of

PVC crystallites inside the material as aging proceeds, which kept increasing in size. However, Tsitsilianis et al. (1989) observed that physical aging of PVC occurs over the entire structure of the material, including the crystalline phase, the amorphous phase and their transition region; there was a significant reduction in the diffusive capacity of the polymer with the presence of crystallite as aging proceeded. Consequently, there is evidence that the PVC polymer undergoes marked stiffening and hardening over time at room temperature. Juijn et al. (1973) found that, during aging of a PVC material with DOP plasticizer, the Young's modulus kept increasing for a period of 5 *years*. The physical aging therefore can most likely be related to the alterations in the mechanical properties of the PVC geosynthetic in the long term. These alterations induced by physical aging, however, can be reversed by reheating the material to processing temperatures (Flores et al., 1994; Matthews, 1996). This is, however, not a practical reality in the context of applications of PVC geosynthetics in landfill.

At high temperatures, however, another degradation issue arises since the PVC polymer has the lowest thermal stability among all carbon-chain polymers (Benavides et al., 2001). At temperatures above $100^{\circ}C$, decomposition of the PVC and the generation of HCl is widely known. The process of such degradation is called *dehydrochlorination* (Arlman, 1954; Bengough and Sharpe, 1963). In the report by Barone et al. (1997), the temperature in the landfill waste increased up to $43^{\circ}C$ due to the generation of the heat by the decomposition of the organic material. Temperatures as high as $70^{\circ}C$ have also been reported (Ramke, 1989; Yoshida et al., 1996); the potential of susceptibility of PVC geosynthetics to thermal degradation is therefore of concern. In the reports by Koerner et al. (1996), however, high temperature is confined to the waste and liner temperature is usually expected to be within the range of $20^{\circ}C$ to $25^{\circ}C$. However, thermal effects should not be neglected. A comprehensive review of the subject of thermal degradation of PVC polymers was conducted by Matthews (1996) (see also Madorsky, 1964). As decomposition proceeds, a colorless unplasticized PVC sample usually becomes yellowed, then brown, and finally black. The thermal degradation product of hydrogen chloride is volatile. Other products, such as aliphatic, unsaturated, aromatic hydrocarbons are generally insoluble in common solvents. The thermal degradation is usually retarded

by the introduction of a thermal stabilizer. Benavides et al. (2001) found that the generation of HCl is retarded during thermal degradation due to the introduction of $CaSt_2$ or $ZnSt_2$. A longer degradation induction period was obtained for a PVC additive with $CaSt_2$ before an accelerated thermal degradation process. Another possible concern for the durability of the geosynthetic due to temperature variation is the temperature-dependent nature of the mechanical response of a PVC specimen. Tsuboi et al. (1998) indicated an exponential reduction of the breaking strength and Young's modulus of the PVC geosynthetic with respect to the temperature. In their study, the 1% secant modulus of the PVC geosynthetic can be reduced two orders of magnitude from $-30^{\circ}C$ to $60^{\circ}C$; this can introduce excessive deformation at locations where the temperature variation is high. On the other hand, the large reduction in the deformability when temperature is reduced in cold weather significantly influences on the ability of the geosynthetic in resisting localized deformations such as localized differential settlement. These authors also studied the stress mobilization due to temperature variations. In their studies, the PVC specimen corresponding to a zero strain at $80^{\circ}C$ could be mobilized to a stress of $0.1MPa$ at $0^{\circ}C$. A stress of $0.1MPa$, however, is usually not a major concern for PVC geosynthetics in most civil engineering uses. The issue of the influence of thermal cycles therefore then only arises where landfill is still in operation without a final cover and subjected to even more harsh and prolonged temperature variations.

Since PVC geosynthetic is actually frequently under stress in the landfill, mechanical degradation of the material is of another important concern. Under extreme cases, stress can introduce chain scission in the PVC main-chain backbone, which results in failure of the material. Most of the mechanical stresses encountered in a landfill are multi-axial. Tensile stress can be mobilized within the various bottom liner components as a result of differential settlement due to the vertical weight from waste, leachate and climatological factors such as rain, snow and ambient temperature, or additional vertical landfill expansion (Stulgis, et al., 1996). Overburden pressures up to $0.68MPa$ can be expected depending on the depth of the fill and cover system (Haxo and Haxo, 1989). On the other hand, the geosynthetic in the cover system can be subjected to gas pressure generated through the decomposition of the organic content inside the waste layer. Figure 1.2 shows

an extreme case where a geosynthetic membrane is subjected to a localized inflation by excessive pressure. The application of a large external stress on a PVC geosynthetic will result in a decrease in its useful lifetime, primarily via a physical process called *creep*. Hamza and Abdel-Hamid (1998) studied the tensile creep behaviour of a PVC material under an external load of $9MPa$ at an elevated temperature of $90^{\circ}C$. A significant decrease in creep rate was obtained for the first period of $40\,days$, with a steady-state creep rate afterwards that showed a dependence on the magnitude of the mechanical stress and the type of stabilizer used. During the design process, the problem of excessive deformation of the PVC geosynthetic as a result of prolonged mechanical loading is usually examined along with the attention to the deformability of the other barrier components such as geotextile, geonet, clay liner and soil base (Koerner, 1994). It should also be noted that other degradation mechanisms may be enhanced under stress (Bishop et al., 2000). Similarly, the reduction in the lifetime of the serviceability of the linear associated with the mechanical effects can also be enhanced by other environmental effects. Hsuan (1998) indicated that the creep lifetime of the geosynthetic could be exponentially reduced when the temperature is elevated; a reduction of temperature from $80^{\circ}C$ to $50^{\circ}C$ leads to an order of magnitude increase in the service life.

A landfill geosynthetic is frequently in contact with the soil containing various living organisms such as bacteria and fungi. Bacteria, fungi and protozoa are also commonly found in the wastes and sludge, with 10^{8} to 10^{9} biological cells per cm^{3} of leachate (Rios and Gealt, 1989). The resistance of the geosynthetic to biological activities, such as fungi, bacteria and animals, needs to be assessed. Elevated temperatures in the landfill can enhance the biological activity. Newman et al. (2001) reported the results of an observation of an exhumed $0.5mm$-thick PVC geosynthetic membrane after service in an aquaculture pond that had been colonized naturally with flora and fauna for 29 *years*. Over time, the pond became congested with dense and persistent strands of cattails and other vegetation. No holes, however, were found in the specimen indicating its superior capacity to resist microorganism attacks. All cattails in the soil layer grew down to the geosynthetic and then extended horizontally along the top surface of geosynthetic; no evidence of roots penetrating the $0.5mm$-thick geosynthetic was found. Surprisingly, this

thin geosynthetic membrane also resisted penetration by roots of a $1.5m$ -tall willow sapling. This is a case of successful application of a PVC geosynthetic. Other research, however, indicates that biological activities can induce the extraction of the plasticizer. The plasticizer can also be a food source for certain bacteria. The issue of the activity of the plasticizer inside a geosynthetic during the biological degradation will be discussed in the next section, *loss of plasticizer*.

Radioactive degradation is most severe in terms of a polymeric chain scission to the PVC molecular backbone which only occurs in situations with a radioactive dosage higher than 10^6 to 10^7 *rads* (Koerner et al., 1996). The containment sites for high-level radioactive wastes generally do not use geosynthetics. The problem of radioactive degradation of PVC geosynthetics occurs when dealing with low-level radioactive waste, such as in uranium mill tailings. The application of the geosynthetic in a low-level radiation containment endeavour dates back to the 1980s (Giroud, 1985; Kane and Widmayer, 1989). The data regarding the durability of PVC geosynthetics in such environments are scarce.

During its service life, a PVC geosynthetic usually experiences several types of environmental effects at the same time. Different environmental mechanisms may have synergistic effects that could accelerate the overall rate of degradation of a PVC geosynthetic. In general, most types of degradation processes can be enhanced at elevated temperatures, where potential thermal degradation can also be of concern. Similarly, degradation can be also accelerated under stress. Stress not only breaks the PVC molecular backbone, it can also lead to an increase in the size of the free volume inside the PVC matrix, further increasing its permeability to moisture and other chemical contaminants. While the subject of the durability of a PVC geosynthetic under a single type of degradation is not completely clear, the synergistic effect is even less well studied. Limited studies on the other types of geosynthetic are available. Maisonneuve et al. (1997) reported an accelerated reduction in the yield strength of a HDPE geosynthetic with a 5% pre-strain during its 8-*month* immersion in a synthetic leachate; their results, however, showed an increase in the yield strain of the geosynthetic after chemical exposure. Barrett (1998) and Barrett et al. (1998) studied the synergistic effects of a

HDPE geosynthetic using the so-called "comprehensive test system" developed at the University of South Florida, Tampa, FL, which was designed for simultaneous application of mechanical loads, chemical exposure and other environmental factors such as temperature variations. The mechanical pressure was applied by a piston through a layer of granular media and additional hydrostatic pressure could be applied from an elevation of water or chemical solvent. The geosynthetic could then be exposed to chemicals at the same time with the intention of simulating the environment in its field conditions. The specimen subjected to vertical pressure and chemical exposure simultaneously, revealed a lower modulus than those exposed to inorganic chemicals.

Due to the complex nature of the landfill conditions, empirical methods have been proposed to predict the lifetime of a geosynthetic (Koerner et al., 1992; Sangam, 2001). The method proposed by Koerner et al. (1992), called *Arrhenius modelling*, considers the accelerated geosynthetic activities at high temperatures (e.g. $50^{\circ}C \sim 70^{\circ}C$) and predicts the material activity at lower temperatures close to the landfill environment. Hsuan and Koerner (1998), by studying the oxidative degradation of the HDPE geosynthetic at elevated temperatures, proposed three characteristic stages of chemical degradation of HDPE geosynthetics. This study concludes that the degradation commences with a loss of the protective additive such as an anti-oxidant. When the protective additive depletes to a certain limit, the degradation process starts; this accounts for the second stage as an induction time. Finally, when all the protective additives are depleted, the degradation accelerates, which is the third stage. Following this approach, Sangam (2001) predicted the lifetime of a HDPE geosynthetic in landfill service at around 200 *years*. As discussed previously, the issue of oxidation is of a less concern to examine reliability of a PVC geosynthetic. Other additives, such as plasticizers, were mainly used for production of the PVC geosynthetic, which is favoured for its modification of an otherwise brittle material. Unlike the process of oxidation, the loss of plasticizer does not significantly alter the chemical structure of a typical PVC material and therefore does not initiate the breakage of the PVC molecular backbone. The loss of the plasticizer can possibly be a governing process in determining the long-term chemical compatibility of a PVC geosynthetic. The

topic of plasticizer loss from a PVC geosynthetic is discussed in more detail in ensuing section.

1.6.3 Loss of plasticizer

Since PVC itself is resistant to attack by most chemicals, it is the stability of plasticizer that determines the longevity of the PVC material (Kamykowski, 1994), and loss of plasticizers is believed to the dominant process in the aging of the plasticized PVC (Jakubowicz et al., 1999). The control of the loss of the plasticizer is possible by special treatment of the PVC specimen surface (Jayakrishnan and Lakshmi, 1998). Gumargalieva et al. (1996) reported a service performance of a PVC material as a wire insulation under darkened conditions for 29 years where temperature during service ranged between $-20^{\circ}C$ and $28^{\circ}C$. In their study, the PVC material exhibited a loss in content of DOP from 35% to 15% along with a reduction in critical elongation from 600% to 300% and a five-fold increase in pore volume from $0.017cm^3/g$ to $0.065cm^3/g$.

The plasticizer loss can take the form of either extraction by contacting media, migration or volatilization (Buszard, 1984; Kovacic and Mrklic, 2002). The *extraction*, in which additives are introduced into the surrounding media, depends on the plasticizer type, its concentration and compatibility with the PVC resin. It is also influenced by the temperature, sheet thickness, environmental conditions, and exposure time. The extraction of additives takes place in a diffusive form (Gumargalieva et al., 1996). Therefore, the loss of plasticizer is highly dependent on the thickness of the PVC material. The diffusion coefficient of dialkylphthalate inside the PVC resin under normal conditions was obtained by Gumargalierva et al. (1999) as $8.2\times10^{-16}m^2/sec$, which is generally four orders smaller than that of an organic chemical inside a PVC material. The *penetration* occurs when additives in direct contact with the surface of another polymer material penetrates into that material. The penetration of the plasticizers is related to its molecular weight, its compatibility with resin and the contacting surface, and the temperature. *Evaporation* occurs when additives are lost into the surrounding gaseous media. Gumargalieva et al. (1996) and Kovacic and Mrklic (2002) found that the evaporation process was the dominant process for various plasticizer losses at

temperatures over $120^{\circ}C$. Jakubowicz et al. (1999) also found that the loss of plasticizer was controlled by evaporation at a temperature range of $80^{\circ}C - 110^{\circ}C$; the evaporation process was a function of plasticizer type, initial plasticizer concentration and temperature. Table 1.5 presents the weight losses through the evaporation process after $24h$ at $85^{\circ}C$ for various types of plasticizers (Matthews, 1996). The initial concentration is determined as the quantity of each plasticizer required to produce a tensile modulus of $7.58MPa$ at 100% tensile strain at $23^{\circ}C$.

Table 1.5 Evaporation losses of various plasticizers after $24h$ at $85^{\circ}C$

Plasticizer	Initial concentration (*phr*)	Weight loss (% plasticizer)
Dibutyl Phthalate	54	21.6
Di-iso-octyl phthalate	64	1.07
Ditridecyl phthalate	74.5	0.74
Di-iso-octyl azelate	56.3	1.02
Dibutyl sebacate	45	10.1
Trixylyl phosphate	75	0.61
Epoxidised soya bean oil	66.5	0.53

The loss of plasticizers in a chemically incompatible liquid media at *low temperature* is presented as an extraction process. Table 1.6 indicates changes in weight percentage of certain plasticizers extracted by a number of liquids (Frissell, 1956). The initial concentration of plasticizer is chosen as the quantity of each plasticizer required to produce a tensile modulus of $7.7MPa$ at a 100% tensile strain at $23^{\circ}C$. Among all the chemicals used, a solution of detergent and toluene is frequently encountered in a MSW landfill (USEPA, 1988). Other solutions can possibly be encountered in a leachate from lagoons, hazard waste sites or industrial waste landfill. The loss of plasticizer was also found to occur in the presence of an alkali solution (Shin et al., 2002). The full amount of plasticizer could be extracted within *days* at the presence of an alkali solution such as $NaOH$ at the temperature range from $80^{\circ}C$ to $120^{\circ}C$, without the occurrence of dehydrochlorination. The extraction of the plasticizer by simulated leachate was reported by Haxo et al. (1985b) during an immersion period which lasted 56 *months*. Duquennoi et al. (1995) also studied laboratory aging of a $1.2mm$-thick PVC material plasticized

with DOP and exposed to landfill leachate collected from a municipal waste landfill at the anaerobic fermentation stage (therefore with an alkali characteristic). The immersion test conducted at $20^{\circ}C$ resulted in up to 20% loss of plasticizer in a region at most within the $25 \times 10^{-6} m$ below the surface of the geosynthetic.

Table 1.6 Extraction of plasticizers (in percentage) by various solvents at $23^{\circ}C$ (after Frissell, 1956)

Extract	Water	1% Soap	1% Detergent	Mineral oil	Iso-octane	Di-iso-butylene	70% iso-octane + 30% toluene
Time of immersion (h)	240	240	240	240	240	240	240
Dibutyl Phthalate	0.5	1	0.9	1.05	1.85	2.1	14.5
Di-iso-octyl phthalate	0.05	0.4	0.5	1.3	20.2	23.4	16.4
Ditridecyl phthalate	0.2	0.05	0.6	20	33	33.8	32.6
Di-iso-octyl azelate	0.15	0.05	0.8	13	26.3	27	19
Dibutyl sebacate	0.2	0.65	0.85	8.95	5.2	7	15.3
Trixylyl phosphate	0.1	0.3	0.25	0.25	0.7	1.7	18.9
Epoxydised soya bean oil	0.1	0.35	0.75	0.7	1.3	3	12.1

As seen from Table 1.6, loss of plasticizer also occurs when a PVC material comes into contact with pure water (see also Duquennoi et al., 1995; Gumargalieva et al., 1996). Djidjelli et al. (2003) studied the effects of boiling water on PVC materials plasticized with DOP and dinonyl adipate up to 9 *hours*. It was observed that the PVC material plasticized with DOP retained its plasticizer content after such operation, while the PVC material plasticized with dinonyl adipate showed a small amount of plasticizer loss. In their studies, mechanical properties altered after interaction with water at elevated temperature near boiling point; the alterations included reductions in both failure stress and failure strain for two both types of PVC materials. Extraction of the plasticizer is accelerated by moving liquids. Studies by the U.S. Bureau of Reclamation on a $0.25mm$-thick PVC geosynthetic used in canal linings showed up to 41% loss of plasticizer after 19 years of service (PVC Geomembrane Institute, 1998); due to the loss of plasticizer, there is alteration in the physical properties of the PVC geosynthetic including a loss in total weight, a slight reduction in sheet thickness, an increase in elastic modulus, an increase in tensile strength and a reduction in ultimate strain. Giroud (1985) performed chemical and mechanical tests on samples of PVC geosynthetic that were used to line

ponds containing acids, up to 45 *months*. A progressive loss of plasticizer and reduction of failure strain was observed. In the tests by Giroud (1985), the loss of plasticizer reached 50% after 50 *months* and the specimen that suffered the greatest plasticizer loss showed a more than 90% reduction in the failure strain. In a bioreactor landfill, the leachate is kept circulated. The problem of the extraction of a plasticizer by a moving liquid is therefore of a concern.

Besides evaporation at high temperature and extraction by chemicals, Decoste (1968) pointed out two other mechanisms for the loss of plasticizer: (a) gases such as oxygen could oxidize the hydrocarbon structures of plasticizers and (b) microorganisms could utilize the carbon from plasticizers as a food in their life cycle. PVC resin, itself, is resistant to the destruction by biological agents, but additives used in formulations, especially the plasticizers, can be susceptible to deterioration by microorganisms, fungi and bacteria. For many geotechnical applications without harsh chemical contact, biodegradation is the primary cause of plasticizer loss and consequently the primary mode of PVC degradation (Decoste, 1968). Gumargalieva et al. (1999) noted that, in the presence of a microscopic fungus, Aspergillus Niger, the migration properties of the dialkylphthalate plasticizer inside the PVC resin increases almost one order of magnitude than under normal conditions. Plasticizers vary by type in their susceptibility to microbial attack. No plasticizer, however, including the *phthalate* plasticizer that is frequently used for PVC geosynthetic, has been shown to be immune to biodegradation (Buszard, 1984). A ranking of susceptibility to fungal attack of several plasticizers was given by Bessems (1988), with phthalate being the most resistant to attack. Among the phthalate plasticizers tested, di-i-nonylphthatlate (DINP) was the most resistant to attack, followed by dihexyl phthalate (DHP), DIOP, DOP and DBP. Decoste (1968) studied soil burial resistance of 21 formulations of PVC material and found that the change in mechanical properties mainly rests with the type of plasticizer. Osman et al. (1972) stated that microbial growth could only occur on samples where organic nutrients, water and sufficient oxygen were present. They also concluded that the rate of biodegradation of PVC formulations depended primarily on the diffusive rate of the plasticizer.

Loss of plasticizer also occurs during weathering. Gumargalieva et al. (1996) pointed out that, while the leaching of the plasticizer acted as the dominant aging process in a darkened and low-temperature environment, in presence of the sunlight, additional photo-degradation and thermal-degradation would occur resulting in dehydrochlorination of the PVC polymer and possible corresponding chemical conversion in the plasticizer. Fayoux (1990) gave an estimate of about 2% plasticizer loss in a PVC geosynthetic after 8 *years* of a single-side exposure to the effects of rainfall and temperature variations during weathering at a site at Marseille, France.

The loss of plasticizer is gaining attention in the design of PVC geosynthetics (Kamykowski, 1994; PVC Geomembrane Institute, 1998). However, the loss of plasticizer and its associated relationship with the alteration in the performance of a PVC geosynthetic is seldom quantitatively characterized. Major decisions are based on empirical or intuitive rules that attempt to either control or limit the loss of plasticizer under certain laboratory conditions. As a part of quality control certification processes, volatility of the plasticizer is evaluated using the testing standards ASTM D1203 and extraction of plasticizer by water is evaluated using ASTM D3083. The test procedure for ASTM D1203 exposes the samples to activated carbon at a temperature of $70^{\circ}C$ for 24 *hours* . In the water extraction test ASTM D3083, the geosynthetic sample is immersed in water for 24 *hours* at a temperature of $50^{\circ}C \pm 2^{\circ}C$. It is expected that these specified requirements assure a low rate of plasticizer loss during the application of a PVC geosynthetic in an aqueous environment, such as in frequent contact with the landfill leachate.

1.7 Implications to the current research

As a summary, PVC polymer is generally a chemically-inert material. It is the activity of the the plasticizer that plays the most important role in determing the serviceability of the PVC geosynthetics under harsh environmental conditions. The loss of plasticizer, as evidenced in various types of degradation process, manifests itself as a dominate phenomenon during the degradation of PVC material. The study on the corresponding alterations in the mechanical behaviour of the PVC material as a result of loss of

plasticizer will be then essential to the knowledge of the subject of durability of the PVC geosynthetic membranes under practical landfill conditions. In this thesis, the phenomenon of the loss of plasticizer of the PVC geosynthetic membranes is studied when exposed to liquid chemicals such as ethanol. By considering the fact that landfill leachate only contains a limited concentration of various chemicals, this thesis studies a spetrum of the concentration of ethanol, ranging from 0%, 50%, 80% to 100%. The field performance of the PVC geosynthetic membranes when exposed to a low concentration of ethanol at 2~3% encountered in landfill (USEPA, 1988) can therefore be extrapolated.

CHAPTER 2
UNIAXIAL BEHAVIOUR OF A CHEMICALLY-TREATED PVC GEOSYNTHETIC

2.1 Introduction

In this chapter, the chemically-induced alteration in the mechanical behaviour of a PVC geosynthetic susceptible to concentrations of ethanol exposure will be examined through uniaxial testing. While the range and complexity of the contaminants in a waste disposal endeavour can be varied, this research is directed to the examination of the performance of PVC geosynthetics exposed to a commonly encountered chemical such as ethanol. Volumetric concentrations of 100%, 80%, 50% and 0% ethanol were used in a water-ethanol mixtures. The focus of the experimental investigations was to assess the effects of exposure to ethanol at various concentrations on the loss of flexibility of the PVC geosynthetic and to correlate such findings with the change in the chemical composition of the PVC geosynthetic.

2.2 Experimental Investigations

2.2.1 Materials and sample preparations

The PVC material tested is a geomembrane with a trade name Solmax 220, manufactured by Canadian General Tower, Inc., ON, Canada and supplied from Groupe Solmax Inc., QC, Canada. The geosynthetic membrane has a thickness of 0.5*mm* and contains PVC resin as a major component (50-70% weight content) along with several types of additives, such as plasticizer, lubricant, pigment and fillers to alter the mechanical behaviour of an otherwise typically brittle PVC polymer (Diebel, 2002). The plasticizer comprises the major part of the additives, amounting for between 25-35% of the total weight. To prepare the PVC geosynthetic material for chemical exposure, specimens

measuring $200mm \times 180mm$ were cut from a large sheet of the supplied material (Figure 2.1).

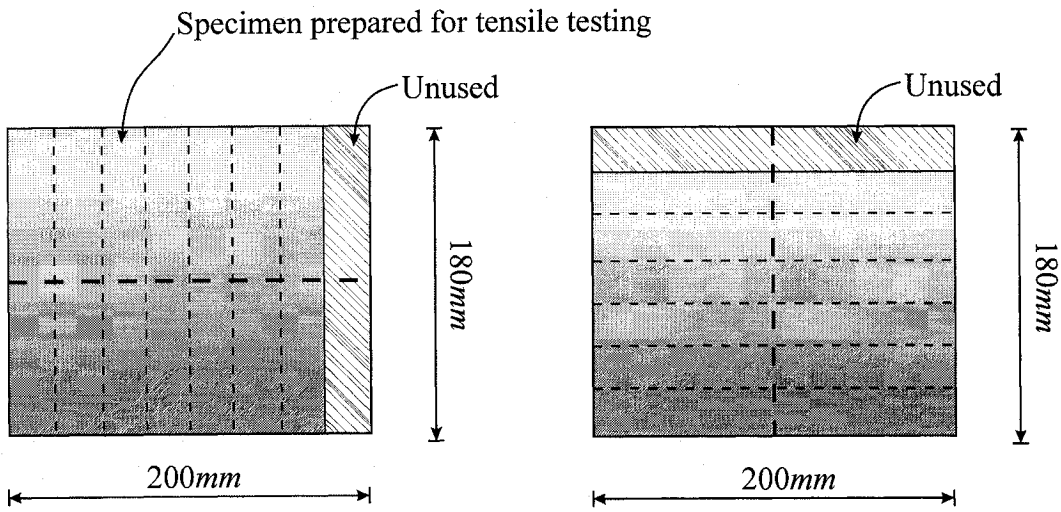

(a) Cut across the machine direction (b) Cut along the machine direction

Figure 2.1 Specimen prepared for the immersion test

PVC sheets are manufactured through calendering techniques (Penn et al., 1971; Koerner, 1994; Diebel, 2002). A characteristic feature of a calendering process is the elimination or reduction in the development of anisotropy in the deformability and strength characteristics (Alfrey et al., 1949a). The development of anisotropy can be minimized through heat treatment and curing processes, which induces thermal relaxation. To determine the possible influences of calendering on the mechanical behaviour, uniaxial tests were also performed on PVC samples (in their as-supplied condition), the axes of which were oriented normal to the calendering direction. Test specimens were prepared both along the machine direction and across the machine direction.

2.2.2 Chemical exposure facility

In the experimental program, the samples of the geosynthetic membrane were subjected to concentrations of ethanol exposure through immersion (Figure 2.2). The samples of the geosynthetic membrane measuring $200mm \times 180mm$, separated by layers of a highly permeable and chemically inert polypropylene (PP) geotextile, were placed in a stainless

steel container. The stack of geosynthetic samples were then covered with the appropriate concentration of ethanol. The stainless container was closed using a stainless steel cover. To reduce the possible loss of ethanol through evaporation, a thin strip of silicon glue was used between the cover and the container. When a stack of geosynthetic samples that were separated by geotextile layers was immersed in a water-ethanol mixture, the geotextile layer with high permeability allowed the liquid to come into *direct* contact with both faces of the PVC geosynthetic membrane.

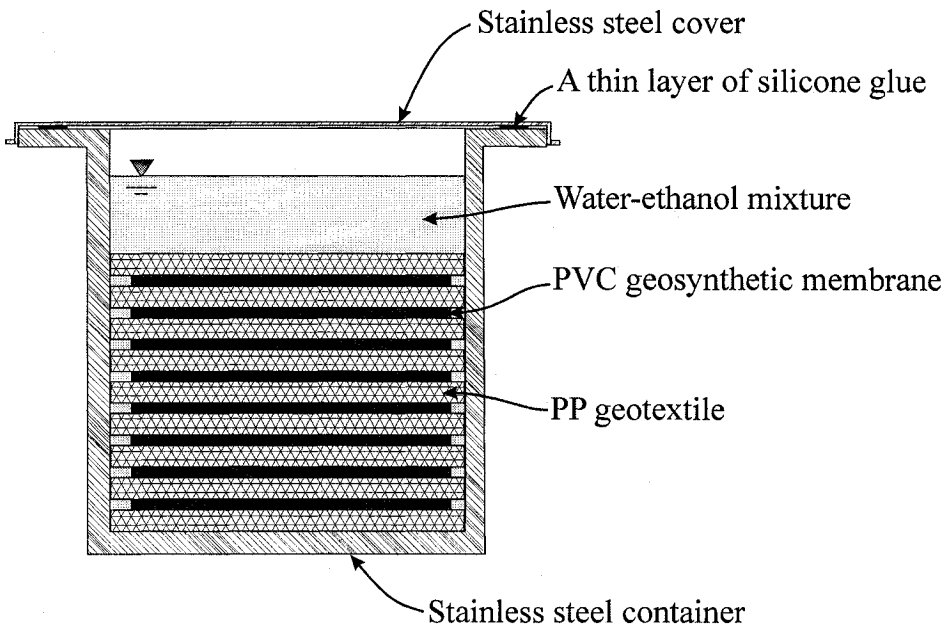

Figure 2.2 Immersion test for PVC geosynthetic membranes subjected to chemical exposure

In view of the highly volatile nature of the ethanol, the entire exposure facility was stored in a ventilated chamber that was maintained at a room temperature between $20^{\circ}C$ and $26^{\circ}C$. The condition of the exposure facility was kept undisturbed except in situations where the samples had to be removed manually, which induced some mixing of the water-ethanol mixture inside the container. There is likelihood that such disturbances can also alter the contact conditions between the water-ethanol mixture and the PVC geosynthetic during an immersion sequence; such effects are, however, not considered to be significant from the experimental point of view. It has also been noted that *direct*

contact between the solid polypropylene geotextile and PVC can also induce plasticizer penetration between the two types of polymer media (Marcilla et al., 2004). The quantitative analysis of such a migration processes is rare due to the absence of definition of the precise contact conditions between the two materials. In the current experiments, it was assumed that the contact area between the geosynthetic and the highly porous geotextile was small (with a contact area ratio corresponding to the *porosity of the geotextile*) and that entire surfaces of the geosynthetic were therefore subjected to exposure to the water-ethanol mixture, enabling free diffusion of the plasticizer from the PVC geosynthetic. Furthermore, the chemical interactions between the water-ethanol mixture and the polypropylene were not considered important to the examination of the interaction between the PVC geosynthetic and the ethanol.

The process governing the *extraction* of the plasticizer from a PVC geosynthetic subjected to ethanol exposure was considered to be diffusive. The process involves both ethanol migration into the PVC geosynthetic and migration of plasticizer from the geosynthetic (Kampouris et al., 1975; Frisch, 1978; Taverdet and Vergnaud, 1984; Papaspyrides and Duvis, 1989; Kondyli et al., 1990). Once a chemical comes into contact with the surface of a PVC geosynthetic membrane, the transport of the chemical to the interior of the material will take place through a concentration-gradient-dependent transport process. This process was identified by Fick (1855) and the equations governing chemical diffusion within the medium can be obtained through a consideration of mass transport (Carslaw and Jaeger, 1959; Crank, 1975; Selvadurai, 2000). In view of the large lateral dimensions of the chemical dosage area in comparison to the thickness of the PVC geosynthetic membrane, the chemical diffusion within it is modelled as a one-dimensional process (Figure 2.3). The one-dimensional diffusion of the chemical through the thickness of a membrane can be obtained from the solution of the governing partial differential equation

$$D\frac{\partial^2 C}{\partial z^2} = \frac{\partial C}{\partial t} \; ; \quad t \geq 0 ; \quad z \in [-H/2, H/2] \tag{2.1}$$

subject to the initial condition

$$C(z,0) = 0 \qquad ; \; z \in [-H/2, H/2] \tag{2.2}$$

and the boundary conditions

$$C(H/2,t) = C_0 \quad ; \quad C(-H/2,t) = C_0 \quad ; \quad t \geq 0 \tag{2.3}$$

respectively, where H is the thickness of the PVC geosynthetic membrane.

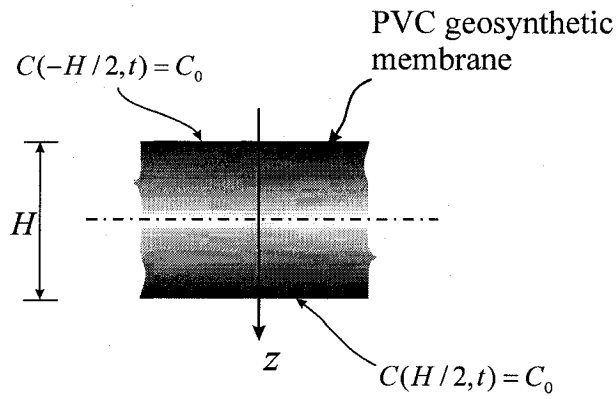

Figure 2.3 Boundary conditions during immersion

In (2.1), $C(z,t)$ is the through-thickness chemical concentration; z is the spatial coordinate, D is a diffusion coefficient and t is time. The linearized form of the diffusion equation (2.1) is a simplification of a much more complicated non-linear process where the diffusion coefficient can be altered as the chemical migration takes place. A further assumption is that the chemical influx is directly related to the loss of plasticizer from the geosynthetic. In practice, when a geosynthetic is used in a waste isolation endeavour, chemical migration to the membrane will take place only through one of its surfaces. In relation to the experimental research that will be conducted, however, it is assumed that the immersed membrane specimen will allow chemical migration to take place from both lateral surfaces as described by the boundary condition (2.3). The solution to the initial boundary value problem is elementary (Carslaw and Jaeger, 1959; Crank, 1975; Seferis et al., 2000; Selvadurai, 2000) and the through-thickness chemical concentration in the membrane is given by

$$\frac{C}{C_0} = 1 - \frac{4}{\pi}\sum_{n=0}^{\infty}\frac{(-1)^n}{(2n+1)}\exp[-(2n+1)^2\pi^2\frac{Dt}{H^2}]\cos[(2n+1)\pi\frac{z}{H}] \tag{2.4}$$

The objective of a diffusion analysis is mainly to ascertain the time required for chemical diffusion to take place over a significant portion of the $0.5mm$ -thick geosynthetic membrane. Theoretically, the elementary diffusion model requires an infinite time for the chemical to completely occupy the membrane. In contrast, only a finite time is required to saturate roughly 90% to 95% of the thickness of the membrane. For example, the time required to achieve 90% saturation of the chemical concentration at the central plane of the membrane is

$$t_{90\%} = \frac{H^2}{4D} \tag{2.5}$$

The critical parameter needed for the estimation of migration time is the diffusion coefficient D. Messadi and Vergnaud (1982) conducted tests to determine the diffusion coefficients for both pure ethanol and an 80% volumetric concentration of ethanol in an ethanol-water mixture. Their results indicated that a PVC membrane plasticized with 38% weight content of DOP plasticizer had a diffusion coefficient $D = 1.0\times10^{-8}cm^2\cdot sec^{-1}$ for pure ethanol at $30^{\circ}C$. Considering (2.4) and (2.5), the time required to saturate in excess of 90% of the central plane of a $0.5mm$-thick PVC membrane will be

$$t_{90\%} = \frac{H^2}{4D} = \frac{(0.05cm)^2}{4\times10^{-8}cm^2\cdot sec^{-1}} \approx 0.7\,days \tag{2.6}$$

Similarly, considering the value of the diffusion coefficient $D = 0.21\times10^{-8}cm^2\cdot sec^{-1}$ for 80% ethanol at $45^{\circ}C$, also given by Messadi and Vergnaud (1982), the time required to saturate more than 90% of the central plane of the $0.5mm$-thick PVC membrane will be

$$t_{90\%} = \frac{H^2}{4D} = \frac{(0.05cm)^2}{4\times0.21\times10^{-8}cm^2\cdot \sec^{-1}} \approx 3.4\,days \tag{2.7}$$

For immersion tests conducted at room temperature and on PVC specimens containing plasticizers other than DOP, the time taken for the ethanol to fully penetrate the specimen is considered to be slightly longer. In view of the results given above it is reasonable to assume that the effective migration will occur at most within 2 *weeks*. Such a short saturation time can allow for a reasonably complete distribution of the water-ethanol mixture within the PVC geosynthetic membrane and this distribution was observed to be almost uniform within a one-*month* immersion period (Contamin and Debeauvais, 1998). In the landfill application, the chemical exposure of the liner only involves one of its faces and a thicker liner ($\geq 1.5mm$) is usually adopted. Therefore a longer time of penetration of the liner by the chemicals is expected. To further retard the migration of chemicals through liner system, a double liner in a configuration shown in Figure 1.3 is generally adopted. Results of fast saturation of a PVC membrane by other organic liquids are also available in the literature; for example, in the experiments conducted by Messadi and Vergnaud (1982), a 3.5*mm*-thick PVC membrane is almost fully saturated by pure ethanol within 5 *days* of exposure at a temperature of $45^{\circ}C$. Liquids such as paraffin oil and white spirit can also fully migrate into a 0.5*mm*-thickness PVC membrane within about 20 *days* at a temperature of $37^{\circ}C$ (Papaspyrides, 1992). These experimental investigations enable the choice of the duration of immersion test for the purposes of achieving chemical exposure of the PVC geosynthetic. The criterion for the selection of the exposure period was basically to allow the alteration in the mechanical behaviour of the PVC geosynthetic. In view of the short duration required for saturation of the PVC samples by both pure and 80% ethanol, in the current experimental investigations, the exposure time was chosen as 1 *week*, 2 *weeks*, 1 *month*, 2 *months*, 7 *months*, and 9 *months*. In cases where there is a faster migration process, shorter exposure periods of 2 *hours* and 1 *day* were chosen. At each exposure stage, three exposed specimens measuring $200mm \times 180mm$ were prepared; these membranes provided adequate samples for mechanical testing. In cases where no significant alteration in the mechanical behaviour of the material was observed during testing, a further 12 PVC geosynthetic specimens were subjected to ethanol exposure to examine the change of mechanical behaviour with prolonged exposure. For ethanol concentrations less than 80%, the information concerning the diffusivity characteristics is not available in the literature; in

this case, a longer period of exposure was attempted. A stack of 12 membrane specimens was prepared for each ethanol concentration (at 50% and 0% respectively). The time interval between tests was decided based on observations concerning the alteration in the mechanical properties of the PVC geosynthetic specimen. For the purpose of comparison, tests were also conducted on samples exposed to air. In these tests, a stack of 12 alternate layers of geosynthetic and geotextiles were placed in a container and located in a sealed and darkened condition maintained at room temperature between $20^{\circ}C$ and $26^{\circ}C$. The samples were kept isolated except when the container was opened for removing samples for testing.

2.2.3 X-ray fluorescence analysis

The loss of the plasticizer content in the exposed membrane was identified through X-ray fluorescence techniques conducted at the Geochemical Laboratories, Department of Earth and Planetary Sciences, McGill University. The sample of the PVC geosynthetic membrane used for this purpose had a circular shape with a radius of 20*mm*. The weight ratio of the oxygen element to the chlorine element in the PVC geosynthetic, defined by $R_{O/Cl}$ (with a resolution and an accuracy of 1%), can be used as an indicator to access the plasticizer content at any stage of exposure of the PVC geosynthetic to ethanol (see Figure 2.4 for the chemical formulation of a phthalate plasticizer). Table 2.1 shows the value of $R_{O/Cl}$ determined at different stages of exposure to pure ethanol. The continuous decrease in this ratio is indicative of the superficial loss of plasticizer in the PVC geosynthetic. The exposure resulted in an appreciable loss of plasticizer during the first 2 *months*. The results of the X-ray fluorescence tests, however, indicate that the rate of extraction was significantly reduced after a 2-*month* exposure. The evidence of loss of plasticizer from a PVC material exposed to low concentrations of ethanol was also observed in other studies (Kawamura et al., 2000; Tsumura et al., 2001; Kim et al., 2003). The X-ray fluorescence technique was also applied to examine the PVC geosynthetic after exposure to 50% ethanol and pure water after 16 *months* and 18 *months*, respectively. Both cases, however, reveal noticeable alterations in the $R_{O/Cl}$ value when compared with the corresponding values for the untreated PVC geosynthetic. The PVC

geosynthetic exposed to 50% ethanol shows a slightly lower value for $R_{O/Cl}$ indicating a faster leaching rate of plasticizer.

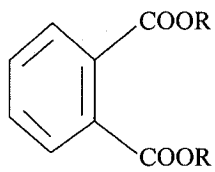

Figure 2.4 Chemical formulation of a phthalate plasticizer (after Wilson, 1995)

Table 2.1 The value of $R_{O/Cl}$ for PVC geosynthetics subjected to ethanol exposure

Specimen	$R_{O/Cl}$
PVC membrane as supplied	6.47%
18-*month* water exposure	5.55%
16-*month* 50% ethanol exposure	5.44%
2-*month* pure ethanol exposure	5.33%
5-*month* pure ethanol exposure	5.20%

2.2.4 Measurement of the mechanical properties

The alteration in the mechanical properties of the PVC geosynthetic subjected to various durations of exposure to ethanol was examined through conventional tensile testing. The testing facility consists of a servo-controlled MTS Machine with a load capacity of 44,000*N* (10,000*lbs*) of the provided load cell. The conventional grips for material testing available in the Material Testing Laboratory were considered to be inadequate for providing fixity at the ends of the specimen. Special grips were therefore fabricated for the current experimental research program. The details of the experimental setup are illustrated in Figure 2.5, which consists of upper and lower sets of grips. During testing, the lower set of grips was fixed and the upper one was moved by the MTS machine in a

displacement-controlled mode. The speed of the cross-head ranges between $0.2mm/sec \sim 80mm/sec$. The PVC membrane specimen was fixed between the two sets of grips and subjected to extension. The rigid connections between the grips and MTS Testing Machine were achieved through the provision of two adaptors. Holes are provided in the grips so that they can be effectively attached to the MTS Testing frame through the use of the special adaptors.

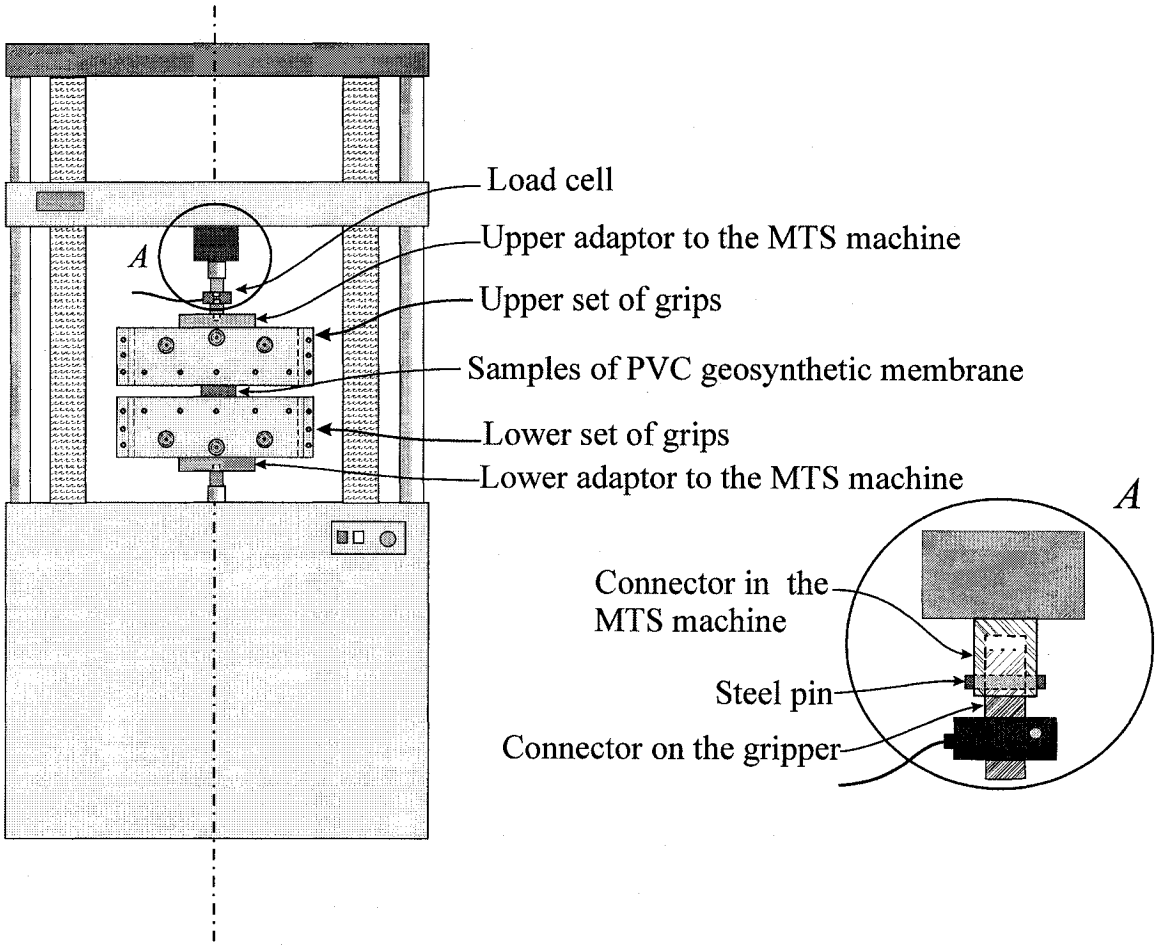

Figure 2.5 Tensile testing facility

The grips, originally designed for testing membrane strips of width $200mm$, were used to test strips of width $25.4mm$. In comparison to the peak load capacity of the MTS machine, the forces involved in the uniaxial testing of the PVC geosynthetic specimens were extremely small. Therefore a lower capacity load cell [$4400N$ ($1000lbs$)] was

incorporated within the upper adaptor. The steel grips were fabricated in such a way that the test specimen could be stretched without development of either an eccentricity or a tilt of the specimen. The details of the grips are shown in Figure 2.6 and Figure 2.7. The sides of the aluminum plates that came into contact with the geosynthetics were roughened to generate adequate frictional forces. The aluminum plates could freely slide on three steel rods within a steel box and 5 adjustable screws were used for alignment.

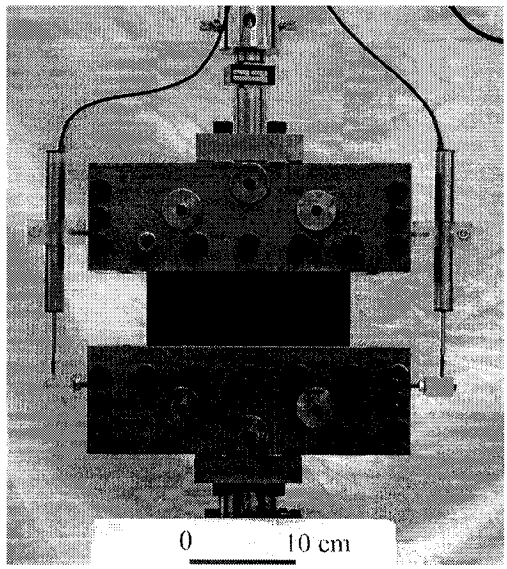

(a) Grip with a wide PVC geosynthetic specimen

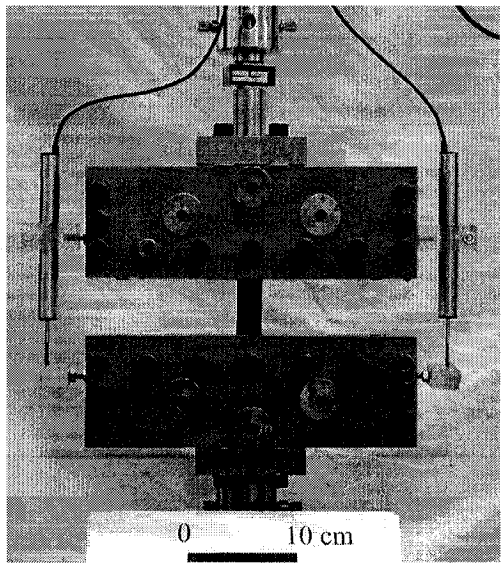

(b) Grip with a narrow PVC geosynthetic specimen

Figure 2.6 Testing a PVC geosynthetic specimen

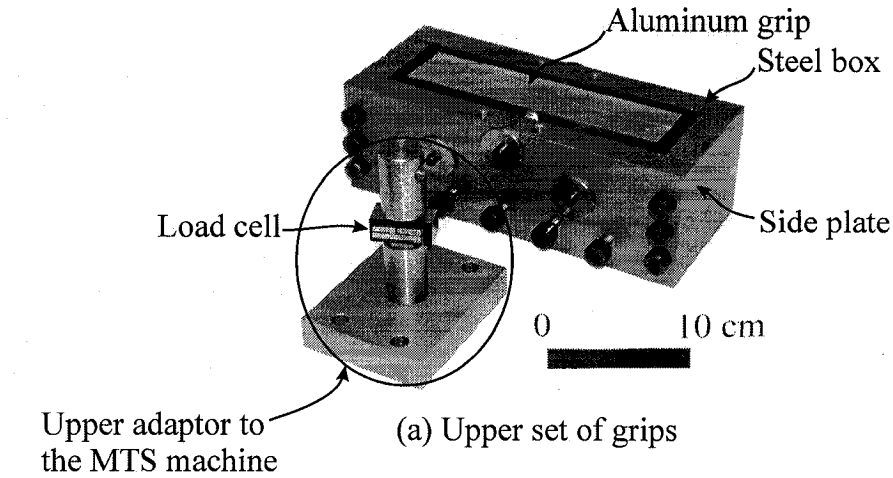

(a) Upper set of grips

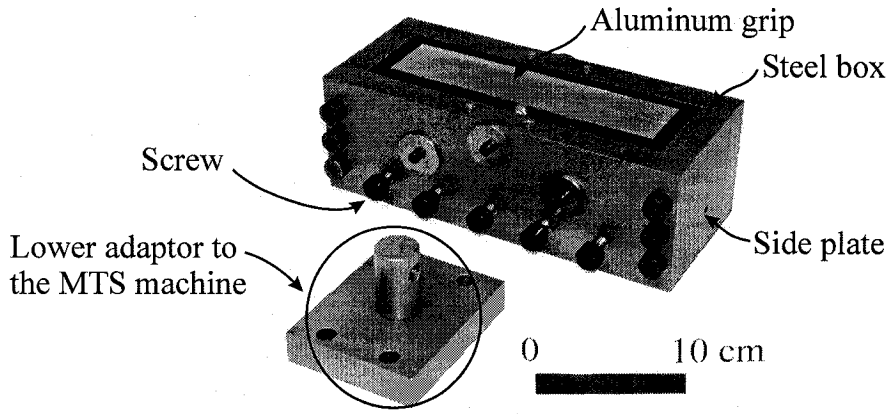

(b) Lower set of grips

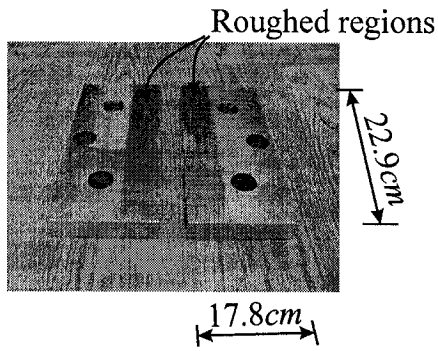

(c) A pair of aluminum grips

Figure 2.7 Design of the sets of grips

To further prevent slip between the specimen and the roughened sections of aluminum plates, an additional layer of the PVC material was bonded to each end of the test

specimen, using a non-reactive LOCTITE ® 404 instant adhesive (Figure 2.8), which increased the thickness of the ends of the PVC geosynthetic specimen. The ends were then tightly clamped between two faces of the aluminum grips. It was found that without the provision of this additional layer, there was insufficient frictional resistance between the surfaces of the membrane and the grips, which resulted in slippage. If the additional layer was not bonded to the PVC geosynthetic sample, the slippage was restricted to a limited extent at small strains but became appreciable at large strain, normally due to the progressive loss of friction between layers of membrane as the test sample contracted in the thickness direction. There is the possibility of chemical reactions between the adhesive and the PVC geosynthetic over long durations. The time-scale of such chemical reactions, however, is expected to be much greater than the duration of a test. Therefore, the influence of the reactivity of the adhesive was not considered in the examination of the experimental results. All test specimens used had an initial cross section area of $25.4mm \times 0.5mm$.

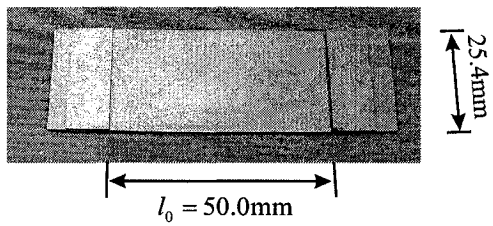

Figure 2.8 Specimen prepared for tensile testing

The experiments were conducted in a Material Testing Laboratory maintained at a room temperature of approximately $24^{\circ}C$. The duration of a tensile test was restricted to about one *hour*. The temperature variation in the laboratory during this period was less than $1^{\circ}C$. The maximum duration of the chemical exposure lasted up to 13 months. During this period, the temperature in the material storage area varied between $20^{\circ}C$ and $26^{\circ}C$. The influence of these temperature fluctuations on either the chemical reaction or on the mechanical properties of the PVC geosynthetic was not considered in this study. During a test, the displacement of the test specimen was initially measured using two LVDTs located on either side of the test specimen. Since the specimen was highly deformable in comparison to the rigid steel grips and the test frame, a machine stiffness correction to the

measured deformations was not considered necessary; the relative extension of the grips was found to be quite close to the average of the LVDT values when the displacement was smaller than $30mm$. At larger extensions, however, the accuracy of the LVDT was significantly reduced. For simplicity and for accuracy, the movement of the grips was therefore taken as the change in the current gauge length l. The initial gauge length was taken as the distance between two edges of the specimen ($l_0 = 50mm$) as indicated in Figure 2.8. The stress σ_0 was defined as the magnitude of applied load divided by the *initial* cross-sectional area of the PVC geosynthetic specimen. The strain was calculated as the percentage change of the *initial gauge length.* All tests were performed at a constant strain-rate $\dot{\varepsilon}_0$, which was defined as

$$\dot{\varepsilon}_0 = \frac{d}{dt}\left(\frac{l - l_0}{l_0}\right) \tag{2.8}$$

The ASTM Standard D4885-1988 for testing of geosynthetics advocates strain-rates in the range of $1\%/min \sim 100\%/min$. The experiments on the geosynthetic material were conducted at three strain-rates $4\%/min$, $40\%/min$ and $160\%/min$.

2.3 Experimental results

2.3.1 PVC geosynthetic as supplied

The results of the uniaxial tests conducted on intact PVC geosynthetics are shown in Figures 2.9-2.11. The untreated PVC geosynthetic undergoes significant large strains during a tensile test. The material exhibits failure at a strain in the range 150%-250%. By examining the continuous stress-strain curve shown in Figure 2.9, it is found that the material exhibited significant creep during the tests. Experiments were also conducted to identify the unloading behaviour of the untreated PVC geosynthetic. Unlike the typical behaviour of hyperelastic rubber-like materials without fillers, where unloading behaviour closely follows the loading curve, the untreated PVC geosynthetic exhibits significant irreversible deformation. Figures 2.9b-c show the responses of the untreated geosynthetic, which is loaded to different levels of maximum strain followed by an

unloading. It is observed that irreversible strain is present over a large range of the strains experienced by the sample. In order to examine the possibility of fully reversible behaviour similar to that of a typical rubber-like material, a test was also conducted at a lower strain-rate of $\dot{\varepsilon}_0 = 0.4\%/min$ and up to a peak strain level of 10%. The results are shown in Figure 2.9a. The existence of an irreversible strain is still noticeable; the amount of the irreversible component is, however, greatly reduced. This indicates the possibility of fully reversible behaviour of the untreated material in situations where the loading rate and maximum strain is considerably restricted. Further results obtained by extracting data from several selective points in a continuous stress-strain curve are shown in Figure 2.10a. The inset Figures shown in Figure 2.10a indicate that the grips, while providing no slippage at the ends, also restricted the lateral contraction at the gripped boundary during uniaxial stretching. This violates the condition necessary for straining the specimen to produce a homogeneous deformation, which is required for any theoretical treatments, particularly related to the development of constitutive relationships. To observe the extent to which the end constraints influence the development of homogeneous straining, a grid was marked on the surface of an undeformed specimen. The grid was made with a marker and had a spacing of $5mm$ between grid lines. As deformation occurred, the horizontal grid lines were used to calculate the real physical gauge lengths for different sections on the PVC geosynthetic specimen (Figure 2.10b). These distances were averaged over the width of the specimen. The deformed configurations of the specimen were recorded using a digital camera (5 Mega pixels). The distances were first measured in image *pixels* and then calibrated against the value of image *pixels* corresponding to a known physical distance. The known physical distance is chosen as the distance between two grips. The distance between two grips is easily obtained in a displacement-controlled experiment. The strains measured by considering different original gauge lengths are presented in Figure 2.10b. Tests results indicate that the effects of the fixity constraints results in an error of 6.8% in average strain range of $\varepsilon_0 = 44\%$ and an error of 2.4% at a larger strain in the range of $\varepsilon_0 = 162\%$. Tests were performed at three different strain-rates, $4\%/min$, $40\%/min$ and $160\%/min$.

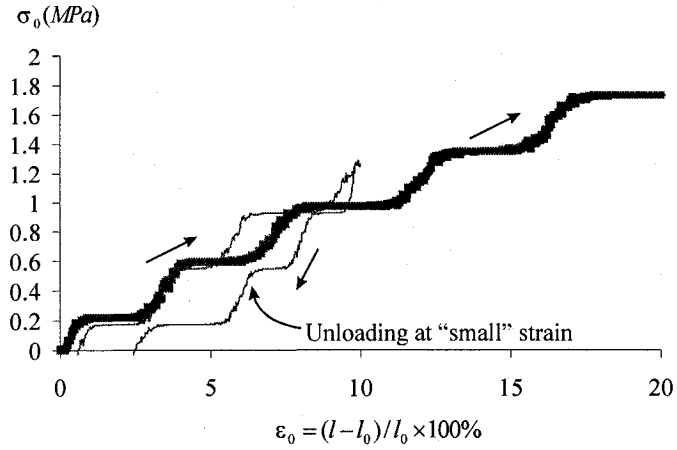

(a) $\dot{\varepsilon}_0 = 0.4\%/min$

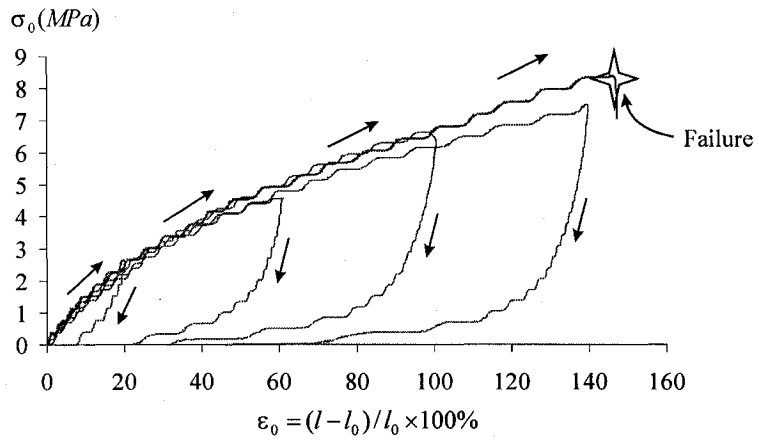

(b) $\dot{\varepsilon}_0 = 4\%/min$

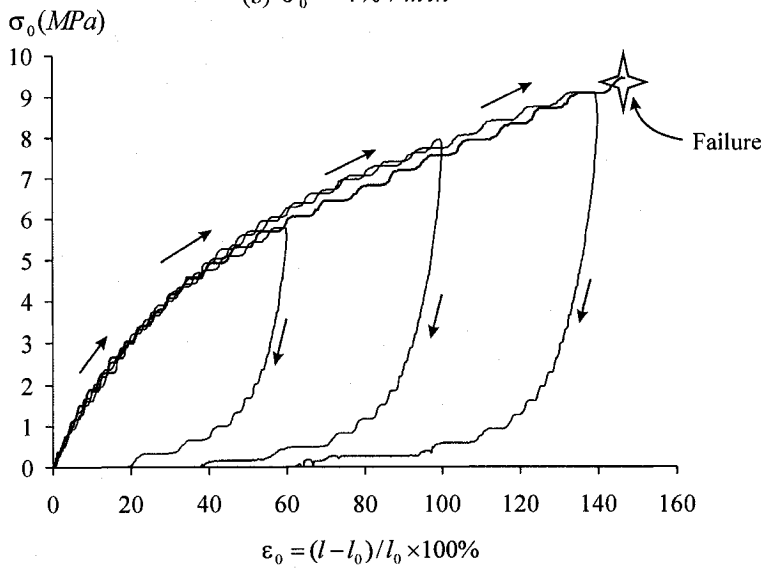

(c) $\dot{\varepsilon}_0 = 40\%/min$

Figure 2.9 Independent stress-strain curves stretched to different peak strains for PVC geosynthetics as supplied

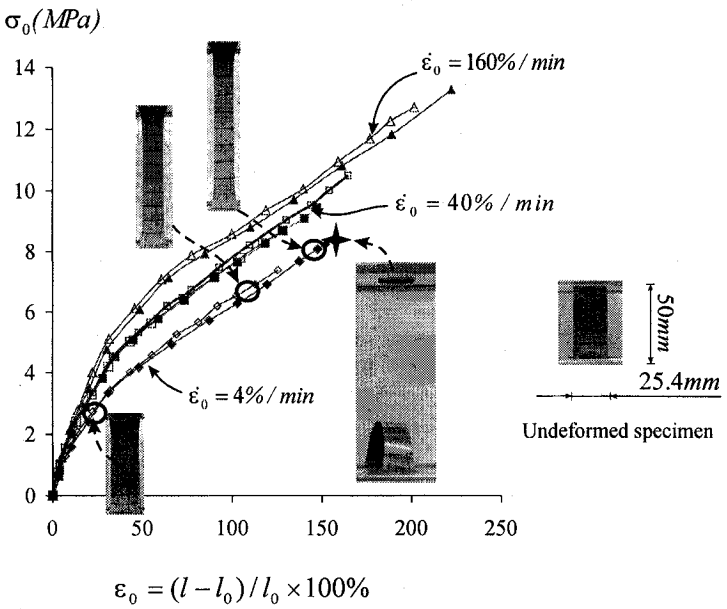

(a) Stress-strain curves

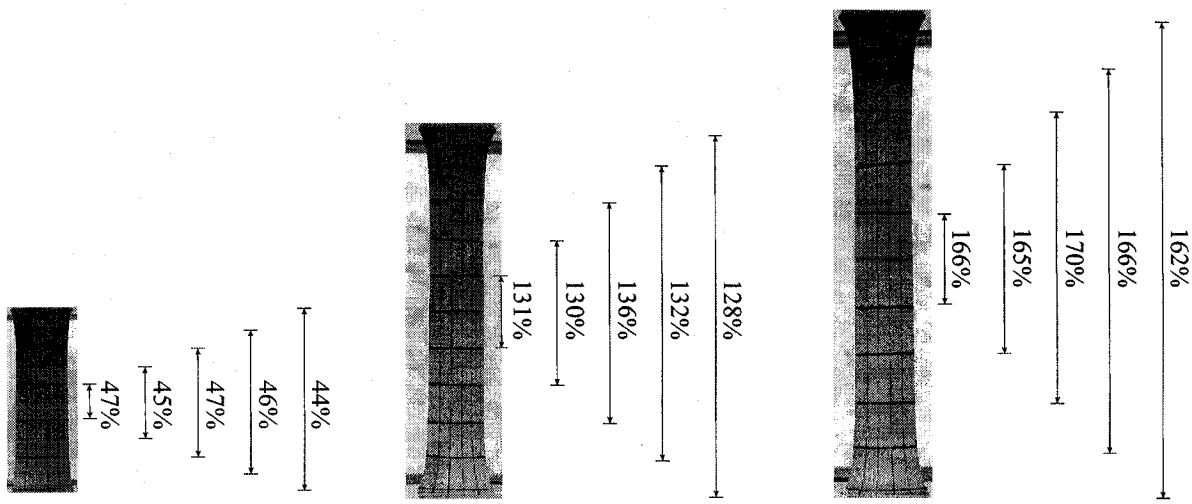

(b) Deformed shapes (with strain measured at different sections of the specimen)

Figure 2.10 Tensile behaviour of a PVC geosynthetic as supplied, with loading at different strain-rates

To establish the presence of any anisotropy in the deformability of the PVC geosynthetic, tests were conducted on samples derived, both along and perpendicular to the calendaring direction. Figure 2.11 shows the corresponding stress-strain curves derived from uniaxial tests conducted at three different strain-rates. There is some evidence of the influence of

manufacturing process on the stress-strain behaviour, but the influences, however, are considered not significant.

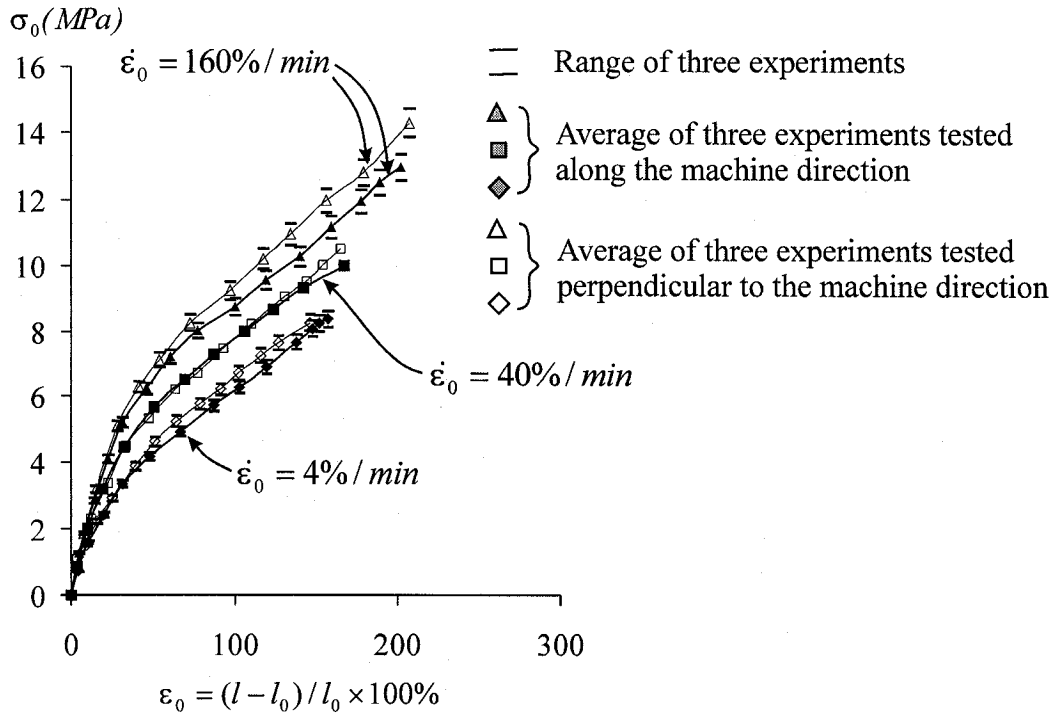

Figure 2.11 Tensile behaviour of untreated an PVC geosynthetic at different strain-rates in two orthogonal directions

2.3.2 Samples subjected to concentrations of ethanol exposure

Figure 2.12 illustrates the typical stress-strain curves for samples subjected to a 7-*month* period of exposure to pure ethanol. The experiments were conducted at a loading rate of $\dot{\varepsilon}_0 = 4\%/min$. During exposure to pure ethanol, the stress-strain behaviour has undergone a significant change. The PVC geosynthetic has developed a pronounced yield point and both strain-softening and strain-hardening regions can be observed. The experiments also show that the material can continue to sustain appreciable post-yield large strains without failure. When unloading is performed, it is evident that a significant amount of the irreversible strain is present when the stresses exceed the initial "yield point" or "yield strain" of the material. Unloading tests were also conducted up to maximum strains that did not exceed the yield strain. It is observed that within this small

strain range, the unloading behaviour closely follows the loading path. The sample exposed to pure ethanol basically exhibits an initial linear elastic response followed by a distinct yield point, a noticeable softening behaviour and a moderate post-yield hardening.

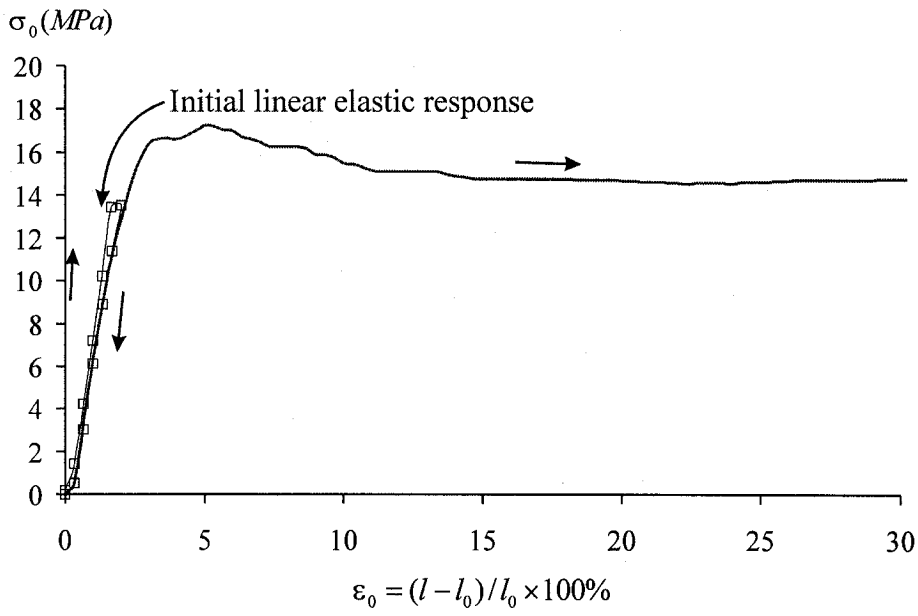

(a) Unloading prior to yield strain

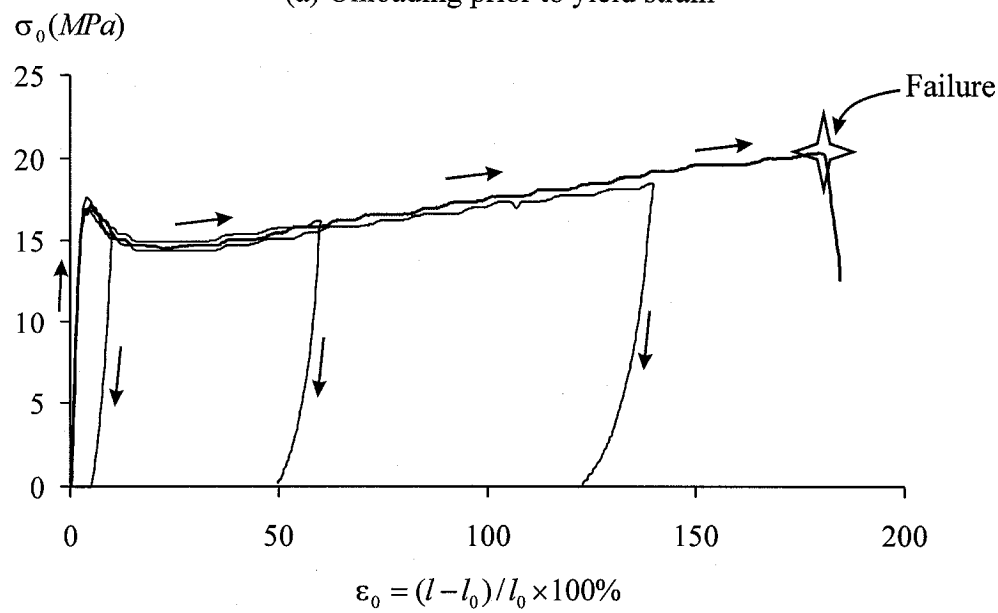

(b) Unloading at various strains that exceed yield strain

Figure 2.12 Independent stress-strain curves stretched to different peak strains for PVC geosynthetics subjected to 7-*month* exposure to pure ethanol ($\dot{\varepsilon}_0 = 4\%/min$)

In order to examine the rate-dependency of the stress-strain curves, experiments were also conducted at loading rates of $\dot{\varepsilon}_0 = 40\%/min$ and $\dot{\varepsilon}_0 = 160\%/min$. The influence of the loading rate on the stress-strain response is also noticeable (Figure 2.13).

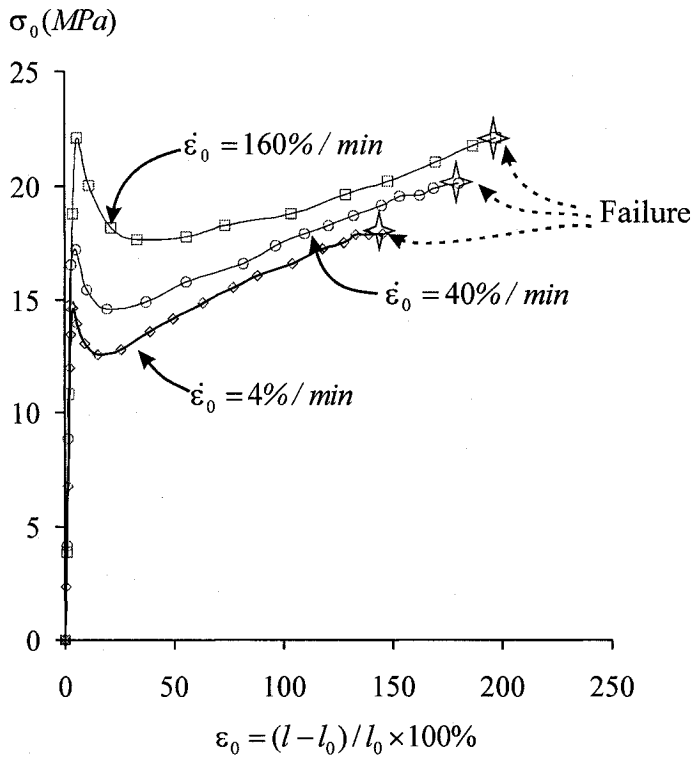

Figure 2.13 Rate dependency of the stress-strain curves of a PVC geosynthetic subjected to 7-*month* exposure to pure ethanol

Figure 2.14 shows the results of the tensile tests conducted on the PVC geosynthetic subjected to different periods of exposure to pure ethanol. These results are representative and indicate a significant continued alteration in the mechanical behaviour of the PVC geosynthetic. It is observed that the sample experiences continued alterations in its mechanical response. The influences of the ethanol exposure include loss of the hyperelastic characteristics (or *embrittlement*) and development of an initial linear modulus and a distinct yield point. The intact material exhibits monotonically increasing hyperelastic behaviour with path dependent partial recoverability of the strain; however, the samples subjected to pure ethanol showed the development of a distinct failure threshold with considerable irrecoverable deformations. The initial linear elastic modulus

and yield stress of the material exhibits a continuous increase up to an exposure period of 2 *months*, after which there is a slight decrease in the peak yield value, which is uninfluenced by further exposure. The rapid alterations in the mechanical behaviour of the PVC geosynthetic within the first two *months* correlate well with the results of an X-ray fluorescence analysis, which indicates a rapid loss of plasticizer during the 2-*month* period. The rate of alteration of the mechanical response of the PVC geosynthetic tends to stabilize after the first 2-*months* of ethanol exposure. This observation correlates with the reduction in the rate of loss of the plasticizer itself. The experimental results also point to the slight reduction in the initial elastic modulus and yield stress in the stress-strain response between the 2-*month* and 7-*month* exposure period. The reasons for the reduction in the initial linear elastic modulus and yield stress in stress-strain response from 2-*month* exposure to a 7-*month* exposure are not entirely clear. A likely reason could be the swelling-induced alteration in the mechanical response, as the PVC samples experience moisture absorption. While there is no conclusive observation of the reduction in the failure strains during the first 9-*month* exposure, the PVC geosynthetic subjected to 13-*months* of exposure to ethanol shows a significant loss of large strain deformability. The material breaks or fractures at a strain that just exceeds the yield strain without exhibiting any post-yield hardening. This possibly indicates a significant chemical alteration in the polymer molecular backbone in the last 4-*month* exposure period, which directly affects its integrity, and subsequently contributes to the failure of the material.

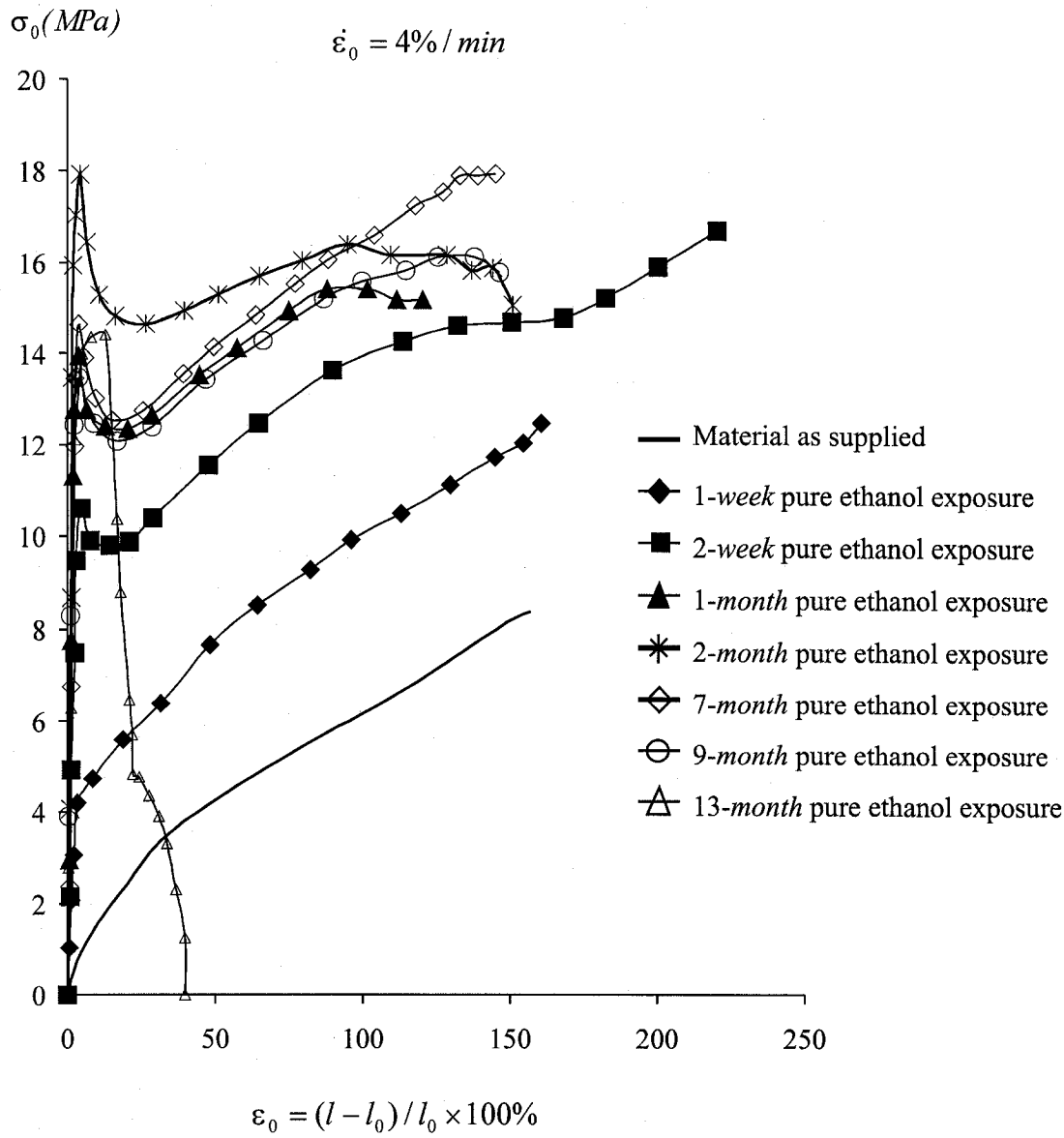

Figure 2.14 Tensile behaviours of a PVC geosynthetic subjected to different periods of pure ethanol exposure

The experiments also investigated the alteration in the mechanical properties of a PVC geosynthetic subjected to exposure at other volumetric concentrations of ethanol, namely 80% and 50% respectively. Lower concentrations of ethanol exposure produced less significant alterations to the PVC geosynthetics than that observed in cases involving exposure to pure ethanol. For this reason, the results of stress-strain data derived from samples subjected to 80% and 50% ethanol are presented for longer exposure times

(Figure 2.15a). The stress-strain curve for the PVC geosynthetic subjected to exposure to 80% concentration of ethanol indicates a slight "hardening" response after a first short exposure period of 17 *days*, which exhibits less deformation under the same external load. A slight increase in the failure strength is also observed in this case. Further exposure to 80% ethanol up to 7 *months* leads to slightly "softening" of the material, which can be possibly caused by the absorption of the moisture and ethanol. To illustrate the effects of their presence, the specimens exposed to 80% ethanol were further exposed to air for 5 *months*, which is considered sufficient to eliminate the content of moisture and ethanol inside the specimen due to their evaporation. The material significantly stiffens when the moisture and ethanol are depleted. The repeatability of the experiments was also examined (Figure 2.15b-g). The specimens that had been subjected to exposure to 80% ethanol were loaded to maximum strains of 60% and 100% respectively, which were then followed by an unloading (Figure 2.15c). The results indicate an experimental scatter of about 3%; this alteration in the stress-strain curves of the PVC geosynthetic after exposure to 80% ethanol is considered significant and not attributable to experimental scatter. The "hardening" response in the stress-strain curve is absent after exposure to 50% ethanol; instead the material became softer after 13-*month* exposure, which can be attributed to the swelling of the material. In comparison, experiments were also conducted on the PVC geosynthetic subjected to exposure to pure water and to air. The stress-strain curve of the PVC geosynthetic exposed to pure water after a period of 15 *months* follows closely the response of the material subjected to exposure to 50% ethanol, indicating a similar chemical and physical mechanism underlying the "softening" of the material. The results from the tests conducted on the PVC geosynthetic exposed to the ambient air after a period of 21 *months*, however, indicate no observable influence due to the exposure. The influence of the ambient air on the test results in other cases of exposure can therefore be disregarded. The results of their experimental research is summarized by Yu and Selvadurai (2005)

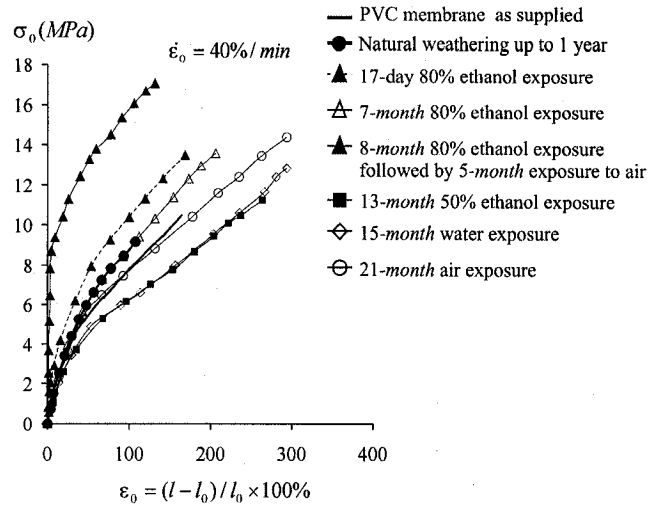

(a) Response of a PVC geosynthetic subjected to exposure to concentrations of ethanol and weathering

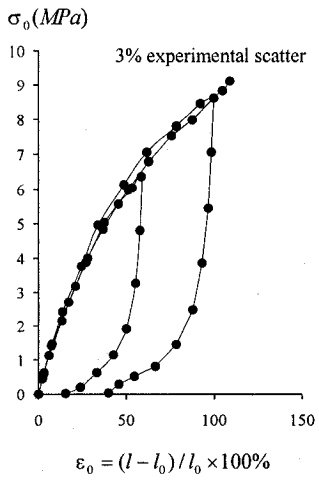

(b) Natural weathering

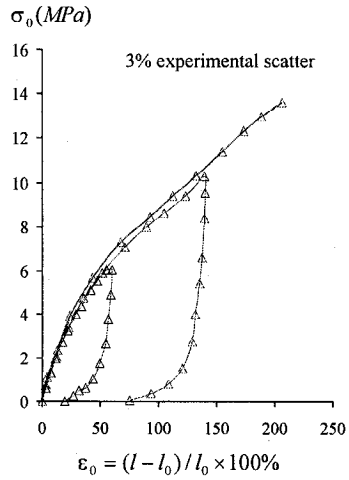

(c) Exposure to 80% ethanol for 7 *months*

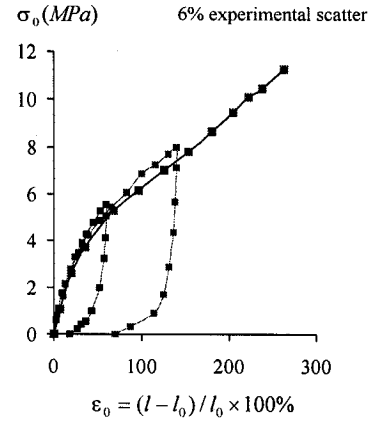

(d) Exposure to 50% ethanol

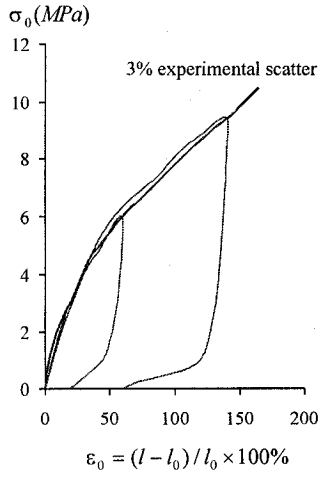

(e) PVC geosynthetic as supplied

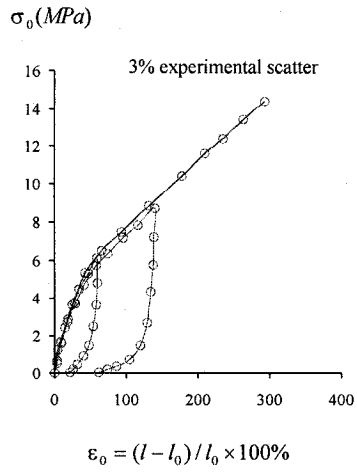

(f) Exposure to air

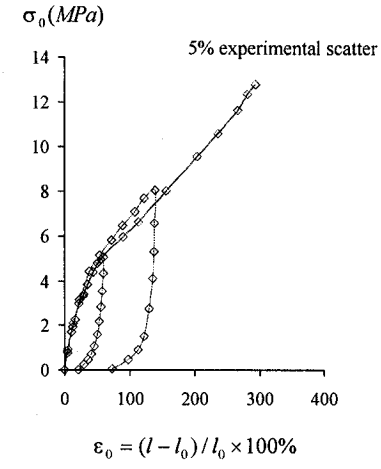

(g) Exposure to pure water

Figure 2.15 Tensile behaviour of a PVC geosynthetic subjected to concentrations of ethanol exposure

2.4 Summary remarks

The exposure of a PVC geosynthetic to an organic liquid chemical, such as pure ethanol, results in two synchronized processes: the first is a fast through-thickness diffusion of the liquid into the PVC geosynthetic and the second is a relatively slower loss of plasticizer in a diffusive manner. The experiments reported in this Chapter deal with the alteration in the mechanical behaviour of a 0.5*mm*-thick PVC geosynthetic membrane subjected to exposure to ethanol at different concentrations. The alteration in the mechanical properties of the PVC geosynthetic subjected to exposure to pure ethanol was a continuing process. The alterations included a progressive loss in the large strain hyperelastic deformability response, the development of embrittlement with an observable initial linear elastic modulus and a distinct yield point. Exposure to pure ethanol up to 13 *months* results in a complete loss in the large deformability of the PVC geosynthetic. The rapid alterations in the mechanical properties of the treated PVC geosynthetic in the first two *months* correlated well with the loss of plasticizer from the PVC geosynthetic, as inferred from the results of X-ray fluorescence. The rate of loss of plasticizer diminished after two *months*, with the resulting reduction in the rate of alteration in the mechanical properties. The exposure to other concentrations of ethanol produced less significant effects. After a 7-*month* period, the PVC geosynthetics exposed to 80% ethanol exhibited a slight "hardening" behaviour; after 13-*months*, however, the PVC geosynthetics subjected to exposure to 50% ethanol became softer. The PVC geosynthetics exposed to pure water for a 15-*month* period exhibited a similar mechanical behaviour as those exposed to 50% ethanol. Both causes of the "softening" behaviour could be attributed to the swelling of the PVC geosynthetics by moisture migration. For the PVC geosynthetics exposed to concentration of ethanol at 2% ~ 3% that is frequently encountered in landfill (USEPA, 1988), similar mechanical response can be expected. The loss of plasticizer was, however, also observed during exposure to lower concentration of ethanol at 80% and 50%. The studies on the PVC geosynthetic exposed to 80% ethanol followed by a certain period of air exposure indicate an eventual stiffening of the material when the absorbed moisture and ethanol is depleted. In a practical context involving landfill application of PVC geosynthetics, the durability of the

PVC liner resulting from the leaching of plasticizer can pose a problem over the long-term, especially when the landfill is subjected to wetting and drying cycles where the leaching of the plasticizer will occur due to prolonged contact with chemicals, whereas swelling is limited due to the evaporation of the moisture during drying period. The loss of flexibility of the PVC geosynthetic as a result of chemical exposure will also induce failure or cracking, when subjected to localized loading.

CHAPTER 3

CONSTITUTIVE CHARACTERIZATIONS

3.1 Introduction

In the last chapter, the mechanical behaviour of a chemically-treated PVC geosynthetic exposed to concentrations of ethanol was examined through sets of uniaxial tests. The effects of exposure to pure ethanol include the reduction in flexibility (or embrittlement) of the PVC geosynthetic and transformation of the material from one capable of large strain hyperelastic behaviour with no observable yield to one that displays a dominant yield behaviour. The objective of this chapter is to develop an approach for modelling the constitutive response of the PVC geosynthetic in its untreated and chemically-treated conditions.

As with rubber-like elastic materials, a characteristic feature of the PVC geosynthetic is its ability to undergo large strain deformations. This is attributed to the nature of its randomly oriented inter-tangled polymer chain network structure. Approaches to modelling the mechanical behaviour of elastic materials through consideration of the polymer network structure and associated kinetic theories are given by a number of investigators including Wall (1942), Treloar (1943,1975), Flory (1969), Edwards (1971), Deam and Edwards (1976), Flory and Erman (1982), Erman and Flory (1982), Doi and Edwards (1987) and Boyd and Philips (1993). More recently, Boyce et al. (1988), Arruda et al. (1995), Sweeney and Ward (1995), Bergström and Boyce (1998), Boyce and Arruda (2000), Makradi et al. (2005) and Gurtin and Anand (2005) have re-examined the kinetic theories and network modelling as applied to the constitutive modelling of polymeric materials that undergo substantially large strains. The phenomenological theories of hyperelastic materials, which will by incorporated into the development of a constitutive model for the PVC material, have been extensively studied in the classical works of Rivlin, Green, Adkins and others,

and extensive reviews of the subject can be found in works by Doyle and Ericksen (1956), Rivlin (1960) (see also Barenblatt and Joseph, 1997), Adkins (1961), Spencer (1970), Truesdell and Noll (1992), Hayes (2001), Selvadurai (2002) and in the volumes by Green and Adkins (1970), Ogden (1984), Lur'e (1990), Drozdov (1996), Dorfmann and Muhr (1999), Fu and Ogden (2001), Besdo et al. (2001) and Busfield and Muhr (2003). In contrast to hyperelastic pure rubber-like materials that have imperceptible irreversible phenomena in terms of permanent deformations and minimal energy dissipation during cycles of loading, a PVC geosynthetic can exhibit appreciable irreversible effects resulting in the development of permanent strains during the loading-unloading cycles and strain-rate effects. Most importantly, such effects can materialize even at moderately large strain levels. The development of constitutive relationships that describe the mechanical behaviour of the PVC geosynthetic therefore has to address three aspects: the influence of large strains, the development of irreversible strains during application of a loading cycle and the strain-rate effects. Furthermore, the constitutive modelling presented in this chapter integrates the influence of prolonged chemical exposure of the PVC geosynthetic on the alteration of its constitutive response. The methodology adopted in the study is mainly a phenomenological approach, since the assessment of the influences of chemical exposure on the alterations in the polymer chain network will require considerably more precise information on both the detailed chemical processes and the manner in which such chemical reactions can be accurately incorporated within the framework of a kinetic theory. Any such developments should also address, simultaneously, material alterations leading to embrittlement and the transformation of the polymeric material to one that exhibits a pronounced yield and strain-rate effects at moderately large strains.

The development of a phenomenological constitutive model for characterizing the irreversible behaviour and strain-rate effects observed in the experiments can be approached via the consideration of either a nonlinear viscoelasticity approach or a nonlinear elasticity approach that is modified to account for a rate-dependency effect. The former approach is a viable one and has been developed and applied to a variety of problems involving rate-sensitive materials undergoing large strains (Rivlin, 1965; Christensen, 1971; Pipkin, 1972; Findley et al., 1976; Betten, 2002). The latter approach is simpler and has been applied by Sweeney and Ward (1995), Septanika and Ernst (1998a,b)

and Amin et al. (2002) to examine the time-dependent behaviour of elastomers. It will be shown that the latter group of constitutive models can be adopted and extended with the aid of the model proposed by Boyce et al. (1988) to develop plausible constitutive models for the PVC material in both its intact and chemically-treated states.

3.2 Constitutive modelling

The development of a plausible constitutive model for describing the mechanical behaviour of the PVC geosynthetic in its intact condition has to address the key aspects as they relate to the presence of large strains, the influence of rate effects and the occurrence of irreversible strains during a loading-unloading cycle. Similarly, the constitutive modelling of the chemically-treated PVC geosynthetic has to address the embrittlement process that leads to the transformation of the material from one capable of large strain hyperelastic behaviour to one that displays dominant yield behaviour, strain-rate sensitivity and associated irreversible strains. An added constraint relates to the suitability of the constitutive model for incorporation into an existing computational procedure for the study of strain-rate sensitive materials that undergo varying degrees of large strain phenomena in both the elastic and irreversible responses. As indicated, there are a variety of methodologies that can be adopted for the development of computational models for the PVC geosynthetic. The purpose of the present exercise is to adopt and extend concepts that have been put forward in the literature for the modelling of both large strain elasticity phenomena, irreversible effects and to accommodate effects of strain-rate sensitivity in such responses.

The equations governing finite strain behaviour of elastic materials are presented in a number of texts and review articles on the subject (see e.g. Rivlin, 1960; Green and Adkins, 1970; Spencer, 1970; Ogden, 1984; Lur'e, 1990) and only the essential points will be summarized. The position of a generic particle in the deformed configuration is denoted by x_i $(i=1,2,3)$, the coordinates of which in the reference configuration are X_A $(A=1,2,3)$. The deformation gradient tensor is

$$\mathbf{F} = \left\| \partial x_i / \partial X_A \right\|. \tag{3.1}$$

At the outset, attention is restricted to incompressible elastic materials for which

$$\det \mathbf{F} = 1. \tag{3.2}$$

The strain measures are defined in terms of the left Cauchy-Green deformation tensor tensor $\mathbf{B}$ given by

$$\mathbf{B} = \mathbf{F}\mathbf{F}^T \; ; \qquad \mathbf{B} = \left\| g_{ij} \right\| \quad ; \quad g_{ij} = f_{iR} f_{jR} = \frac{\partial x_i}{\partial X_R} \frac{\partial x_j}{\partial X_R} \tag{3.3}$$

The invariants of $\mathbf{B}$ are

$$I_1 = g_{ii} = \lambda_1^2 + \lambda_2^2 + \lambda_3^2 \quad ; \quad I_2 = \frac{1}{\lambda_1^2} + \frac{1}{\lambda_2^2} + \frac{1}{\lambda_3^2} \quad ; \quad I_3 = \lambda_1 \lambda_2 \lambda_3 \tag{3.4}$$

and λ_i $(i = 1,2,3)$ are the principal stretches. For isotropic incompressible elastic materials, the Cauchy stress $\mathbf{T}$ is an isotropic function of $\mathbf{B}$ and takes the form

$$\mathbf{T} = -p\mathbf{I} + \psi_1 \mathbf{B} + \psi_2 \mathbf{B}^2 \tag{3.5}$$

where p is an arbitrary scalar pressure, $\mathbf{I}$ is the unit matrix and ψ_1 and ψ_2 are functions of the invariants of $\mathbf{B}$, with the restriction that $\det \mathbf{B} = I_3 = 1$. The constitutive equation (3.5) is a generalized relationship that can be made specific by invoking energetic/thermodynamic concepts. The incompressible hyperelastic material is assumed to possess a strain energy function W and considering energy conservation and invariance requirements applicable to an isotropic elastic material, it can be shown (Rivlin, 1960; Spencer, 1970) that the generalized constitutive relationship for an incompressible elastic material undergoing finite strains can be written in Cartesian tensor notation as follows:

$$T_{ij} = -p\delta_{ij} + 2[(\frac{\partial W}{\partial I_1} + I_1 \frac{\partial W}{\partial I_2})g_{ij} - g_{ik} g_{jk} \frac{\partial W}{\partial I_2}] \tag{3.6}$$

The constitutive relationship (3.6) can also be made more specific through the introduction of a strain energy function with an explicit dependence on the invariants I_1 and I_2. The

development of such relationships invariably relies on experimental data and the approaches adopted can range from the use of kinetic theories to phenomenological approaches. These are adequately covered in the references cited previously in connection with the modelling of rubber-like elastic materials. The most widely used phenomenological form of the strain energy function is the Mooney-Rivlin form (Mooney, 1940; Rivlin, 1948) given by

$$W(I_1, I_2) = C_1(I_1 - 3) + C_2(I_2 - 3) \tag{3.7}$$

where C_1 and C_2 are material constants. This form of the strain energy function is considered adequate for the purposes of modelling rubber-like elastic materials that are subjected to moderately large strains (Green and Adkins, 1970; Spencer, 1970; Selvadurai, 1973,1974). The strain energy function is also the most general form that is applicable for modelling problems in second-order elasticity theory (Rivlin, 1953; Green and Spratt, 1954; Selvadurai and Spencer, 1972; Selvadurai et al., 1988; Selvadurai, 2002). Ogden (1972) presented an alternative form of the strain energy function, which uses the principal stretches λ_1 and λ_2 as opposed to the strain invariants: i.e.

$$W(\lambda_1, \lambda_2) = \sum_n \frac{\mu_n}{\alpha_n}(\lambda_1^{\alpha_n} + \lambda_2^{\alpha_n} + \lambda_1^{-\alpha_n}\lambda_2^{-\alpha_n} - 3) \tag{3.8}$$

with the stability constraint $\alpha_n \mu_n \geq 0$. It can capture the stress-strain response for an extensive range of strains encountered in highly deformable rubber-like materials. Further discussions of the strain energy functions derived through phenomenological considerations are given by Treloar (1975), Ogden (1984) and Drozdov (1996). Along the same lines, Arruda and Boyce (1993) propose the following form of the strain energy function that accommodates the 8-chain model derived from a kinetic theory:

$$W = \tilde{\mu}\lambda_m[\beta\lambda_{chain} + \lambda_m \ln(\frac{\beta}{\sinh\beta})]; \quad \beta = L^{-1}(\frac{\lambda_{chain}}{\lambda_m}); \quad L(\beta) = \coth\beta - \frac{1}{\beta} \tag{3.9}$$

where $\tilde{\mu}$ and λ_m are, respectively, the linear elastic shear modulus and limiting extensibility of the material such that the strain energy tends to infinity as λ_{chain} approaches λ_m. The current chain length λ_{chain} is defined in terms of principal stretches as follows:

$$\lambda_{chain} = [\frac{1}{3}\{\lambda_1^2 + \lambda_2^2 + \lambda_3^2\})]^{1/2} \tag{3.10}$$

An account of further models derived from kinetic theories is given by Boyce and Arruda (2000). Figure 3.1 shows a comparison of the modelling of the tensile behaviour of the untreated PVC material for different forms of the strain energy function.

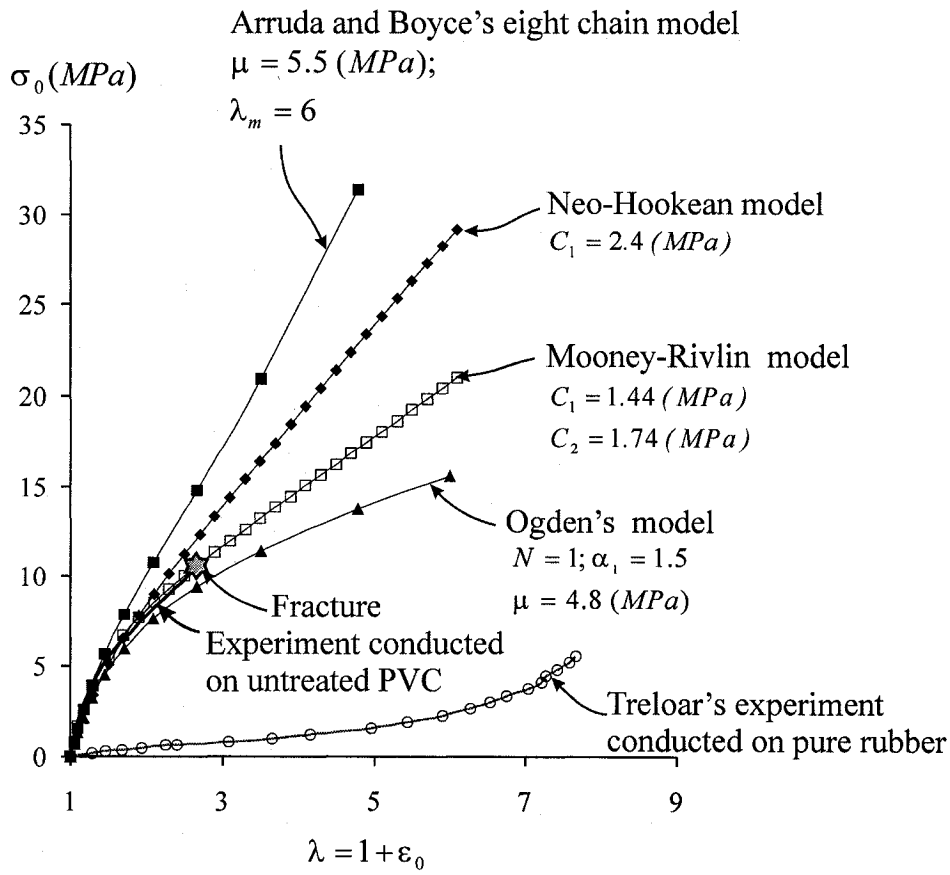

Figure 3.1 Constitutive modelling of the stress-strain curve for an untreated PVC geosynthetic (corresponding to a loading rate of $\dot{\varepsilon}_0 = 40\%/min$) using different forms of strain energy functions

3.2.1 A model for the untreated PVC geosynthetic

From an inspection of the results of uniaxial tests conducted on the untreated PVC geosynthetic (Figure 2.10a), it is evident that the material experiences only moderately large strains during uniaxial stretching and that the stress-strain response is sensitive to the strain-rate, particularly during the loading path. The response of the material during unloading appears to be relatively insensitive to the loading rate (Figure 2.9b-c) during a loading-unloading cycle, and the material experiences a large irreversible strain. The insensitivity of the unloading behaviour to strain-rate effects and the presence of large irreversible strains after a loading-unloading cycle are also observed in experiments conducted on other polymeric material such as Polyphenylene oxide (Krempl and Khan, 2003) and polytetrafluoroethylene (Khan and Zhang, 2001). The development of a constitutive model for the untreated PVC geosynthetic therefore has to address the three aspects of moderately large strains and strain-rate sensitivity during loading, relative insensitivity to strain-rate effects during unloading, and the development of irreversible strains during a load cycle. This last aspect is an important consideration in the modelling of PVC geosynthetics as opposed to pure rubber, which experiences little or no irreversible strains during a loading cycle. A pure rubber can, however, exhibit hysterisis effects, which is usually referred to as the "Mullins effect" (see e.g. Mullins, 1947, 1969; Farris, 1971; Dorfmann and Ogden, 2004), to varying degrees, depending upon the composition of the chemicals and additives in the rubber. The conventional theory of finite elasticity for moderately large deformations thus needs to be modified to take into consideration these additional material responses. It is highly debatable whether such a modification can be accomplished in a unique way to satisfy all possible polymeric materials even under the same test conditions. The exercise is made more complicated by the presence of the plasticizer in the PVC material. The objective here is to achieve the modifications through the introduction of a rate-dependent component in the definition of the strain energy function. Following the developments presented by Sweeney and Ward (1995) and Amin et al. (2002), the strain energy function for the untreated PVC geosynthetic is assumed to be expressed in the functional form of

$$W^e = W^e(\dot{\gamma}_0, I_1^e, I_2^e) \tag{3.11}$$

where W^e, I_1^e and I_2^e are written more explicitly in relation with the elastic deformation gradient $\mathbf{F}^e$; in cases where the irreversible deformations are absent, the total deformation gradient $\mathbf{F}$ coincides with the elastic deformation gradient $\mathbf{F}^e$, i.e., $\mathbf{F} = \mathbf{F}^e$. In (3.11), $\dot{\gamma}_0$ is a generalized form of a combined stretch-rate that depends only on the total principal stretches λ_i $(i = 1,2,3)$ of the material, such that

$$\dot{\gamma}_0 = \frac{d\gamma_0}{dt} \quad ; \quad \gamma_0 = \left[(\bar{\lambda}_1 - 1)^{\frac{1}{\alpha}} + (\bar{\lambda}_2 - 1)^{\frac{1}{\alpha}} + (\bar{\lambda}_3 - 1)^{\frac{1}{\alpha}} \right]^{\alpha} \tag{3.12}$$

where $\bar{\lambda}_i$ now have a *conditional dependence* on λ_i to take into effect *only* the stretching response: i.e.

$$\bar{\lambda}_i = \begin{cases} \lambda_i & ; \quad (\lambda_i \geq 1) \quad ; \quad i = (1,2,3) \\ 1 & ; \quad (\lambda_i < 1) \quad ; \quad i = (1,2,3) \end{cases} \tag{3.13}$$

and α is a material parameter that accounts for combined stretch. When the specimen is subjected to a uniaxial stretch, the principal stretches in the other two directions are less than unity and therefore the definition of γ_0 reduces to that for the uniaxial strain ε_0. The conditional dependency indicated in (3.13) is primarily to accommodate for the observed influences of strain-rate effects when the material is subjected to stretch, and the relatively marginal influence in directions where the principal stretches are less than unity, especially when the material is in the form of a membrane. The combined stretch γ_0 depends on the principal invariants I_1 and I_2 through (3.4), although the resulting forms are not required for purposes of parameter identification. It now remains to specify the explicit form for the strain energy function defined by (3.11). The form of the strain energy function should reduce to an appropriate finite strain equivalent in the absence of strain-rate effects. The basic functional form of the strain energy function proposed by Sweeney and Ward (1995) is adopted, and the strain energy function with a Mooney-Rivlin form is selected as the limiting case. This latter choice is dictated by the observation that the untreated PVC geosynthetic generally experiences only moderately large strains even up to failure (Figure 3.1). The form of strain energy function corresponding to (3.11) is taken as

$$W^e(\dot{\gamma}_0, I_1^e, I_2^e) = C_1'(I_1^e - 3) + C_2'(I_2^e - 3) \tag{3.14}$$

with

$$\begin{aligned} C_1' &= C_1 + \begin{cases} \kappa_1 \ln(|\dot{\gamma}_0| / \dot{\gamma}_c^{<1>}) ; & (|\dot{\gamma}_0| \geq \dot{\gamma}_c^{<1>}) \\ 0 ; & (|\dot{\gamma}_0| < \dot{\gamma}_c^{<1>}) \end{cases} ; \\ C_2' &= C_2 + \begin{cases} \kappa_2 \ln(|\dot{\gamma}_0| / \dot{\gamma}_c^{<2>}) ; & (|\dot{\gamma}_0| \geq \dot{\gamma}_c^{<2>}) \\ 0 ; & (|\dot{\gamma}_0| < \dot{\gamma}_c^{<2>}) \end{cases} \end{aligned} \tag{3.15}$$

where C_1' and C_2' are the modified Mooney-Rivlin parameters, κ_1 and κ_2 are parameters that related to strain-rate sensitivity; and $\dot{\gamma}_c^{<1>}$, $\dot{\gamma}_c^{<2>}$ are defined as *rate-independent threshold strain-rates* for parameters C_1' and C_2', respectively. The rate-dependency of the hyperelastic parameters for polymeric materials has also been observed by Amin et al. (2002). The constitutive postulates presented thus far are sufficient if attention is strictly focused on *monotonic loading* paths with no provision for observation of unloading behaviour, where the viscous deformation is assumed absent and the total deformation gradient $\mathbf{F}$ coincides with the elastic deformation gradient $\mathbf{F}^e$. From (3.6) with a Mooney-Rivlin form of strain energy function (3.14), the stress σ_0 in a uniaxial PVC geosynthetic can be expressed by the following relation (see also Rivlin and Saunders, 1951; Treloar, 1975):

$$\frac{\sigma_0}{2(\lambda - \dfrac{1}{\lambda^2})} = C_1' + \frac{C_2'}{\lambda} \tag{3.16}$$

where λ is the uniaxial stretch in the test direction. It can be shown that for $1/\lambda \in [0.4, 0.9]$, the slope of the linear relation (3.16) gives the value of C_2' and its intercept (as $1/\lambda \to 0$) gives the value of C_1' (Figure 3.2a).

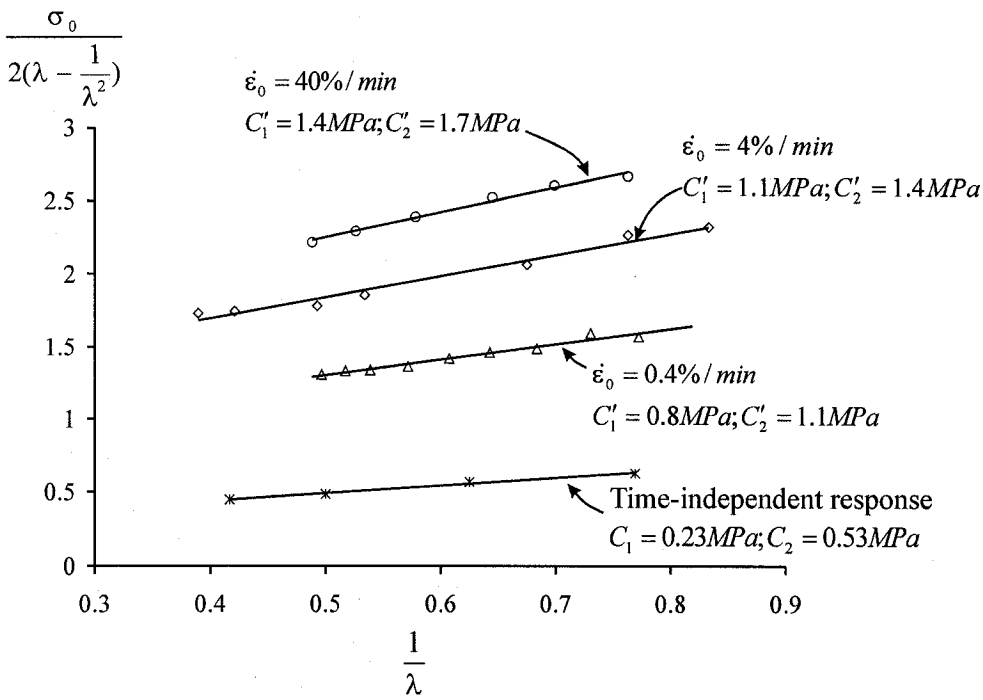

(a) Determination of the modified elastic parameters

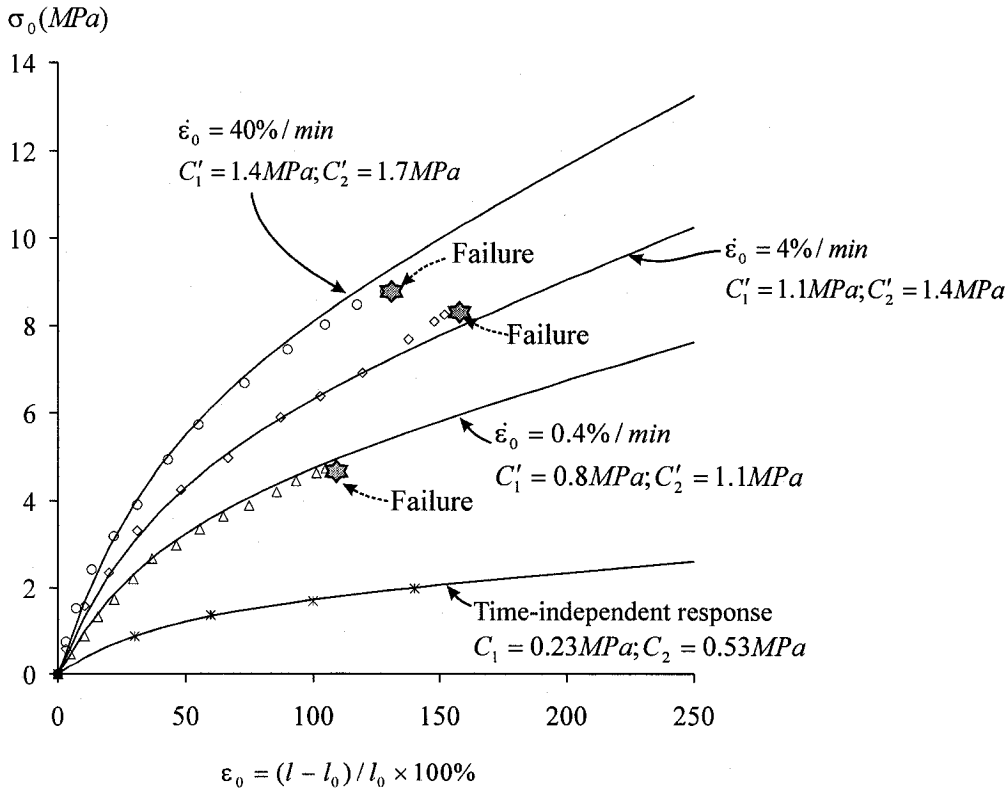

(b) Curve-fitting of the stress-strain curves at various loading rates

Figure 3.2 Curve-fitting for the loading part of the stress-strain curves of an untreated PVC geosynthetic

The model representations of the monotonic loading behaviour using these derived elastic parameters are presented in Figure 3.2b along with the experimental data. The calculations then indicate the following rate-dependency of C_1' and C_2' on $\dot{\gamma}_0$ (see also Figure 3.3):

$$\begin{aligned} C_1' &= [0.13\ln(\dot{\gamma}_0) + 2.1]MPa \\ C_2' &= [0.13\ln(\dot{\gamma}_0) + 2.4]MPa \end{aligned} \tag{3.17}$$

It is noted that C_1' and C_2' essentially present a similar rate-sensitivity, i.e., $\kappa_1 = \kappa_2 = \kappa \approx 0.13$.

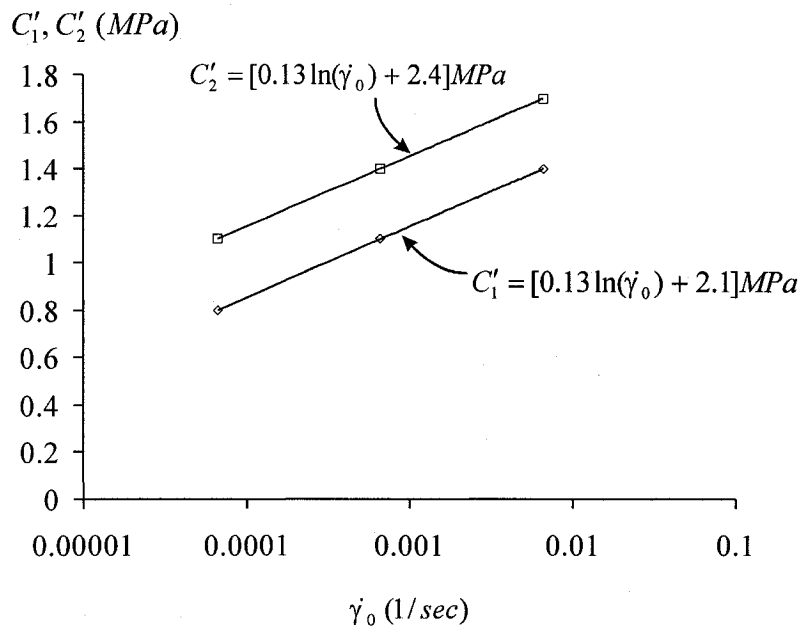

Figure 3.3 Rate dependencies of C_1' and C_2' on $\dot{\gamma}_0 (= \dot{\varepsilon}_0)$ for an untreated PVC geosynthetic

The difficulty encountered is to obtain the time-independent elastic parameters C_1 and C_2, where experiments must be conducted at a loading rate $0 < \dot{\varepsilon}_0 (= \dot{\gamma}_0) < \min(\dot{\gamma}_c^{<1>}, \dot{\gamma}_c^{<2>})$. An alternative approach is adopted for determining the rate-independent material properties through a relaxation test, where the specimen is first stretched to a certain fixed strain; then, due to inelastic effects in the material, the uniaxial stress in the specimen will continuously decrease until it reaches a stable value. Examples of such relaxation tests are

given by Bergström and Boyce (1998), Amin et al. (2002) and Qi and Boyce (2004). A plot of strains and the stabilized relaxation stresses produces the proposed time-independent response of the PVC geosynthetic (see Figure 3.2b) giving rise to the elastic parameters: $C_1 \approx 0.23MPa$; $C_2 \approx 0.53MPa$. The mechanical responses of the PVC geosynthetics during relaxation, however, can be possibly affected by temperature drift (maximum $3^{\circ}C$) over a maximum test duration of $24hours$. Therefore by allowing a 20% variation of C_1, an interval of $\dot{\gamma}_c^{<1>} \in [3.7\times10^{-7}sec^{-1}, 7.6\times10^{-7}sec^{-1}]$ is obtained by noticing that $C_1' = C_1$ at loading rates $\dot{\gamma}_0 = \dot{\gamma}_c^{<1>}$ in (3.15). Similarly, the value of $\dot{\gamma}_c^{<2>}$ will fall within a similar interval. $\dot{\gamma}_c^{<1>}$ and $\dot{\gamma}_c^{<2>}$ are therefore assumed essentially to have the same value and can be taken as an average value of their variation (i.e., $\dot{\gamma}_c^{<1>} = \dot{\gamma}_c^{<2>} = \dot{\gamma}_c \approx 5.67\times10^{-7}sec^{-1}$).

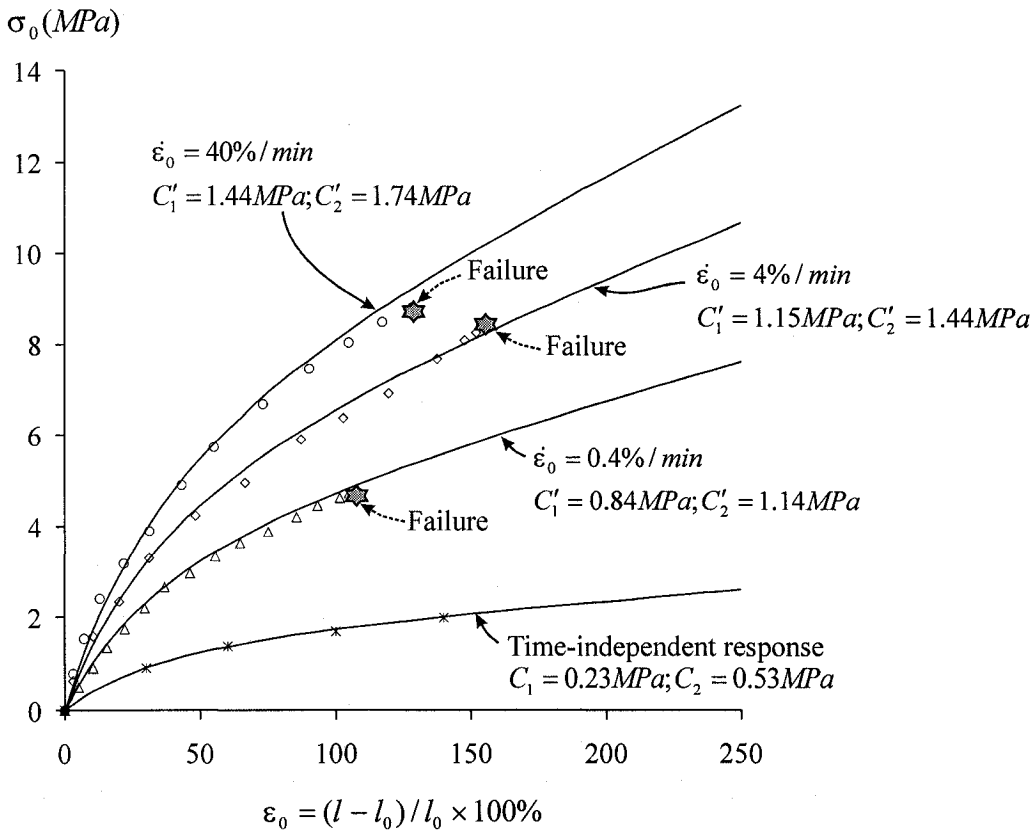

Figure 3.4 Model representations using Equation (3.18) for the loading part of the stress-strain curves of an untreated PVC geosynthetic

The equation (3.15) can then be finalized in the following form:

$$C_1' = C_1 + \begin{cases} \kappa \ln(|\dot{\gamma}_0|/\dot{\gamma}_c); & (|\dot{\gamma}_0| \geq \dot{\gamma}_c) \\ 0 & ; \quad (|\dot{\gamma}_0| < \dot{\gamma}_c) \end{cases} ;$$
$$C_2 = C_2 + \begin{cases} \kappa \ln(|\dot{\gamma}_0|/\dot{\gamma}_c); & (|\dot{\gamma}_0| \geq \dot{\gamma}_c) \\ 0 & ; \quad (|\dot{\gamma}_0| \geq \dot{\gamma}_c) \end{cases} \tag{3.18}$$

where $C_1 \approx 0.23MPa$; $C_2 \approx 0.53MPa$; $\kappa \approx 0.13$; $\dot{\gamma}_c \approx 5.67 \times 10^{-7} sec^{-1}$. The model representations of the monotonic loading behaviour of the untreated PVC geosynthetic at different loading rates are determined using (3.18) are presented in Figure 3.4.

The constraints introduced by (3.18) correspond to the absence of strain-rate effects upon unloading with complete reversal of strains. An inspection of the unloading response of the untreated PVC geosynthetic (Figures 2.9b-c), however, indicates that the initial slope of the unloading response is significantly higher than that for the loading mode and that permanent deformation accompanies unloading behaviour. Furthermore, the permanent strains themselves are also in the moderately large strain range. In general, the mechanisms contributing to such irreversible phenomena can include both elastic and visco-plastic effects. Following these observations and assumptions, this thesis considers additional constitutive responses, which are then added in series to the elastic constitutive component represented by the modified form of the Mooney-Rivlin strain energy function (3.18). The model can be visualized as including an elastic component *A* of the finite strain contributing to the elastic recovery, in parallel with a visco-plastic component *B* accounting for viscous effects during unloading (Figure 3.5 shows a schematic arrangement of the constitutive components). If the modelling of the finite strains during loading is accommodated through a Mooney-Rivlin model applicable to moderately large strains, then it is sufficient that the finite strain elastic recovery behaviour of the unloading response can also be modelled through the use of a strain energy function of the Mooney-Rivlin form of an elastic component *A*:

$$W^u(I_1^u, I_2^u) = E_1'(I_1^u - 3) + E_2'(I_2^u - 3) \tag{3.19}$$

where E_1' has the conditional constraint

$$E_1' = \begin{cases} \to \infty; & (\dot{\gamma}_0 \geq -\dot{\gamma}_c^v) \\ 0 \quad ; & (\dot{\gamma}_0 < -\dot{\gamma}_c^v) \end{cases} \tag{3.20}$$

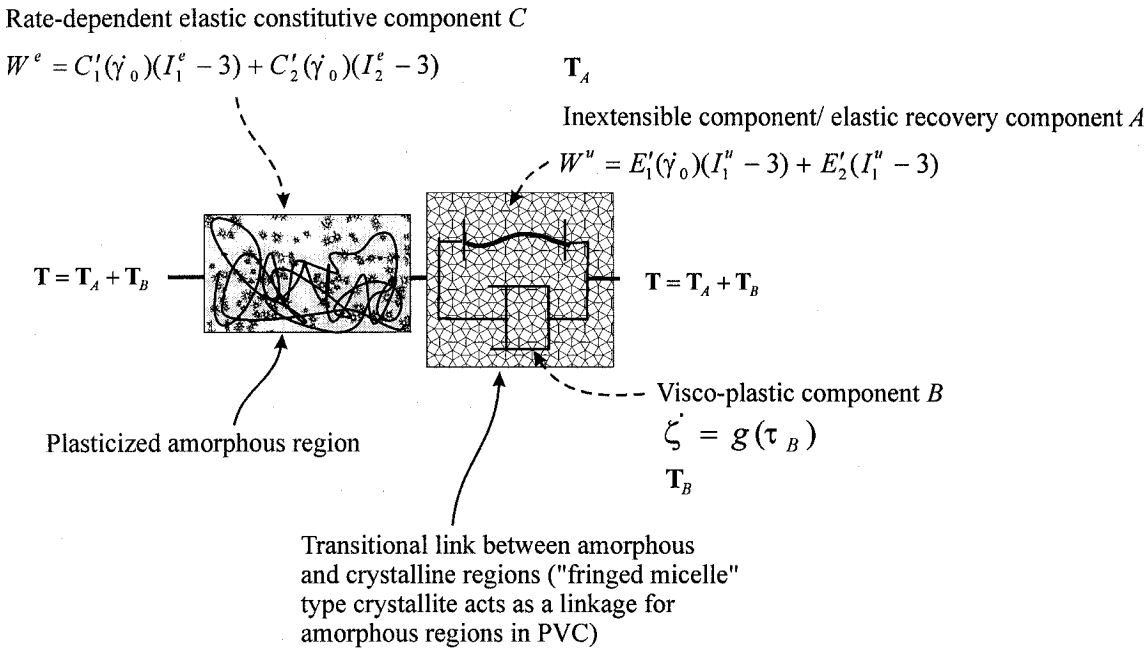

Figure 3.5 Schematic representation of the constitutive components

The special treatment of E_1' is intended to take into account the fully elastic behaviour at loading stage $\dot{\gamma}_0 > 0$, where any development of visco-plastic deformation is restricted due to the infinite value of E_1'. It is further assumed that, at sufficiently low loading rates, say, lower than a *viscous threshold strain-rate* $\dot{\gamma}_c^v$ (i.e. $|\dot{\gamma}_0| \leq \dot{\gamma}_c^v$), strain-rate effects are absent. Upon unloading (i.e. $\dot{\gamma}_0 < -\dot{\gamma}_c^v$), however, the visco-plastic deformation is fully activated due to the zero value of E_1'. The elastic parameter E_2' is then the only remaining elastic parameter that contributes to the elastic recovery during unloading. E_2' is assumed to be both time- and history-independent. It is also possible to interpret the special behaviour of modulus E_1' in terms of the transformations of the polymer chain network through a

transitional link between the amorphous regions and the crystalline regions and by considering the response of such links during both loading and unloading. The inextensible transitional link can only accommodate incremental loading, but zero incremental unloading. The work of Boue et al. (1988), Jones and Marques (1990) and Drozdov and Dorfmann (2003) also deals with the concept of an inextensible strand connecting two neighboring junctions in a polymeric material, which contributes to this form of response. The existence of the "fringed micelle" type crystallite that acts as a linkage for the amorphous network was experimentally confirmed by Aiken et al. (1947) and Alfrey et al. (1949a,b). In particular, Alfrey et al. (1949b) found that the crystallites formed an oriented structure after a pre-stretch history. Therefore, due to the oriented alignment between the amorphous network and the crystallite, the region in the vicinity of a connection is assumed to process negligible loading capacities during an unloading immediately following a monotonic loading. The procedure adopted here, however, is mainly phenomenological with the modelling based on experimental observations.

The modelling of the visco-plastic component B that contributes to the development of irreversible strains during unloading is now discussed. A model proposed by Boyce et al. (1988) assumes that the finite irreversible strain-rate tensor $\mathbf{D}^u$ is related to the deviatoric component of the effective stress tensor $\mathbf{N}_B$ associated with the visco-plastic effects through a relationship of the form

$$\mathbf{D}^u = \dot{\zeta}\,\mathbf{N}_B \;; \quad \mathbf{N}_B = \frac{3}{2\tau_B}\mathbf{T}'_B \;; \quad \tau_B = \left[\frac{3}{2} tr(\mathbf{T}'^2_B)\right]^{1/2} \tag{3.21}$$

where $\mathbf{T}'_B$ is the deviatoric component of the Cauchy stress tensor $\mathbf{T}_B$ applicable to the visco-plastic phenomena, as pictorially depicted in Figure 3.5 (see also Sweeney and Ward, 1995). Also, in (3.21) the visco-plastic strain-rate $\dot{\zeta}$ is generally assumed to be a function of the effective stress τ_B (in MPa) and the strain-rate $\dot{\gamma}_0$, i.e.

$$\dot{\zeta} = g(\tau_B, \dot{\gamma}_0) \tag{3.22}$$

An explicit form of (3.22) is a relationship in the form of a power law

$$\dot{\zeta} = \left(\frac{\tau_B}{q}\right)^{1-s} |\dot{\gamma}_0| \begin{cases} \dfrac{1}{(|\dot{\gamma}_0|/\dot{\gamma}_c^v)^s} & ; \quad (|\dot{\gamma}_0| \geq \dot{\gamma}_c^v) \\ 1 & ; \quad (|\dot{\gamma}_0| < \dot{\gamma}_c^v) \end{cases} \tag{3.23}$$

or

$$d\zeta = \left(\frac{\tau_B}{q}\right)^{1-s} |d\gamma_0| \begin{cases} \dfrac{1}{(|\dot{\gamma}_0|/\dot{\gamma}_c^v)^s} & ; \quad (|\dot{\gamma}_0| \geq \dot{\gamma}_c^v) \\ 1 & ; \quad (|\dot{\gamma}_0| < \dot{\gamma}_c^v) \end{cases} \tag{3.24}$$

where q (in MPa) can be interpreted as a *static yield stress* of the material and s is the *viscous sensitivity* to rate-effects. At sufficiently low strain-rates $|\dot{\gamma}_0| \leq \dot{\gamma}_c^v$, the material behaviour is assumed rate-independent. There are two possible categories of behaviour involving rate-independency: either time-independent or time- and history- independent behaviour. The time-independent behaviour mainly manifests in the form of an *elasto-plastic* response, whereas the time- and history-independent behaviour results in a purely *elastic* response. Therefore, when the strain-rate satisfies the constraint $|\dot{\gamma}_0| < \dot{\gamma}_c^v$, the *incremental viscous strain* $d\zeta$ is independent of the time effect in spite of a possible history-dependency. Hence, in this case, $d\zeta$ should be referred to as an *incremental plastic strain* rather than *incremental viscous strain.* Also, as s becomes small (i.e. $s \to 0$), the time-dependency of the *incremental viscous strain* $d\zeta$ on $\dot{\gamma}_0 / \dot{\gamma}_c^v$ is also highly restricted. Therefore, in the stress-strain responses for the tested samples conducted at $|\dot{\gamma}_0| \geq \dot{\gamma}_c^v$, the rate-insensitivity of the unloading behaviour of the untreated material can be attributed to the low value of s. The finite irreversible strain-rate $\mathbf{D}^u$ is obtained by considering the product decomposition of the deformation gradient tensor into its elastic and irreversible components, as suggested by Kröner (1960) and Lee (1969) (see also, Lubarda, 2004; Gurtin and Anand, 2005): i.e.

$$\mathbf{F} = \mathbf{F}^e \mathbf{F}^u \tag{3.25}$$

and the strain-rate and irreversible strain-rate are defined (Malvern, 1969; Spencer, 2004) by

$$\begin{aligned}
&\mathbf{L} = \dot{\mathbf{F}}\mathbf{F}^{-1} = \mathbf{D} + \mathbf{W} = \dot{\mathbf{F}}^{e}(\mathbf{F}^{e})^{-1} + \mathbf{F}^{e}[\dot{\mathbf{F}}^{u}(\mathbf{F}^{u})^{-1}](\mathbf{F}^{e})^{-1} \\
&\mathbf{L}^{u} = \dot{\mathbf{F}}^{u}(\mathbf{F}^{u})^{-1} \\
&\mathbf{D}^{u} = \frac{1}{2}\left[\mathbf{L}^{u} + (\mathbf{L}^{u})^{T}\right]
\end{aligned} \tag{3.26}$$

with $tr\mathbf{D}^{u} = 0$. For a uniaxially stressed element

$$D_{11}^{u} = \frac{\partial \dot{x}_1^{u}}{\partial x_1^{u}} = \frac{\partial \dot{x}_1^{u}}{\partial X_1}\frac{\partial X_1}{\partial x_1^{u}} = \frac{\dot{\lambda}_1^{u}}{\lambda_1^{u}} = \dot{\zeta} \, . \tag{3.27}$$

Finally, following Boyce et al. (1988) (see also Wang et al., 2001), the stress states in the elastic recovery and the visco-plastic responses applicable to the unloading paths are added to generate the Cauchy stress. Denoting the stress due to the elastic recovery response by $\mathbf{T}_A$ (see Figure 3.5) and the stress due to the visco-plastic response by $\mathbf{T}_B$, the total Cauchy stress tensor $\mathbf{T}$ in the PVC geosynthetic can be expressed as

$$\mathbf{T} = \mathbf{T}_A + \mathbf{T}_B \, . \tag{3.28}$$

The results of uniaxial test data derived from the untreated PVC geosynthetic are first used to determine the constitutive parameters associated with the above modelling approach. Although the experiments were conducted at three different strain-rates, $\dot{\varepsilon}_0 = 4\%/min$, $\dot{\varepsilon}_0 = 40\%/min$ and $\dot{\varepsilon}_0 = 160\%/min$ respectively, only the results for *two* of these strain-rates ($\dot{\varepsilon}_0 = 4\%/min$ and $\dot{\varepsilon}_0 = 40\%/min$) will be used to determine the material parameters and the third set of data is used to assess the predictive capabilities of the parameter identification exercise. The curve-fitting is carried out using the MATLAB © program through a least square method.

The rate-insensitivity of the unloading behaviour essentially indicates a near-zero value of s. As discussed previously, when $s \approx 0$, the viscous model reduces to a time-independent plastic model; therefore the *viscous threshold critical strain-rate* $\dot{\gamma}_c^{v}$ is inapplicable for the

untreated material. In cases where the viscous effect is important, the exact non-zero value of s needs to be determined. Also, since there is no distinct yield point in the time-independent stress-strain behaviour, the *static yield stress* q also becomes irrelevant for the untreated PVC material. The parameter q, however, essentially determines the steepness of the unloading part of the stress-strain curve at the transitional point from loading to unloading. By curve-fitting of the data derived from the unloading response of the untreated material at the loading rates $\dot{\varepsilon}_0 = 4\%/min$ and $\dot{\varepsilon}_0 = 40\%/min$, $q \approx 2.0MPa$ is obtained. The final parameter E_2' determines the amount of the elastic recovery. The value of $E_2' \approx 0.5MPa$ gives the best fit of the results at a peak strain of 140%. The material parameters determined can now be used to evaluate the model response for strain-rates of $\dot{\varepsilon}_0 = 4\%/min$ and $\dot{\varepsilon}_0 = 40\%/min$. The representations correlate well with the experimental data obtained for tests conducted up to peak strain of 140% (Figure 3.6). The results at other peak strains of 60% and 100% are predicted. The predictions of the constitutive model for the strain-rate corresponding to a loading rate of $\dot{\varepsilon}_0 = 160\%/min$ are included in a subsequent section.

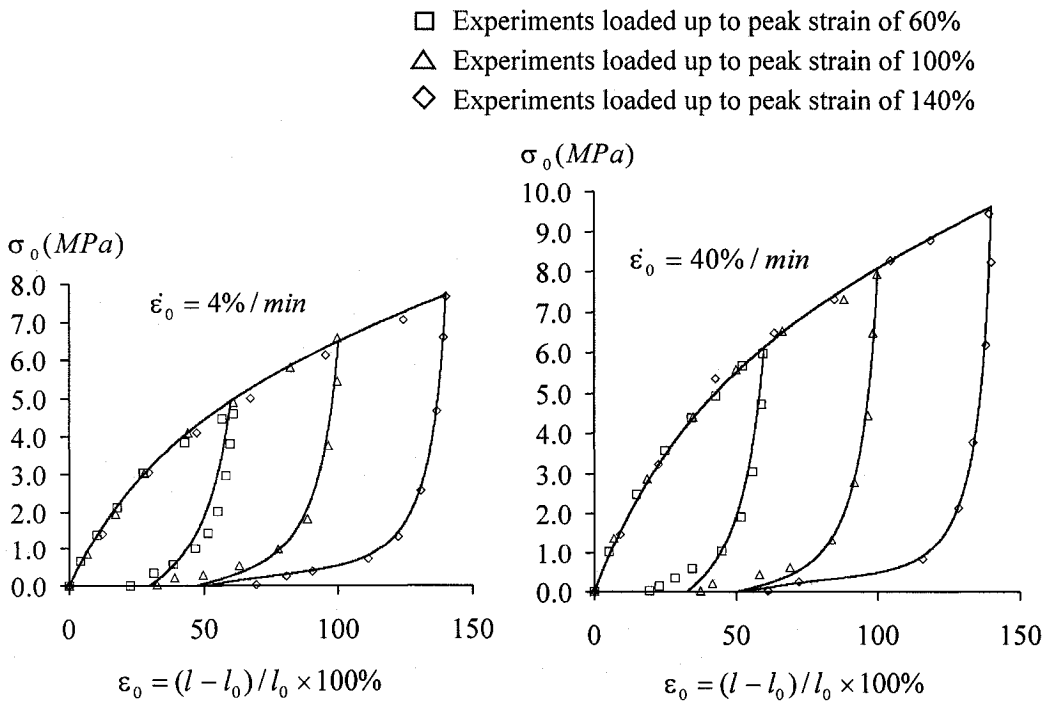

Figure 3.6 Model duplicatioin for the stress-strain curves of an untreated PVC geosynthetic involving loading and unloading

As a concluding remark, the assumption of incompressibility of the material was explicitly invoked in the development of the constitutive relationships for model *A*. The validity of this assumption was assessed by examining the lateral contraction of the membrane specimen during monotonic stretching where the total deformation gradient **F** coincided with the elastic deformation gradient $\mathbf{F}^e$ for the model *A*. The results of these correlations were restricted to the region of the membrane that exhibited a near homogeneous deformation (Figure 2.10). It was found that the strain ratio gave a near incompressibility condition characterized by a third invariant with a value of approximately 0.982 to 0.993 (it is explicitly assumed that, during stretching, the lateral contractive strain in the thickness direction of the specimen was identical to the lateral contractive strain over the width of the specimen).

3.2.2 A model for the chemically-treated PVC geosynthetic

The experimental investigations indicate the progressive loss of the hyperelastic characteristic responses of the treated PVC geosynthetic during exposure to ethanol (Figure 2.14). Ideally, the development of a comprehensive model for a PVC geosynthetic subjected to chemical exposure should address the issue of the progressive change in the mechanical behaviour, in a time-dependent fashion. A further observation is that there is a limiting mechanical response resulting from chemical exposure, beyond which continued exposure does not result in an appreciable change in the strength of the PVC. For this reason, the model development for the mechanical behaviour of the PVC focuses on the commencement of the limiting level of material strength corresponding to 7 *months* of exposure to pure ethanol. The most noticeable observation in this case is the drastic increase in the stiffness of the PVC geosynthetic due to chemical alterations associated with the ethanol migration and the removal of the plasticizer. The characteristic hyperelastic large strain phenomena associated with loading paths of the untreated PVC geosynthetic have completely disappeared, the material has developed a pronounced yield point along with both strain softening and strain hardening responses. Finally, the material continues to sustain appreciable post yield large strain without failure at most exposure periods (Figure 2.12b). The constitutive model should therefore address these specific aspects. As far as permissible, the concepts put forward for the constitutive modelling of

the untreated PVC geosynthetic will also be adopted to define the mechanical behaviour of the chemically-treated PVC geosynthetic. Admittedly, a classical Hookean isotropic incompressible elastic model without the consideration of large strain effects can adequately describe the initial elastic behaviour of the chemically-treated PVC geosynthetic. To conform to the description of the model for the untreated material, a neo-Hookean form of the strain energy function is adopted, which can be derived from a Mooney-Rivlin form of strain energy function with $C_2' \approx 0$ and it reduces to the classical Hookean isotropic incompressible elastic model in cases when an infinitesimal strain measurement is adopted. As with (3.14), the strain energy function for the chemically-treated material contributing to the loading range of the stress-strain curve becomes

$$W^e(\dot{\gamma}_0, I_1^e, I_2^e) = C_1'(I_1^e - 3) \tag{3.29}$$

with

$$C_1' = C_1 + \begin{cases} \kappa_1 \ln(|\dot{\gamma}_0| / \dot{\gamma}_c^{<3>}) & ; \quad (|\dot{\gamma}_0| \geq \dot{\gamma}_c^{<3>}) \\ 0 & ; \quad (|\dot{\gamma}_0| < \dot{\gamma}_c^{<3>}) \end{cases} \tag{3.30}$$

The function for C_1' can also be obtained from a series of loading tests at loading rates $\dot{\varepsilon}_0 = 0.4\%/min$, $4\%/min$ and $40\%/min$. The procedure reveals the following logarithmic dependency of C_1' on $\dot{\gamma}_0$ (see also Figure 3.7):

$$C_1' = [12.06 \ln(\dot{\gamma}_0) + 180.32] MPa \tag{3.31}$$

A series of relaxation tests are conducted to investigate the time-independent response of the chemically-treated PVC geosynthetic. The results of the time-independent response are shown in Figure 3.8, which indicates $C_1 \approx 14.2 MPa$. The value $\dot{\gamma}_c^{<3>} = 1.0 \times 10^{-6} sec^{-1}$ for the chemically-treated PVC geosynthetic can be obtained by invoking $C_1' = C_1$ at $\dot{\gamma}_0 = \dot{\gamma}_c^{<3>}$. It is noted that $\dot{\gamma}_c^{<1>}$, $\dot{\gamma}_c^{<2>}$ and $\dot{\gamma}_c^{<3>}$ are essentially close. They therefore can be assumed to be characterized by a single *rate-independent threshold strain-rate* $\dot{\gamma}_c$ (i.e. $\dot{\gamma}_c^{<1>} = \dot{\gamma}_c^{<2>} = \dot{\gamma}_c^{<3>} = \dot{\gamma}_c = 5.67 \times 10^{-7} sec^{-1}$), which is also uninfluenced by the duration to

chemical exposure. In summary, the rate-dependency of the hyperelastic parameter C_1' for the chemically-treated PVC geosynthetic advocating equation (3.30) can be described by the following set of parameters: $C_1 \approx 14.2MPa$; $\kappa_1 \approx 12.06$; $\dot{\gamma}_c \approx 5.67 \times 10^{-7}\ sec^{-1}$.

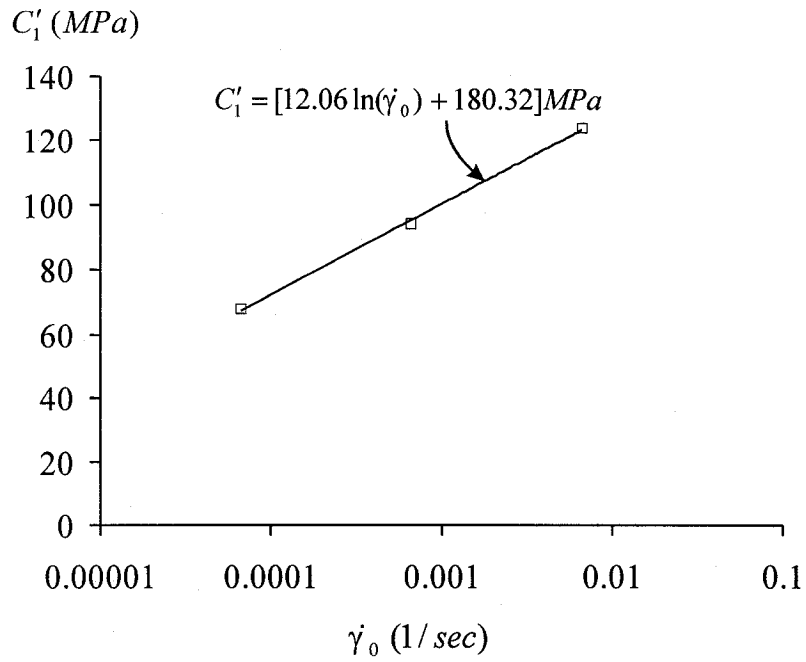

Figure 3.7 Rate dependency of C_1' on $\dot{\gamma}_0 (= \dot{\varepsilon}_0)$ for a chemically-treated PVC geosynthetic

Also the deviation from elastic behaviour commences with the initial yield of the chemically-treated PVC geosynthetic. The yield strain obtained from the data corresponds to $\zeta_y \approx 2.8\%$. This result indicates that ζ_y is relatively insensitive to the duration of chemical exposure. The yield point can be interpreted as that resulting from the breakage of the transitional link between the crystallite and the amorphous regions, which occurs at a critical strain $\varepsilon_0 = \gamma_0 = \zeta_y$. Its pronounced presence is then determined by the degree of susceptibility of the transitional link to the chemical exposure. The value of the yield strain is, however, uninfluenced by the duration of the chemical exposure. The breakage of the transitional link is assumed to cause changes in the elasticity parameters of the elastic recovery model *A*. Wilson (1995) indicated that it was the amorphous regions that accepted plasticizer while the crystallite regions preserved their structures during plasticization.

During the monotonic loading and prior to yield, therefore, the transitional link or the crystallite region can be viewed completely rigid in comparison to the deformability of the plasticized amorphous network. When the strain within the material reaches a critical value, the transitional link or the crystallite breaks, while preserving certain ability to prevent further large deformations. The abrupt breakage of the transitional link or the crystallite therefore contributes to the development of the *softening behaviour* of the material immediately beyond the yield. It remains a question, however, whether the modulus of the transitional link or the crystallite is zero after breakage. The existence of the non-zero elastic modulus of the transitional link can account for the slight *hardening behaviour* of the chemically-treated geosynthetic at larger deformations (e.g. $\varepsilon_0 = 100\% \sim 150\%$).

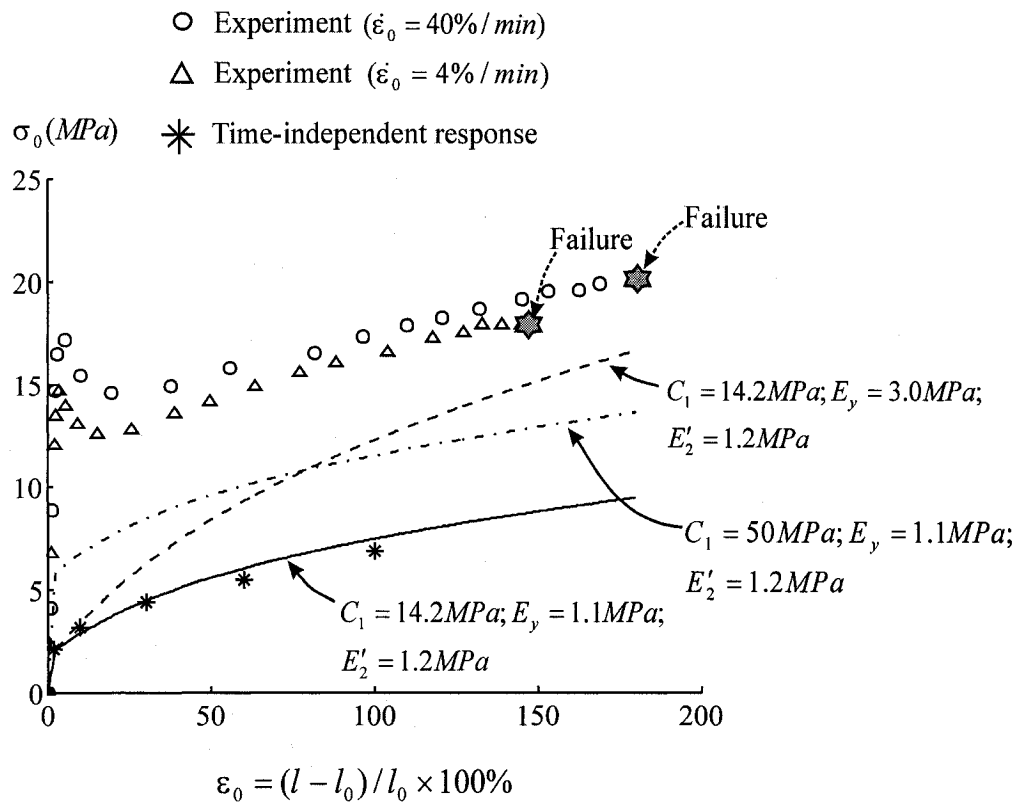

Figure 3.8 Curve-fitting of *hardening behaviour* of the time-independent response of the chemically-treated PVC geosynthetic

Therefore, as with the untreated PVC geosynthetic, the elastic parameter E_2' is assumed to be a constant, but E_1' considers the yield of the material and takes the form

$$E_1' = \begin{cases} \to \infty & ; \quad (\dot{\gamma}_0 \geq -\dot{\gamma}_c^v \quad \text{and} \quad \gamma_0 \leq \zeta_y) \\ E_y' & ; \quad (\dot{\gamma}_0 \geq -\dot{\gamma}_c^v \quad \text{and} \quad \gamma_0 > \zeta_y) \\ 0 & ; \quad (\dot{\gamma}_0 < -\dot{\gamma}_c^v) \end{cases} \tag{3.32}$$

where ζ_y is the yield strain and E_y' is the non-zero post-yield *hardening modulus*. The special representation for E_1' can take into account the fully elastic behaviour of the chemically-treated geosynthetic prior to yield at a loading rate $\dot{\gamma}_0 \geq -\dot{\gamma}_c^v$, where the visco-plastic deformation is restricted due to the infinite value of E_1'. A non-zero finite value of E_1' beyond the yield point, however, results in the development of visco-plastic deformation, which leads to a softening behaviour of the material and subsequent hardening behaviour in the large strain range (e.g. $\varepsilon_0 = 100\% \sim 150\%$). Upon unloading (i.e. $\dot{\gamma}_0 < -\dot{\gamma}_c$), the visco-plastic deformation is fully activated due to the zero value of E_1', which leads to appreciable irreversible visco-plastic permanent strains. The possibility of the rate-dependency of E_y' is also considered; i.e.

$$E_y' = E_y + \begin{cases} \kappa_y \ln(|\dot{\gamma}_0| / \dot{\gamma}_c^v) & ; \quad (|\dot{\gamma}_0| \geq \dot{\gamma}_c^v) \\ 0 & ; \quad (|\dot{\gamma}_0| < \dot{\gamma}_c^v) \end{cases} \tag{3.33}$$

where κ_y is the rate-sensitivity and E_y is the *rate-independent hardening modulus*. To further describe the visco-plastic responses in the chemically-treated PVC geosynthetic, the form of either (3.23) or (3.24) is adopted. Unlike with the untreated geosynthetic, the visco-plastic response in the chemically-treated PVC geosynthetic is not only dominant in the unloading process, but also accounts for the softening behaviour of the material beyond the yield point ζ_y.

The parameter identification for the visco-plastic responses begins with an examination of the time-independent response (Figure 3.8). In the chemically-treated PVC geosynthetic, there is a distinct yield point in the proposed time-independent stress-strain response. Softening behaviour is, however, absent, which proves the validity of the assumption

concerning the absence of a viscous effect at limiting loading rates less than $\dot{\gamma}_c^v$. The *static yield stress* $q(=6C_1\zeta_y) \approx 2.4MPa$ can be determined as a yield stress in the rate-independent stress-strain curve. From (3.32), it is inferred that, at a loading rate $|\dot{\gamma}_0| \le \dot{\gamma}_c^v$ and prior to the yield point, stresses in model A are zero as the elastic modulus $E_1' \to \infty$, which restricts any deformation in model A. The total external stresses applied to the material are then taken by model B according to (3.28). Therefore, at the instant of yield (i.e. $\varepsilon_0 = \gamma_0 = \zeta_y$), the relation of $\tau_B = q$ obtain, which gives rise to $d\zeta = d\gamma_0 = d\varepsilon_0$ in (3.24), which means that the contribution of the visco-plastic model C (Figure 3.5) to the time-independent response is marginal beyond the yield. All the subsequent hardening responses of the material then rely on the presence of the non-zero finite modulus of E_y and E_2' in model A. The values of E_y and E_2' can be obtained by matching the *slope* of the hardening behaviour of the time-independent stress-strain curve; this gives $E_y \approx 1.1MPa$ and $E_2' \approx 1.2MPa$ (see Figure 3.8).

Similarly, for the stress-strain responses conducted at a particular loading rate higher than the critical value $\dot{\gamma}_c^v$ (i.e. $|\dot{\gamma}_0| > \dot{\gamma}_c^v$), at large strains (e.g. $100\% - 150\%$), the effective stress $\tau_B \to q$; the visco-plastic response in model B is therefore nearly independent of the stress level of τ_B in (3.24). It is the values of E_y' and E_2' that determine the *slope* of the hardening behaviour of the material at this loading rate. The rate-dependency of the parameter E_y' can be obtained by matching the slope of the hardening responses for a series of loading tests conducted at the loading rates $\dot{\varepsilon}_0 = 4\%/min$ and $40\%/min$. The relevant constitutive parameters are: $E_y \approx 1.13MPa$; $\kappa_y \approx 0.13$; $\dot{\gamma}_c^v \approx 3.2 \times 10^{-10}\ sec^{-1}$. The remaining undetermined material parameter is the *viscous sensitivity* s. When s is close to zero, the unloading behaviour of the material, with $E_1' = 0$, is relatively insensitive to the loading rate. In the material softening region, where $E_1' \neq \infty$, the rate-sensitivity is noticeable even though s is close to zero. Therefore, the value of s has a significant influence on the softening behaviour of the material where E_1' abruptly transforms from an

infinite value to a finite value E_y' beyond the yield point (i.e. $\varepsilon_0 = \zeta_y$). Figure 3.9b shows the influence of the value of s on the quality of model representations. The curve fitting exercise is performed on the stress-strain curves at loading rates $\dot{\varepsilon}_0 = 4\%/min$ and $40\%/min$. The practice determines an appropriate estimate for $s \approx 0.1$ (Figure 3.9a).

Therefore all the parameters for describing the irreversible behaviour of the chemically-treated PVC geosynthetic are obtained. The relevant constitutive parameters for model A are: $E_y \approx 1.13MPa$; $\kappa_y \approx 0.13$; $E_2' = 1.2MPa$, and the parameters defining the visco-plastic component B are: $q \approx 2.4MPa$; $s \approx 0.1$; $\dot{\gamma}_c^v \approx 3.2 \times 10^{-10}\ sec^{-1}$. The material parameters determined can now be used to duplicate the experimental response for strain-rates of $\dot{\varepsilon}_0 = 4\%/min$ and $\dot{\varepsilon}_0 = 40\%/min$. The representations correlate well with the experimental data obtained for tests conducted up to peak strain of 140% (Figure 3.9c). The results at other peak strains 10% and 60% are predicted.

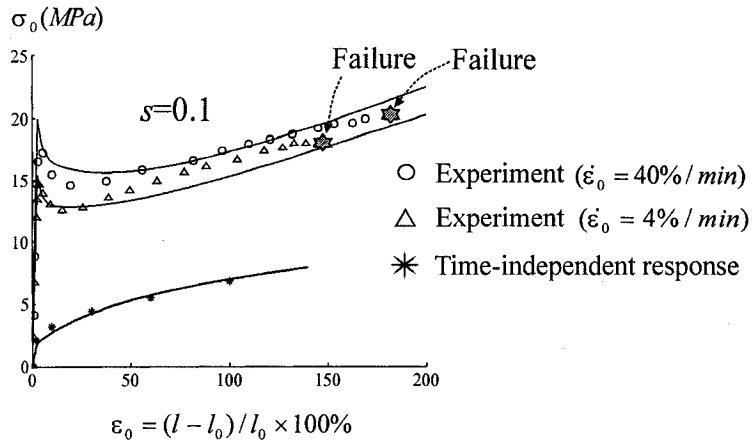

(a) Modelling of the stress-strain curves up to failure

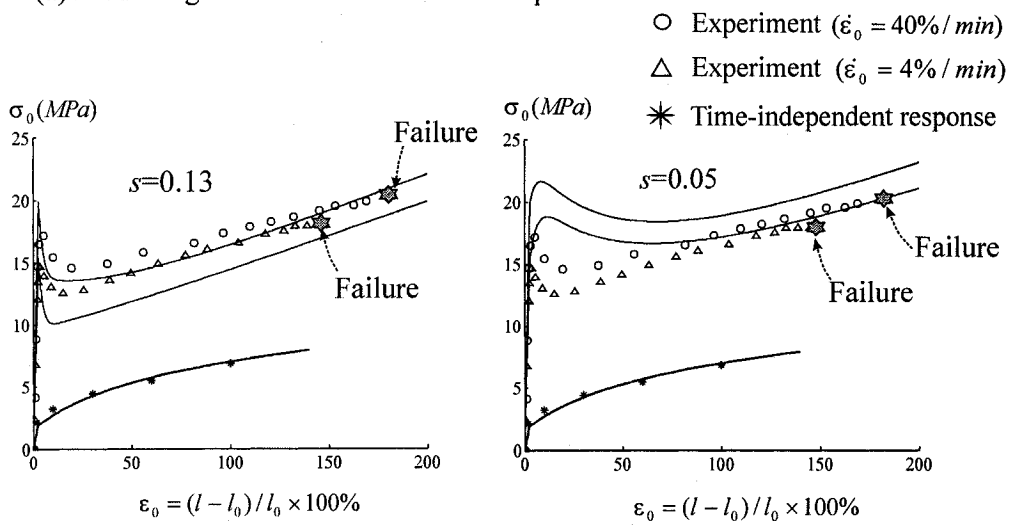

(b) Influence of the value of s on the quality of model representations

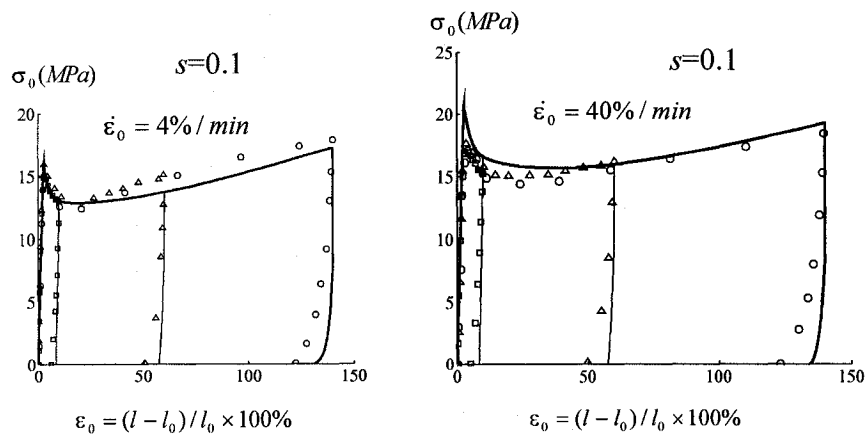

(c) Modelling of the stress-strain curves involving loading and unloading

Figure 3.9 Constitutive representations of the stress-strain responses of the chemically-treated PVC geosynthetic exposed to pure ethanol for 7 *months*

3.3 Summary of the constitutive models and predictions

A *single* generalized form of a constitutive model that accounts for large strain hyperelastic behaviour, strain-rate effects and moderately large irreversible plastic strains has been developed for modelling *both* the *untreated* and *chemically-treated* PVC geosynthetic. The mechanical response of the *untreated* material, however, has to distinguish between loading and unloading sequences through a selective treatment of the elastic parameters of the elastic recovery component. During loading, the visco-plastic deformation of the *untreated* material is restricted and the only deformation is attributed to elastic effects; upon unloading, however, the visco-plastic component is fully activated and unloading behaviour is accompanied by irreversible deformations. For the *chemically-treated* material, the material responses additionally take into account the yield of the material. Prior to yield (as defined by a ζ_y), the visco-plastic deformation is restricted; beyond yield, however, the visco-plastic component is activated, which accounts for further softening and hardening behaviour. Tables 3.1 and 3.2 give, respectively, the summaries of the equations used for describing the general forms of the constitutive models for both the *untreated* and *chemically-treated* PVC.

Table 3.1 Constitutive equations for *untreated* PVC geosynthetic

Components	Deformation gradient	Component A ($\mathbf{T}_A$)	Component B ($\mathbf{T}_B$)	Component C ($\mathbf{T}_C$)
Loading	$\mathbf{F} = \mathbf{F}^e$	Deformation restricted	Deformation restricted	Eq. (3.12), (3.13), (3.14),(3.18)
Unloading	$\mathbf{F} = \mathbf{F}^e\mathbf{F}^u$	Eq. (3.19) with $E_1' = 0$	Eq. (3.21), (3.23) or (3.24)	

Table 3.2 Constitutive equations for *chemically-treated* PVC geosynthetic

Components	Deformation gradient	Component A ($\mathbf{T}_A$)	Component B ($\mathbf{T}_B$)	Component C ($\mathbf{T}_C$)
Loading prior to yield point	$\mathbf{F} = \mathbf{F}^e$	Deformation restricted	Deformation restricted	Eq. (3.12), (3.13), (3.29) or (3.14) with $C_2' = 0$, (3.30)
Loading beyond yield point	$\mathbf{F} = \mathbf{F}^e\mathbf{F}^u$	Eq. (3.19) with $E_1' = E_y'$ and (3.33)	Eq. (3.21), (3.23) or (3.24)	
Unloading	$\mathbf{F} = \mathbf{F}^e\mathbf{F}^u$	Eq. (3.19) with $E_1' = 0$	Eq. (3.21), (3.23) or (3.24)	

The constitutive model developed is now used to *predict* the uniaxial response of the untreated and chemically-treated PVC geosynthetic exposed to pure ethanol for 7 *months*, which are tested at the loading rate $\dot{\varepsilon}_0 = 160\%/min$. The predictive capabilities of the models for a complete stress-strain curve that involve both loading and unloading have also been examined. The constitutive modelling for the chemically-treated geosynthetic should take into account the yield point and softening behaviour of the material. Figure 3.10 shows the comparisons between the results of the model and the corresponding test data. The results show good correlations between the two sets of results, particularly as loading-unloading cycles are carried out up to three levels of strain.

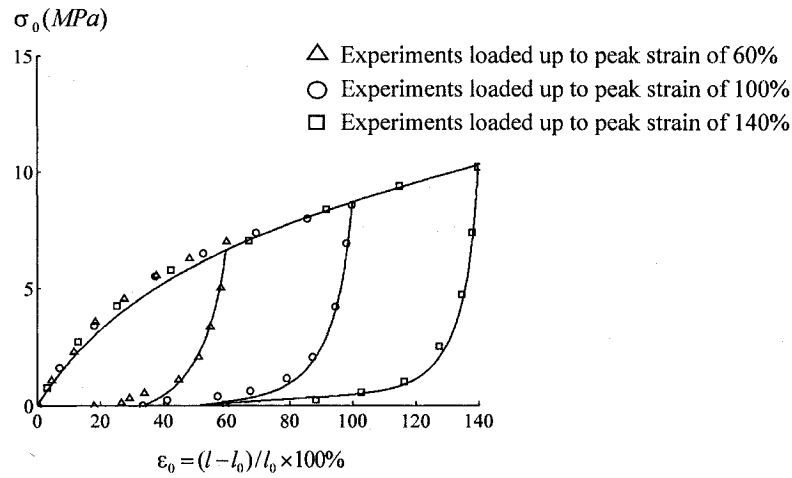

(a) Untreated PVC geosynthetic

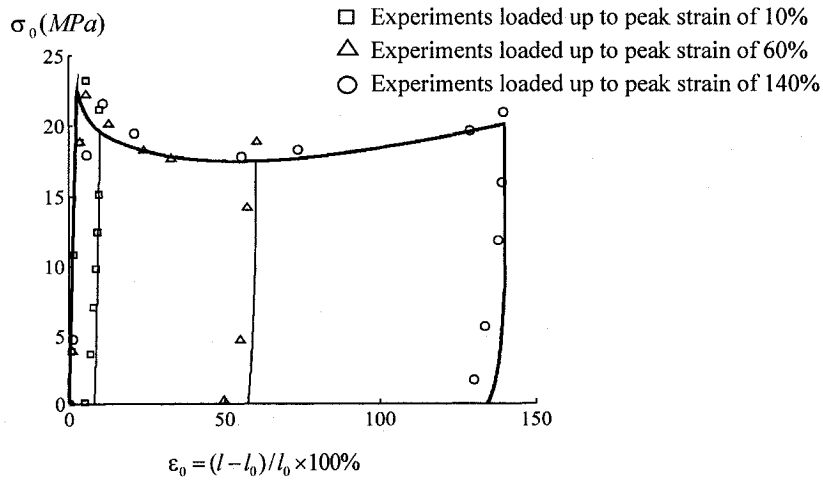

(b) Chemically-treated PVC geosynthetic exposed to pure ethanol for 7-*months*

Figure 3.10 Computational *predictions* for the stress-strain responses ($\dot{\varepsilon}_0 = 160\%/min$; symbols represent experimental results)

3.4 Samples subjected to varying durations of chemical exposure

It can be shown that the constitutive model developed for the untreated PVC geosynthetics and samples exposed to pure ethanol for 7 *months* can also be adopted for the description of the chemically-treated PVC geosynthetics that experienced varying durations of chemical exposure. Table 3.3 gives a summary of the material parameters for the samples at various durations of exposure to pure ethanol. It is noted that there is a set of material parameters that are essentially uninfluenced by the duration of chemical exposure; these are $\zeta_y = 2.8\%$; $\dot{\gamma}_c \approx 5.67\times10^{-7} sec^{-1}$; $\dot{\gamma}_c^v \approx 3.2\times10^{-10}\ sec^{-1}$; $E_2' \approx 1.2MPa$. The model representations of the experimental data conducted up to failure at loading rates $\dot{\varepsilon}_0 = 4\%/min$ and $\dot{\varepsilon}_0 = 40\%/min$ for samples subjected to different durations of exposure are presented in Figure 3.11.

Table 3.3 Material parameters of the chemically-treated PVC geosynthetic at varying periods of exposure to pure ethanol

Exposure period to pure ethanol	Parameters that are influenced by exposure duration						Parameters that are uninfluenced by duration of chemical exposure
	Component *A*		Component *B*		Component *C*		
	$E_y(MPa)$	κ_y	s	$q = 6C_1\zeta_y$ (MPa)	$C_1(MPa)$	κ_1	$\zeta_y \approx 2.8\%$; $\dot{\gamma}_c \approx 5.67\times10^{-7} sec^{-1}$; $\dot{\gamma}_c^v \approx 3.2\times10^{-10}\ sec^{-1}$; $E_2' \approx 1.2MPa$;
1 *week*	3.4	0.13	0.06	2	11.9	2.0	
2 *month*	2.88	0.087	0.115	2.3	13.7	13.0	
7 *months*	1.13	0.13	0.10	2.4	14.3	12.06	
9 *months*	1.90	0.087	0.09	2.6	15.0	9.0	
5 *months* followed by 7-*month* air exposure	4.13	0.087	0.11	4.2	25.0	19.0	

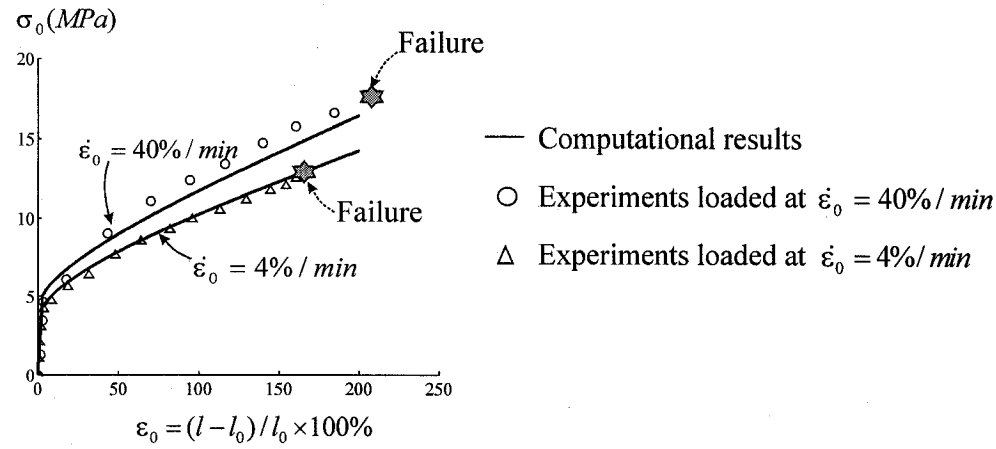

(a) 1-*week* exposure to pure ethanol

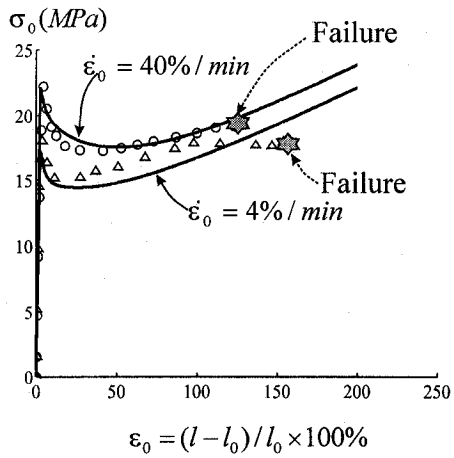

(b) 2-*month* exposure to pure ethanol

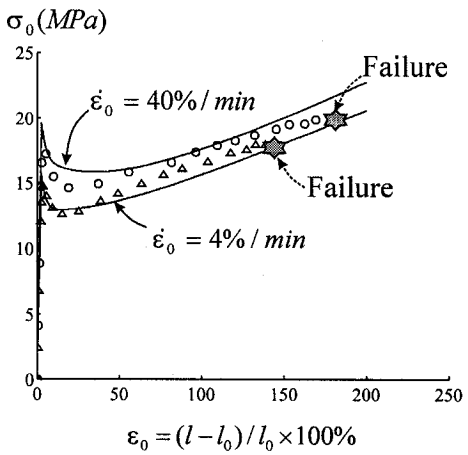

(c) 7-*month* exposure to pure ethanol

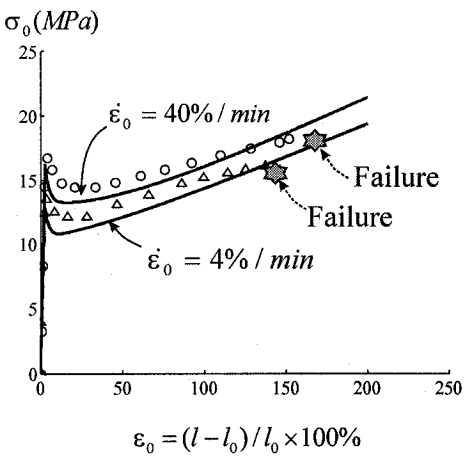

(d) 9-*month* exposure to pure ethanol

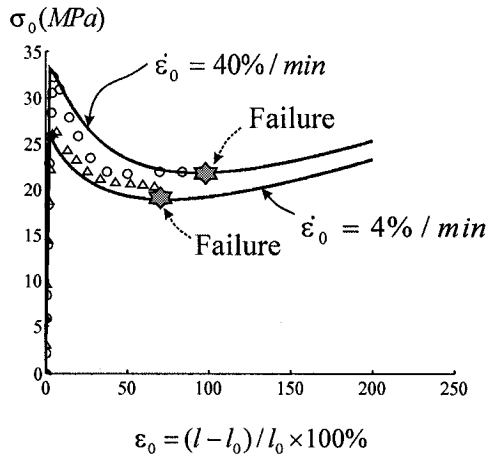

(e) 5-*month* exposure to pure ethanol followed by 7-*month* exposure to air

Figure 3.11 Model representations of the loading behaviour of PVC geosynthetics subjected to different durations of exposure to pure ethanol

3.5 The determination of α

The results of the uniaxial tests are insufficient to determine the parameter α [see Equation (3.12)] that accounts for effects of combined stretch. The influence of this parameter becomes appreciable when the PVC geosynthetic experiences bi-axial or inhomogenous stretching. The inhomogenous stretching of the PVC geosynthetic was achieved by stretching a square specimen fixed along oblique directions inclined at 45° to the axis of loading (see Figure 3.12a). Fixity was enforced at the boundaries of the tested specimen using a pair of aluminum grips. (At the time of conducting this type of test, the specimens subjected to 9 *months* of exposure to pure ethanol had all been used to conduct the uniaxial and membrane indentation tests.) The material parameter α was determined by conducting tests on samples of the PVC geosynthetic subjected to 5 *months* of exposure to ethanol followed by 7 *months* of exposure to air. The experiments were first conducted on samples of the untreated PVC. Observations of the distortion of a grid marked on the test specimen indicate that regions of the test specimen do experience biaxial effects at large deformations. These experiments were repeated using a PVC geosynthetic subjected to 5 *months* of exposure to pure ethanol followed by a 7-*month* exposure to air. It is concluded that the swelling phenomenon due to the absorption of the moisture resulted in the possible "softening" of the PVC geosynthetic at longer durations of exposure to pure ethanol (see Figure 2.14). Exposure to air leads to the removal of moisture and ethanol within the chemically-treated PVC geosynthetic; therefore, the response of a chemically-treated specimen subjected to prolonged exposure to air results in a stiffer mechanical response (Figure 3.11e) when compared to the stress-strain responses of the chemically-treated PVC geosynthetic in the absence of exposure to air. The constitutive model proposed in this chapter, together with the set of material parameters shown in Table 3.3, were used to examine the computational responses of the uniaxial test with oblique fixity. Since the plasticizer loss appears to stabilize after 5 *months* of exposure to pure ethanol (Table 2.1), it may be concluded that the material parameter α is relatively uninfluenced by the duration of chemical exposure. The material parameter $\alpha \approx 3$ is therefore considered to be applicable to PVC geosynthetics exposed to pure ethanol for a period of 7 *months*. The

particular value of $\alpha \approx 3$ is possibly indicative of equal contributions from the three principal stretch directions of the polymeric material in the definition of $\dot{\gamma}_0$.

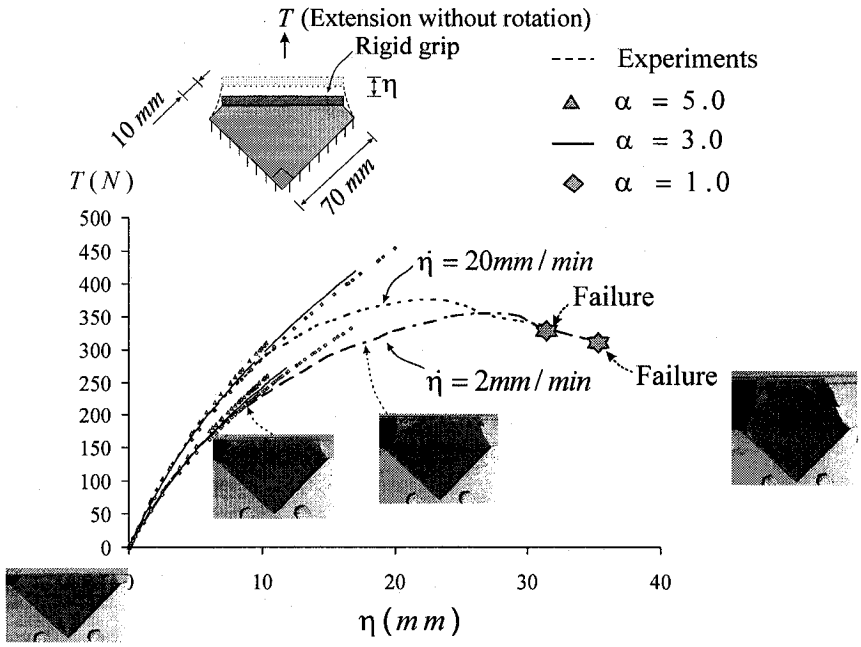

(a) Untreated PVC

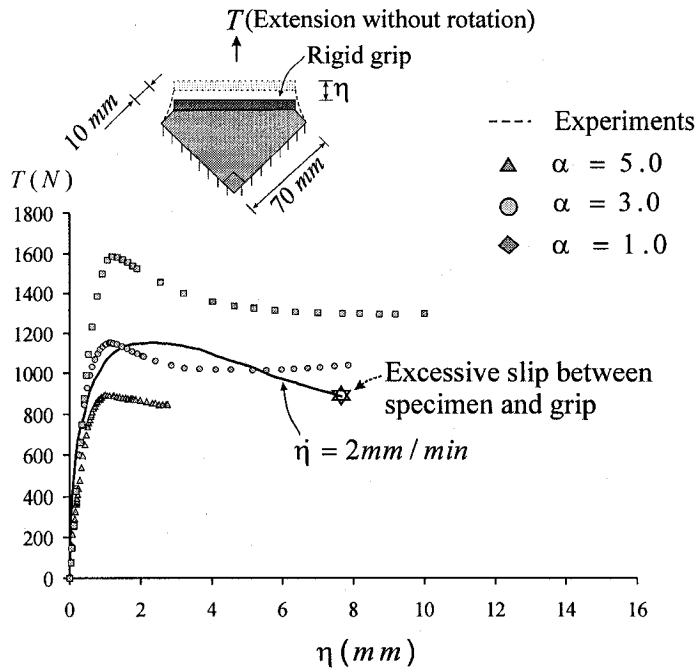

(b) PVC subjected to 5 *months* of exposure to pure ethanol followed by a 7-*month* exposure to air

Figure 3.12 Experimental determination of the material parameter α

3.6 Summary remarks

The accurate modelling of the mechanical response of a PVC geosynthetic has important implications to the engineering applications of such materials. The results of the experiments conducted in connection with the research program indicates that, in its natural condition the PVC geosynthetic is only capable of undergoing moderately large strains, the finite strain response of which can be modelled by appeal to a strain energy function of the Mooney-Rivlin form. Unlike natural rubber at moderately large strains, which is virtually void of irreversible phenomena and strain-rate effects, the PVC geosynthetic exhibits a strong rate-dependency and irreversible effects. Furthermore, the irreversible strains themselves can be within the realm of moderately large strains. This chapter used the results of a series of uniaxial tests described in the previous chapter to develop a plausible constitutive model that incorporates both strain-rate effects and moderately large irreversible strains. The parameter identification is conducted using the results of two sets of strain-rates and the results of a third series of tests are used to validate the constitutive model. The calibration exercise yields highly satisfactory correlations between the predictions and the experiments, although the range of applicability of the constitutive model is strictly limited to the basic Mooney-Rivlin form of the strain energy function with the constitutive parameters that are now strain-rate-dependent.

A majority of the investigations dealing with the constitutive modelling of rubber-like and highly deformable materials assume that the constitutive properties of the model remain invariant throughout the lifetime of their use. The role of chemically-induced alterations in the constitutive properties of rubberlike and PVC geosynthetic is gaining attention as the impact of such alterations on the functional properties becomes a topic of concern. With PVC-type materials it is found that their interaction with chemicals such as ethanol and acetone leads to embrittlement, with the attendant loss of their desirable highly elastic characteristics. The constitutive model development also addresses the loss of elasticity and the development of a distinct yield point in the stress-strain response of the chemically-treated PVC geosynthetic. It is shown that the basic constitutive responses involving large strain hyperelastic behaviour, strain-rate effects and moderately large irreversible plastic strains can also be modelled through the basic constitutive approaches adopted for the

description of the untreated PVC geosynthetic. Here again, the constitutive model developed uses a restricted data set for parameter identification and the predictive capabilities of the model are validated through the remaining data set. The correlations between the predictions of the constitutive model and the experimental data are considered to be highly satisfactory. It is noted that the PVC geosynthetic exposed to 13-*month* chemical exposure shows only moderate strain deformability with a failure strain at about 20% (Figure 2.14). This corresponds to an extreme case that can be possibly reached after hundreds of years of service in the field by considering a limited ethanol concentration of 2%-3% in the landfill (USEPA, 1988). On the other hand, experimental evidence found that, a PVC material that exhibited brittle behaviour at a particular loading rate could recover its large strain deformability at loading rates orders lower than the above rate (Pezzin et al., 1972). The constitutive model that is generally developed for large strain modelling is then considered also applicable to the specimen that experiences the longest exposure period and is only capable of experiencing moderate strains at the loading rate used in connection with the experimental program. In general, the constitutive model development for both the untreated and chemically-treated PVC geosynthetic results in correlations of satisfactory quality that permits the use of the models in the study of boundary value problems involving PVC geosynthetic membranes. The constitutive models developed are also in a sufficiently generalized form that enables their incorporation in advanced computational codes that have been developed in the literature for the modelling of membranes that can exhibit rate-sensitive responses in addition to the development of moderately large elastic and irreversible plastic strains.

CHAPTER 4

FRICTIONAL CHARACTERISTICS OF UNTREATED AND CHEMICALLY-TREATED PVC GEOSYNTHETIC

4.1 Introduction

In the previous chapters, the mechanical behaviour of PVC geosynthetic samples that were either untreated or subjected to concentrations of ethanol exposure was studied. The effect of pure ethanol exposure leads to the loss of flexibility or "embrittlement" of the PVC geosynthetic during an exposure period of *months*. In this chapter, the influence of chemical exposure as a result of the alteration in the mechanical behaviour on the frictional behaviour of the PVC geosynthetic will be discussed. Figure 4.1 shows aerial views of a landfill falure prior to and after failure, discharging $160{,}000\,m^3$ waste to a valley below (Brink et al., 1999). According to Brink et al. (1999), inadequate friction between the nearly-placed and orginal waste layers and that between the new waste layer and a layer of geomembrane placed underneath were reported to cause this catastrophe.

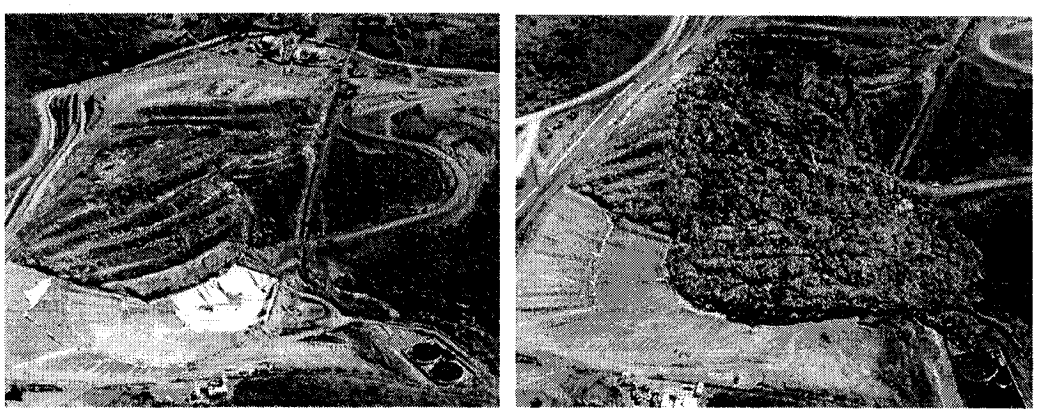

(a) Prior to failure (b) After failure

Figure 4.1 Aerial views of a landfill failure resulting from inadequate friction between a newly-placed waste layer and other landfill components (after Brink et al., 1999)

Attention is focused on the friction between a brass surface and the untreated PVC geosynthetic or samples exposed to pure ethanol for duration of 9 *months*. This will provide useful information about the possible influence of the friction coefficient between a brass indentor and the membrane specimen for the study of the mechanics of indentation of an untreated and a chemically-treated geosynthetic in subsequent chapters. Experiments reported in the literature (Pooley and Tabor, 1972) indicate that the friction coefficient between an untreated PVC material and a rigid glass surface varies between $\mu \in [0.30, 0.38]$. The coefficient of friction can, however, be influenced by the content of the additives such as plasticizer in the PVC material (Grosch, 1963; Masada et al., 1994). Barquins and Courtel (1975) also pointed out that untreated and irradiated material exhibited different frictional behaviour. Due to the rate-dependent nature of the mechanical responses of the parent polymeric material, the relative velocity between the contacting surfaces can influence the frictional behaviour (Schallamach, 1953; Pascoe and Tabor, 1956; James and Newell, 1980; Briscoe, 1981; Gascó et al., 1998). The frictional behaviour at very low speeds is governed by the presence of adhesion between two surfaces (Grosch, 1963; Barquins and Courtel, 1975). The adhesion forces can influence the true contact areas formed between the asperities in two surfaces (Pascoe and Tabor, 1956). Similarly, the normal pressure could also influence the frictional behaviour (Schallamach, 1952; Santner and Czichos, 1989). It is therefore necessary to conduct independent experiments to assess the friction between the brass surface and the untreated and the chemically-treated PVC geosynthetics used in the current research program.

4.2 Concept of frictional measurement

The frictional behaviour between the PVC geosynthetic and a metallic surface can be examined by inducing a specified displacement or a rate of displacement of a rigid surface of finite dimension that is larger than thickness of the PVC geosynthetic membrane (Figure 4.2). To ensure the fixity, the membrane specimen with a thickness of H is glued on a flat rigid base. A normal stress $\sigma_n (= F_n / A)$ is applied using static weights through the load transfer of the movable rigid plate on the contact surface, where A is the contact area. In order to minimize the influence of the vertical deformation of

the membrane specimen, the applied normal load is kept to a minimum. A friction force F_s between the rigid block and the PVC geosynthetic can then be generated by inducing a relative displacement φ of the movable plate at a controlled rate. The frictional behaviour between the PVC geosynthetic and the rigid surface can then be recorded as a relation between the average frictional stress $\tau_f (= F_s / A)$ and normalized sliding displacement φ / H. Furthermore, the ratio between F_s and F_n (or τ_f / σ_n) gives the frictional coefficient μ between the plate and the PVC geosynthetic. It is desirable that the friction forces F_s generated directly pass through the contact plane so that any overturning moment can be minimized (James and Newell, 1980). In the experiments, the amount of the overturning moment can be minimized by reducing the thickness of the movable plate, provided that the flexibility of the plate does not induce any non-uniform displacements either in the direction of the normal load or in the direction of the shear force.

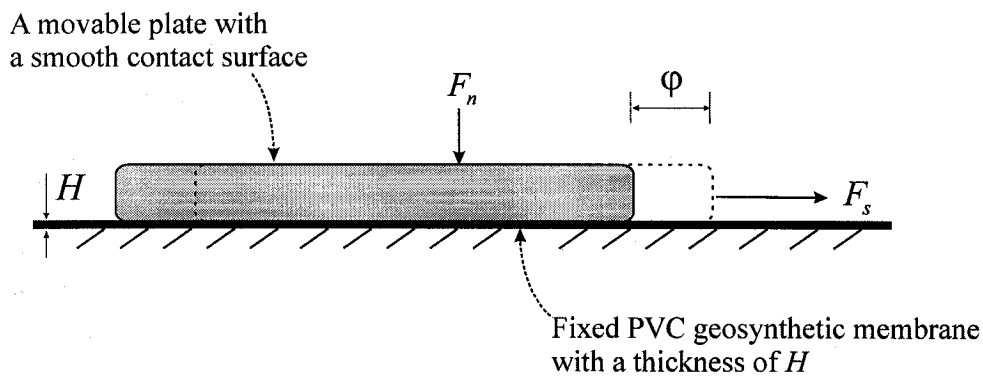

Figure 4.2 Concept of the frictional measurement

4.3 Experimental details

4.3.1 Preparations of the movable plate

A brass plate with a self-weight of $11.7N$ and with dimensions $127mm \times 127mm \times 9.5mm$ ($5inch \times 5inch \times \frac{3}{8} inch$) was used as the contact element (see also Figure 4.3a). For the purpose of friction measurement, the plate was considered thin enough to minimize the overturning moment; it is, however, also assumed to be stiff

enough so that it can sustain a normal weight of less than $100N$ without appreciable bending. As an estimation of the stiffness of the plate in the direction of the load F_s, the maximum in-plane extension of the plate is estimated to be $2\times10^{-4}mm$. Similarly, under the normal load F_n, the maximum differential deflection induced by bending of the plate is $4\times10^{-4}mm$. Before the friction experiments, the contacting flat surface was polished to a maximum asperity difference of $0.75\mu m$. Figure 4.3b shows the spatial distribution of maximum asperity height difference measured by the Surface Measurement Machine, at the Machine Tool Laboratory, Department of Mechanical Engineering, McGill University. The maximum asperity height difference was measured at nine equally-spaced points over a distance $10mm$ in the direction shown.

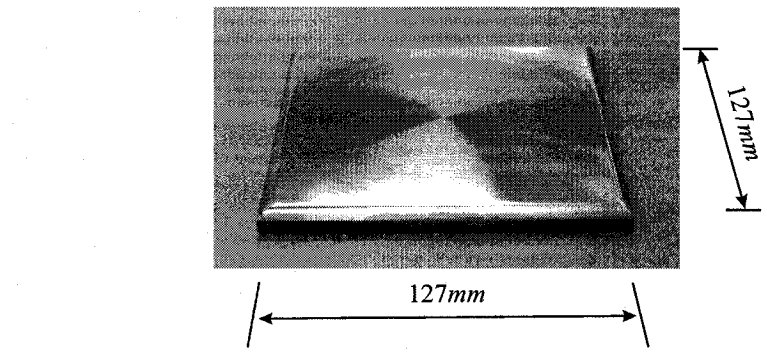

(a) Polished contact surface

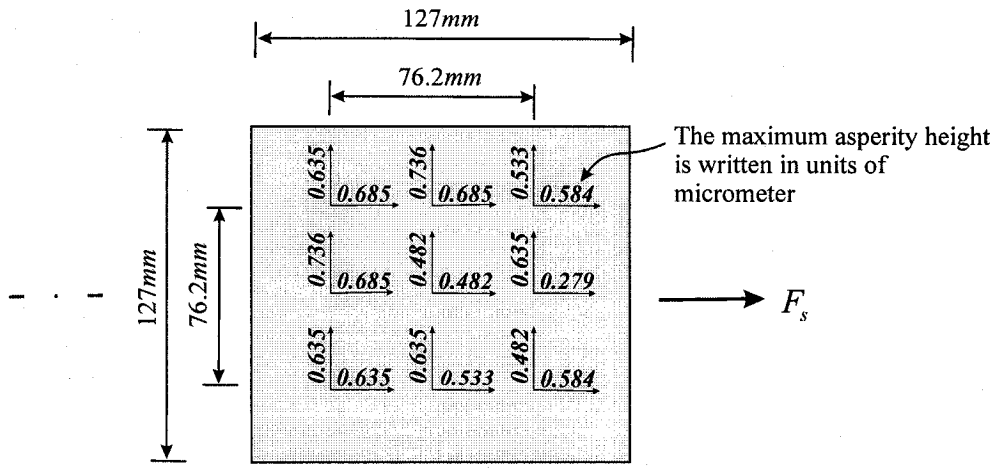

(b) Spatial distribution of the maximum asperity height of a contact surface

Figure 4.3 The geometry of the brass plate and asperity characteristics

4.3.2 Experimental setup

The experimental setup for measurement of friction consisted of a stationary platform that contained a surface of the membrane specimen glued to a flat Plexiglas plate. The membrane was bonded using a non-reactive LEPAGE 5© flexible plastic adhesive. The rigid plate was moved by a linear actuator that induced a relative displacement φ. The purpose of providing a fixed platform was to ensure the development of a flat contact plane between the brass surface and the membrane specimen. During the test, the sliding speed $\dot{\varphi}$ was maintained constant. To eliminate relative motion between the platform and the linear actuator, both components were fixed to a stationary aluminum plate (see Figure 4.4a).

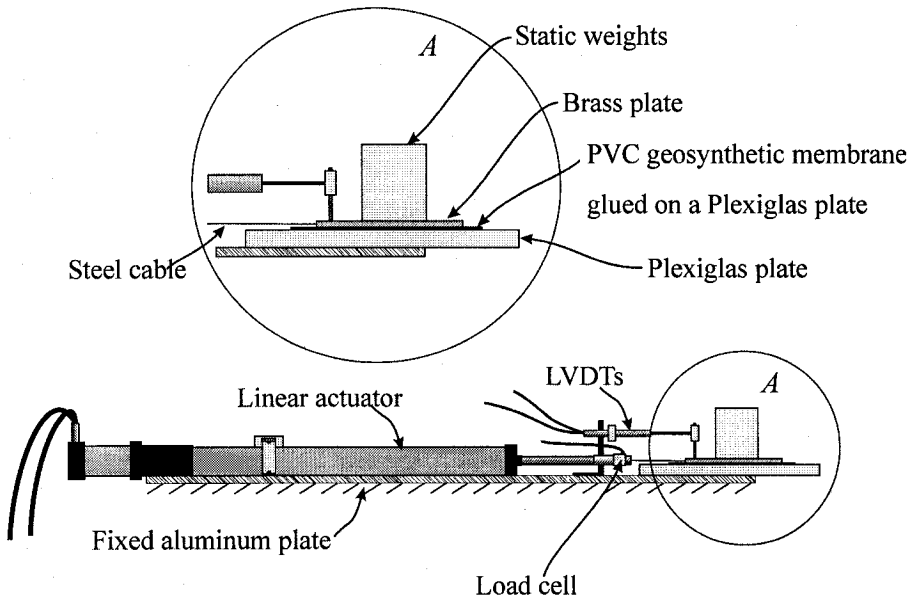

(a) Schematic view of the friction measurement device

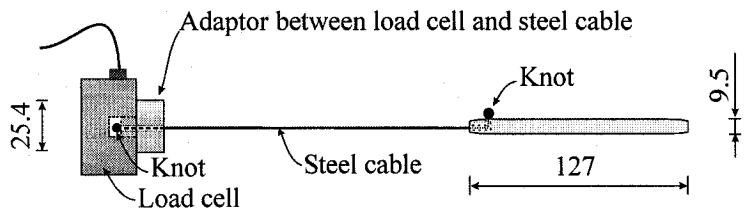

(b) The connection between the load cell and brass plate (all dimensions in *mm*)

Figure 4.4 Schematic view of the experimental setup for friction determination

The peak load capacity of the linear actuator that induced the relative displacement was $3100N$ and its maximum linear travel distance was $650mm$ at an accuracy of $\pm 0.025mm$. It was able to provide a maximum velocity of $\pm 0.4m/sec$. The frictional load F generated during the movement of the rigid plate was recorded by a load cell with a peak capacity of $4400N$ ($1000lbs$). The connection between the load cell and the movable brass plate was achieved through a horizontal inextensible cable of length $254mm$ ($10inches$) and diameter $0.5mm$ (see Figure 4.4b for details of the connection). The steel cable was situated horizontally in order to avoid any asymmetric movement that could be introduced to the metal plate. In principle, however, the tilt of the cable does not make an appreciable difference to the frictional forces induced at the contact plane, as long as the axis of the linear actuator remains parallel to the contact plane. Since the platform and linear actuator were both fixed to a rigid flat aluminum plate, this assumption is satisfied by the experimental configuration. The load cell and the cable were further connected by a cylindrical adaptor with a hole of $1mm$ diameter drilled through its axis. To prevent the detachment of the cable from the cylindrical adaptor, a knot was made at the end of the cable. The other end of the steel cable was connected to the movable brass plate in a similar manner. To minimize the vertical deformation of the membrane specimen, a low normal load F_n was applied. The magnitude of the vertical load was $87.3N$ and this load gave rise to a normal pressure of $6.14kPa$ at the contact plane. In the literature, friction between a metal surface and a polymer surface is usually measured at much larger normal pressure over $1MPa$ (Schallamach, 1952; Pooley and Tabor, 1972). The work of Pascoe and Tabor (1956) and Santner and Czichos (1989) pointed out that the friction at low normal stresses (less than $1000kPa$) mainly resulted from adhesion between the contacting surfaces, which accumulated as a function of time. Therefore to avoid excessive adhesion between the two contacting regions, the contact time between the brass plate and the PVC geosynthetic was kept to less than $30sec$ prior to the start of a frictional test. In order to record any occurrence of rotation of the brass plate during sliding, two LVDTs spaced $76.2mm$ apart were used to measure the displacement of the plate in the shear direction (see Figure 4.5). The LVDT readings during a frictional test conducted on an untreated PVC geosynthetic are presented in Figure 4.6. The readings between two LVDTs exhibit a maximum difference of 7% for a given maximum

displacement of 25.4*mm*. The influence of the rotation of the brass plate on the friction measurement is therefore neglected. On the other hand, the average reading of the two LVDTs is very close to the displacement provided by the linear actuator (with a maximum difference of 4%). The value of the displacement recorded from the linear actuator is therefore selected as the relative displacement between the brass plate and the membrane specimen.

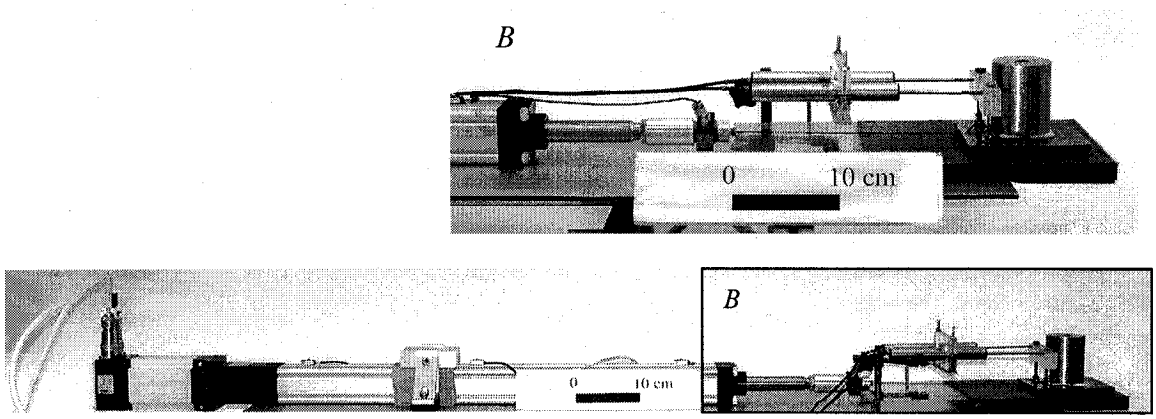

Figure 4.5 Friction measurement facility

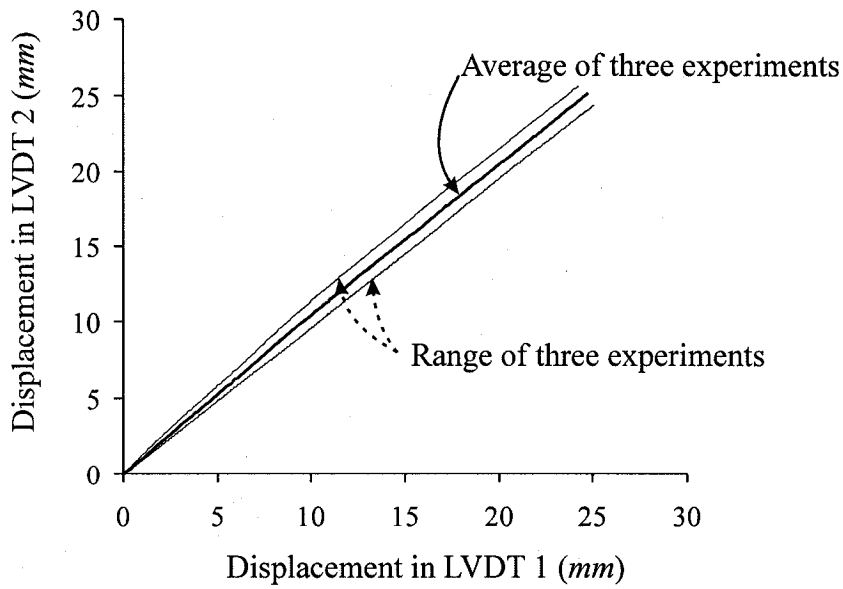

Figure 4.6 LVDT readings during friction tests

4.4 Experimental results

The experimental program first examined the frictional behaviour between the brass surface and the untreated membrane specimen. Due to the time-dependent mechanical behaviour of the polymeric material, the friction between a metal surface and the PVC surface will be influenced by the speed of the relative displacement (Schallamach, 1953; Grosch, 1963; Barquins and Courtel, 1975; Briscoe, 1981; Gascó et al., 1998; Persson, 1998; Zhang, 1998). A preliminary testing program was conducted by varying the displacement rate $\dot{\varphi}$ from $0.025mm/sec$ to $0.50mm/sec$. The upper limit for the speed was chosen such that it was the maximum speed of movement of the indentor in the membrane indentation test, which will be discussed in subsequent chapters. At the upper limit of maximum speed, the friction coefficient increased by 10%. The influence of the relative velocity on the friction was considered to be negligible and friction was evaluated at the relative velocity $\dot{\varphi} = 0.50mm/sec$. The variation in the frictional stress F_s/A with normalized relative displacement φ/H are shown in Figure 4.7. The differences between the static friction and the dynamic friction coefficients are negligible compared to the variability in the experimental data. In the experiment conducted by Pooley and Tabor (1972), these two values were also relatively close, for contacts between a PVC material and a rigid glass surface. Results of the current series of experiments indicate that the coefficient of friction for the contact between the untreated PVC geosynthetic and the brass plate can be estimated at $\mu = 0.52$. An identical experiment was performed to determine the coefficient of friction between the chemically-treated PVC geosynthetic and the brass plate. The results of the experiments are shown in Figure 4.7. As can be observed, the coefficient of friction is significantly lowered as a result of exposure to the PVC geosynthetic to pure ethanol. The estimated value of coefficient of friction is $\mu = 0.08$ for the chemically-treated PVC geosynthetic.

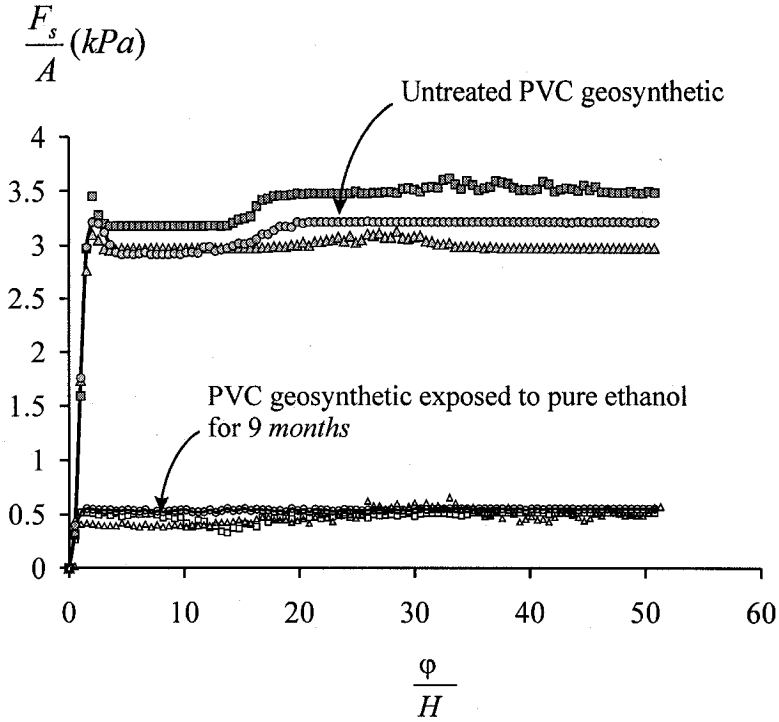

Figure 4.7 Frictional behaviour between a brass plate and a PVC geosynthetic (under normal pressure of $\sigma_n = 6.14kPa$; F_s : frictional force; A : contact area; φ : relative displacement between brass plate and PVC geosynthetic membrane; H : thickness of the PVC geosynthetic membrane)

4.5 Summary remarks

This chapter examines the frictional behaviour of both untreated and chemically-treated PVC geosynthetics that are in contact with a brass plate with a prescribed surface roughness defined by a maximum asperity height of $0.736\times10^{-6}m$. The experiments focus on PVC geosynthetics exposed to pure ethanol for duration of 9 *months*. Chemical exposure leads to a substantial reduction in the friction coefficient between a brass plate and a PVC geosynthetic membrane. The reduction in friction coefficient is considered to be attributed to the embrittlement in the mechanical behaviour of the chemically-treated material (see also Grosch, 1963). As such, the friction coefficient of a PVC geosynthetic membrane in contact with other geomaterials such as geotextile and soil can possibly expected to be reduced (Masada et al., 1994). Although the friction between a

geosynthetic membrane and a brass plate does not directly represent the field condition experienced in the landfill, the alterations in its friction coefficient constitute an index of loss of its performance in landfill slope applications as a result of chemical exposure. In conventional geotechnical practice, the design of slope stability of the landfills is generally based on the laboratory values of friction coefficient of the PVC geosynthetic membrane in its untreated condition and therefore plausible (Koerner, 1994; Qian et al., 2002).

CHAPTER 5

INDENTATION OF AN UNTREATED PVC GEOSYNTHETIC MEMBRANE

5.1 Introduction

In the previous chapters, the constitutive characterization of the alterations in the mechanical behaviour after chemical exposure has been examined through a coordinated set of uniaxial tests. This chapter focuses on the study of the mechanics of a flat PVC geosynthetic membrane subjected to lateral indentation. The specific problem chosen for the experimental study is that of a PVC geosynthetic membrane that is fixed along a circular boundary and subjected to either an axisymmetric or asymmetric indentation through a loaded rigid spherical indentor (Figure 5.1).

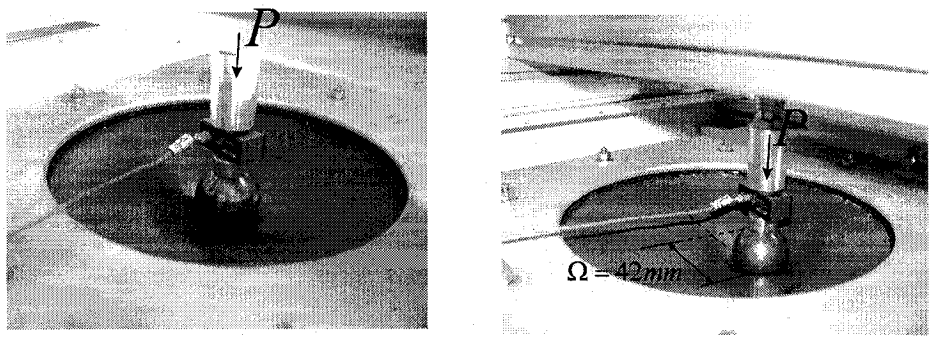

(a) Axisymmetric indentation (b) Asymmetric indentation

Figure 5.1 Indentation of a PVC geosynthetic membrane

The problem simulates situations that involve localized loading of membranes used in placement and construction or operation of the landfill and serves as a useful method for calibrating the constitutive responses of the PVC geosynthetic determined from conventional uniaxial testing. The indentation test can also give useful information

concerning the behaviour of a PVC geosynthetic material that may be subjected to ballooning as a result of the buildup of gas pressure (Figure 1.2).

The literature on the mechanics of membranes, in general, is quite extensive and no attempt will be made to review of all available articles. The history of the study of mechanics of membranes dates back to the work of Föppl, Hencky, Clebsch, Schwerin, Girkmann, von Karman and others and useful historical reviews are given by Timoshenko (1953), Timoshenko and Woinowsky-Krieger (1959), Naghdi (1972) and Libai and Simmonds (1988). Many of the classical studies dealing with the mechanics of membranes focus on the modelling of the large deflection-large rotation response of membranes composed of an elastic material with a linear Hookean response. Since the scope of the present paper relates to materials that can exhibit large strain hyperelastic phenomena with consistent constitutive modelling, it is pertinent to present here a brief account of developments that are germane to the themes discussed in the thesis. These include topics such as pressurization and indentation of flat circular membranes comprised of hyper-elastic materials, localized loading of hyper-elastic materials, indentation of membranes with classical linear elastic constitutive responses, mechanics of membranes with inelastic and time-dependent responses and experimental evaluation of membrane behaviour. An investigation of a membrane indentation problem presented by Bhatia and Nachbar (1968) examines the axisymmetric indentation of a pre-stressed elastic membrane with a linear elastic constitutive response. The theoretical developments were also used by these authors to interpret the results of experiments obtained from indentation tests conducted on stretched Mylar sheets. Kao and Perrone (1971) examined the problem of the transverse loading of a circular membrane, formulating the problem using the non-linear partial differential equations arising from the large deflections of membranes, albeit using only linear elastic stress-strain relationships. These authors also examined the problem of the axisymmetric indentation of the membrane by a rigid circular disc. Seide (1977) investigated the problem of the transverse loading of a rectangular membrane by a uniform pressure. Here again, the analysis was restricted to the non-linear equations governing large deflections of the membrane with linear elastic constitutive response. Dickey (1967) considered the

geometrically nonlinear problem of the deflection of a plane circular elastic surface under the action of a normal pressure occupying the entire area. Although the constitutive behaviour was restricted to classical Hookean elasticity, the paper addressed several topics related to the existence and uniqueness of the nonlinear problem. Allman (1982) has presented a variational solution to the problem of the non-linear deflection of an annular membrane subjected to an axial load. The problem of the non-linear behaviour of a circular membrane subjected to a concentrated force was presented by Dickey (1983). Both these investigations are restricted to membrane behaviour characterized by the classical theory of elasticity. An early application of the theory of finite elasticity to the problem of the inflation of a membrane is due to Adkins and Rivlin (1952), who considered the inflation of a plane sheet to a nearly spherical shape. In their study, the experimental results by Treloar (1943) were complemented by a comprehensive finite elasticity analysis of the problem for various types of rubber-like elastic materials, with different forms of the strain energy functions. Klingbeil and Shield (1964) used a central difference analysis of a pressurized flat circular rubber membrane problem to determine the empirical forms of the relevant strain energy functions. Foster (1967) examined a similar study of the inflation of a flat circular membrane to a nearly spherical shape, and presented comparisons with analytical solutions developed for a Neo-Hookean material. The problem of the stress concentration due to stretching a rubber sheet containing either a circular hole or a rigid circular inclusion was examined by Yang (1967); numerical results were presented for a rubber-like elastic material with a strain energy function of the Mooney-Rivlin type. Hart-Smith and Crisp (1967) also presented a very comprehensive study of the stretching of a rubber membrane and the theoretical developments are discussed in relation to the experimental results obtained by Treloar (1943). These authors also highlight the advantage of using the membrane inflation problem as a technique for determining the constitutive parameters for the rubber-like materials. Wu (1970a) considered the problem of the deformation of a tube of hyperelastic material that transforms the tube to an annulus and presented an exact solution to the problem, applicable to hyperelastic materials with strain energy functions of the Mooney-Rivlin and Neo-Hookean type. Wu (1971) also applied methodologies to examine certain contact problems associated with the immersion of a pressurized

cylindrical membrane beneath a fluid, due to the action of a rigid indentor. Pipkin (1968) and Wu (1970b) considered solutions to hyper-elastic membrane problems where the undeformed surface corresponds to a cylindrical surface. In this case the equation of equilibrium for the direction tangent to the meridian curve can be integrated exactly. Of related interest are the papers by Kydoniefs (1969) and Kydoniefs and Spencer (1969) who examined the hyper-elastic problems related to the behaviour of an initially axisymmetric cylindrical membrane and the interaction of an initially cylindrical membrane enclosing a rigid body. References to further studies are also given in the review article by Spencer (1970). Yang and Feng (1970) examined the problem of the inflation of a flat circular membrane due to uniform pressure. The numerical technique proposed in the paper was applied to develop solutions for the inflation of a circular membrane or sheet, the constitutive behaviour of which is modelled by a Mooney-Rivlin material. Extensive numerical results are provided for the membrane profile at different stages of the inflation process. The problem of the axisymmetric indentation of a circular membrane by a spherical indentor was studied by Yang and Hsu (1971); again, the governing non-linear equations were solved for the case of a Mooney-Rivlin material. The problem discussed in the paper by Yang and Hsu (1971) has a close resemblance to the study that will be discussed in this chapter except that the constitutive response of the PVC geosynthetic material is markedly different from that of the rubber-like elastic material. Similar results have been obtained by Feng and Yang (1973), Yang and Lu (1973), Feng et al. (1974), and Feng and Huang (1975) for both inflation and inflation-induced contact problems related to circular and rectangular membranes. Problems related to the axisymmetric inflation of a circular membrane containing a rigid disc inclusion and the inflation of an ellipsoidal membrane were examined by Tielking and Feng (1974), using a minimum potential energy approach. Feng et al. (1974) extended these studies to develop a solution to the problem of an edge-constrained square membrane subjected to uniform pressure and included a situation where a contact constraint is induced by a rigid smooth obstacle on the deformed membrane. The problem of the radial deformation related to a plane-sheet containing either a circular hole or a rigid circular inclusion has been examined by Verma and Rana (1978). The measure of strain used in their study is that due to Seth (1964) and the solution differs from that

given by Yang (1967). Pujara and Lardner (1978) discuss the inflation problem for a flat circular membrane and present results for two classes of rubberlike elastic materials, including the Mooney-Rivlin material and one suitable for the blood cell membrane, proposed by Skalak et al. (1973). Wu (1979) examined the finite strain problem related to a membrane; the treatment in the paper is relatively general, although explicit results are given for the problem of a plane circular membrane of a Neo-Hookean material that transforms to a near-spherical surface. Feng (1987) also examined the problem of the indentation of a membrane by an indentor in the form of a paraboloid of revolution. Numerical results are presented for the case where a square membrane composed of a Mooney-Rivlin material is indented by a paraboloid of revolution. The study by Fulton and Simmonds (1986) considers the large deformations resulting from edge loading of annular membranes. Results are presented for hyperelastic materials with strain energy functions of the Neo-Hookean and Mooney-Rivlin forms and for the strain energy function proposed by Rivlin and Saunders (1951). The problem of the finite deformation of a circular elastic membrane containing an axially-loaded concentric rigid inclusion was considered by Tezduyar et al. (1987). The resulting non-linear problem is solved for the special case of a Mooney-Rivlin material using a Newton-Raphson procedure. Pamplona and Bevilacqua (1992) considered a similar problem for both Neo-Hookean and Mooney-Rivlin materials, using a numerical scheme based on Picard-iteration technique to solve the non-linear problem. The review article by Beatty (1987) contains further references to topics of interest to membrane problems. The problem of the finite deformation and stability of spherical membranes under axisymmetric concentrated loads have been investigated both experimentally and computationally, by Glockner and Vishwanath (1972), Szyszkowski and Glockner (1987), and Dacko and Glockner (1988). The analysis presented by Li and Steigmann (1995) considers the point loading of a spherical elastic membrane with a relaxed strain energy function derived from the three-term strain energy function given by Ogden (1984). Useful experimental results concerning nano-indentation of polymeric surfaces are given by Poliane et al. (2000) although the results are largely related to linear elastic analysis of the indentation problem. The problem of the inflation of a rubber-like elastic material studied by Rachik et al. (2001) presents a useful account of the use of the experimental results for the

purposes of material parameter identification, both directly and indirectly, for a strain energy function of the following forms: generalized Mooney-Rivlin, Yeoh (1993), Arruda and Boyce (1993), Ogden (1984) and van der Waal's model. Arroyo and Belytschko (2002) also examine the finite deformation problem for a membrane in the context of the modelling of nano-tubes. In their study, a continuum model is presented for a one-atom thick crystalline film. An inter-atomic potential of the Born-type is used to construct the strain energy function applicable to the equivalent continuum. These authors have implemented the constitutive model in an advanced computational scheme that can accommodate large strain elasticity phenomena. Computational results presented illustrate the development of global and local instabilities in nano-tubes. The applications of non-linear theories that incorporate time- and rate-effects in the finite strain constitutive responses are not extensive. The axisymmetric inflation of a non-linear viscoelastic membrane by lateral pressure is presented by Wineman (1976). The solution of a system of non-linear Volterra-type integral equations is used to generate results for the time-dependent constitutive relationship of a vulcanized styrene-butadiene rubber (McGuirt and Lianis, 1970). In a further study by Wineman (1978) dealing with the problem of the inflation of a circular membrane by lateral pressure considers a fluid-like material such as polyisobutylene with deformability characteristics that are history-dependent. Feng (1992) has considered the time-dependent problem of finite deformation of a membrane with a constitutive response of the non-linear viscoelastic-type; the study also presents experimental investigations of the inflation of a plane circular membrane. Wineman and Huntley (1994) considered deformation-induced microstructural changes to the rubbery material and studied the axisymmetric inflation of an elastic membrane with an original strain energy function of a Neo-Hookean type. The above brief review is by no-means complete but suggests that much of the literature pertaining to mechanics of membranes undergoing finite deformations has focused on rubber-like membranes with time-independent constitutive responses. The focus of this study is to apply the relevant constitutive responses that were developed in Chapter 3 to investigate the behaviour of a plane circular membrane that is subjected to indentation. Attention is restricted to the untreated PVC geosynthetic membrane and constitutive modelling takes into consideration the influence of large strains and both elastic and visco-plastic effects.

These constitutive models are implemented in the general-purpose ABAQUS/Standard finite element code, to develop computational estimates of the deformations of the PVC geosynthetic membrane with a circular platform, which is subjected to both axisymmetric and asymmetric indentation by a rigid spherical indentor.

5.2 The test facility

The membrane indentation facility shown in Figure 5.2a is designed to apply a controlled movement to a rigid spherical indentor (with a diameter of $50.8mm$) that interacts with a membrane specimen. The test facility has provisions for securing a plane membrane specimen in a fixed condition along a circular boundary. The diameter of the flat PVC geosynthetic membrane sample that is subjected to indentation is approximately $250mm$. The fixed boundary condition is achieved by clamping two aluminum plates that are secured with $4mm$ screws. To reduce the stress concentration near the clamped edge, the boundary of the aluminum plates is bevelled to a circular cross section. Previous tests conducted on the PVC geosynthetic membrane indicated the possibility of slippage at the fixed end. To eliminate this effect, a rubber sheet of thickness $3mm$, which contains an opening of diameter $250mm$ was bonded to the PVC specimen, using a non-reactive (LOCTITE ® 404) instant adhesive (Figure 5.2b). The test specimen was clamped between two aluminum plates ($5mm$ in thickness) to form a specimen assembly as shown in Figure 5.2c. During the axisymmetric indentation, contact was established at the center of the membrane (Figure 5.1a). The indentation was achieved by moving a polished brass indentor (with roughness corresponding to a maximum asperity difference $0.2\times10^{-3}mm$) against the membrane at a prescribed rate. The rate of indentation $\dot{\Delta}$ is set constant during a test. A computer controlled linear actuator is used to move the spherical indentor. The applied displacement can be measured to a maximum accuracy of $0.025mm$. The loads applied to the indentor are low enough to neglect any elastic deformation of both the linear actuator and the connecting devices.

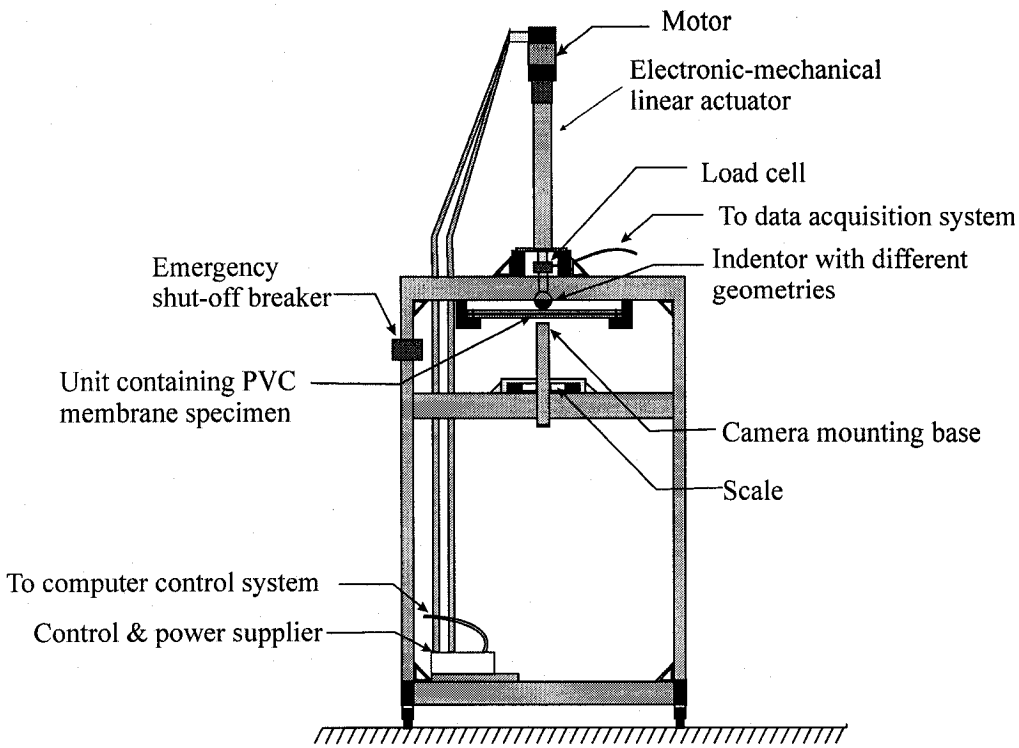

(a) Schematic view of the test frame

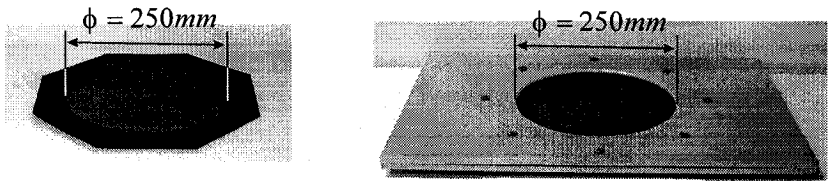

(b) PVC test specimen (c) Clamped plate assembly

Figure 5.2 Membrane indentation test facility

The measurement of the deformed shape of the membrane forms an important component of the experimental results that will be subsequently used in the calibration of the computational predictions. The three-dimensional shape of the deformed geometry can be measured using quite sophisticated optical techniques including holography and Moire interferometry. However, in the current experimental research, attention was restricted to the measurement of the deformed profile using a simplified optical technique. A visual image of the deformed profile was first captured using a high precision (5 Mega pixels)

digital camera, which was mounted on the test frame and positioned $1.5m$ from the axis of the test specimen. The (x, z) coordinates of the deflected profile were determined using an image analysis procedure (Klette, et al., 1998). In this procedure, the coordinates were first measured in terms of image *pixels* and subsequently calibrated against the known dimensions of two scales that were located on the test frame. The centers of the two scales were aligned on a plane passing through the optical axis of the camera, which was also normal to the image plane. The camera was positioned to capture a representative image through the plane of deformationed symmetry of the membrane, equidistant from the center of the membrane. The load (P) transmitted through the indentor was measured using a load cell with a peak capacity of $4400N$ ($1000lbs$). The loads were continuously recorded through a data acquisition system (National Instruments) with appropriate software (Labview System). The indentation response was prescribed through the application of the indentation displacement in an incremental manner up to a maximum displacement of $\Delta_{max} = 76.2\,mm$. The ratio of the maximum axial displacement to the membrane diameter reached approximately 0.30 during the axisymmetric loading of the circular PVC geosynthetic membrane. This corresponds to an overall average strain of 17% in the radial direction; preliminary computations, however, indicate that the maximum strain reaches 40% at the line of separation between a contact. The load-displacement response during axisymmetric indentation is shown in Figure 5.3a. The results show a good repeatability between sets of experiments. The inset figures in Figure 5.3a indicate the configuration of the deformed membrane. The PVC geosynthetic membrane exhibits irreversible deformations after a loading-unloading cycle. During asymmetric indentation, the contacts were initiated at a distance Ω from the axis of the circular membrane (Figure 5.1b). The image analysis of the deflected shape indicates that $\Omega \approx 42mm$, which is close to the measured value of $41.5mm$. The maximum indentation displacement applied during the asymmetric indentation was also $\Delta_{max} = 76.2\,mm$. This displacement gave rise to an overall average strain of approximately 20%; preliminary computations, however, indicate that the maximum strain reaches 50% at the line of separation between a contact. In comparison to the case of axisymmetric indentation, slightly larger forces were needed to induce asymmetric indentation (Figure 5.3).

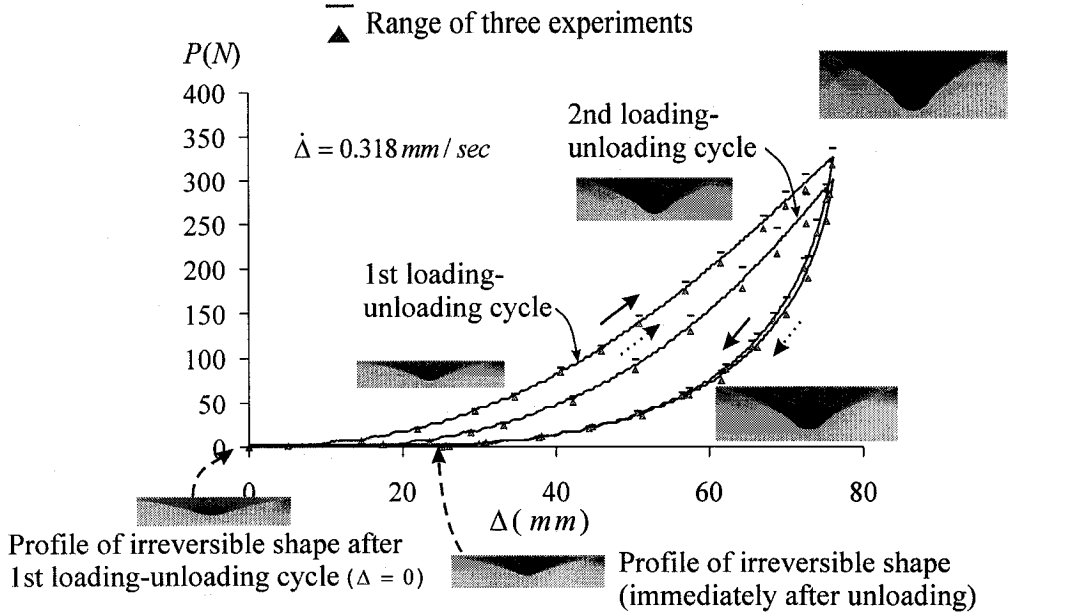

(a) Axisymmetric indentation

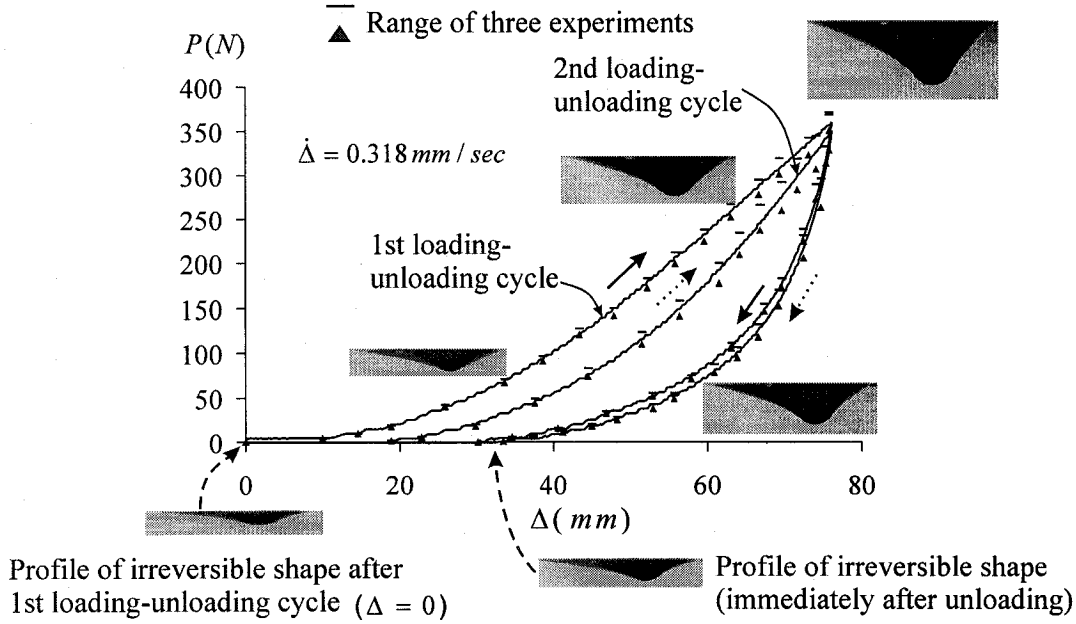

(b) Asymmetric indentation

Figure 5.3 Load-displacement responses of the indentor

The frictional characteristics between the PVC membrane and brass indentor can influence the measured indentation responses. Schallamach (1953) indicated that the normal pressure could influence the friction coefficient for a polymeric material. The

axisymmetric indentation of the membrane gave an estimated maximum normal pressure of $170kPa$ and the asymmetric indentation of the membrane produced an estimated normal pressure of $200kPa$. In the frictional test described in Chapter 4, normal stresses applied were as low as $6.14kPa$ to avoid the vertical compression of the PVC membrane. Santner and Czichos (1989) indicate that at normal pressures less than $1000kPa$, the friction coefficient has an inverse relation with the amount of the normal pressure applied. It can be inferred that the coefficient of friction during the indentation process is likely to be smaller than the value determined. However, for the purpose of conducting the computational modelling, the value of the coefficient of friction is assigned a range of $\mu \in [0.0, 0.6]$. The lower limit considers a frictionless contact between the indentor and PVC geosynthetic membrane; and the upper limit is chosen to be approximately 5% higher than that determined from the experiment.

5.3 Computational implementations

The computational modelling of the indentation of the PVC geosynthetic membrane was conducted using the general-purpose finite element code ABAQUS (ABAQUS/Standard, 2004). There are several computational features in ABAQUS/Standard that are relevant to the computational modelling of the axisymmetric and asymmetric membrane indentation problem. These include consideration of large strain phenomena, implementation of the contact conditions, and most importantly, the ability to implement the constitutive model derived in Chapter 3 in the computational algorithm. Complete descriptions of these procedures are given in the user manul for ABAQUS/Standard.

5.3.1 The small sliding formulation

Considering the observation that the indentation of the membrane involves only a limited amount of relative slip between the membrane and the indentor, the *small sliding formulation* that is available in the ABAQUS/Standard code is considered sufficient for purposes of modelling the contact. With this formulation, the relative movement between the contacting surfaces is limited, although the arbitrary rotation of contacting surfaces is permitted. For the computational modelling associated with the membrane indentation,

the finite geometry of the indentor profile will induce finite rotations at the contact zone and exterior to it. ABAQUS/Standard considers an interaction between surfaces that are designated as *master* and *slave* surfaces. In the small sliding formulation, the algorithm in the ABAQUS/Standard code attempts to locate a potential contact point on the master surface for every node defined in the slave surface. Consider a potential contact between a node n in the slave surface and a segment of the master surface described by nodes n_1, $n_2 \ldots n_m$, where m is the number of the surface nodes of the contact element on the master surface. The interaction of the two surfaces then involves a relative change of the distance of the node n to the master surface and a tangential slip of this node.

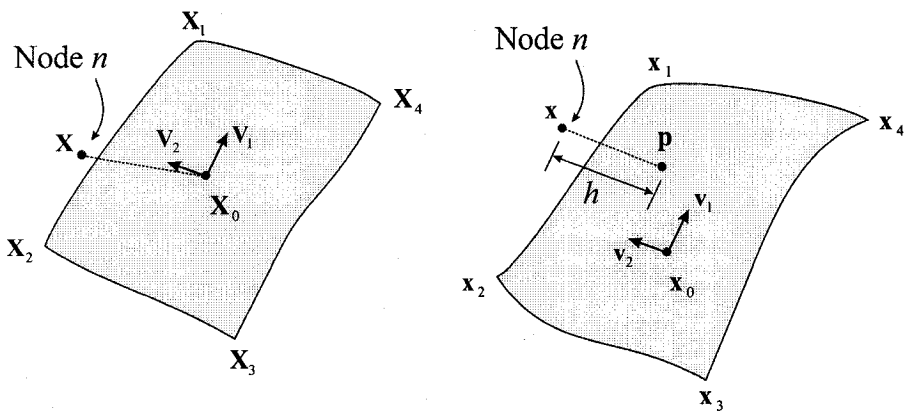

(a) Undeformed configuration (b) Deformed configuration

Figure 5.4 Contact of a node with a segment of the master surface

In the undeformed configuration, the potential contact node n with coordinates $\mathbf{X}$ is considered. It is supposed to contact a point $\mathbf{X}_0$ on the segment of the master surface which is formed by the nodes n_1, $n_2 \ldots n_m$ whose coordinates are defined as $\mathbf{X}_1$, $\mathbf{X}_2 \ldots \mathbf{X}_m$, respectively (see Figure 5.4). Since the point $\mathbf{X}_0$ is on the segment of the master surface, its coordinates can be expressed in terms of the coordinates of the nodes n_1, $n_2 \ldots n_m$: i.e.

$$\mathbf{X}_0 = \sum_{i=1}^{m} N_i(g_1, g_2)\mathbf{X}_i \tag{5.1}$$

where $N_i(g_2,g_2)$ are the interpolation functions for node n_i. The position (g_1,g_2) of the contact point $\mathbf{X}_0$ is established based on the condition that $\mathbf{X}-\mathbf{X}_0$ is normal to the segment of the master surface at point $\mathbf{X}_0$: i.e.

$$\begin{aligned}(\mathbf{X}_0-\mathbf{X})\bullet\mathbf{V}_1=0\\(\mathbf{X}_0-\mathbf{X})\bullet\mathbf{V}_2=0\end{aligned} \tag{5.2}$$

with

$$\begin{aligned}\mathbf{V}_1=\frac{\partial\mathbf{X}_0}{\partial g_1}=\sum_{i=1}^{m}\frac{\partial N_i(g_1,g_2)}{\partial g_1}\mathbf{X}_i;\\\mathbf{V}_2=\frac{\partial\mathbf{X}_0}{\partial g_2}=\sum_{i=1}^{m}\frac{\partial N_i(g_1,g_2)}{\partial g_2}\mathbf{X}_i;\end{aligned} \tag{5.3}$$

In the deformed configuration, coordinates $\mathbf{x}$ for node n in the slave surface and coordinates $\mathbf{x}_1$, $\mathbf{x}_2\ldots\mathbf{x}_m$ for nodes n_1, $n_2\ldots n_m$ are written in lower case letters. With the small sliding formulation, the contact point $\mathbf{p}$ in the deformed configuration is assumed to lie on the tangential plane defined by $\mathbf{v}_1$ and $\mathbf{v}_2$ at point $\mathbf{x}_0$ with

$$\begin{aligned}\mathbf{v}_1=\frac{\partial\mathbf{x}_0}{\partial g_1}=\sum_{i=1}^{m}\frac{\partial N_i(g_1,g_2)}{\partial g_1}\mathbf{x}_i;\\\mathbf{v}_2=\frac{\partial\mathbf{x}_0}{\partial g_2}=\sum_{i=1}^{m}\frac{\partial N_i(g_1,g_2)}{\partial g_2}\mathbf{x}_i;\end{aligned} \tag{5.4}$$

where (g_1,g_2) is determined by (5.2) that is assumed to remain unchanged when slip occurs. Therefore, the contact point $\mathbf{p}$ can be expressed in terms of $\mathbf{v}_1$ and $\mathbf{v}_2$: i.e.

$$\mathbf{p}(\xi_1,\xi_2)=\mathbf{x}_0+\xi_1\mathbf{v}_1+\xi_2\mathbf{v}_2 \tag{5.5}$$

where parameters (ξ_1,ξ_2) are determined such that

$$\begin{aligned}\mathbf{v}_1\bullet[\mathbf{p}(\xi_1,\xi_2)-\mathbf{x}]=0\\\mathbf{v}_2\bullet[\mathbf{p}(\xi_1,\xi_2)-\mathbf{x}]=0\end{aligned} \tag{5.6}$$

The distance or the over-closure h (Figure 5.4) between the node $\mathbf{x}$ and the contact plane defined by $\mathbf{v}_1$ and $\mathbf{v}_2$ is then defined as

$$h = |\mathbf{p}(\xi_1, \xi_2) - \mathbf{x}| \tag{5.7}$$

or

$$h\mathbf{n} = \mathbf{p}(\xi_1, \xi_2) - \mathbf{x} \tag{5.8}$$

where $\mathbf{n}$ is the unit normal of the tangential contact surface. Linearization of Equation (5.8) gives

$$\delta h\mathbf{n} + h\delta\mathbf{n} = \delta\mathbf{x}_0 + \delta\xi_1\mathbf{v}_1 + \delta\xi_2\mathbf{v}_2 + \xi_1\delta\mathbf{v}_1 + \xi_2\delta\mathbf{v}_2 - \delta\mathbf{x} \tag{5.9}$$

Taking the dot product of Equation (5.9) with $\mathbf{n}$ results in following expression for δh:

$$\delta h = \mathbf{n} \bullet (\delta\mathbf{x}_0 + \xi_1\delta\mathbf{v}_1 + \xi_2\delta\mathbf{v}_2 - \delta\mathbf{x}) \tag{5.10}$$

Similarly, the variation of the *first slip component* can be defined as

$$\delta\bar{s}_1 = \delta\xi_1|\mathbf{v}_1| = \delta\xi_1\frac{\mathbf{v}_1 \bullet \mathbf{v}_1}{|\mathbf{v}_1|} = \delta\xi_1\mathbf{v}_1 \bullet \mathbf{t}_1 = -\mathbf{t}_1 \bullet (\delta\mathbf{x}_0 + \xi_1\delta\mathbf{v}_1 + \xi_2\delta\mathbf{v}_2 - \delta\mathbf{x}) \tag{5.11}$$

where $\mathbf{t}_1 = \mathbf{v}_1/|\mathbf{v}_1|$. The variation of the *second slip component* can be defined as

$$\delta\bar{s}_2 = \delta\xi_2|\mathbf{v}_2| = \delta\xi_2\frac{\mathbf{v}_2 \bullet \mathbf{v}_2}{|\mathbf{v}_2|} = \delta\xi_2\mathbf{v}_2 \bullet \mathbf{t}_2 = -\mathbf{t}_2 \bullet (\delta\mathbf{x}_0 + \xi_1\delta\mathbf{v}_1 + \xi_2\delta\mathbf{v}_2 - \delta\mathbf{x}) \tag{5.12}$$

5.3.2 The Coulomb friction model

In the classical Coulomb friction model, it is assumed that, when the two planar surfaces are in contact, there is no relative movement between surfaces in contact until the frictional stress $\bar{\tau}$ reaches a critical stress $\bar{\tau}_{crit} = \mu\bar{p}$, where μ is the coefficient of friction and $\bar{p}$ is the pressure normal to contact plane (see Figure 5.5a). In the modified Coulomb friction model that is adopted in the ABAQUS/Standard code, the notion of

elastic stiffness in slip is introduced and the maximum elastic slip is restrained by the failure of asperities at the contacting surfaces. The interface slip occurs in a linearly elastic fashion prior to the attainment of shear failure: i. e.

$$\tau = k_s \bar{s} \qquad ; \qquad \bar{s} = \sqrt{\bar{s}_1^2 + \bar{s}_2^2} \tag{5.13}$$

where $\bar{s}$ is the magnitude of the slip; $\bar{s}_1$ and $\bar{s}_2$ are defined in (5.11) and (5.12). In (5.13), $k_s = \bar{\tau}_{crit} / \bar{s}_{crit} = \mu \bar{p} / \bar{s}_{crit}$ is the stiffness during slip and $\bar{s}_{crit}$ is the maximum elastic slip. The formulation for the shear behaviour of the frictional surface takes the form of

$$d\bar{\tau} = \begin{cases} k_s d\bar{s} + \dfrac{\mu \bar{s}}{\bar{s}_{crit}} d\bar{p} & ; \quad \bar{\tau} < \bar{\tau}_{crit} (= \mu \bar{p}) \\ \mu d\bar{p} & ; \quad \bar{\tau} \geq \bar{\tau}_{crit} \end{cases} \tag{5.14}$$

The modified Coulomb frictional model is illustrated in Figure 5.5b.

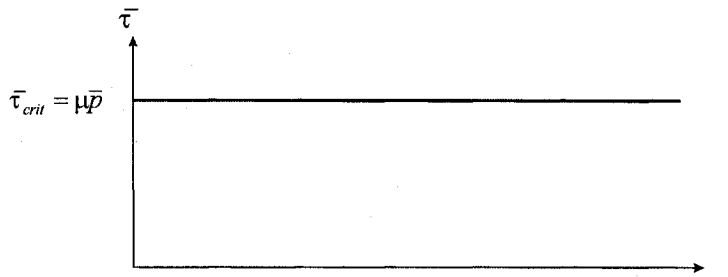

(a) The Classical Coulomb friction model

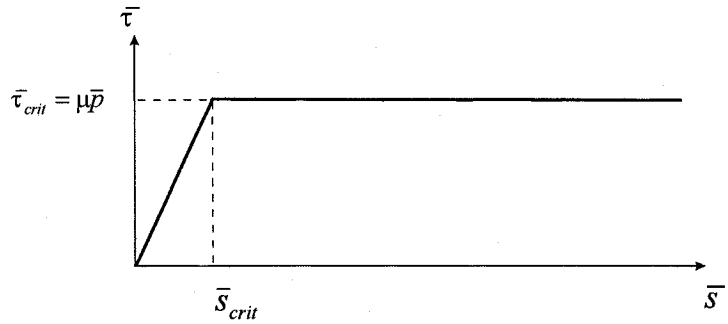

(b) Elastic-sticky friction model used in the ABAQUS/Standard code ($d\bar{p} = 0$)

Figure 5.5 Two types of friction models [model (b) reduces to model (a) when $\bar{s}_{crit} \to 0$]

The presence of the elastic stiffness k_s in slip is mainly attributed to the interlock of the asperities in the contacting surfaces. The experimental program presented in Chapter 4, however, is insufficient to determine this parameter since it involves significant amount of elastic and inelastic deformation of the parent material of the PVC geosynthetic membrane during contact. Preliminary computations also show that this parameter has no appreciable influence on the computational results involving the axisymmetric and asymmetric indentation of a PVC membrane as thin as $H = 0.5mm$. Therefore, a very small value of $\bar{s}_{crit}$ (compared to the thickness of the membrane) for the modified Coulomb friction model is considered, which reduces to the classical friction model as $\bar{s}_{crit} \to 0$.

5.3.3 Incorporation of the constitutive model

Complete descriptions of the procedures for the incorporation of the constitutive model are discussed in the User Defined Subroutine UMAT (ABAQUS/Standard, 2004). In this study, only the salient features will be presented. In nonlinear analysis using ABAQUS/Standard code, each step is divided into iteration increments. The user suggests the size of the first increment, and ABAQUS/Standard automatically chooses the size of subsequent increments. During each increment, ABAQUS employs a Newton-Raphson algorithm to perform the iteration and the requirements for equilibrium is determined through consideration of the principle of virtual work

$$\int_{V^{<t+\Delta t>}} \mathbf{T}^{<t+dt>} : \delta\mathbf{D}^{<t+dt>} dV^{<t+dt>} = \int_{S^{<t+\Delta t>}} \mathbf{t}^{<t+dt>} \bullet \delta\mathbf{v} dS^{<t+dt>} + \int_{V^{<t+\Delta t>}} \mathbf{f}^{<t+dt>} \bullet \delta\mathbf{v} dV^{<t+dt>} \tag{5.15}$$

where $\mathbf{T}$ is the Cauchy stress; $\delta\mathbf{D}$ is the incremental strain-rate; $\delta\mathbf{v}$ is a vector of virtual displacements; $\mathbf{t}$ is a vector of externally applied surface tractions on a unit surface of S; and $\mathbf{f}$ is a body force vector on a unit volume of V; and $^{<t+dt>}$ denotes a state evaluated at time $t + dt$. For the Newton-Raphson algorithm, the Jacobian of the finite element is required for equilibrium equations. The Jacobian, which is obtained by taking the variation of Equation (5.15), can be written as:

$$\int_{V^{<t+dt>}}\left(d\mathbf{T}^{<t+dt>}:\delta\mathbf{D}^{<t+dt>}+\mathbf{T}^{<t+dt>}:d\delta\mathbf{D}^{<t+dt>}\right)dV^{<t+dt>}$$
$$=\int_{S^{<t+dt>}}\left(d\mathbf{t}^{<t+dt>}\bullet\delta\mathbf{v}+\mathbf{t}^{<t+dt>}\bullet\delta\mathbf{v}\frac{dA}{A}\right)dS^{<t+dt>} \tag{5.16}$$
$$+\int_{V^{<t+dt>}}\left(d\mathbf{f}^{<t+dt>}\bullet\delta\mathbf{v}+\mathbf{f}^{<t+dt>}\bullet\delta\mathbf{v}\frac{dJ}{J}\right)dV^{<t+dt>}$$

where

$$A=\frac{dS^{<t+dt)}}{dS^{<t>}};\quad J=\frac{dV^{<t+dt)}}{dV^{<t>}} \tag{5.17}$$

A is surface area ratio between time $t+dt$ and t; and V is volume ratio between time $t+dt$ and t. Right side of the Equation (5.16) is defined by the boundary conditions involving the loading conditions and displacement constraints. On the left side, the expressions for the strain-rate $\mathbf{D}$ and its variations $d\mathbf{D}$ and $d\delta\mathbf{D}$ in terms of the virtual displacement are defined by the displacement interpolation function used in the element definition. It has been shown (ABAQUS/Standard, 2004) that the left side equation (5.16) can be expressed in a more explicit form:

$$\int_{V^{<t+dt>}}\left\{d\mathbf{D}^{<t+dt>}:\mathbf{C}^{<t+dt>}:\delta\mathbf{D}^{<t+dt>}-\frac{1}{2}\mathbf{T}^{<t+dt>}:\left[2\mathbf{D}^{<t+dt>}\bullet\mathbf{D}^{<t+dt>}-(\mathbf{L}^{t+dt})^{T}\bullet\mathbf{L}^{t+dt}\right]\right\}dV^{<t+dt>}$$

where $\mathbf{C}$ is a fourth-order tangential stiffness tensor defined by

$$\mathbf{C}=\frac{\partial d\mathbf{T}}{\partial d\mathbf{D}} \tag{4.4}$$

Information on both $\mathbf{C}$ and $\mathbf{T}$ is defined by the constitutive response for the PVC geosynthetic through a subroutine UMAT. The flow chart of the computational procedure used in the ABSQUS/Standard code is presented in Figure 5.6. The ABAQUS/Standard further utilizes a backward-Euler scheme as a default finite difference scheme to update variables. Those variables that are determined from a previous iteration and which do not change during the iteration between $[t,t+dt]$ are defined as *state variables*. The *state*

variables adopted in this analysis include the components of irreversible deformation gradient $\mathbf{F}^u$ at time t and stress tensors $\mathbf{T}_A$ and $\mathbf{T}_B$ at time t in the visco-plastic component including models A and B, respectively.

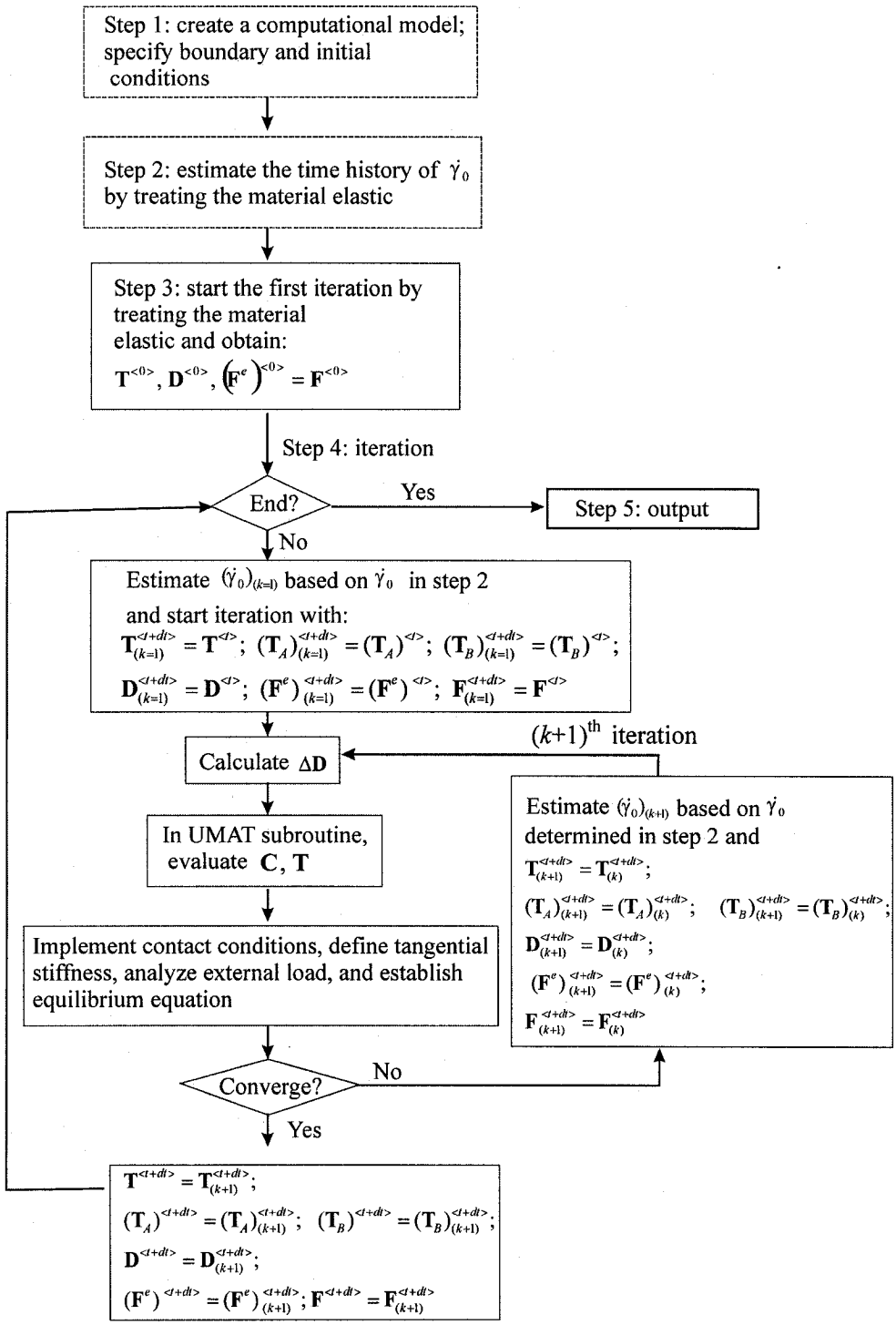

Figure 5.6 Computational procedure used in ABAQUS

By implementing a fully backward-Euler finite difference scheme in time, however, the updating of $\dot{\gamma}_0$ requires information on the material configuration at $t+dt$. The constitutive model will have an influence on the choice of $\dot{\gamma}_0$. The value of $\dot{\gamma}_0$ is thus assumed to remain unchanged during an iteration and taken as a further *state variable*. This approach is valid when the deformations are moderate (e.g. $\gamma_0 \leq 60\%$). In situations that involve significant amount of total and viscoplastic deformations, the convergence in this approach is slow. A possible way of overcoming this deficiency is to use an approximate estimate of the time-history of $\dot{\gamma}_0$ while considering the material to be fully elastic prior to the start of the computations (see Figure 5.6). When the time-history of $\dot{\gamma}_0$ for a particular element is estimated at a number of displacement increments, the value of $\dot{\gamma}_0$ for that element at a particular displacement can then be interpolated. The computational program also involves the comparison of the results by using different types of elements. The preliminary computational results indicate no noticeable differences between them. A 6-node prism solid element is used, which adopts a linear first-order interpolation function (see Figure 5.7). This approach showed stable numerical results and was adopted for the model representations of the uniaxial test data for the untreated PVC geosynthetic with an initial gauge length of $50mm$ and a cross section of $25.4mm \times 0.5mm$ (see also Figure 2.8). Although the time history of $\dot{\gamma}_0$ is estimated, the computations only slightly overestimate the experimental results (see Figure 5.8) due to the fixity at the edge of the specimen with a finite size. The computations for a narrower specimen with a cross section of $1.0mm \times 0.5mm$ show a better correlation with the experimental results. The computational results in this case follow more closely with those represented by MATLAB software (see Figure 3.6). The slight (maximum 6%) overestimation of the computational results by ABAQUS/Standard finite element is then neglected. The computational approach presented here is adopted for the modelling of both axisymmetric and asymmetric indentation of the untreated circular PVC geosynthetic membrane.

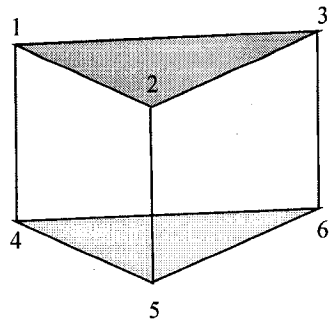

Figure 5.7 A 6-node prism solid element

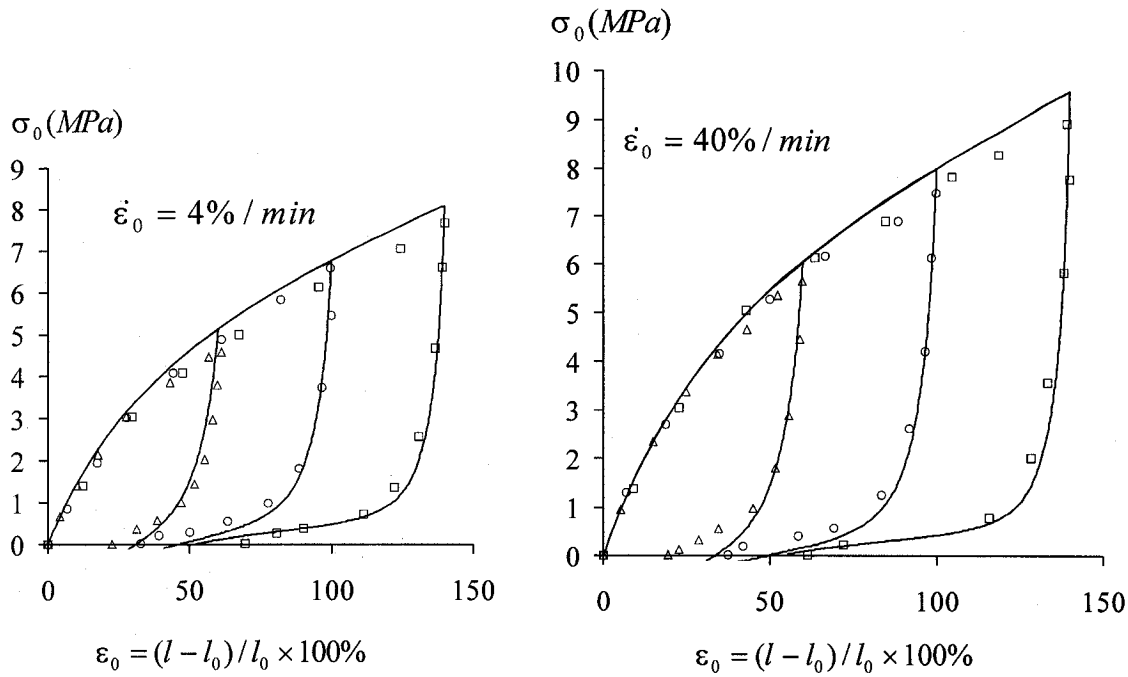

Figure 5.8 Model representations by ABAQUS software of the stress-strain responses involving loading and unloading of the untreated PVC geosynthetic

5.4 Computational results

The geometry of the membrane indentation problem for axisymmetric deformation is illustrated in Figure 5.9a. The boundary conditions and finite element discretization used in the computational modelling are indicated in Figure 5.9b. For the axisymmetric indentation problem, the spherical indentor with a rigid profile is configured to move normal to membrane fixed along the boundary, by achieving contact at the center of the membrane. The contact conditions between the indentor and the membrane have been

chosen as standard hard contact in the ABAQUS/Standard code. The computational modelling of the axisymmetric indentation involves a loading rate of $\dot{\Delta} = 0.318 mm/sec$. The computations first consider the case where the contact between the indentor and the PVC geosynthetic membrane is frictionless. Figure 5.10a shows the comparison of the load-displacement responses between the computational predictions and the experimental results during axisymmetric indentation with a loading rate of $\dot{\Delta} = 0.318 mm/sec$. For the purposes of comparison, results are also presented for the unloading mode. The computations slightly underestimate the experimental responses. The computations further consider the case involving much a higher friction coefficient $\mu = 0.6$ which is approximately 5% higher than the value determined from the experiments described in Chapter 4. As observed both experimentally and computationally, the axisymmetric indentation of the PVC geosynthetic membrane involves almost zero relative slip between the indentor and the PVC geosynthetic membrane. Therefore the influence of the variability in friction coefficient on the axisymmetric load-displacement response is marginal. The computation also attempts to correlate the predicted deflected shapes with those determined from the experiments. The computations are preformed with the value of the friction coefficient $\mu = 0.52$ determined from friction experiments. The computational estimates for the deflected profiles at different loading-unloading stages are presented in Figure 5.11. (The profiles are presented in the $x - z$ plane through the center of the indentor, which is also parallel to the image plane of the mounted digital camera.) The results are presented for three indentation displacements $\Delta = 25.4 mm$, $50.8 mm$ and $72.6 mm$, respectively. Due to the visco-plastic effects in the untreated PVC geosynthetic membrane, the membrane will undergo irreversible deformation after a loading-unloading cycle. As a result, the deflected profiles during loading differ from that determined during the unloading range. When the indentation displacement Δ reduces to zero after a full loading-unloading cycle, the membrane exhibits a permanent deformation. The computations show an accurate prediction of the deflected profile at the loading stage, while it slightly overestimates the irreversible deflections during complete release of the applied load. To further test the predictive capability of the computational approach, the computations also consider the problem of the axisymmetric indentation at a loading rate of $\dot{\Delta} = 0.032 mm/sec$, which is ten times lower than the value used

previously (Figure 5.10b). It can be seen that, although the computation tends to slightly underestimate the experimental results, it gives a reasonable prediction of the experimental trend of the load-displacement responses covering different loading rates.

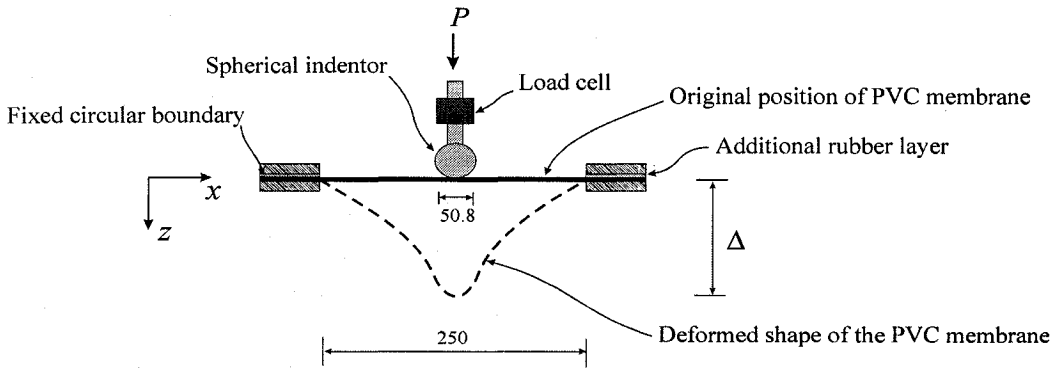

(a) Axisymmetric indentation (dimensions in *mm*)

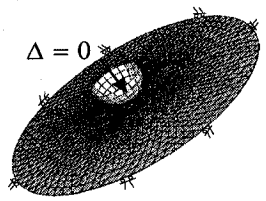

(b) Mesh configuration and boundary conditions
(Total number of elements: 2086)

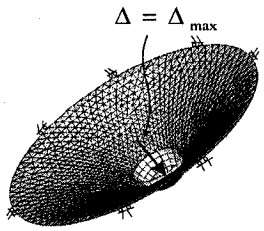

(c) Deformed shape during maximum indentation

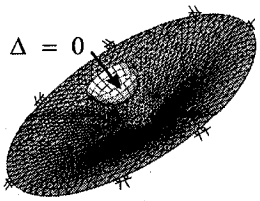

(d) Irreversible shape after a loading-unloading cycle

Figure 5.9 Computational results for axisymmetric indentation of a PVC geosynthetic membrane

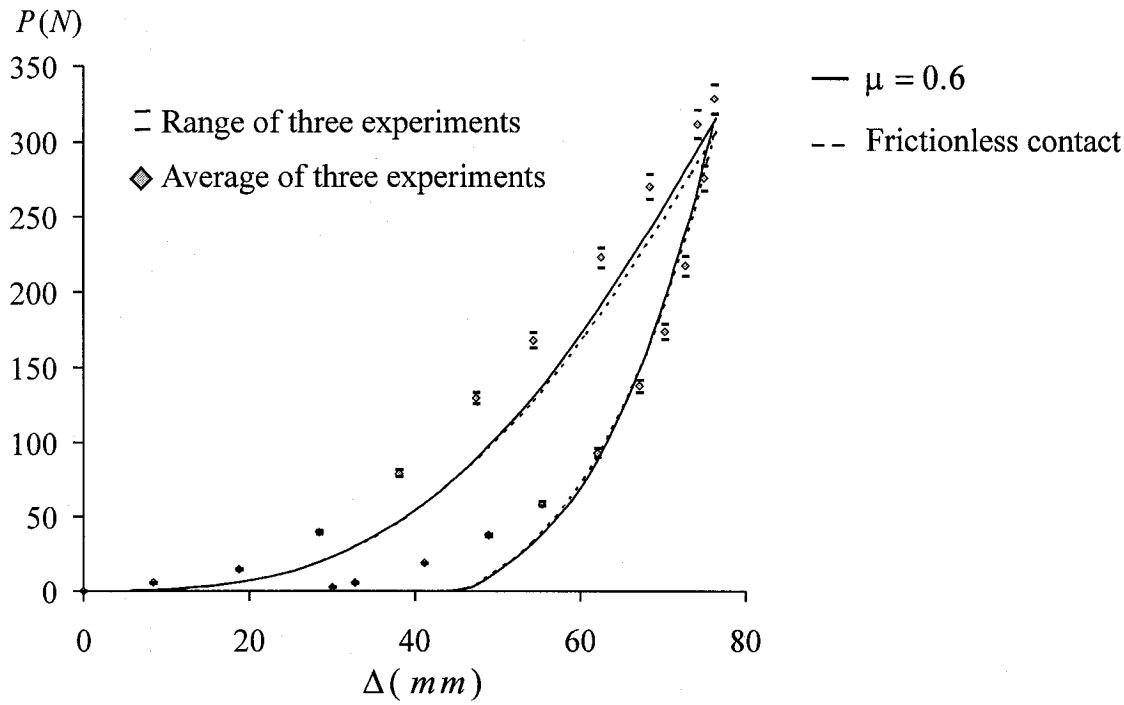

(a) $\dot{\Delta} = 0.318\,mm/sec;\quad \mu \in [0.0, 0.6]$

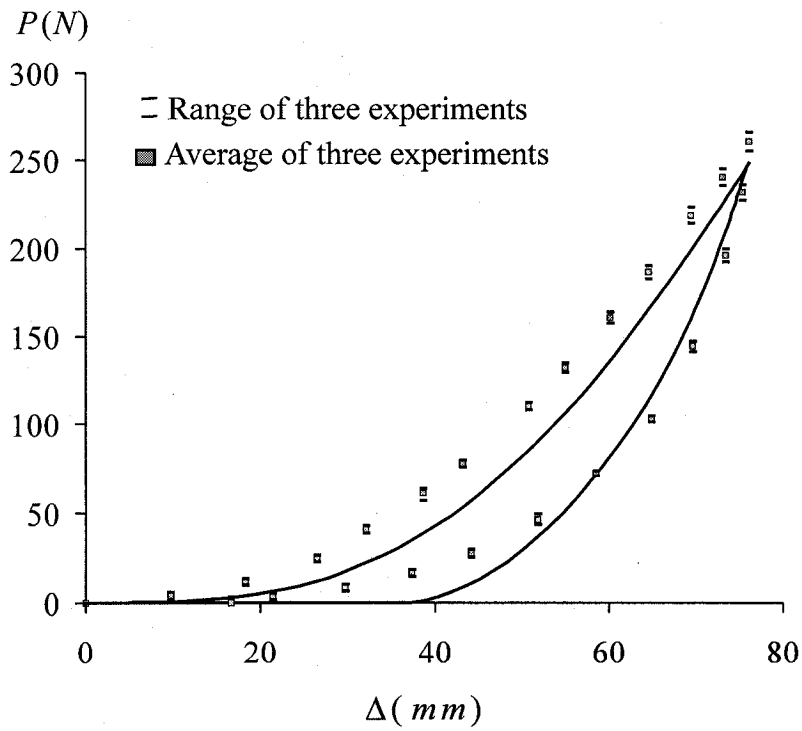

(b) $\dot{\Delta} = 0.032\,mm/sec;\quad \mu = 0.52$

Figure 5.10 Load-displacement responses of the PVC geosynthetic membrane subjected to axisymmetric indentation

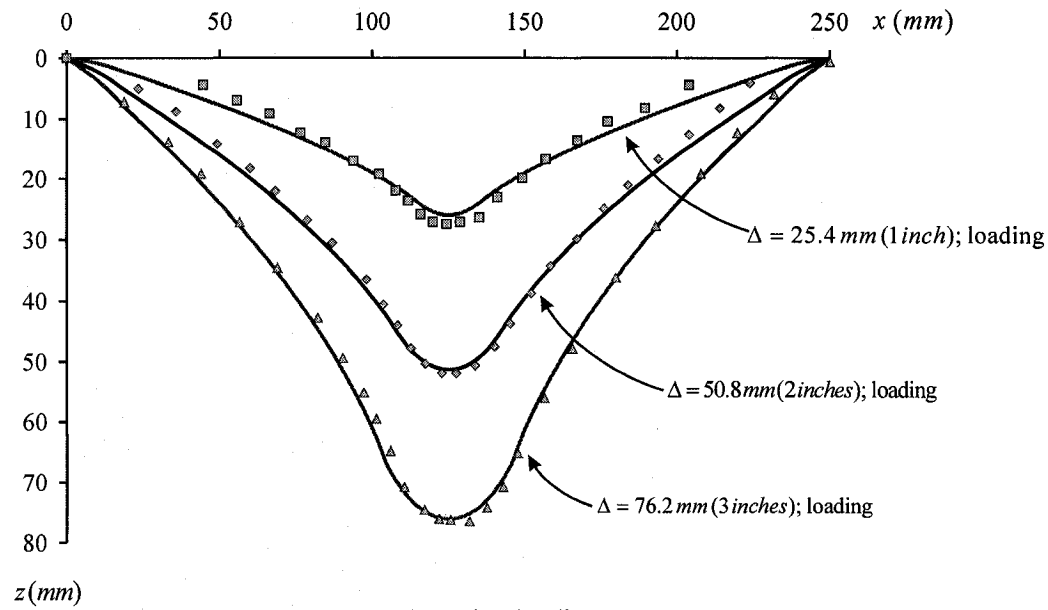

(a) During loading

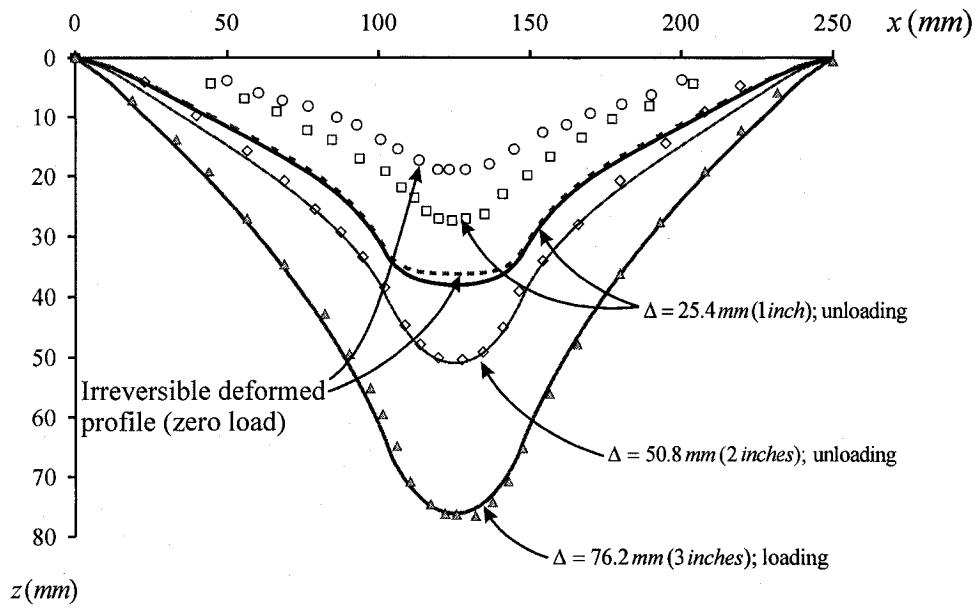

(b) During unloading

Figure 5.11 Deflected shapes of the PVC geosynthetic membrane during axisymmetric indentation ($\dot{\Delta} = 0.318\, mm/sec$; $\mu = 0.52$; symbols represent experimental data)

The problem involving asymmetric indentation of the untreated PVC geosynthetic membrane is now studied. Figure 5.12a illustrates the geometry of the membrane, the location of the asymmetric indentation and the boundary conditions. The mesh

discretization is shown in Figure 5.12b. In the case of the asymmetric indentation, contact is established at a distance $\Omega = 42mm$ from the center of the circular membrane.

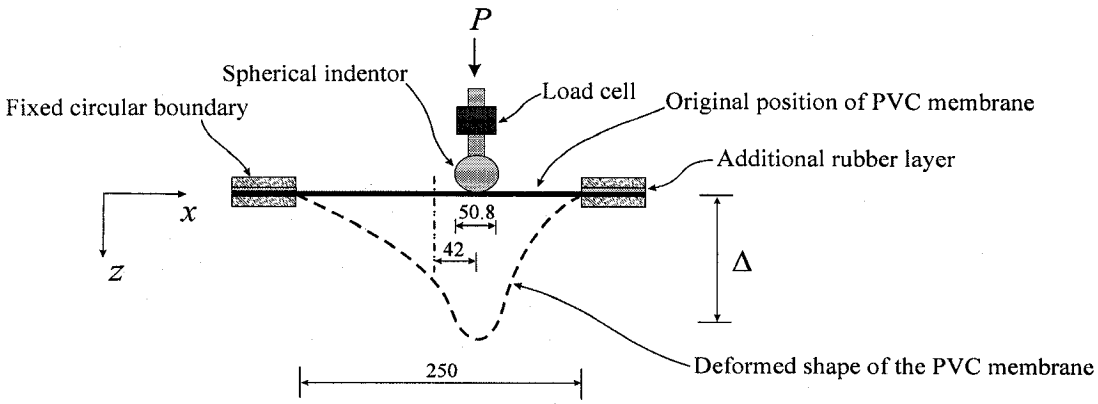

(a) Asymmetric indentation (dimensions in *mm*)

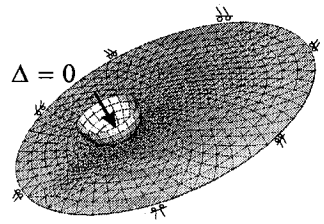

(b) Mesh configuration and boundary conditions
(Total number of elements: 1246)

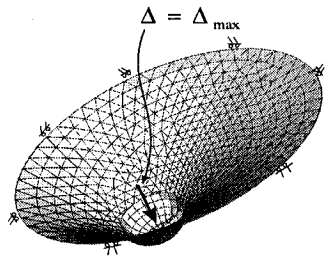

(c) Deformed shape during maximum indentation

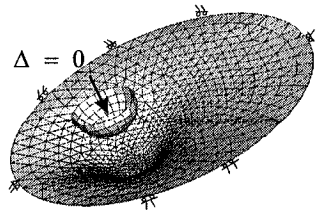

(d) Irreversible shape after a loading-unloading cycle

Figure 5.12 Computational results for asymmetric indentation of a PVC geosynthetic membrane

The study of the asymmetric indentation also involves a loading rate of $\dot{\Delta} = 0.318 mm/sec$. The computation first considers a case involving a frictionless contact between the indentor and the PVC geosynthetic membrane (Figure 5.13). The underestimation of the indentation loads by the computation is less significant during the asymmetric indentation. Furthermore, the computations consider the case involving a much higher coefficient of friction $\mu = 0.6$. The asymmetric indentation of the PVC geosynthetic membrane can involve relative slip between the indentor and PVC geosynthetic membrane; therefore the influence of the variation in the coefficient of friction is more noticeable when compared with the results obtained for the modelling involving axisymmetric indentation. The comparisons between the computed deflected profiles and the experimental results are presented for the case involving a coefficient of friction $\mu = 0.52$ that is determined from experiments (Figure 5.14). As with the modelling of the axisymmetric indentation problem, the computations provide an accurate representation for the deflected profiles during the loading stage, whereas the modelling slightly overestimates the irreversible deformation during complete unloading of the membrane.

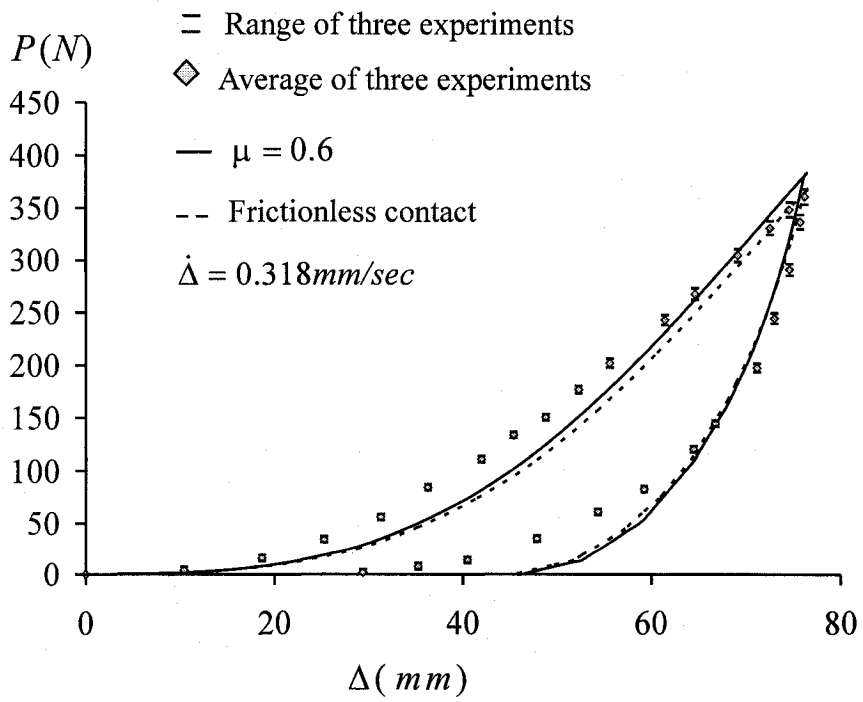

Figure 5.13 Load-displacement response of the PVC geosynthetic membrane subjected to asymmetric indentation

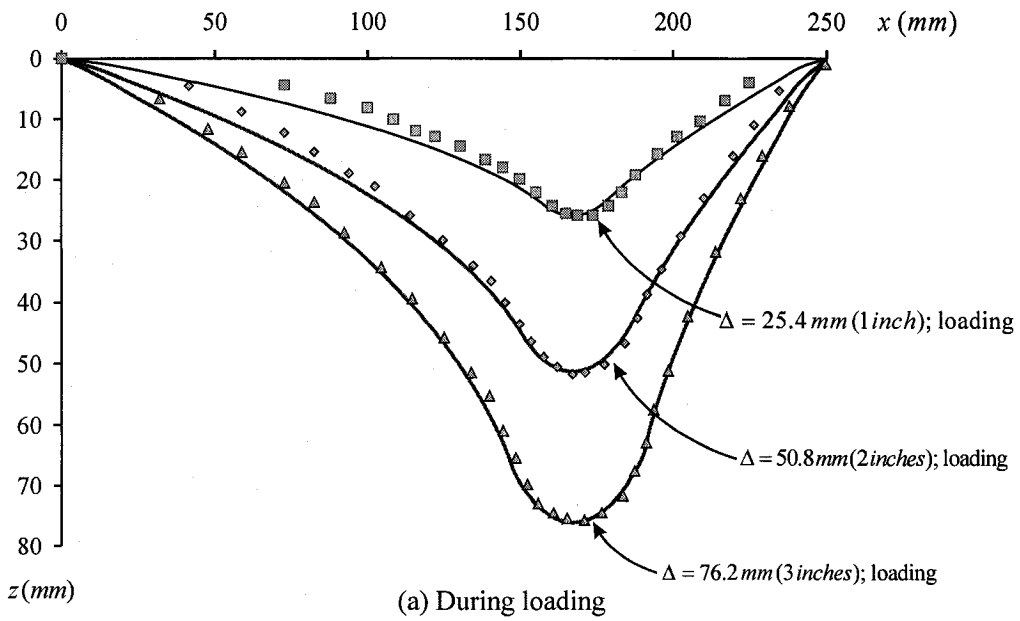

(a) During loading

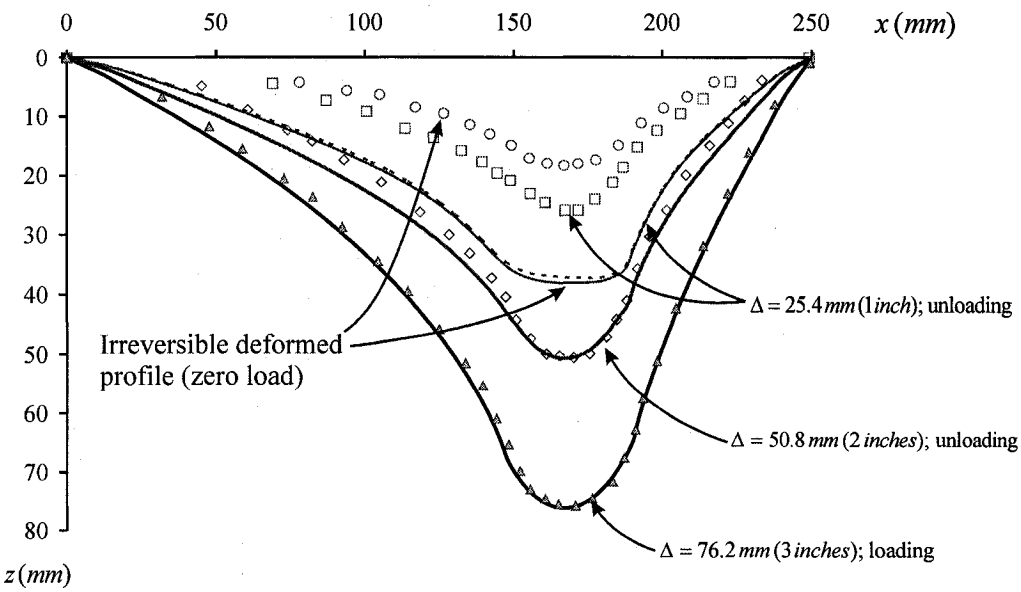

(b) During unloading

Figure 5.14 Deflected shapes of the PVC geosynthetic membrane during asymmetric indentation ($\mu = 0.52$; $\dot{\Delta} = 0.318\,mm/sec$; symbols represent experimental data)

5.5 Summary remarks

In this chapter, the constitutive model which is specifically developed for modelling the mechanical behaviour of untreated PVC geosynthetics as described in Chapter 3, has

been implemented in the commercial finite element ABAQUS/Standard code. The finite element method is used to examine the problem of a flat circular geosynthetic membrane subjected to both an axisymmetric indentation and an asymmetric indentation. The material parameters, validated through the uniaxial tensile tests, have been used to predict the mechanical response. The results show that the computations can accurately capture the experimental response for both types of indentation tests. In general, the deflected shapes predicted by computations correlate well with experimental data. A slight overestimation of the irreversible deformation is observed during unloading of the indentation. The predictive capacities of the methodology adopted here permit a further study of the problem of the indentation of a chemically-treated PVC geosynthetic membrane. The membrane indentation test on the chemically-treated PVC geosynthetic would allow the assessment of the influence of flexibility reduction on the mechanics of the chemically-treated membrane.

CHAPTER 6

INDENTATION OF A CHEMICALLY-TREATED PVC GEOSYNTHETIC MEMBRANE

6.1 Introduction

The exposure of the PVC geosynthetic membrane to chemicals such as pure ethanol, however, leads to the deterioration of the flexibility of the material. The chemically-treated PVC geosynthetic membrane stiffens and displays dominant yield behaviour. By considering axisymmetric and asymmetric indentation tests, the experimental program described in this chapter further studies the indentation behaviour of a chemically-treated PVC geosynthetic membrane exposed to levels of concentrations of ethanol. The research also involves a computational study that allows the incorporation of the constitutive model developed in Chapter 3 for the chemically-treated PVC geosynthetic membrane that takes into consideration large strains, yield type phenomena, irreversible deformations and strain-rate effects. The focus is on the prediction of the indentation behaviour of a PVC geosynthetic membrane exposed to pure ethanol up to 9 *months*. This problem serves as a useful tool for assessing the influence of the loss of flexibility of the PVC geosynthetic membrane subjected to chemical exposure in situations that involve localized loading of membranes. It also provides a useful method for calibrating the constitutive responses developed for describing the behaviour of chemically-treated PVC geosynthetics.

6.2 Experimental results

The experimental setup used to examine the indentational response of the untreated PVC geosynthetic membrane was adopted for the study of the chemically-treated PVC geosynthetic membrane exposed to pure ethanol for 9 *months*. The loading rate adopted

was $\dot{\Delta} = 0.318 mm/sec$. During axisymmetric loading of the chemically-treated PVC, the contact was established at the center of the circular membrane (Figure 6.1a). The indentation response was prescribed through the application of the indentation displacement in an incremental manner up to a maximum displacement of $\Delta_{max} = 50.8 mm$. The ratio of the maximum axial displacement to the membrane diameter reached approximately 0.20 which gave rise to an average strain of approximately 8% in the radial direction; the prelimanry computation, however, indicates a maximum strain of 20% in the vicinity of contact. The load (P)-indentor displacement (Δ) response during axisymmetric indentation and the displaced profiles of the chemically-treated PVC geosynthetic membrane are shown in Figure 6.2a. The results show a good repeatability between the sets of experiments. The visual images of the deflected shapes were recorded using the same technique employed in the testing of the untreated PVC geosynthetic membrane. The chemically-treated PVC geosynthetic exhibits pronounced irreversible deformations after a loading-unloading cycle. During asymmetric indentation, contact was initiated at a distance of $42mm$ from the central axis of the circular membrane (Figure 6.1b). The indentation responses were examined up to a maximum displacement of $\Delta_{max} = 38.1 mm$, which gave rise to an average strain of approximately 10% in radial direction; the prelimanry computation, however, indicates a maximum strain of 27% at the line of separation between a contact. In comparison to the case of the axisymmetric indentation, larger forces are needed to induce the same indentational displacement (Figure 6.2b).

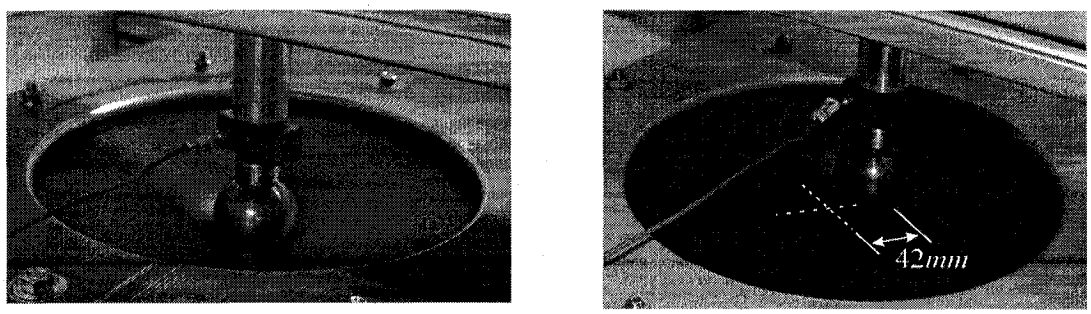

(a) Axisymmetric indentation (b) Asymmetric indentation

Figure 6.1 Indentation of a chemically-treated PVC membrane

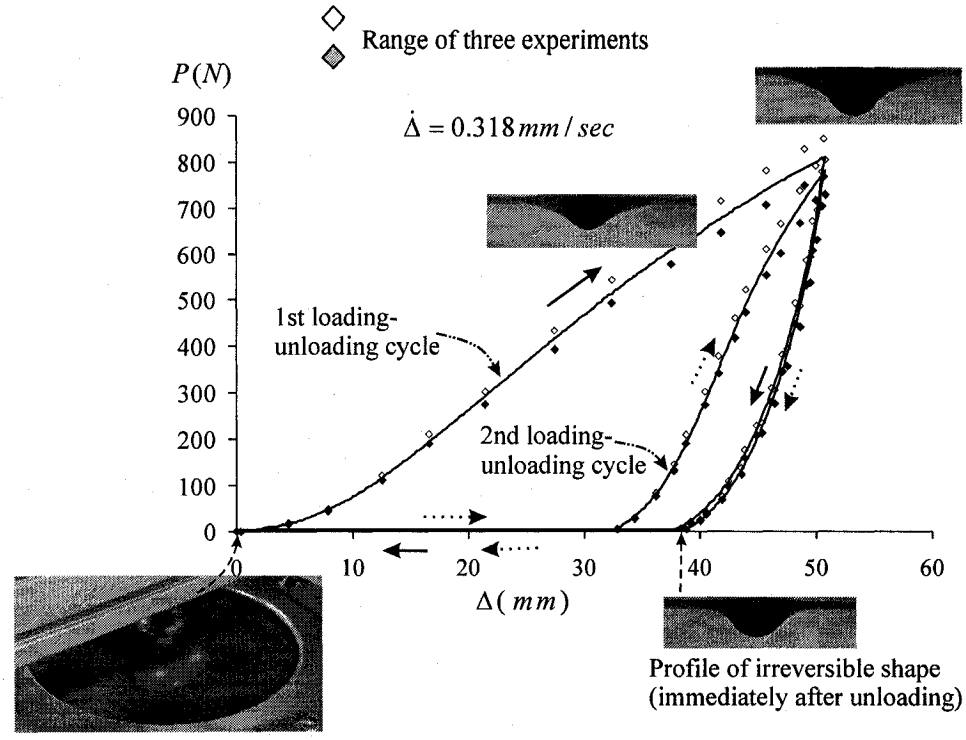

(a) Axisymmetric indentation

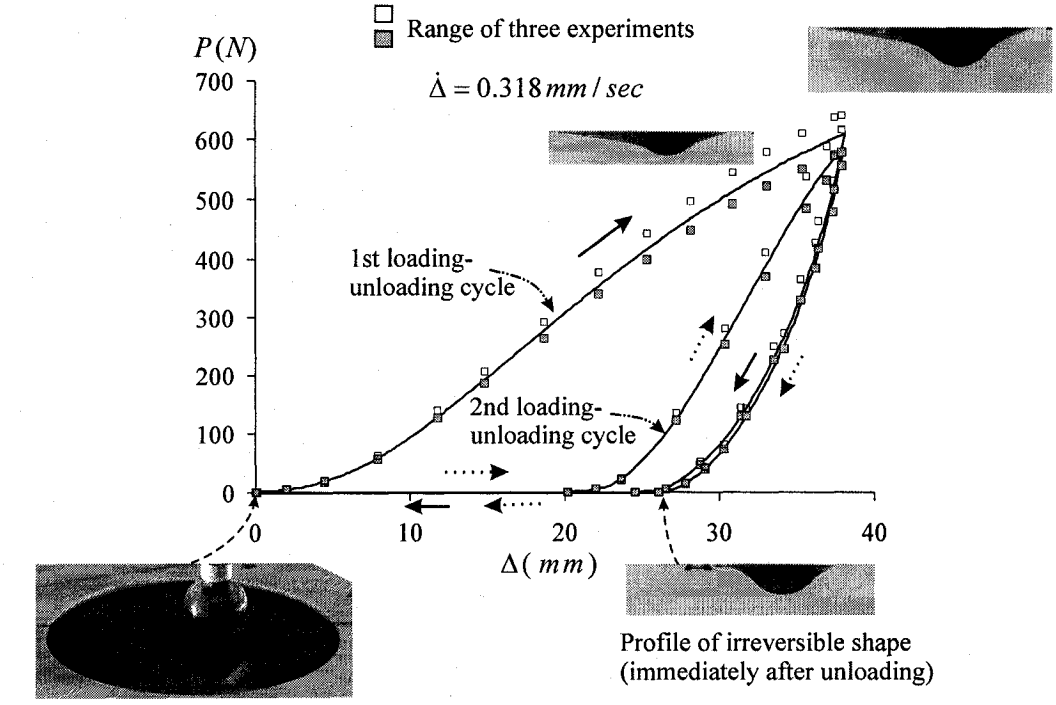

(b) Asymmetric indentation

Figure 6.2 Load-displacement responses of indentation of a chemically-treated PVC geosynthetic membrane exposed to pure ethanol for 9 *months* (solid line represents a typical experiment)

The research program dealing with the membrane indentation problem also examined the axisymmetric indentation responses conducted on samples exposed to ethanol concentrations of 50% and 80%. At these concentrations the chemically-treated PVC geosynthetic membrane exhibited a slower rate of leaching of the plasticizer (Table 2.1) and generally maintained their hyperelastic large strain deformability characteristics (Figure 2.15a). In particular, the PVC geosynthetic exposed to a 50% ethanol solution 'softened' after a prolonged exposure indicating better flexibility in resisting the localized loading compared to those exposed to pure ethanol. The possible cause of the "softening" behaviour could be attributed to the swelling of the PVC due to moisture absorption over a prolonged exposure. The membrane indentation tests conducted on the chemically-treated PVC membranes subjected to a maximum displacement of $\Delta_{max} = 76.2\,mm$ gave rise to an average radial strain of 17%. Figure 6.3 shows the load-indentor displacement responses during the indentation of the chemically-treated PVC geosynthetic membranes subjected to lower levels of ethanol concentrations. As the ethanol concentration is reduced, much lower indentational loads are required to attain the same indentational displacement.

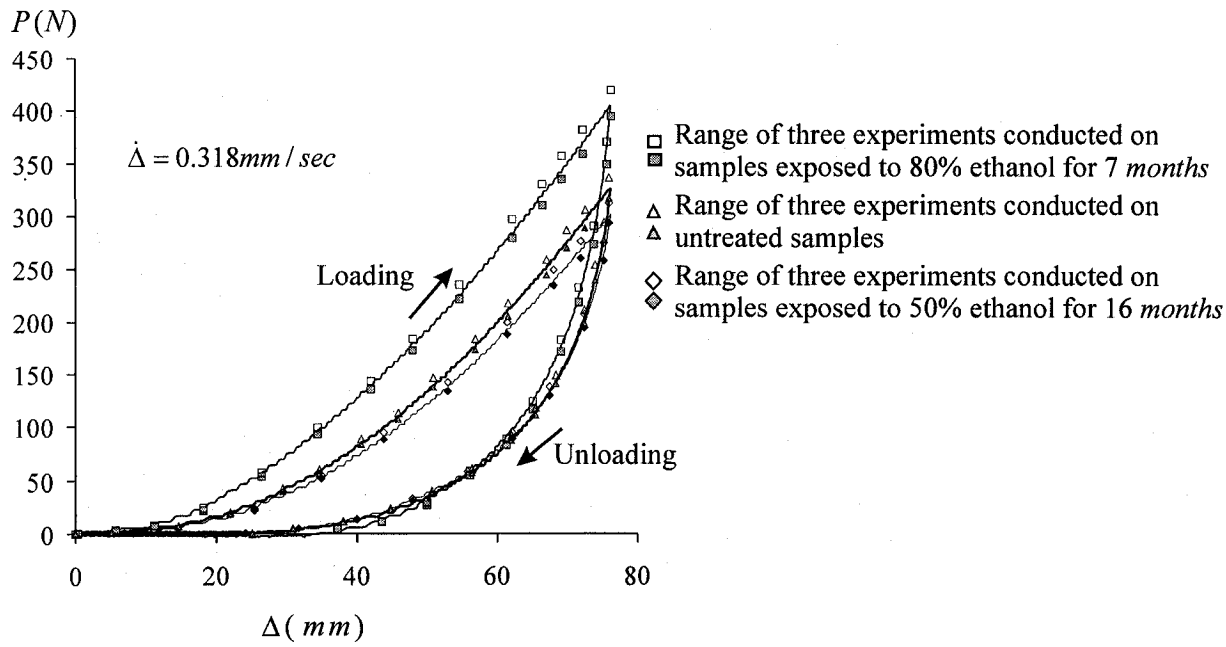

Figure 6.3 Load-displacement responses of the chemically-treated PVC geosynthetic membrane exposed to lower levels of ethanol concentrations during axisymmetric indentation (solid line represents average of three experiments for each level of exposure)

6.3 Computational results

The computational procedure used in ABAQUS/Standard that are relevant to the computational modelling are mainly described in the previous chapter. The model representations (by the ABAQUS/Standard finite element code) of the stress-strain curves up to failure of the samples exposed to pure ethanol for 9 *months* are shown in Figure 6.4.

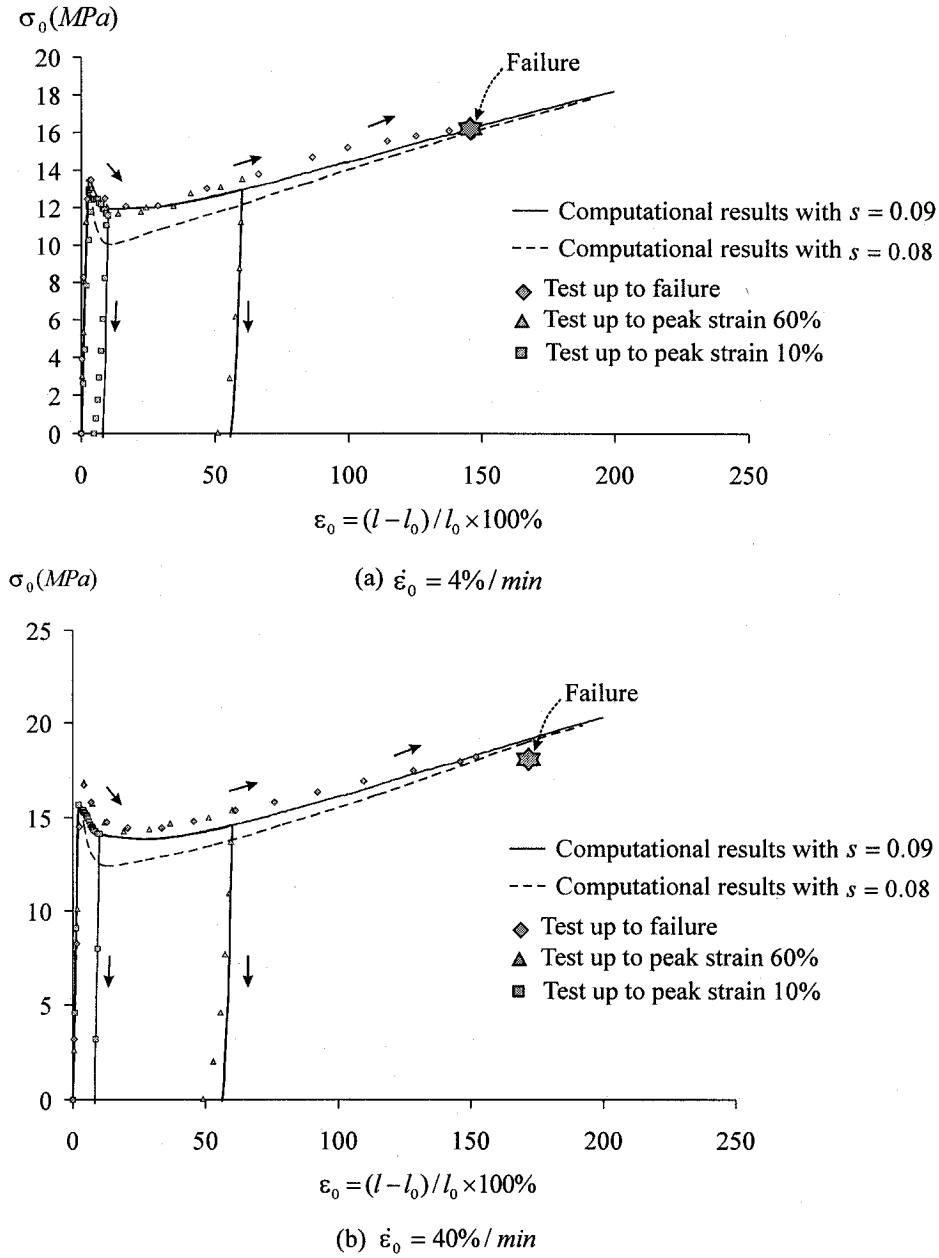

Figure 6.4 Model representation by ABAQUS software of the stress-strain responses involving loading and unloading of the chemically-treated PVC exposed to pure ethanol for 9 *months*

The specimens examined have an initial gauge length of $50mm$ and a cross section of $25.4mm \times 0.5mm$. The constitutive equations used are presented in Table 3.2 and the material parameters are given in Table 3.3. The computational results at two different peak strains $\varepsilon_0 = 10\%, 60\%$ are predicted responses. Although the time history of $\dot{\gamma}_0$ is estimated, the computations show a good correlation with the experimental results. These results, however, are slightly larger than those represented by MATLAB software (see Figure 3.11) due to the fixity at the edge of the specimen. While the preliminary computations on the axisymmetric membrane indentation with $s \approx 0.09$ give a good correlation with the experimental results at indentation range $\Delta \in [0,30mm]$, the results tend to overestimate the the mechanical response at larger indentation displacement. The uniaxial results represented by ABAQUS software with $s \approx 0.08$, however, follow more closely with those represented by MATLAB software (see Figure 3.11). They give less overestimation at higher indentation displacement and produce a better overall correlation with the axisymmetric membrane indentation results. The computational approach (with $s \approx 0.08$) is then adopted for the modelling of both the axisymmetric and the asymmetric indentation of the chemically-treated circular membrane.

The geometry of the membrane indentation problem for axisymmetric deformation is illustrated in Figure 6.5a. The boundary conditions and the finite element discretization used in the computational modelling are indicated in Figure 6.5b. In the case of the axisymmetric indentation problem, a spherical indentor with a rigid surface is configured to move normal to the fixed membrane by achieving contact at the center of the membrane.

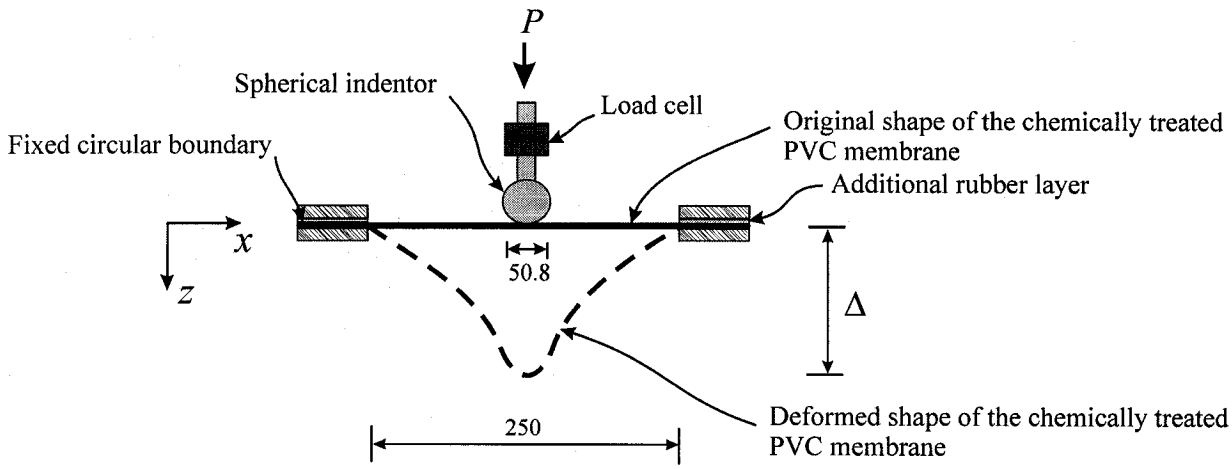

(a) Axisymmetric indentation (all dimensions in *mm*)

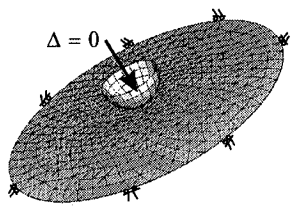

(b) Mesh configurations and boundary conditions
(Total number of elements: 862)

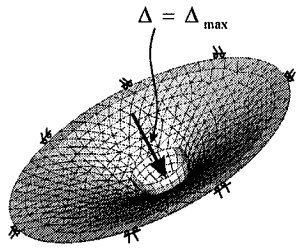

(c) Deformed shape during maximum indentation

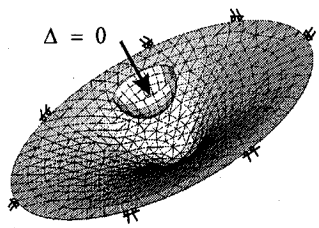

(d) Irreversible shape after a loading-unloading cycle

Figure 6.5 Computational results of axisymmetric indentation of a chemically-treated PVC geosynthetic membrane

The contact conditions between the indentor and the membrane have been chosen as the standard hard contact option available in the ABAQUS/Standard code. Considering the fact that the friction was measured at a much lower normal stress than that experienced by the membrane during indentation (involving maximum normal pressure of approximately $450kPa$), in the computational modelling, the value of the coefficient of friction is assigned a range of $\mu \in [0, 1.0]$, where the lower limit corresponds to frictionless contact between the indentor and the chemically-treated membrane specimen and the upper limit corresponds to a coefficient of friction an order of magnitude higher than that determined from experiments. The computational modelling of the axisymmetric indentation is performed for a loading rate of $\dot{\Delta} = 0.318mm/sec$. The computation first considers the case where the contact between the indentor and the chemically-treated PVC geosynthetic is frictionless. Figure 6.6 shows the comparison of the load-displacement response determined from the computational modelling with equivalent results derived from the axisymmetric indentation with a specified loading rate. For purposes of comparison, results are also presented for the unloading mode. The computations were also carried out to include the case where the coefficient of friction was determined from experiments (i.e. $\mu = 0.08$) and the case where the friction coefficient was an order of magnitude higher than that determined from experiments (i.e. $\mu = 1.0$). As observed, the computational results at $\mu = 0.08$ tend to match the experimental data more accurately.

The computations also attempt to correlate the predicted deflected shapes with those recorded in the experiments. The computational estimates for the deflected profiles at different loading-unloading stages are presented in Figure 6.7. Figure 6.7a presents results for three indentational displacements $\Delta = 12.7mm$, $25.4mm$ and $50.8mm$ obtained during the loading stage and Figure 6.7b shows the profile of the deflected shape in the completely unloaded state. Due to the visco-plastic effects in the polymeric material, the membrane experiences irreversible deformations after a complete loading-unloading cycle. As a result, the deflected profiles during loading differ from those determined during the unloading stage. When the indentation displacement Δ reduces to zero after a complete loading-unloading cycle, the membrane exhibits a pronounced

permanent deformation. The computational results show an accurate prediction of the deflected profile during the loading stage, whereas the procedure slightly overestimates magnitude of these irreversible deflections. The overestimation of the irreversible deformation is also visible in the load-displacement response shown Figure 6.6.

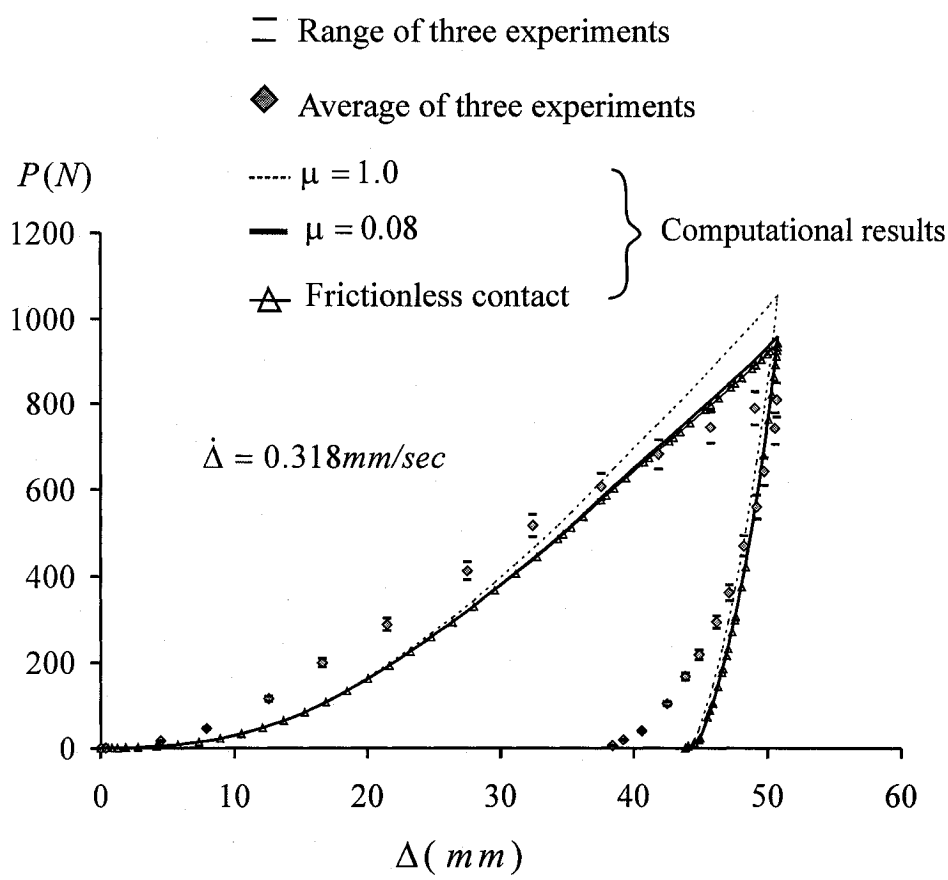

Figure 6.6 Load-displacement responses of the chemically-treated PVC geosynthetic membrane subjected to axisymmetric indentation

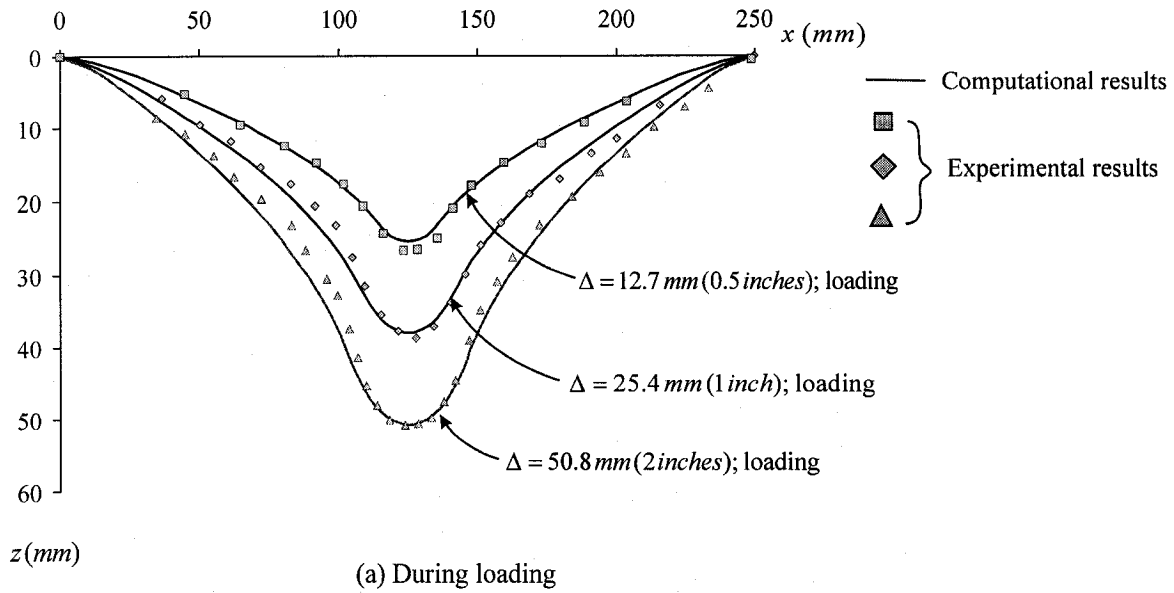

(a) During loading

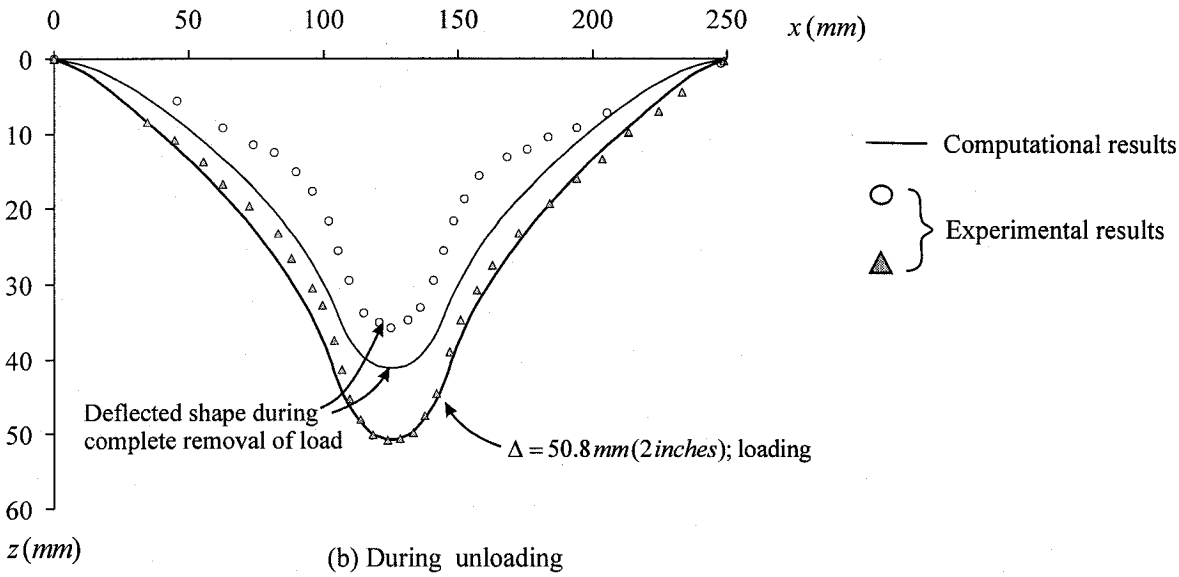

(b) During unloading

Figure 6.7 Deflected shape of a chemically-treated PVC geosynthetic membrane during axisymmetric indentation ($\mu = 0.08$; $\dot{\Delta} = 0.318 mm/sec$)

The problem involving asymmetric indentation of the chemically-treated PVC geosynthetic membrane is now focused. Figure 6.8a illustrates the geometry of the membrane, the location of the asymmetric indentation and the boundary conditions. The mesh discretization is shown in Figure 6.8b. In the case of the asymmetric indentation, contact is established at a distance $\Omega = 42mm$ from the center of the circular membrane.

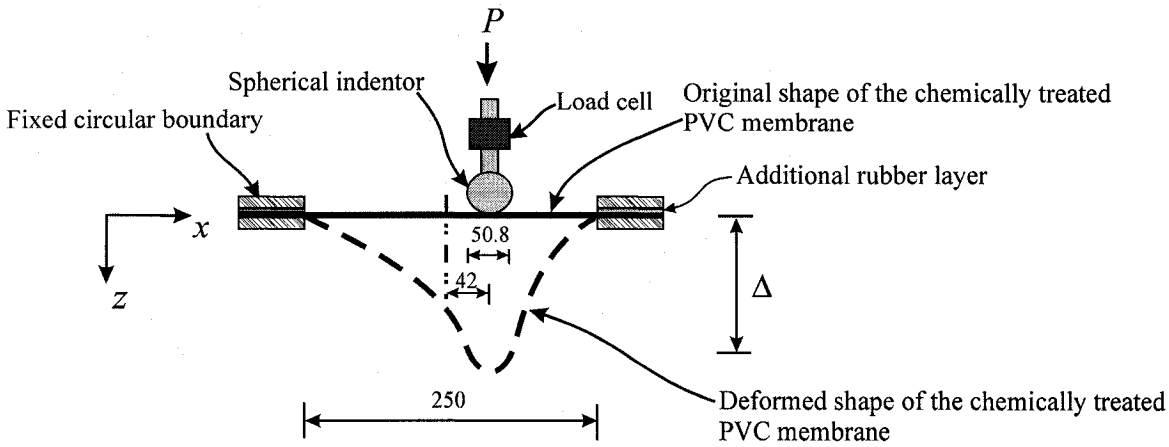

(a) Asymmetric indentation (dimensions in *mm*)

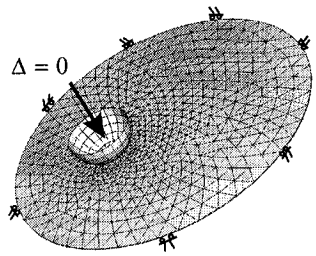

(b) Mesh configurations and boundary conditions
(Total number of elements: 1198)

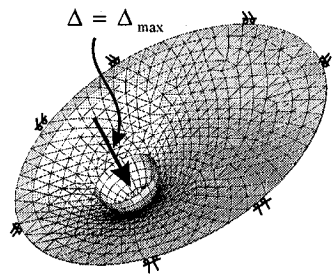

(c) Deformed shape during maximum indentation

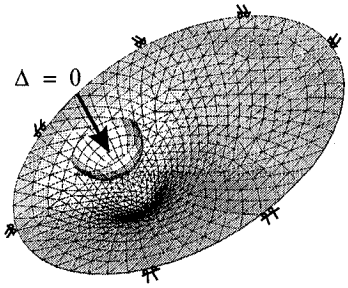

(d) Irreversible shape after a loading-unloadingt cycle

Figure 6.8 Computational results of asymmetric indentation of a chemically-treated PVC geosynthetic membrane

The study of the asymmetric indentation also involves a loading rate of $\dot{\Delta} = 0.318mm/sec$. The computations first consider the case involving frictionless contact between the indentor and the chemically-treated PVC geosynthetic membrane (Figure 6.9). The discrepancy between the experimentally derived load-displacement responses and the computational equivalents is more pronounced for the case involving asymmetric indentation. The asymmetric indentation of the chemically-treated PVC membrane can involve greater relative slip between the indentor and the PVC geosynthetic membrane than is the case for the axisymmetric indentation. Therefore the influence of the variation in the friction coefficient is more noticeable.

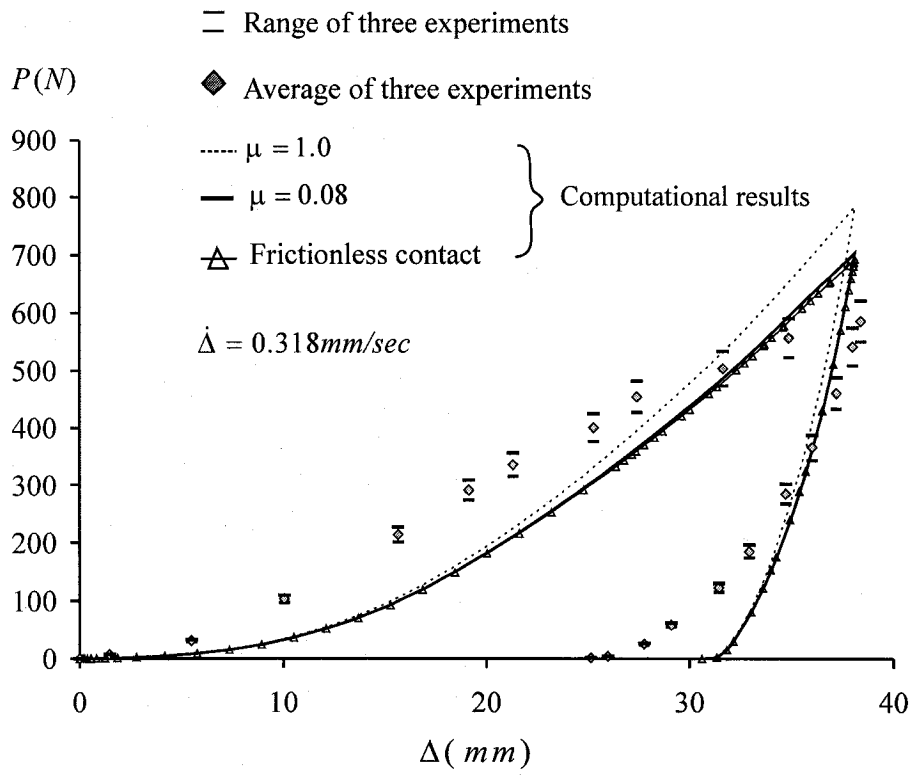

Figure 6.9 Load-displacement responses of the chemically-treated PVC membrane subjected to asymmetric indentation

Figure 6.10 presents a comparison between the deflected profiles derived from computational modelling and experimental results derived for the case involving a friction coefficient $\mu = 0.08$. The results are presented for three indentation displacements $\Delta = 25.4mm$, $31.8mm$ and $38.1mm$. As with the situation involving

axisymmetric indentation, the computations provide an accurate representation for the deflected profiles during the loading stage, whereas the modelling slightly overestimates the irreversible deformation during complete unloading of the chemically-treated PVC geosynthetic membrane. The overestimation of the irreversible deformation is also evident in the load-displacement response presented in Figure 6.10b.

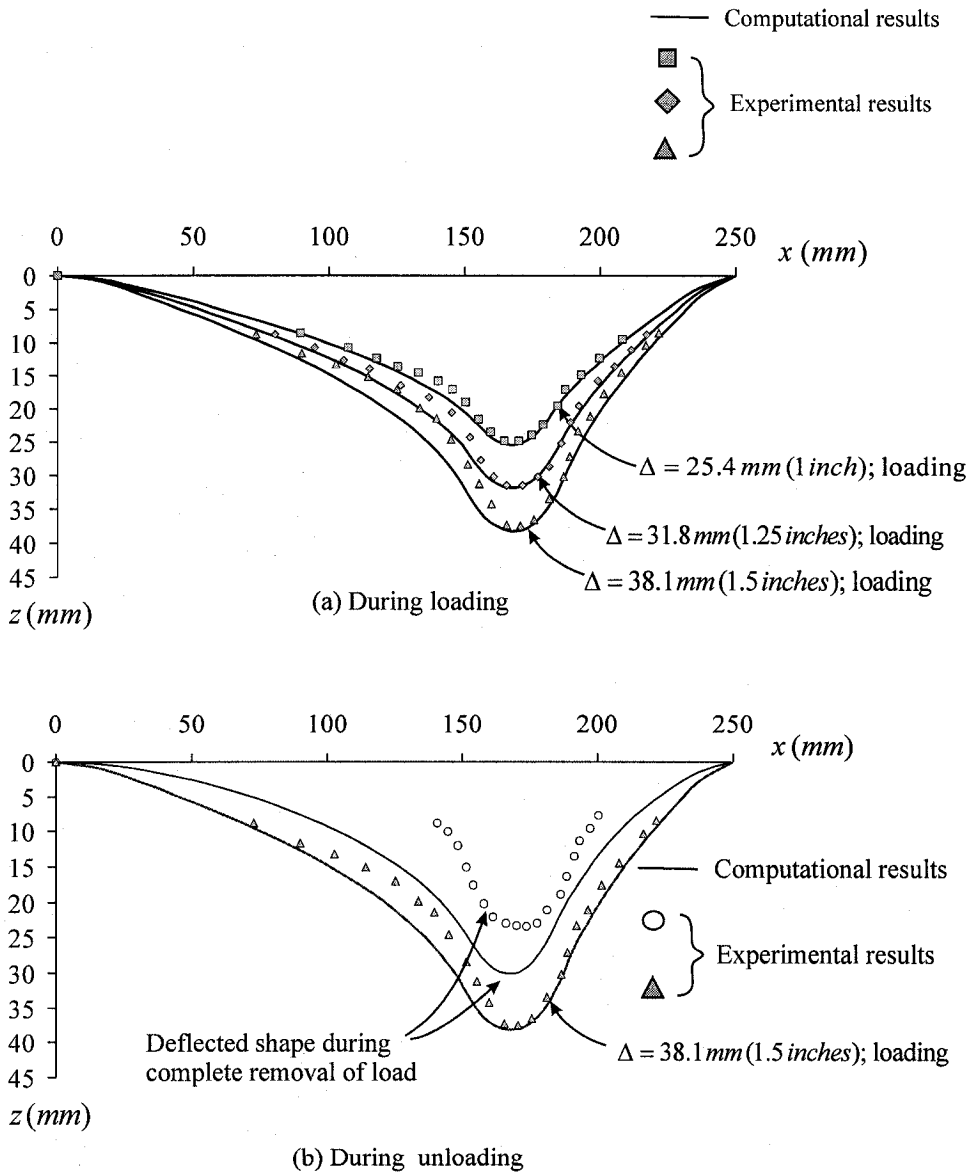

Figure 6.10 Deflected shapes of a chemically-treated PVC geosynthetic membrane during asymmetric indentation ($\mu = 0.08$; $\dot{\Delta} = 0.318\,mm/sec$)

6.4 Summary remarks

In this chapter, the mechanical behaviour of a chemically-treated PVC geosynthetic membrane subjected to various levels of ethanol exposure was examined via an indentation test. The experimental research dealt with a chemically-treated flat circular membrane specimens that were fixed at its boundary and subjected to both axisymmetric and asymmetric indentations. The indentation problem provides a useful technique for assessing the loss of the flexibility of the PVC geosynthetic membrane subjected to various levels of exposure to ethanol. The response of the PVC geosynthetic membrane subjected to pure ethanol exposure indicates a stiffness increase and a loss of flexibility and these effects diminish as the level of concentration of ethanol decreases. In particular, the constitutive model proposed for describing the mechanical behaviour of PVC geosynthetics subjected to a 9-*month* exposure to pure ethanol, that incorporates yield-type phenomena, large strain deformability, irreversible effects and strain-rate sensitivity effects. The constitutive model for the chemically-treated PVC geosynthetic is implemented in a computational code, and used to predict the response of the membrane to indentation. The results show that the computations can reasonably duplicate the trends in the experimental responses for the cases involving axisymmetric and asymmetric indentation of the clamped circular membrane. The deflected shapes predicted from the computational approach correlate well with the experimental data particularly in the loading stage. An overestimation of the irreversible deformation is observed during the unloading stage.

CHAPTER 7

CONCLUSIONS

7.1 Summary and concluding remarks

In this thesis, the chemically-induced alteration in the mechanical behaviour of a PVC geosynthetic membrane has been studied. The experimental program involves the immersion of the test specimens in concentrations of ethanol for a range of durations of exposure. This chapter summarizes the research activities and the results obtained:

- Alteration in the mechanical behaviour of a chemically-treated PVC geosynthetic due to chemical exposure was first investigated via a series of uniaxial tests. Exposure to pure ethanol resulted in a reduction in flexibility, or embrittlement and transformation of the material from one capable of large strain hyperelastic behaviour with no yield threshold to one that displayed dominant yield behaviour. These alterations included a progressive loss of large deformability characterized by hyperelastic behaviour, buildup of embrittlement and development of an initial linear elastic modulus and a distinct yield point. The results of exposure to pure ethanol up to 13 *months* indicate a complete loss of the large strain deformability of the material. The rapid alterations in the mechanical properties of the membrane specimens during the first two *months* correlated well with the X-ray Fluorescence results, which also indicated a rapid loss of plasticizer during this period. The rate of plasticizer loss reduced after two *months*, corresponding to a reduction in the rate of alteration in the mechanical properties.

- Exposure of the PVC geosynthetic samples to lower volumetric concentrations of ethanol at 80% and 50%, and pure water produced less changes compared to the cases exposed to pure ethanol; the large strain deformability of the PVC

membrane sample, characterized by hyperelastic behaviour was unaltered after an exposure to more than one *year*. The PVC geosynthetic subjected to exposure to 50% ethanol and pure water after longer periods became softer; such a phenomenon can possibly be due to the swelling of the material as a result of the water absorption. Loss of plasticizer, however, is also observed during the exposure of PVC geosynthetic membrane to these concentrations. The PVC geosynthetic samples exposed to 80% ethanol followed by a period of air exposure eventually stiffens due to the evaporation of moisture and ethanol. Although in practical situations, the ethanol that comprises one component of landfill leachte reaches only a maximum concentration of 2% ~ 3% (USEPA, 1988), the embrittlement of the PVC geosynthetic barrier as result of the leaching of plasticizer can pose a problem over the long-term, especially when the landfill is subjected to wetting and drying cycles where the leaching of the plasticizer will occur due to prolonged contact with chemicals, whereas swelling is limited due to the evaporation of the moisture during drying periods.

- The influence of the natural storage under ambient conditions was also investigated; results of exposure to air for up to 21 *months* indicated no evidence of alterations in the mechanical properties. It should, however, be noted that PVC materials can experience degradation with time even in the absence of any interaction with other agents. In the context of PVC geosynthetics, however, these effects can also be neglected.

- The results of the experiments conducted in connection with the research program indicate that, in its natural condition, the PVC geosynthetic is only capable of undergoing moderately large strains, the finite strain response of which can be modelled by appealing to a strain energy function of the Mooney-Rivlin form. Unlike natural rubber at moderately large strains, which is virtually void of irreversible phenomena and strain-rate effects, the PVC geosynthetic exhibits a strong rate-dependency. It was shown that the loading part of the stress-strain behaviour of the untreated PVC geosynthetic can be characterized by a basic Mooney-Rivlin form of the strain energy function with the constitutive parameters

that show a logarithmic dependence on the strain-rate that is defined as the rate of change of a combined stretch.

- The PVC geosynthetic also exhibits irreversible behaviour upon unloading depending on the level of the peak strains. An inspection of the unloading response of the untreated PVC geosynthetic indicates that the initial unloading elastic modulus is significantly higher than that for the loading mode. Furthermore, the permanent strains themselves are also in the moderately large strain range. The mechanisms contributing to such irreversible phenomena were considered to include both elastic and visco-plastic effects. Visco-plastic effects are fully restricted during incremental loading due to an infinite value of the elastic parameters of the component contributing to the elastic recovery, which, however, is fully activated upon unloading. It is possible to interpret the presence of a high elastic modulus in terms of the deformability of a transitional link between the plasticized amorphous regions and the crystalline regions and by considering the selective response of such links to either loading or unloading. Due to the oriented alignment of the structure of the amorphous and crystallite region during extension, the transitional link at their connection can take only zero incremental unloading immediately following the loading stage. The procedure adopted here, however, is purely phenomenological with the model representations based on experimental observations.

- The constitutive model development also addresses the loss of elasticity and the development of a distinct yield point in the stress-strain response of the chemically-treated PVC geosynthetic. It is shown that the basic form of the constitutive responses that are developed for the untreated PVC material involving large strain behaviour, strain-rate effects and moderately large irreversible plastic strains can also be used to describe the chemically-treated PVC geosynthetic by adopting a different set of constitutive parameters. The presence of the yield point can be considered as possibly attributable to the breakage of the transitional link or the crystallite that is also responsible for the activation of the visco-plastic component (the approach presented, however, was

mainly phenomenological). Using such an interpretation, the breakage of the transitional link leads to an abrupt reduction of the elastic parameter of the elastic recovery component, from an infinite value to a non-zero final value, which results in material softening immediately beyond the yield and subsequent hardening at larger strains. The correlations between the predictions of the constitutive model and the experimental data are considered to be satisfactory, but nonetheless open to improvement.

- As a method for the calibration of the developed constitutive model, this thesis also examines the mechanical response of a flat PVC geosynthetic membrane subjected to a uniaxial test that induces inhomogeneous strains. The material parameter α, which accounts for the combined stretch effects during multiaxial behaviour, was identified by conducting tests on a uniaxial specimen fixed along oblique planes inclined at 45° to the axes of loading. A computational investigation is needed to identify the parameter α. The material parameter $\alpha \approx 3$ was found to be uninfluenced by the durations of chemical exposure.

- The constitutive model developed thus far is complete in a sense that its parameters can be determined through conventional experimental procedures and the model representation give a reasonable correlation with the experimental data. The constitutive model, therefore, along with the material parameters derived, can be implemented into a computational model and used as a predictive tool for examining the behaviour of a geosynthetic subjected to localized loading. The specific problem chosen for the study is that of a membrane specimen that is fixed along a circular boundary and subjected to either an axisymmetric or asymmetric indentation through a loaded rigid spherical indentor. The problem simulates situations that can occur during localized loading of PVC geosynthetic membranes either during installation and construction or during operation of the landfill. It also serves as a useful method for calibrating the constitutive responses of the PVC geosynthetic determined from conventional uniaxial testing. The results show that the computation gives a reasonably accurate prediction of the

experimental responses for both cases of indentation conducted at different loading rates.

- The results of the indentation of the chemically-treated PVC geosynthetic exposed to pure ethanol indicate an appreciable "stiffening" of the material. The chemically-treated PVC geosynthetic shows a significant loss of flexibility and therefore tends to exhibit much less flexibility for resisting a localized loading. The loss of flexibility of the PVC geosynthetic will also induce failure or cracking, when subjected to localized loading.

7.2 Statement of originality and contributions

The author's original contributions, through this research program, to the advancement of knowledge in this field can be summarized as follows:

- This research determined that the loss of plasticizer was the governing factor that causes the embrittlement of the PVC liner. The results are sufficient to bring into public attention the possible influence of chemical exposure to the performance of the PVC geosynthetlic liner existing in the interior of current landfills. Most previous research studied the PVC geosynthetic membranes exposed to chemical exposure for a short period with no observation of the loss of plasticizer.

- This study required development of a coordinated experimental program to investigate the mechanical behaviour of the chemically-treated PVC geosynthetic membranes which is practical for field application. The previous studies, however, were concerned with the variation of chemical composition of the PVC material subjected to various environmental loading.

- The friction coefficients of the PVC geosynthetic were noted to be significantly reduced after prolonged chemical exposure in this research. Most existing design procedures for landfill slope are based on friction coefficient of the geosynthetic in its intact condition and therefore possibly plausible.

- To study the mechanical behaviour of the uniaxial samples of chemically-treated PVC geosynthetic membrane, a special experimental setup was developed to provide adequate grips at the edges of each sample. The specimen was allowed to experience a near-homogeous deformation during testing, which was essential to the development of the constitutive models.

- An experimental setup to study the experimental behaivour of a circular polymeric membrane subjected to axisymmetric and asymmetric indentation was developed. This provided a performance index of the chemically-treated PVC geosynthetic membrane in resisting the localized large-strain deformations resulting from puncture of the sharp objectives contained in the soil layer or uneven local differential settlement that could occur in landfill application.

- The constitutive model was developed in this research for the chemically-treated PVC material. The subject of constitutive modelling of the mechanical behaviour of the degradated polymeric material can be of interest to the field of polymer engineering. The research results currently available in the literature deal mainly with the material in its untreated condition.

- The elastic and irreversible deformations of the plasticizer PVC material were examined for the influence of the plasticizer and the orientation of the crystallite. Most existing constitutive models developed for polymer have discussed its rate-effects and irreversible deformation in a purely phenomenological approach without consideration of the governing microstructure of the polymer.

- In this research, the predictive capacity of the constitutive model was tested for the circular membrane subjected to an axisymmetric and an asymmetric indentation. It would assistant in modeling the membrane subjected to any arbitary loading. Almost all constitutive models developed so far for polymers examine only the behaviour of the material subjected to uniaxial loading.

7.3 Implications to the design exercises

- Geosynthetics are man-made materials and as such they have a finite life. Waste disposal activities on the other hand are expected for perpetuity. The use of any engineered material with a finite life in containment activities should therefore be approached with caution and care. In most existing design process, a design life of 100 years for geosynthetic membranes is proposed (Rowe and Sangam, 2002). In this research, the design life is suggested to be extended to at least 1000 years, until when human being is expected to develop sufficient mature techniques that help to deal with exhumed waste and facilitate the replacement of the failed geosynthelic liner system.

- The PVC geosynthetic membranes can experiences embrittlement and lose its large deformability in resisting localized loading when exposed to various concentrations of chemical. Such effect can be further pronounced in long term. So the design of the critical deformation for geosynthetic membranes should be paid a high satefy factor by considering a significant reduction in the critical strain for the specimen experienced longest duraction of exposure to pure ethanol. A value of 7~8 is suggested in this thesis.

- Also the friction coefficient of the PVC geosynthetic membranes in contact with other geomaterials, such as geotextiles and soils, can be highly disturbed by the prolong action of chemical exposure. The reduction of friction coefficient between a PVC geosynthetic membrane and a brass surface servces as an index of the variation of friction coefficient as a result of chemical action. The safety factor during the design of the landfill slope stability should be then paid a high value of at least 6.

7.4 Scope for future research

- While this thesis is primarily concerned with the study of chemically-induced alterations in the mechanical behaviour of unstressed PVC geosynthetics, the influences of the coupling of initial stress effects and chemical action can also be

a topic of interest to the service life of a PVC geosynthetic. The orientation of the polymer molecules during applications of stresses and the resulting influence on the chemical diffusion pattern will also be an important consideration.

- In this thesis, the effects of chemical exposure are studied by immersion of PVC geosynthetics in a commonplace chemical such as ethanol. The main reason for the choice of ethanol is its non-toxicity and its abundant presence in landfills. Other chemicals such as acetone or a leachate taken directly from a landfill can also impose a similar threat to the integrity of PVC geosynthetic membrane. While it is acknowledged that chemicals such as a leachate taken directly from a landfill can provide more relevant information about the serviceability of the PVC geosynthetic in a landfill environment, these chemical are generally highly toxic and need special precautions to induce exposure and to conduct subsequent material testing.

- The loss of plasticizer was considered to be the most common phenomenon that would contribute to the alterations in the mechanical behaviour of the PVC geosynthetic. In this thesis, the loss of plasticizer was estimated through X-ray fluorescence techniques and interpreted through observation of the mechanical behaviour for highly-plasticized or weakly-plasticized PVC materials. The alterations in the mechanical behaviour induced by other degradation mechanisms such as UV degradation, weathering, aging, thermal degradation, radioactive degradation and biological degradation, should also be the subject of further research.

Appendix A Thermodynamic Considerations of the Rate-dependent Internal Energy Function $W(\Xi, I_1, I_2)$

The microstructure of a polymeric material alters during deformation either in a form of "breaking" or forming of the network chains (Tobolsky, 1944; Green and Tobolsky, 1946). As a result, there can be corresponding alterations in the internal energy function $W(I_1, I_2, I_3)$ of the material (see Lubliner, 1985). Septanika and Ernst (1998) proposed that the current state of the microstructure of the material can be described by an internal variable $\Xi(t)$ at time t. In the case of an incompressible material where $I_3 = 1$, the internal energy function W can be written as a function of the internal variable Ξ, i.e. (see also Simo, 1987; Septanika and Ernst, 1998):

$$W = W(\Xi, I_1, I_2) \tag{A.1}$$

The second law of thermodynamics requires that the evolution of the internal energy function on the internal variable Ξ satisfies the condition that (see also Lubliner, 1972 and 1985; Simo, 1987; Kamlah and Haupt, 1998; Huber and Tsakmakis, 2000):

$$\frac{\partial W}{\partial \Xi}\dot{\Xi} \leq 0 \tag{A.2}$$

The state variable Ξ can be interpreted as a damage parameter of the microstructure (Simo, 1987). In this case, the restriction (A.2) can be satisfied on the condition that the material only experiences damage without healing (i.e., $\partial W / \partial \Xi \leq 0$ and $\dot{\Xi} \geq 0$). In cases where both self-healing and damage of the microstructure are possible, the evolution history of Ξ can be arbitrary; therefore the approach to use parameter Ξ for the description of the state of the microstructure does not obey the second law of thermodynamics in a first sense. This appendix then addresses the possibility of an arbitrary evolution of the internal variable Ξ that satisfies the second law of thermodynamics.

The first fundamental assumption made here is that, for any fixed combination (I_1, I_2), W is a *continuous* function of the internal variable Ξ. As such, the dependency can, however, be either positive or negative. Let us first look into those intervals of Ξ (say $\Xi \in [\beta_0, \beta_1]$) where $\partial W / \partial \Xi \geq 0$.

Now consider an arbitrary *continuous* evolution history $\Xi = \Xi(t)$, where t denotes the time. At those time intervals where $\dot{\Xi} < 0$, the constraint (A.2) imposed by second law of thermodynamics can be automatically satisfied. The time intervals where $\dot{\Xi} \geq 0$ is now focused on. Following Septanika and Ernst (1998), these history where a state variable $\Xi(t)$ shows an increment (i.e., $\dot{\Xi} \geq 0$) can be discretized into series of step-intervals $t \in (t_i, t_{i+1})$, where $i = 0,1,2..$ is an integer, such that, at their transition, the slope of $\Xi = \Xi(t)$ with respect to time t varnishes (see Figure A.1), i.e.

$$\dot{\Xi} = 0 \qquad \text{at } t = t_0, t_1 .. t_i \tag{A.3}$$

At time $t \in (t_i, t_{i+1})$, however, $\dot{\Xi} \geq 0$. The second thermodynamic requirement (A.2) therefore prescribes that

$$\frac{\partial W}{\partial \Xi} = 0 \qquad \text{at} \quad t \in (t_i, t_{i+1}); \qquad (i = 0,1,2..) \tag{A.4}$$

or

$$W(\Xi, I_1, I_3) = \text{constant} \quad ; \qquad \Xi \in (\Xi_i, \Xi_{i+1}) \tag{A.5}$$

Combine (A.3) and (A.4), the second law of thermodynamics is satisfied on the condition that

$$\frac{\partial W}{\partial \Xi} \dot{\Xi} = 0 \tag{A.6}$$

This means that the material with a internal energy function $W(\Xi, I_1, I_2)$ experiences actually an *elastic* deformation from time t_{i-1} to t_{i+1} (see Lubliner, 1972).

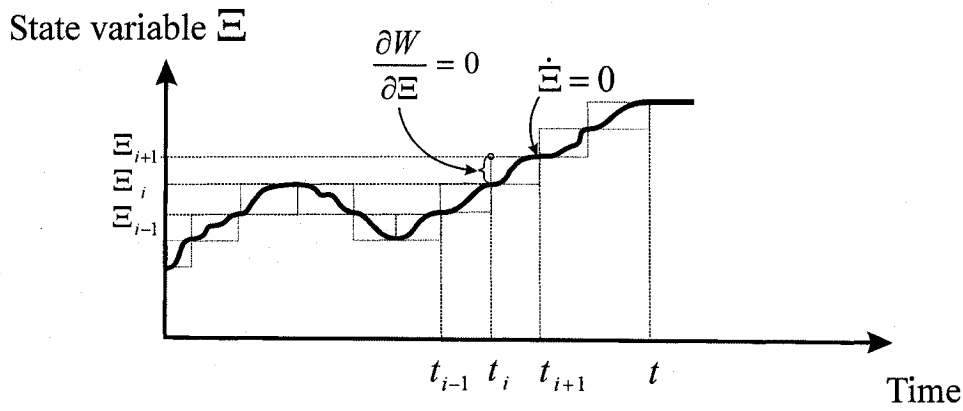

Figure A.1 A discretized evolution of a state variable

Let us further think that the dependence of the internal energy function W on the internal variable Ξ is significant from time t_{i-1} to t_{i+1}. (If the dependence of the internal energy function W on the internal variable Ξ is insignificant, the second law of thermodynamics is automatically satisfied with $\partial W / \partial \Xi = 0$). Therefore, internal energy differs at levels of Ξ_i ($i = 0,1,2..$), i.e.,

$$W(\Xi_i) < W(\Xi_{i+1}) \quad ; \quad (i = 0,1,2..) \tag{A.7}$$

Discrepancy of (A.5), however, arises when $(\Xi_{i+1} - \Xi_i) \to \infty$, which means that the internal energy function W has no dependency on Ξ. In order to resolve this, a concept of "sensitivity" parameter Ξ_c of the material is introduced such that values of internal energy differs at two material states with a difference larger than Ξ_c, i.e.,

$$W(\Xi_i, I_1, I_2) < W(\Xi_i + \Xi_c, I_1, I_2) \tag{A.8}$$

or

$$W(\Xi_i + \delta, I_1, I_2) = \begin{cases} W(\Xi_i, I_1, I_2) & ; \ 0 \le \delta < \Xi_c \\ W(\Xi_i + \Xi_c, I_1, I_2) & ; \ \delta \ge \Xi_c \end{cases} \tag{A.9}$$

The existence of the "sensitivity" parameter Ξ_c of the material then comprises our second fundamental assumption.

In order for both (A.5) and (A.9) to come true, Ξ_i and Ξ_{i+1} must satisfy a relation that

$$\Xi_{i+1} - \Xi_i \geq \Xi_c \tag{A.10}$$

Let us first assume that $\Xi_{i+1} - \Xi_i > \Xi_c$, therefore a positive value $\tilde{\beta} > 0$ can be found such that $\Xi(= \Xi_i + \Xi_c + \tilde{\beta}) < \Xi_{i+1}$. Since $\Xi \in (\Xi_i, \Xi_{i+1})$, (A.5.) can lead to

$$W(\Xi, I_1, I_2) = W(\Xi_i, I_1, I_2) \tag{A.11}$$

However, since $\Xi(= \Xi_i + \Xi_c + \tilde{\beta}) > \Xi_i + \Xi_c$, (A.9) can lead to

$$W(\Xi, I_1, I_2) = W(\Xi_i + \Xi_c, I_1, I_2) \tag{A.12}$$

The discrepancy between (A.8) and (A.11 and A.12) then allows us to say that

$$\Xi_{i+1} - \Xi_i = \Xi_c \tag{A.13}$$

or

$$\Xi_i = \Xi_0 + i\Xi_c \tag{A.14}$$

At those intervals of Ξ (say $\Xi \in [\beta_1, \beta_2]$) where $\partial W / \partial \Xi \leq 0$, similar comments as (A.14) can be addressed. (A.14) therefore states that internal energy function W actually shows a *continuous* "step-wise" dependency on the *continuous* internal variable Ξ. While the internal energy function in a form of $W(\Xi, I_1, I_2)$ is *continuous*, it can only alter at certain discrete state variables of Ξ_0, Ξ_1 ... Ξ_i where $\partial W / \partial \Xi \neq 0$. Other permissible sources of energy, such as radiation, mechanical work or other potential energy, can be transformed with internal energy only at these discrete state variables. At discrete state variables of Ξ_0, Ξ_1 ... Ξ_i, however, the levels of internal energy is undetermined. The difference of each discrete state is then characterized by a *sensitivity parameter* Ξ_c (See Figure A.2). This is similar to the concepts of "*natural units*" or "*quanta*" discovered by Planck (1901) in study of blackbody radiation, discrete energy levels around a hydrogen atom interpreted by Bohr (1913), and discrete molecular states introduced by Einstein (1917). The authors clearly had no desire to explain the existence of discrete material states Ξ_0, Ξ_1 ... Ξ_i with these fundamental concepts in physics. They are provided to illustrate the possibility of a continuous step-wise evolution of an

internal energy potential (with a basic physical constraint that $|W(\Xi_i, I_1, I_2) - W(\Xi_{i+1}, I_1, I_2)| \geq h$, where $h = 6.626 \times 10^{-34} m^2 kg / sec$ is the Planck's constant).

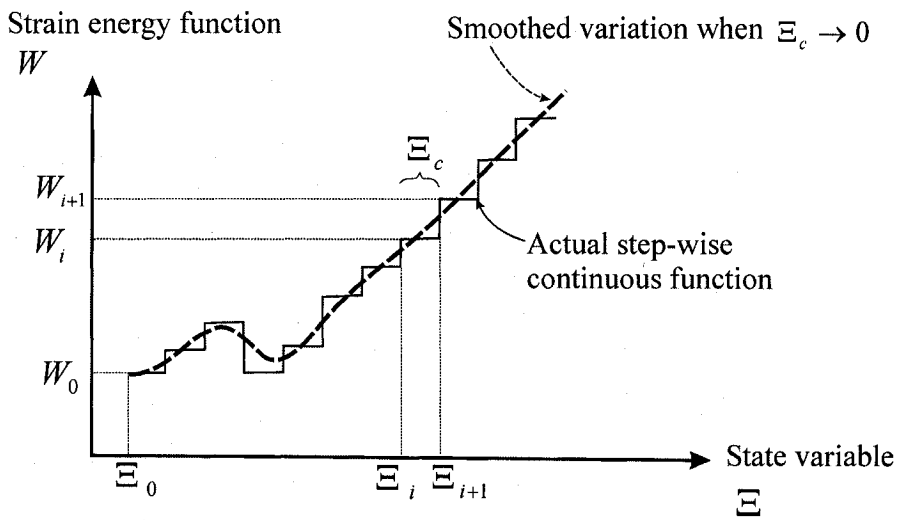

Figure A.2 A step-wise internal energy function

From (A.9), it can be known that the level of the internal energy can stay stable with a maximum disturbance of Ξ_c at discrete variables Ξ_0, $\Xi_1 \ldots \Xi_i$. With $i = 0$, it should be noted that the original configuration of the material can resist a maximum disturbance of Ξ_c to Ξ_0, i.e.,

$$W(\Xi, I_1, I_2) = W(\Xi_0, I_1, I_2) \quad ; \quad \Xi \in (\Xi_0 - \Xi_c, \Xi_0 + \Xi_c) \tag{A.15}$$

When Ξ_c is sufficiently small, so does the difference between each evolution step $|\Xi_{i+1} - \Xi_i|$. The continuous step-wise relation between W and Ξ can approximately be smoothed with a continuous form of its slope (shown in Figure A.2).

Now the internal variable is interpreted as the absolute value of the strain rate defined in the paper (i.e. $\Xi = |\dot{\gamma}_0|$). The *original* value of Ξ then becomes $\Xi_0 = 0$. Therefore there should be an extremely low value of strain rate $\dot{\gamma}_c$ between which the internal energy function is independent from $\dot{\gamma}_0$, i.e.,

$$W = \begin{cases} W(\dot{\gamma}_c, I_1, I_2) & ; \ |\dot{\gamma}_0| \le \dot{\gamma}_c \\ W(\dot{\gamma}_0, I_1, I_2) & ; \ |\dot{\gamma}_0| > \dot{\gamma}_c \end{cases} \tag{A.16}$$

where W is a *smoothed* function; and $\dot{\gamma}_c$ is called the *rate-independent threshold strain-rate* defined in the paper for model *C* (see Figure 7). The detail experimental procedures for the determination of the form of $W(\dot{\gamma}_0, I_1, I_2)$ and value of $\dot{\gamma}_c$ are described in the paper.

The internal variable can be further interpreted as the value of the strain rate (i.e., $\Xi = \dot{\gamma}_0$; see also Sweeney and Ward, 1995). In this case, the internal variable can take either in a positive or a negative form, and $\Xi_0 = 0$. From previous analysis, it is then allowable that the internal energy is independent from $\dot{\gamma}_0$ at $\dot{\gamma}_0 < -\dot{\gamma}_c^v$. Therefore the internal energy function can then be written as (see Figure A.3)

$$W = \begin{cases} \widetilde{C}(I_1, I_2) & ; \ \dot{\gamma}_0 < -\dot{\gamma}_c^v \\ W(\dot{\gamma}_c^v, I_1, I_2) & ; \ |\dot{\gamma}_0| < \dot{\gamma}_c^v \\ W(\dot{\gamma}_0, I_1, I_2) & ; \ \dot{\gamma}_0 \ge \dot{\gamma}_c^v \end{cases} \tag{A.17}$$

where W is a *smoothed* function at $\dot{\gamma}_0 > \dot{\gamma}_c^v$; $\widetilde{C}(I_1, I_2) \ge 0$ and $\partial \widetilde{C} / \partial \dot{\gamma}_0 = 0$; and $\dot{\gamma}_c^v$ is called the *viscous threshold strain-rate* defined for model *A* (see also Figure 3.5).

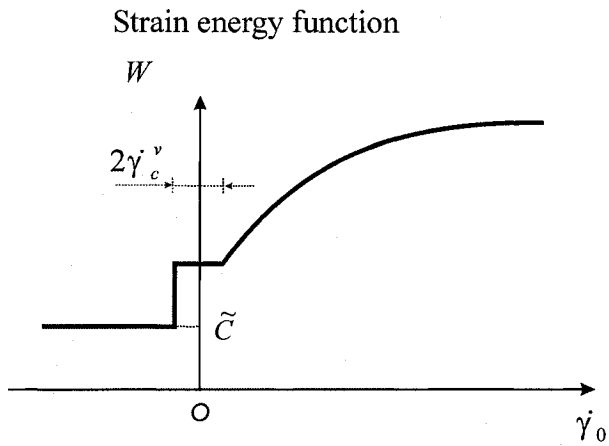

Figure A.3 Internal energy as a function of strain rate $\dot{\gamma}_0$

References

ABAQUS/Standard (2004) *A General-Purpose Finite Element Program*, Hibbitt, Karlsson & Sorensen, Inc., Pawtucket, RI, USA.

Adkins, J.E. (1961) Large elastic deformations, in: Sneddon, I.N. and Hill, R. (Eds.), *Prog. in Solid Mech.*, **Vol. 2**, pp. 2-60.

Adkins, J.E. and Rivlin, R.S. (1952) Large elastic deformations of isotropic materials. 9. The deformation of thin shells, *Phil. Trans. Roy. Soc.*, **Vol. A244**, pp. 505-531.

Aiken, W., Alfrey, T., Janseen, A. and Mark, H. (1947) Creep behavior of a plasticized vinylite VYNW, *J. Polym. Sci.*, **Vol. 2**, pp. 178-198.

Alfrey, T., Wiederhorn, N. and Stein, R. and Tobolsky, A. (1949a) Plasticized polyvinyl chloride: structure and mechanical behavior, *Ind. Eng. Chem.*, **Vol. 41**, No.4, pp. 701-703.

Alfrey, T., Wiederhorn, N., Stein, R. and Tobolsky, A. (1949b) Some studies of plasticized polyvinyl chloride, *J. Colloid. Sci.*, **Vol. 4**, pp. 211-227.

Allman, D. J. (1982) Variational solutions for the nonlinear deflection of an annular membrane under axial load, *Int. J. Mech. Sci.*, **Vol. 24**, pp. 749-753.

American Society for Testing and Materials (ASTM) (1999) *Annual Book of ASTM Standards, Vol. 04.09, Soil and Rock (II): D4943-latest; Geosynthetics*, ASTM, Philadelphia, PA.

Amin, A.F.M.S., Alam, M.S. and Okui, Y. (2002) An improved hyperelasticity relation in modeling viscoelasticity response of natural and high damping rubbers in compression: experiments, parameter identification and numerical verification, *Mech. Mat.*, **Vol. 34**, pp. 75-95.

Aminabhavi, T.M. and Naik, H.G. (1999) Chemical compatibility testing of linear low density polyethylene geomembrane, *J. Polym. Eng.*, **Vol. 19**, No. 5, pp. 315-332.

Arlman, E.J. (1954) Thermal and oxidative decomposition of polyvinyl chloride, *J. Polym. Sci.*, **Vol. 7**, pp. 547-558.

Arroyo, M. and Belytschko, T. (2002) An atomistic-based finite deformation membrane for single layer crystalline films, *J. Mech. Phys. Solids*, **Vol. 50**, pp. 1941–1977.

Arruda, E.M. and Boyce, M.C. (1993) A three dimensional constitutive model for the large stretch behavior of rubber elastic materials, *J. Mech. Phys. Solids*, **Vol. 41**, No. 2, pp. 389-412.

Arruda, E.M., Boyce, M.C. and Jayachandran, R. (1995) Effects of strain rate, temperature and thermomechanical coupling on the finite strain deformation of glassy polymers, *Mech. Mat.*, **Vol. 19**, pp. 193-212.

Assmuth, T. and Penttilae, S. (1995) Characteristics, determinants and interpretations of acetic lethality in diploids exposed to complex waste leachates, *Aquat. Toxicol.*, **Vol. 31**, pp. 125-141.

ASTM (American Society for Testing and Materials) (1999) D4833-88: standard test method for index puncture resistance of geotextiles, goemembranes, and related products, annual Book of ASTM Standards, Vol. 04.09, Soil and Rock (II): D4943-latest; Geosynthetics. ASTM, Philadelphia, PA.

Bacaloglu, R. and Fisch, M. (1995) Degradation and stabilization of poly (vinyl chloride). V. reaction mechanism of poly(vinyl chloride) degradation, *Polym. Degrad. Stab.*, **Vol. 47**, pp. 33-57.

Barenblatt, G.I. and Joseph, D.D. (Eds.) (1997) *Collected Papers of R.S. Rivlin*, **Vols. I and II**, Springer-Verlag, Berlin.

Barlaz, M.A., Schaefer, D.M. and Ham, R.K. (1989) Bacterial population development and chemical characteristics of refuse decomposition in a simulated sanitary landfill, *Appl. Environ. Microbiol.*, **Vol. 55**, pp. 55-65.

Barlaz, M.A. and Ham, R.K. (1993) Leachate and gas generation, in: Daniel, D.E. (Eds.), *Geotechnical Practice for Waste Disposal*, Chapter 6, London; New York: Chapman & Hall.

Barone, F.S., Costa, J.M.A. and Ciardullo, L. (1997) Temperatures at the base of a municipal solid waste landfill, *50th Canadian Geotechnical Conference of the Canadian Geotechnical Society, 20-22 October, 1997*, Ottawa, Ontario, pp. 144-152.

Barquins, M. and Courtel, R. (1975) Rubber friction and the rheology of viscoelastic contact, *Wear*, **Vol. 32**, pp. 133-150.

Barrett, W.M. (1998) *Determination of the Effect of Exposure to Gasoline Components On A High Density Polyethylene Geomembrane Using the Comprehensive Test System*, Ph.D. thesis, University of South Florida.

Barrett, W.M., Stessel, R.I. and Fetterly, III, F.A. (1998) Evaluation of chemical compatibility testing of goemembranes using the comprehensive test system, *J. Air Waste Manage. Assoc.*, **Vol. 49**, pp. 1027-1038.

Beatty, M.F. (1987) Topics in finite elasticity: hyperelasticity of rubber, elastomers, and biological tissues-with examples, *Appl. Mech. Rev.*, **Vol. 40**, pp. 1699-1734.

Benavides, R., Castillo, B.M., Castaneda, A.O., Lopez, G.M. and Arias, G. (2001) Different thermo-oxidative degradation routes in poly(vinyl chloride), *Polym. Degrad. Stab.*, **Vol. 73**, pp. 417-423.

Bengough, W.I. and Sharpe, H.M. (1963) The thermal degradation of polyvinylchloride in solution, I. the kinetics of the dehydrochlorination reaction, *Macromol. Chem. Phys.*, **Vol. 66**, pp. 31-44.

Benson, C.H., Abichou, T.H. and Olson, M.A. (1995) Winter effects on hydraulic conductivity of compacted clay, *J. Geotech. Geoenviron. Eng.*, **Vol. 121**, pp. 69-79.

Bergström, J.S. and Boyce, M.C. (1998) Constitutive modeling of the large strain time-dependent behavior of elastomers, *J. Mech. Phys. Solids*, **Vol. 46**, No. 5, pp. 931-954.

Besdo, D., Schuster, R.H. and Ihlemann, J. (Eds.) (2001) *Constitutive Models for Rubber II, Proc. 2nd European Conf. Constitutive Models for Rubber*, Hannover, Germany, A.A. Balkema, Lisse.

Bessems, E. (1988) The biodeterioration of plasticized PVC and its prevention, *J. Vinyl Technol.*, **Vol. 10**, No. 1, pp. 3-6.

Betten, J. (2002) *Creep Mechanics*, Springer-Verlag, Berlin.

Bhatia, N.M. and Nachbar, W. (1968) Finite indentation of an elastic membrane by a spherical indenter, *Int. J. Non-Linear Mechanics*, **Vol. 3**, pp. 307-324.

Billmeyer, F.W. (1971) *Textbook of Polymer Science*, Wiley Interscience: New York.

Bishop, S., Isaac, D.H., Hinksman, P. and Morrissey, P. (2000) Environmental stress cracking of poly(vinyl chloride) in alkaline solutions, *Polym. Degrad. Stab.*, **Vol. 70**, pp. 477-484.

Blundell, D.J. (1979) Small-angle X-ray study of microdomains in rigid PVC, *Polymer*, **Vol. 20**, pp. 934-938.

Bohr, N. (1913) On the constitution of atoms and molecules. Part II-systems containing only a single nucleus, *Phil. Mag.*, **Vol. 26**, pp. 476-502.

Boue, F., Edwards, S.F. and Vilgis, T.A. (1988) The entropy of a network of rod molecules, *J. Phys.*, **Vol. 49**, pp. 1635-1645.

Borek, J. and Oscoba, W. (1996) Free volume in plasticized polyvinyl chloride, *J. Polym. Sci., B, Polym. Phys.*, **Vol. 34**, pp. 1903-1906.

Bort, D.N., Zegel'man, V.I. and Kargin, V.A. (1968) Supermolecular formulations in crystalline polyvinylchloride, *Polym. Sci. USSR.*, **Vol. 10**, pp. 1498-1505.

Boyce, M.C., Parks, D.M. and Argon, A.S. (1988) Large inelastic deformation of glassy polymers, part I: rate dependent constitutive model, *Mech. Mat.*, **Vol. 7**, pp. 15-33.

Boyce, M.C. and Arruda, E.M. (2000) Constitutive models of rubber elasticity, a review, *Rubber Chem. and Tech.*, **Vol. 73**, No. 3, pp. 504-523.

Boyd, R.H. and Philips, P.J. (1993) *The Science of Polymer Molecules*, Cambridge University Press, Cambridge.

Bozkurt, S., Moreno, L. and Neretnieks, I. (1999) Long-term fate of organics in waste deposits and its effect on metal release, *Sci. Total Environ.*, **Vol. 228**, pp. 135

Bozkurt, S., Moreno, L. and Neretnieks, I. (2000) Long-term processes in waste deposits, *Sci. Total Environ.*, **Vol. 250**, pp. 101-121.

Brandrup, J. Immergut, E.H. and Grulke, E.A. (1999) *Polymer Handbook*, Fourth edition, John Wiley & Sons.

Brink, D., Day, P.W. and Du Freez, L. (1999) Failure and remediation of Bulbul Drive landfill: Kwazulu-Natal, South Afria, Cazzuffi, *Proceedings Sardinia' 99, Seventh International Landfill Symposium*, pp. 100-108.

Briscoe, B. (1981) Wear of polymers: an essay on fundamental aspects, *Tribol. Int.*, **Vol. 14**, pp. 231-243.

Bruins, P.F. (1965) *Plasticizer Technology*, **Vol. 1**, Reinhold Publishing, New York.

Busfield, J.J.C. and Muhr, A.H. (Eds.) (2003) Constitutive Models for Rubber III, *Proc. 2nd European Conf. Constitutive Models for Rubber*, London, U.K., A.A. Balkema, Lisse.

Buszard, D.I. (1984) Properties of plastcized PVC, in: Titow, W.V. (Eds.), *PVC Technology*, Elsevier, London, pp. 181-214.

Burton, S.Q. and Watson-Craik, I.A. (1998) Ammonia and nitrogen fluxes in landfill sites: application to sustainable landfilling, *Waste Manage. Res.*, **Vol. 16**, pp. 41-54.

Cameron, R.D. and Koch, F.A. (1980) Toxicity of landfill leachates, *J. Water Pollut. Control Fed.*, **Vol., 52**, pp. 760-769.

Carrega, M. (1977) Polyvinyl-chloride–general discussion on properties, *J. Macromol Sci., Phys.*, **Vol. B14,** pp. 585-591.

Carslaw, H.S. and Jaeger, J.C. (1959) *Heat Conduction in Solids*, Clarendon Press, Oxford.

Cassidy, P.E., Mores, M., Kerwick, D.J., Koeck, D.J., Verschoor, K.L. and White, D.F. (1991) Chemical resistance of geosynthetic material, *Geotext. Geomembr.*, **Vol. 11**, pp. 61-98.

Cazzuffi, D., Fede, L., Villa, C., Montanelli, F. and Rimoldi, P. (1995) The assessment of the effects of natural and lab weathering exposure of geosynthesics, *Proceedings Sardinia' 95, Fifth International Landfill Symposiu*m, pp. 387-396.

Chamberlain, E.J., Erickson, A.E. and Benson, C.H. (1995) Effects of frost action on compation of compacted clay barriers, *Proceeding of GeoEnvironment 2000, ASCE*, Geotechnical Special Publication, No. 46, New Orleans, LA, USA, pp. 702-717.

Christensen, R.M. (1971) *Theory of Viscoelasticity*, Academic Press, New York.

Christensen, T.H. Kjeldsen, P., Albrechtsen, H.J., Heron, G. Nielsen, P.H., Bjerg, P.L. and Holm, P.E. (1994) Attenuation of landfill leachate pollutants in aquifers, *Crit. Rev. Environ. Sci. Technol.*, **Vol. 24**, pp. 119.

Christensen, T.H. and Kjeldsen, P. (1995) Landfill emissions and environmental impact: an introduction, in: Christensen, T.H., Cossu, R. and Stegmann, R. (Eds.), *SARDINIA 95, Fifth International Landfill Symposium, Proceedings*, **Vol. III**, CISA, Cagliari, Italy, pp. 3-27.

Christensen, T.H., Kjeldsen, P., Bjerg, P.L., Jensen, D.L., Christensen, J.B., Baun, A., Albrechtsen, H.J., Heron, G. (2001) Biogeochemistry of landfill leachate plumes, *Appl. Geochem.*, **Vol. 16**, pp. 659-718.

Christoph, H., Volker, M.S., Virginia, S.H., Ursula, G., Carmen, K. Lu, W., Fekadu, K., Rolf, S.H. and Siegfried, K. (1996) Comparative evalution of four bacterial assays for the detection of genotoxic effects in the dissolved water phases of acqueous matrices, *Environ. Sci. Technol.*, **Vol. 30**, No. 3, pp. 897-907.

Clement, B. and Merlin, G. (1995) The contribution of ammonia and alkalinity to landfill leachate toxicity to duckweed, *Sci. Total Environ.*, **Vol. 170**, pp. 71-79.

Clement, B., Persoone, G., Janssen, C., Le Du-Delepierre, A. (1996) Estimation of the hazard of landfills through toxicity testing of leachates, *Chemosphere*, **Vol. 33**, No. 11, pp. 2303-2320.

Collette, D. (1994) The calendering process in geomembrane manufacturing, in: Husan, Y.G. and Koerner, R.M. (Eds.), *Geosynthetic Resins, Formulations and Manufacturing*, Industrial Fabrics Associated Internatinal, pp. 153-155.

Contamin, B. and Debeauvais, V. (1998) *The Effect of Ethanol Exposure on Burst Strength of a Geomembrane*, Research Report, McGill University.

Crank, J. (1975) *The Mathematics of Diffusion*, Clarendon Press, London.

Dacko, A.K. and Glockner, P.G. (1988) Spherical inflatable under axisymmetric loads: another look, *Int. J. Non-Linear Mechanics*, **Vol. 23**, pp. 393-407.

Daniel, D.E. and Wu, Y.K. (1993) Compacted clay liners and covers for arid sites, *J. Geotech. Eng.*, **Vol. 119**, pp.223-237.

Deam, R.T. and Edwards, S.F. (1976) The theory of rubber elasticity, *Phil. Trans. Roy. Soc.*, **Vol. 280**, pp. 317-353.

Decoste, J.B. (1968) Soil Burial resistance of vinyl chloride plastics, *Ind. Eng. Chem. Prod. Res. Dev.*, **Vol. 7**, pp. 238-247.

Dickey, R.W. (1967) The plane circular membrane under normal pressure, *Arch. Rat. Mech. Analysis*, **Vol. 26**, pp. 219-236.

Dickey, R.W. (1983) The non-linear circular membrane under a vertical force, *Quart. Appl. Math.*, **Vol. 41**, pp. 331-338.

Diebel, P. (2002) Formulation, manufacturing and physical properties of PVC geomembranes, in: *PVC Geomembrane Institute Technology Program: Constructing with PVC Geomembrane: Video Series*, Lecture 1, PVC Geomembrane Institute, University of Illinois at Urbana-Champaign.

Djidjelli, H., Kaci, M., Boukerrou, A., Benachour, D. and Martinez-Vega, J.J. (2003) Hydrothermic aging of plasticized poly(vinyl chloride): its effect on the dielectric, thermal, and mechanical properties, *J. Appl. Polym. Sci.*, **Vol. 89**, pp. 3447-3457.

Doi, M. and Edwards, S.F. (1987) *The Theory of Polymer Dynamics*, Oxford University Press.

Dorfmann, A. and Muhr, A. (Eds.) (1999) *Constitutive Models for Rubber*, A.A. Balkema, Rotterdam.

Dorfmann, A. and Ogden, R.W. (2004) A constitutive model for the Mullins effect with permanent set in particle-reinforced rubber, *Int. J. Solids Struct.*, **Vol. 41**, pp. 1855-1878.

Dorrestijn, A., Keijzers, A.E. and te Nijenhuis, K. (1981) Correlation between viscoelastic behaviour and small angle X-ray scattering of thermoreversible polyvinyl chloride gels, *Polymer*, **Vol. 22**, pp. 305-312.

Doyle, T.C. and Ericksen, J.L. (1956) Nonlinear elasticity, *Adv. Appl. Mech.*, **Vol. 4**: 53-115.

Doyle, R.A. and Baker, K.C. (1989) Weathering of geomembranes, in: Koerner, R.M. (Eds.), *Durability and Aging of Geosynthetics*, Elsevier: London and New York, pp. 152-158.

Drozdov, A.D. (1996) *Finite Elasticity and Viscoelasticity*, World Scientific, Singapore.

Drozdov, A.D. and Dorfmann, A. (2003) A micro-mechanical model for the response of filled elastomers at finite strains, *Int. J. Plast.*, **Vol. 19**, pp. 1037-1067.

Dubault, A., Bokobza, L., Gandin, E. and Halary, J.L. (2003) Effect of molecular interations on the viscoelastic and plastic behavior of plasticized poly(vinyl chloride), *Polym. Int.*, **Vol. 52**, pp. 1108-1118.

Duquennoi, C., Bernhard, C. and Gaumet, S. (1995) Laboratory aging of geomembranes in landfill leachates, *Sardinia 95: Fifth International Landfill Symposium*, pp. 397-404.

Earth Technology (1988) *In-place stability of landfill slopes, Puente Hills Landfill, Los Angeles, California, Report No. 88-614-1*, The Earth Technology Corp., Long Beach, CA.

Edwards, S.F. (1971) Statistical mechanics of rubber, in: Chompff, A.J. and Newman, S. (Eds.), *Polymer Networks: Structural and Mechanical Properties*, Plenum Press, New York, pp. 83-110.

Einstein, A. (1917) Zur Quantentheorie der Strahlung (in German; Quantum theory of radiation), *Zeit. Phys.*, **Vol. 18**, pp. 121-128.

Elicegui, A., del Val, J.J., Bellenger, V. and Verdu, J. (1997) A study of plasticization effects in poly(vinyl chloride), *Polymer*, **Vol. 38**, No. 7., pp. 1647-1657.

Endo, K. (2002) Synthesis and structure of poly(vinyl chloride), *Prog. Polym. Sci.*, **Vol. 27**, pp. 2021-2054.

Erman, B. and Flory, P.J. (1982) Relationships between stress, strain and molecular constitution of polymer networks. Comparison of theory with experiments, *Macromolecules*, **Vol. 15**, pp. 806-811.

Farris, R.J. (1971) The stress-strain behaviour of mechanically degradable polymers, in, *Polymer Networks: Structural and Mechanical Properties*, in: Chompff, A.J. and Newman, S. (Eds.), Plenum Press, New York, pp. 341-392.

Fayoux, D. (1990) Durability of PVC geomembranes and resistance to mechanical puncturing, in: Hoedt, G.D. (Eds.), *Geotextiles, Geomembranes and Related Products*, **Vol. II**, Balkema, Brookfield, pp. 561-565.

Faulkner, P.G. (1975) The use of a temperature programmable behavior mixing head for the evalution of the processing characteristics of poly(vinyl) chloride, *J. Macromol. Sci., Phys.*, **Vol. B11**, pp. 251-279.

Feng, W.W. (1987) Indentation of a plane membrane with a rigid paraboloid, *Int. J. Non-Linear Mechanics,* **Vol. 22**, pp. 261-265.

Feng, W.W. (1992) Viscoelastic behavior of elastomeric membranes, *J. Appl. Mech.*, **Vol. 59**, S29-S35.

Feng, W.W. and Yang, W.H. (1973) On the contact problem of an inflated spherical nonlinear membrane, *J. Appl. Mech.*, **Vol. 40**, pp. 209-214.

Feng, W.W., Tielking, J.T. and Huang, P. (1974) The inflation and contact constraint of a rectangular Mooney membrane, *J. Appl. Mech.*, **Vol. 41**, pp. 979-984.

Feng, W.W. and Huang, P. (1975) On the general contact problem of an inflated nonlinear plane membrane, *Int. J. Solids Structures*, **Vol. 11**, pp. 437-448.

Fick A. (1855) Ueber Diffusion, *Annln. Phys.*, **Vol. 170**, pp. 59-86.

Findley, W.N., Lai, J.S. and Onaran, K. (1976) *Creep and Relaxation of Nonlinear Viscoelastic Materials, with an Introduction to Linear Viscolasticity*, North-Holland Publ. Co., The Netherlands.

Flores, R., Perez, J., Cassagnau, P., Michel, A. and Cavaille, J.Y. (1994) α mechanical relaxation in poly(vinyl chloride): effect of ageing and crosslinking, *Polymer*, **Vol., 35**, pp. 2800-2808.

Flory, P.J. (1969) *Statistical Mechanics of Chain Molecules*, Wiley Interscience, New York.

Flory, P.J. and Erman, B. (1982) Theory of Elasticity of Polymer Networks. 3, *Macromolecules*, **Vol. 15**, pp. 800-806.

Foster, H.O. (1967) Inflation of a plane circular membrane, *J. Eng. Ind.*, **Vol. 89**, pp. 403-407.

Frascari, D., Bronzini, F., Giordano, G., Tedioli, G. and Nocentini, M. (2004) Long term characterization, lagoon treatment and migration potential of landfill leachate: a case study in an active Italian landfill, *Chemosphere*, **Vol. 54**, pp. 335-343.

Frisch, H.L. (1978) Simultaneous nonlinear diffusion of a solvent and organic penetrant in a polymer, *J. Polym. Sci., Polym. Phys. Ed.*, **Vol. 16**, pp. 1651-1664.

Frissell, W.J. (1956) Volatility of vinyl plasticizers, *Ind. Eng. Chem.*, **Vol. 48**, pp. 1096-1099.

Fu, Y.B. and Ogden, R.W. (Eds.) (2001) *Nonlinear Elasticity: Theory and Applications*, Cambridge Univ. Press, Cambridge.

Fulton, J.P. and Simmonds, J.G. (1986) Large deformations under vertical edge loads of annular membranes with various strain energy densities, *Int. J. Non-Linear Mechanics*, **Vol. 21**, pp. 257-267.

Gascó, M.C., Rodriguez, F. and Long, T. (1998) Polymer-polymer friction as a function of test speed, *J. Appl. Polym. Sci.*, **Vol. 67**, pp. 1831-1836.

Giardino, V.G. and Guglielmetti, J.L. (1997) Long-term performance of a hazardous waste landfill, *Geotext. Geomembr.*, **Vol. 15**, pp. 255-267.

Gibbons, W. S., Patel, H.M. and Kusy, R.P. (1997) Effects of plasticizers on the mechanical properties of poly (vinyl chloride) membranes for electrodes and biosensors, *Polymer*, **Vol. 38**, No.11, pp. 2633-2642.

Gibbons, W. S. and Kusy, R.P. (1998) Influence of plasticizer configurational changes on the mechanical properties of highly plasticized poly(vinyl chloride), *Polymer*, **Vol. 39,** No. 26, pp. 6755-6765.

Gilbert, M. (1994) Crystallinity in poly(vinyl chloride), *J. Macromol. Sci., Rev. Macromol. Chem. Phys.*, **Vol. C34**, No. 1, pp. 77-136.

Gilbert, M. and Mulla, M.I. (1983) Use of solvent sorption to detect structural changes in rigid PVC compounds, *Polym. Test.*, **Vol. 3**, No. 3, pp. 171-182.

Giroud, J.P. (1985) Aging of PVC geomembranes in uranium mine tailing ponds, in: Giroud, J.P. (Eds.), *Geotextiles and Geomembranes-Definitions, Properties, and Design*, Industrial Fabrics Association International, St. Paul, Minnesota, pp. 311-316.

Giroud, J.P. and Bonaparte, R. (1989) Leakage through liners constructed with geomembranes, - part 1. geomembrane liners, *Geotext. Geomembr.*, **Vol. 8**, pp. 27-67.

Giroud and Soderman (1995) Comparison of geomembranes subjected to different settlement, *Geosynth. Int.*, **Vol. 2**, No. 6, pp. 953 – 969.

Glenda, G (1997) The state of garbage in Canada, *BioCycle*, **Vol. 38**, pp. 78-82.

Glockner, P.G. and Vishwanath, T. (1972) On the analysis of non-linear membranes, *Int. J. Non-Linear Mechanics*, **Vol. 7**, pp. 361-394.

Gray, A. and Gilbert, M. (1975) Solvent sorption of heat-treated vinyl chloride polymers , *Polymer*, **Vol. 16**, pp. 387-389.

Green, A.E. and Adkins, J.E. (1970) *Large Elastic Deformations*, Oxford University Press, London.

Green, A.E. and Spratt, E.B. (1954) Second-order effects in the deformation of elastic bodies, *Proc. Roy. Soc.*, **A224**: 347-361.

Green, M.S., Tobolsky, A.V. (1946) A new approach to the theory of relaxing polymeric media, *J. Chem. Phys.*, **Vol. 14**, pp. 80-92.

Grosch, K.A. (1963) Relation between the friction and visco-elastic properties of rubber, *Proc. Roy. Soc.*, **Vol. A274**, pp. 21-39.

Guerreto, S. J. (1989) Antiplasticization and crystallinity in poly(vinyl chloride), *Macromolecules*, **Vol. 22**, pp. 3480-3485.

Gumargalieva, K.Z., Ivanov, V.B., Zaikov, G.E., Moiseev, Ju. V. and Pokholok, T.V. (1996) Problems of aging and stabilization of poly(vinyl chloride), *Polym. Degrad. Stab.*, **Vol. 52**, pp. 73-79.

Gumargalieva, K.Z., Zaikov, G.E., Semenov, S.A. and Zhdanova, O.A. (1999) The influence of biodegradation on the loss of a plasticizer from poly(vinyl chloride), *Polym. Degrad. Stab.*, **Vol. 63**, pp. 111-112.

Gurtin, M.E. and Anand, L. (2005) The decomposition $\mathbf{F} = \mathbf{F}^e\mathbf{F}^p$, material symmetry, and plastic irrotationality for solids that are isotropic-viscoplastic or amorphous, *Int. J. Plast.* (in press)

Haedrich, T. (1995) *The Effect of Chemical Exposure on the Burst Strength of a Geomembrane*, Master Thesis, Carleton University, Ottawa.

Hamza, S.S. and Abdel-Hamid, M. (1998) The effect of thermal aging and type of stabilizer on creep characteristics of poly(vinyl chloride), *Polym. Degrad. Stab.*, **Vol. 62**, pp.171-174.

Hart-Smith, L. J. and Crisp, J. D. C. (1967) Large elastic deformations of thin rubber membranes, *Int. J. Engng. Sci.*, **Vol. 5**, pp. 1-24.

Hattori, T., Tanaka, K. and Matsuo, M. (1972) Fusion of particulate structure in polyvinyl chloride during power extrusion, *Polym. Eng. Sci.*, **Vol. 12**, pp. 199-207.

Haxo, H.E. (1990) Determining the transport through geomembranes of various permeants in different applications, in: *Geosynthetic Testing for Waste Containment Applications, Las Vegas, Nevada, USA*, ASTM Special Technical Publication 1081, Philadelphia, pp. 75-94.

Haxo, H.E., Miedema, J.A. and Nelson, N.A. (1984) Permeability of polymeric membrane lining materials, *Proceedings of International Conference on Geomembranes, 20-24 June, 1984, Denver, Co., USA*, **Vol. 1**, pp. 151-168.

Haxo, H.E., Nelson, N.A. and Miedema, J.A. (1985a) Solubility parameters for predicting membrane-waste liquid compatibility, *Proceeding of the Conference on Hazardous Waste, April, 1985, Cincinnati, Ohio*, pp. 198-212.

Haxo, H.E., White, R.M., Haxo, P.D. and Fong, M.A. (1985b) Liner materials exposed to municipal solid waste leachate, *Waste Manage. Res.*, **Vol. 3**, pp. 41-45.

Haxo, H.E. and Haxo, P.D. (1989) Environmental conditions encountered by geosynthetics in waste containment applications, in: Koerner, R.M. (Eds.), *Durability and Aging of Geosynthetics*, Elsevier, London and New York, pp. 28-47.

Hayes, M.A. (Eds.) (2001) *Topics in Finite Elasticity*, CISM Lecture Notes 424, Springer, Wien.

Hjertberg, T. and Sorvik, E.M. (1984) Degradation of Stability of PVC, in: Owen, E.D., *Degradation and Stabilization of PVC*, Elsevier, London, Charpter 1.

Hollande, S. and Laurent, J.L. (1997) Study of discolouring change in PVC, plasticizer and plasticized PVC films, *Polym. Degrad. Stab.*, **Vol. 55**, pp. 141-145.

Holtz, R.D., Christopher, B.R. and Berg, R.R. (1997) *Geosynthetic Engineering*, Bitech Publishers, Richmond, BC, Canada.

Hsuan, Y.G. (1998) Temperature effect on the stress crack resistance of high density polyethylene geomembrane, in: *The Sixth International Conference on Geosynthetics*, **Vol. 1**, pp. 371-374.

Hsuan, Y.G. and Koerner, R.M. (1998) Antioxidant depletion lifetime in high density polyethylene geomembranes, *J. Geotech. Geoenviron. Eng.*, **Vol. 124**, pp. 532-541.

Huber, H. and Tsakmakis, C. (2000) Finite deformation viscoelasticity laws, *Mech. Mat.*, **Vol. 32**, pp. 1-18.

Jackson, W.J. and Caldwell, J.R. (1967) Antiplasticization. 3. Characteristics and properties of antiplasticizable polymers, *J. Appl. Polym. Sci.*, **Vol. 11**, pp. 227-244.

Jakubowicz, I., Yarahmadi, N. and Gevert, T. (1999) Effects of accelerated and natural ageing on plasticized polyvinyl chloride (PVC), *Polym. Degrad. Stab.*, **Vol. 66**, pp. 415-421.

James, D.I. and Newell, W.G. (1980) A new concept in friction testing, *Polym. Test.*, **Vol. 1**, pp. 9-25.

Jayakrishnan, A. and Lakshmi, S. (1998) Immobile plasticizer in flexible PVC, *Nature*, **Vol. 396**, pp. 638.

Jones, J.L. and Marques, C.M. (1990) Rigid polymer network models, *J. Phys.*, **Vol. 51**, pp. 1113–1127.

Juijn, J.A., Gisolf, J.H. and de Jong, W.A. (1973) Calorimetric study of first order transitions in polyvinyl chloride, *Kolloid-Z.Z. Polym.*, **Vol. 235**, pp. 1157-1161.

Kamlah, M. and Haupt, P. (1998) On the macroscopic description of stored energy and self heating during plastic deformation, *Int. J. Plast.*, **Vol. 13**, pp. 893-911.

Kampouris, E.M., Regas, F., Rokotas, S., Polychronakis, S. and Pantazoglou, M. (1975) Migration of PVC plasticizers into alcohols, *Polymer*, **Vol. 16**, pp. 840-844.

Kamykowski, G.W. (1994) Durability consideration for PVC formulations used in geosynthetics: a review, *Polym.-Plast. Technol. Eng.*, **V.33**, p. 281-293.

Kane, J.D. and Widmayer, D.A. (1989) Considerations for the long-term performance of geosynthetics at radioactive waste disposal facilities, in: Koerner, R.M. (Eds.), *Durability and Aging of Geosynthetics*, Elsevier, London and New York, pp. 13-27.

Kao, R. and Perrone, N. (1971) Large deflections of axisymmetric circular membranes, *Int. J. Solids Structures*, **Vol. 7**, pp. 1601-1612.

Kawamura, Y., Maehara, T., Wakui, C. and Yamada, T. (2000) Migration of plasticizers and nonylphenol from polyvinyl chloride gloves (in Japanese), *Journal of the Food Hygienic Society of Japan*, **Vol. 41**, pp. 330-334.

Khalifa, B.A., Morsi, S.E., Khalifa, W.M. and Barsoum, S. (1979) The effect of ultraviolet radiation on the physical properties of stabilized poly(vinyl chloride), *Br. Polym. J.*, **Vol. 11**, No. 1, pp. 13-16.

Khan, A. and Zhang, H. (2001) Finite deformation of a polymer: experiments and modeling, *Int. J. Plast.*, **Vol. 17**, pp. 1167-1188.

Kim, K.K.U., Hong, S.M. and Kim, B.C. (1987) A study on the antiplasticization of polyvinylchloride, *Journal of the Korean Society of Textile Engineers and Chemists*, **Vol. 24**, pp. 29-34.

Kim J.H., Kim S.H., Lee C.H. and Nah, J-W and Hahn, A. (2003) DEHP migration behavior from excessively plasticized PVC sheets, *Bull. Korean Chem. Soc.*, **Vol. 24**, pp. 345-349.

Kinjo, N. and Kakagawa, T. (1973) Antiplasticization in slightly plastifized polyvinyl-chloride, *Polym. J.*, **Vol. 4**, pp. 143-153.

Kjeldsen, P. and Christensen, T.H. (2001) A simple model for the distribution and fate of organic chemicals in a landfill: MOCLA, *Waste Manage. Res.*, **Vol. 19**, pp. 201-216.

Kjeldsen, P., Barlaz, M.A., Rooker, A.P., Baun, A., Ledin, A. and Christensen, T.H. (2002) Present and long-term composition of MSW landfill leachate: a review, *Crit. Rev. Environ. Sci. Technol.*, **Vol. 32**, No. 4, pp. 297-336.

Klette, R., Karsten, S. and Andreas, K. (1998) *Computer Vision: Three Dimensional Data from Images*, Springer-Verlag, Singapore.

Klingbeil, W.W. and Shield, R.T. (1964) Some numerical investigations on empirical strain energy functions in large axi-symmetric extensions of rubber membranes, *J. Appl. Math. Phys. (ZAMP)*, **Vol. 15**, pp. 608.

Koerner, R.M. (1990) *Durability and Aging of Geosynthetics*, Elsevier, London and New York.

Koerner, R.M. (1994) *Designing with Geosynthetics*, third edition, Prentice Hall, Upper Saddle River, New Jersey.

Koerner, R.M., Halse, Y.H. and Lord, A.E. (1990) Long-term durability and aging of geomembrane, in: Bonaparte, R. (Eds.), *Waste Containment Systems: Construction, Regulation, and Performance: Proceeding of a Symposium/ASCE*, pp.147-158.

Koerner, R.M., Lord, Jr, A.E. and Hsuan, Y.H. (1992) Arrhenius modelling to predict geosynthetic degradation, *Geotext. Geomembr.*, **Vol. 11**, pp. 151-183.

Koerner, G.R., Yazdani, R. and Mackey, R.E. (1996) Long term temperature monitoring of landfill goemembranes, *Proceedings, SWANA Conference on Landfills, No. 4-6, 1996, Publ. GR D0401*, Silver Spring, MD, pp.61-63.

Kondyli, E, Demertzis, P.G. and Kontominas, M.G. (1990) Migration of dioctylphthalate and dioctyladipate plasticizer from polyvinylchloride films into olive oil, *Food Chem.*, **Vol. 36**, pp. 1-10.

Kovacic, T. and Mrklic Z. (2002) The kinetic parameters for the evaporation of plasticizers from plasticized poly(vinyl chloride), *Thermochim. Acta*, **Vol. 381**, pp. 49-60.

Krempl, E. and Khan, F. (2003) Rate (time)-dependent deformation behavior: an overview of some properties of metals and solid polymers, *Int. J. Plast.*, **Vol. 19**, pp. 1069-1095.

Kröner, E. (1960) Allgemeine kontinuumstheorie der versetzungen und eigenspannungen, *Arch. Ration. Mech. Anal.*, **Vol. 4**, pp. 273–334.

Kydoniefs, A.D. (1969) Finite axisymmetric deformations of an initially cylindrical elastic membrane enclosing a rigid body, *Quart. J. Mech. Appl. Math.*, **Vol. 22**, pp. 319-331.

Kydoniefs, A.D. and Spencer, A.J.M. (1969) Finite axisymmetric deformations of an initially cylindrical elastic membrane, *Quart. J. Mech. Appl. Math.*, **Vol. 22**, pp. 87-95.

LaGatta, M.D., Boardman, B.T., Cooley, B.H., and Daniel, D.E. (1997) Geosynthetic clay liners subjected to differential settlement, *J. Geotech. Geoenviron. Eng.*, **Vol. 123**, pp. 402-410.

Landva, A.O. and Clark, J.I. (1990) Geotechnics of waste fill, in: Landva A.O. and Knowles G.D. (Eds.), *Geotechnics of Waste Fills-Theory and Practice, ASTM STP 1070*, Philadelphia, pp. 86-103.

Lauwers, D.C. (1994) PVC resin–the key to a flexible geomembrane, Geosynthetic Resins, in: Hsuan, Y.G. and Koerner, R.M. (Eds.), *Geosynthetic Resins, Formulations and Manufacturing*, Industrial Fabrics Associated Internatinal, pp. 47-54.

Lee, E.H. (1969) Elastic-plastic deformation at finite strains, *J. Appl. Mech.*, **Vol. 36**, pp.1-6.

Li, X. and Steigmann, D.J. (1995) Point loads on a hemispherical elastic membrane, *Int. J. Non-Linear Mechanics*, **Vol. 30**, pp. 569-581.

Libai, A. and Simmonds, J.G. (1988) *The Nonlinear Theory of Elastic Shells: One Spatial Dimension*, Academic Press, Boston.

Loehr, R.C. and Haikola, B.M. (2003) Long term landfill primary and secondary leachate production, *J. Geotech. Geoenviron. Eng*, **Vol. 129**, No.11, pp. 1063-1067.

Loizidou, M. and Kapetanios, E.G. (1993) Effect of leachate from landfills on underground water quality, *Sci. Total Environ.*, **Vol. 128**, pp. 69-81.

Lubarda, V.A. (2004) Constitutive theories based on the multiplicative decomposition of deformation gradient: thermoelasticity, elastoplasticity, and biomechanics, *Appl. Mech. Rev.*, **Vol. 57**, pp. 95-108.

Lubliner, J. (1972) On the thermodynamic foundations of non-linear solid mechanics, *Int. J. Non-Linear Mechanics*, **Vol. 7**, pp. 237-254.

Lubliner, J. (1985) A model of rubber viscoelasticity, *Mech. Res. Comm.*, **Vol. 12**, pp. 93-99.

Lur'e, A.I. (1990) *Nonlinear Theory of Elasticity*, North-Holland, Amsterdam.

Madorsky, S.L. (1964) *Thermal Degradation of Organic Polymers*, Interscience, New York.

Maisonneuve, C., Pierson, P., Duquennoi, C. and Morin, A. (1997) Accelerated aging tests for geomembranes used in landfills, *SARDINIA 97: Sixth International Landfill Symposium: Proceedings.*

Makradi, A., Ahzi, S., Gregory, R.V. and Edie, D.D. (2005) A two-phase self-consistent model for the deformation and phase transformation behavior of polymers above the glass transition temperature: application to PET, *Int. J. Plast.*, **Vol. 21**, pp. 741-758.

Malvern, L.E. (1969) *Introduction to the Mechanics of a Continuous Medium*, Prentice-Hall, Upper Saddle River.

Manson, J.A., Iobst, S.A. and Acosta, R. (1972) Preparation of poly(vinyl chloride) at low temperature by a photochemical method, *J. Polym. Sci., Polym. Chem. Ed.*, **Vol. 10**, pp. 179.

Marcilla, A., Garcia, S. and Garcia-Quesada, J.C. (2004) Study of the migration of PVC plasticizers, *J. Anal. Appl. Pyrolysis*, **Vol. 71**, pp. 457-463.

Martinez, J.G., Oliverio S.R.F., Santiago S.L. Eduardo, R.V. and Norman, S. Allen (1996) Prediction of photoageing stability of plasticised PVC films containing UV-stabiilisers, *Polym. Degrad. Stab.*, **Vol. 54**, pp. 49-55.

Marvel, C.S., Sample, J.H. and Roy, M.F. (1939) The Structure of Vinyl Polymers. VI.[1] Polyvinyl Halides, *J. Am. Chem. Soc.*, **Vol. 61**, pp. 3241.

Masada, T., Mitchell, G.F., Sargand, S.M. and Shashikumar, B. (1994) Modified direct shear study of clay liner-geomembrane interfaces exposed to landfill leachate, *Geotext. Geomembr.*, **Vol. 13**, pp. 165-179.

Matthews, G. (1996) *PVC: Production, Properties and Uses*, The Institute of Materials, London.

McBean, E.A., Rovers, F.A., and Farquhar, G.J. (1995) *Solid Waste Landfill Engineering and Design*, Prentice Hall PTR, Englewood Cliffs, NJ.

McGuirt, C.W. and Lianis, G. (1970) Constitutive equations for viscoelastic solids, *Trans. Soc. Rheol.*, **Vol. 14**, pp. 117-134.

Messadi, D. and Vergnaud, J.M. (1982) Plasticizer transfer from plasticized PVC into ethanol-water mixtures, *J. Appl. Polym. Sci.*, **Vol. 27**, pp. 3945-3955.

Mooney, M. (1940) A theory of large elastic deformation, *J. Appl. Phys.*, **Vol. 11**, pp. 583-593.

Mueller, W., Jakob, R., Tatzky-Gerth, and August, H. (1998) Solubilities, diffusion and partitioning coefficients of organic pollutants in HDPE geomembranes: experimental results and calculations, in: *The Sixth International Conference on Geosynthetics*, pp. 239-248.

Mullins, L. (1947) Effect of stretching on the properties of rubber, *J. Rubber Res.*, **Vol.16**, pp. 275-289.

Mullins, L. (1969) Softening of rubber by deformation, *Rubber Chem. Technol.*, **Vol. 42**, 339-362.

Naghdi, P.M., 1972. The theory of shells and plates, in: Flugge, S. (Eds.), *Handbuch der Physik*, Vol. Iia/2. Truesdell, C. (Eds.), *Mechanics of Solids II*, Springer-Verlag, Berlin, pp. 425-640.

Nass, L.I. and Heiberger, C.A. (1985) *Encyclopedia of PVC, Vol. 1, Resin Manufacture and Properties*, Secondary Edition, Revised and Expanded, Marcel Dekker: New York.

Newman, E., Stark, T. D. and Rohe, F.P. (2001) Features-PVC aquaculture liners stand the test of time-after three decades of performance, exhumed geomembrane retains strength and flexibility, *Geotechnical Fabric Report*, **Vol. 19**, No. 7, pp. 16-18.

Neilson, L.E., Buchhahl, R. and Levreault, R. (1950) Mechanical and electrical properties of plasticized vinyl chloride compositions, *J. Appl. Phys.*, **Vol. 21**, No. 6, pp. 607-614.

Ogden, R.W. (1972) Large deformation isotropic elasticity-on the correlation of theory and experiment for incompressible rubberlike solids, *Proc. Roy. Soc.*, **Vol. A326**, pp. 565-584.

Ogden, R.W. (1984) *Non-Linear Elastic Deformations*, Ellis-Horwood, Chichester.

Okuno, H., Renzo, K. and Uragami, T. (1993) Influence of casting solution additive, degree of polymerization, and polymer concentration on poly(vinyl chloride) membrane properties and performance, *J. Membr. Sci.*, **Vol. 83**, pp. 199-209.

Osman, J.L., Klausmeier, and Jamison, E.I. (1972) Rate-limiting factors in biodeterioration of plastics, in: Walters, A.H. (Eds.), *Biodeterioration of Materials*, Halsted Press Division, Wiley, New York, pp. 66-75.

Pamplona, D.C. and Bevilacqua, L. (1992) Large deformations under axial force and moment loads of initially flat annular membranes, *Int. J. Non-Linear Mechanics*, **Vol. 27**, pp. 639-650.

Papaspyrides, C.D. (1992) Transport phenomena into and out of plasticized PVC sheet: the influence of sample history, *J. Appl. Polym. Sci.*, **Vol. 44**, pp. 1145-1152.

Papaspyrides, C.D. and Duvis, T. (1989) Plasticizer transfer from plasticized poly(vinyl chloride) sheets to petroleum oils, *J. Appl. Polym. Sci.*, **Vol. 38**, pp. 1573-1580.

Pascoe, M.W. and Tabor, D. (1956) The friction and deformation of Polymers, *Proc. Roy. Soc.*, **Vol. A235**, pp. 210-224.

Park, J.K. and Nibras, M. (1993) Mass influx of organic chemicals through polyethylene geomembranes, *Water Environ. Res.* , **Vol. 65**, pp. 227-237.

Pavelka, C., Loehr, R.C. and Haikola, B. (1993) Hazardous waste landfill leachate characteristics, *Waste Management*, **Vol. 13**, No. 8, pp. 573-580.

Penn, W.S., Titow, W.V. and Lanham, B.J. (1971) *PVC Technology*, third edition, Elsevier, London and New York.

Persson, B.N.J. (1998) On the theory of rubber friction, *Surf. Sci.*, **Vol. 401**, pp. 445-454.

Pezzin, G., Ajroldi, T., Casiraghi, T., Garbuglio, C. and Vittadini, G. (1972) Dynamic-mechanical and tensile properties of poly(vinyl chloride). influence of thermal history and crystallinity, *J. Appl. Polym. Sci.*, **Vol. 16**, pp. 1839-1849.

Pipkin, A.C. (1968) Integration of an equation in membrane theory, *J. Appl. Math. Phys. (ZAMP)*, **Vol. 19**, pp. 818-819.

Pipkin, A.C. (1972) *Lectures on Viscoelasticity Theory*, Springer-Verlag, Berlin.

Pita, V.J.R.R., Sampaio, E.E.M. and Monteiro, E.E.C. (2002) Mechanical properties evaluation of PVC/plasticizers and PVC/thermoplastic polyurethane blends from extrusion processing, *Polym. Test.*, **Vol. 21**, pp. 545-550.

Planck, M. (1901) Uber das gesetz der energieverteilung im normalspectrum (in German; Law of energy distribution in normal spectra), *Ann. Physik.*, **Vol. 4**, pp. 553-563.

Poilane, C., Delobelle, P., Lexeceller, C., Hayashi, S. and Tobushi, H. (2000) Analysis of the mechanical behavior of shape memory polymer membranes by nanoindentation, bulging and point membrane deflection tests, *Thin Solid Films*, **Vol. 379**, pp. 156-165.

Pooley, C.M. and Tabor, D. (1972) Friction and molecular structure: the behaviour of some thermoplastics, *Proc. Roy. Soc.*, **Vol. A329**, pp. 251-274.

Prasad, T.V., Brown, K.W. and Thomas, J.C. (1994) Diffusion coefficients of organics in high-density polyethylene (HDPE), *Waste Manage. Res.*, **Vol. 12**, pp. 61-71.

Pujara, P. and Lardner, T. J. (1978) Deformations of elastic membranes-effect of different constitutive relations, *J. Appl. Math. Phys. (ZAMP)*, **Vol. 29**, pp. 315-327.

PVC Geomembrane Institute (1994) Identification and behavior of PVC geomembrane components, *PGI Technical Bulletin, April 1994*, PVC Geomembrane Institute, University of Illinois at Urbana-Champaign, IL, USA.

PVC Geomembrane Institute (1998) Case study of PVC goemembrane durability, *PGI Technical Bulletin, July 1998*, PVC Geomembrane Institute, University of Illinois at Urbana-Champaign, IL, USA.

PVC Geomembrane Institute (1999) Benefits of PVC geomembranes for landfill covers, *PGI Technical Bulletin, January 1999*, PVC Geomembrane Institute, University of Illinois at Urbana-Champaign, IL, USA.

Qi, H.J. and Boyce, M.C. (2004) Stress-strain behavior of thermoplastic polyurethanes, *Mech. Mat.* (in press).

Qian, Xuede, Koerner, R.M. and Gray, D.H. (2002) *Geotechnical Aspects of Landfill Design and Construction*, Prentice-Hall, Upper Saddle River, New Jersey.

Rachik, M., Schmidt, F., Reuge, N., Le Maoult, Y., Abbe, F. (2001) Elastomer biaxial characterization using bubble inflation technique. II: numerical investigation of some constitutive models, *Polym. Eng. Sci.*, **Vol. 41**, pp. 532--541.

Ramke, H.G. (1989) Leachate collection systems in sanitary landfill, in: Christensen, T.H., Cossu, R. and Stegmenn, R. (Eds.), *Technology and Environmental Impact*, Academic Press, London, pp. 343-364.

Recyc-Québec (2002) *Gestion des matières résiduelles au Québec : Bilan 2002.*

Rios, N.Y. and Gealt, M.A. (1989) Biological growth in landfill leachate collection systems, in: Koerner, R.M. (Eds.), *Durability and Aging of Geosynthetics*, Elsevier: London and New York, pp.244-259.

Rivlin, R.S. (1948) Large elastic deformations of isotropic materials. IV. Further developments of the general theory, *Phil. Trans. Roy. Soc.*, **Vol. A241**: 379-397.

Rivlin, R.S. (1953) The solution of problems in second-order elasticity, *J. Rational Mech. Anal.*, **Vol. 2**, pp. 53-81.

Rivlin, R.S. (1960) Some topics in finite elasticity, in: Goodier, J.N. and Hoff, N.J. (Eds.), *Structural Mechanics*: *Proc. 1st Symp. Naval Struct. Mech.*, Pergamon Press, pp. 169-198.

Rivlin, R.S. (1965) Non-linear viscoelastic solids, *SIAM Review*, **Vol. 7**, pp. 323-340.

Rivlin, R.S. and Saunders, D.W. (1951) Large elastic deformations of isotropic materials-VII. Experiments on the deformation of rubber, *Phil. Trans. Roy. Soc.*, **A243**, pp. 251-288.

Rowe, R.K. (1995) Leachate characterization for MSW landfills, in: *SARDINIA 95: Fifth International Landfill Symposium: Proceedings*, pp. 327-344.

Rowe, R.K. (1998) Geosynthetics and minimization of contaminant migration through barrier systems beneath solid waste, in: *The Sixth International Conference on Geosynthetics*, **Vol. 1**, pp. 27-102.

Rowe, R.K. and Sangam, H.P. (2002) Durability of HDPE geomembranes, *Geotext. Geomembr.*, **Vol. 20**, pp. 77-95.

Rowe, R.K, Sangam, H.P. and Lake, C.B. (2003) Evaluation of an HDPE geomembrane after 14 years as a leachate lagoon liner, *Can. Geotech. J.*, **Vol. 40**, pp. 536-550.

Sangam, H.P. (2001) *Performance of HDPE Geomembrane Liners in Landfill Applications*, Ph.D. thesis, University of Western Ontario.

Sangam, H.P. and Rowe, R.K. (2001) Migration of dilute aqueous organic pollutants through HDPE geomembranes, *Geotext. Geomembr.*, **Vol. 19**, pp. 329-357.

Santner, E. and Czichos, H. (1989) Tribology of polymers, *Tribol. Int.*, **Vol. 22**, pp. 103-109.

Sarvetnick, H.A. (1969) *Polyvinyl Chloride*, Van Nostrand Reinhold, New York, pp. 14-36.

Schallamach, A. (1952) The load dependence of rubber friction, *Proc. Phys. Soc.*, **Vol. B65,** pp. 657-661.

Schallamach, A. (1953) The velocity and temperature dependence of rubber friction, *Proc. Phys. Soc.,* **Vol. B66**, pp. 386-392.

Schrab, G.E. Brown, K.W. and Donnelly, K.C. (1993) Acute and genetic toxicity of municipal landfill leachate, *Water Air Soil Pollut.*, **Vol. 69**, pp. 99-112.

Sears, J.K. and Darby, J.R. (1982) *The Technology of Plasticizers*, John Wiley & Sons, New York.

Seferis, J.C., Chung, K., Buehler, F.U. and Takatoya, T. (2000) Heat and water mass transfer modeling in polymide based advanced composites, *Polym. Degrad. Stab.*, **Vol. 68**, pp. 43-51.

Seide, P. (1977) Large deflections of rectangular membranes under uniform pressure, *Int. J. Non-Linear Mechanics*, **Vol. 12**, pp. 397-406.

Selvadurai, A.P.S. (1973) Plane strain problem in second-order elasticity theory, *Int. J. Non-linear Mechanics*, **Vol. 8**, pp. 551-563.

Selvadurai, A.P.S. (1974) Second-order effects in the torsion of a spherical annular region, *Int. J. Eng. Sci.*, **Vol. 12**, pp. 295-310.

Selvadurai, A.P.S. (2000) *Partial Differential Equations in Mechanics*, **Vol. 1**, Springer-Verlag, Berlin.

Selvadurai, A.P.S. (2002) Second-order elasticity for axisymmetric torsion: a spheroidal coordinate formulation, in: Croitoro, E. (Eds.), *Proc. 2nd Canadian Conf. on Nonlinear Solid Mechanics*, Vancouver, **Vol. 1**, pp. 27-49.

Selvadurai, A.P.S. and Spencer, A.J.M. (1972) Second-order elasticity with axial symmetry. I. General theory, *Int. J. Engng. Sci.*, **Vol. 10**, pp. 97-114.

Selvadurai, A.P.S., Spencer, A.J.M. and Rudgyard, M.A. (1988) Second-order elasticity with axial symmetry, II spherical cavity and spherical rigid inclusion problems, *Int. J. Eng. Sci.*, **Vol. 26**, pp. 343-360.

Septanika, E.G. and Ernst, L.J. (1998a) Application of the network alteration theory for modeling the time-dependent constitutive behaviour of rubbers. Part I. General theory, *Mech. Mat.*, **Vol. 30**, pp. 253-263.

Septanika, E.G. and Ernst, L.J. (1998b) Application of the network alteration theory for modeling the time-dependent constitutive behaviour of rubbers. Part II. Further evaluation of the general theory and experimental verification, *Mech. Mat.*, **Vol. 30**, pp. 265-273.

Seth, B.R. (1964) Second-order effects in elasticity. Plasticity and fluid dynamics, in: Görtler, H., (Eds.), *Proc. XI Int. Cong. Appl. Mech., Munich, Germany*, pp. 383-389.

Shin, S.M., Jeon, H.S., Kim, Y.H., Yoshioka, T. and Okuwaki, A. (2002) Plasticizer leaching from flexible PVC in low temperature caustic solution, *Polym. Degrad. Stab.*, **Vol. 78**, pp. 511-517.

Shtarkman, B.P., Lebedev, V.P., Yatsynina, T.L., Kosmynin, B.P., Gerasimov, V.I., Genin, Ya., V. and Tsvankin, D.Ya, (1972) Very small-angle X-ray scattering by plasticized polyvinyl chloride, *Polym. Sci. USSR*, **Vol. 14**, pp. 1826-1837.

Simo, J.C. (1987) On a fully three-dimensional finite-strain viscoelastic damage model: formulation and computational aspects, *Comp. Meth. Appl. Mechs. Engg.*, **Vol. 60**, pp. 153-173.

Smith, M. Orman, M. and Queja, C. (1994) Copper heap leaching-a case for PVC liners, *PGI Technical Bulletin May 1997*, PVC Geomembrane Institute, University of Illinois at Urbana-Champaign.

Skalak, R., Tozeren, A., Zarda, R.P. and Chien, S. (1973) Strain energy function of red blood cell membranes, *Biophys. J.*, **Vol. 13**, pp. 245-264.

Spencer, A.J.M. (1970) The static theory of finite elasticity, *J. Inst. Math. Appl.*, **Vol. 6**, pp. 164-200.

Spencer, A.J.M. (2004) *Continuum Mechanics*, third Edition, Dover Publ., London.

Struik, L.C.E. (1978) Physical aging in plastics and other glassy materials, *Polym. Eng. Sci.*, **Vol. 17**, pp. 165-173

Stulgis, R.P., Soydemir, C., Telgener, R.J. and Hewitt, R.D. (1996) Use of geosynthetics in 'Piggyback Landfills': a case study, *Geotext. Geomembr.*, **Vol. 14**, pp. 341-364.

Sweeney, J. and Ward, I.M. (1995) Rate dependent and network phenomena in the multiaxial drawing of poly(vinyl chloride), *Polymer*, **Vol. 36**, pp. 299-308.

Szyszkowski, W. and Glockner, P. G. (1987) Spherical membranes subjected to vertical concentrated loads: an experimental study, *Engng. Struct.*, **Vol. 9**, pp. 183-192.

Taylor, R.B. and Tobolsky, A.V. (1964) Viscoelastic properties of plasticized poly(vinyl chloride), *J. Appl. Polym. Sci.*, **Vol. 8**, pp. 1563-1575.

Taverdet, J.L. and Vergnaud, J.M. (1984) Study of transfer process of liquid into and plasticizer out of the plasticized PVC by using short tests, *J. Appl. Polym. Sci.*, **Vol. 29**, pp. 3391-3400.

Tezduyar, T. E., Wheeler, L. T. and Graux, L. (1987) Finite deformation of circular elastic membrane containing a concentric rigid inclusion, *Int. J. Non-Linear Mechanics*, **Vol. 22**, pp. 61-72.

Tielking, J.T. and Feng, W.W. (1974) The application of the minimum potential energy principle to nonlinear axisymmetric membrane problems, *Appl. Mech.*, **Vol. 41**, pp. 491-496.

Timoshenko, S. (1953) *History of Strength of Materials: with a Brief Account of the History of Theory of Elasticity and Theory of Structures*, McGraw-Hill, New York.

Timoshenko, S. and Woinowsky-Krieger, S. (1959) *Theory of Plates and Shells,* Second Edition, McGraw-Hill, New York.

Titow, W.V. (1986) *PVC Technology*, Elsevier, London, Fourth Editon.

Tobolsky, A.V., Prettyman, I.B. and Dillon, J.H. (1944) Stress relaxation of natural and synthetic rubber stocks, *J. Appl. Phys.*, **Vol. 15**, pp. 380-395.

Treloar, L.R.G. (1943) Stress-strain rate for vulcanized rubber under various types of deformation, *Trans. Faraday Soc.*, **Vol. 39**, pp. 59-70.

Treloar, L.R.G. (1975) *Rubber Elasticity*, 3rd Ed., Oxford University Press, London.

Truesdell, C. and Noll, W. (1992) *The Non-Linear Field Theories of Mechanics*, second Edition, Springer-Verlag, Berlin.

Tsitsilianis, C., Tsapatsis, M. and Economou, Ch. (1989) Effects of crystallinity on ageing phenomena in poly(vinyl chloride), *Polymer*, **Vol. 30**, pp. 1861-1866.

Tsuboi, M., Imaizumi, S. and Miyaji, H. (1998) Effect of the temperature on tensile behavior of geomembranes, in: *The Sixth International Conference on Geosynthetics*, **Vol. 1**, pp. 201-204.

Tsumura, Y., Ishimitsu, S., Kaihara, A., Yoshii, K., Nakamura, Y. and Tonogai, Y. (2001) Di(2-ethylhexyl) phthalate contamination of retail packed lunches caused by PVC gloves used in the preparation of foods, *Food Addit. Contam.*, **Vol. 18**, pp. 569-579.

USEPA (1988) *Summary of Data on Municipal Solid Waste Landfill Characteristics-Critreia for municipal Solid Waste Landfills (40CFR Part 258)*, OSWER, U.S. Environmental Protection Agency, EPA/530—SW-88-038.

Verma, P.D.S. and Rana, O.H. (1978) Radial deformation of a plane sheet containing a circular hole or inclusion, *Int. J. Non-Linear Mechanics*, **Vol. 13**, pp. 223-232.

Wall, F.T. (1942) Statistical thermodynamics of rubber. II, *J. Chem. Phys.*, **Vol. 10**, pp. 485-488.

Wang Y., Arruda E.M. and Przybylo, P.A. (2001) Characterization and constitutive modeling of a plasticized poly(vinyl) chloride for a broad range of strain rates, *Rubber Chem. and Technol.*, **Vol. 74**, pp. 560-573.

Wenig, W. (1978) The microstructure of poly(vinyl chloride) as revealed by X-ray and light scattering, *J. Polym. Sci., Polym. Phys. Ed.*, **Vol. 16**, pp. 1635-1649.

Wilson, A.S. (1995) *Plasticisers: Principles and Practice*, Institute of Material, London.

Wineman, A. S. (1976). Large axisymmetric inflation of a nonlinear viscoelastic material by lateral pressure, *Trans. Soc. Rheol.*, **Vol. 20**, pp. 203-225.

Wineman, A. S. (1978) On axisymmetric deformations of nonlinear viscoelastic membranes, *J. Non-Newtonian Fluid Mech.*, **Vol. 4**, pp. 249-260.

Wineman, A.S. and Huntley, H.E. (1994) Numerical simulation of the effect of damaged induced softening on the inflation of a circular rubber membrane, *Int. J. Solids Structures*, **Vol. 3**, pp. 3295-3313.

Wu, C.-H. (1970a) Tube to Annulus. An exact nonlinear membrane solution, *Quart. Appl. Math.*, **Vol. 27**, pp. 489-496.

Wu, C.-H. (1970b) On certain integrable nonlinear membrane solutions, *Quart. Appl. Math.*, **Vol. 28**, pp. 81-90.

Wu, C.-H. (1971) On the contact problems of inflated cylindrical membranes with a life raft as an example, *J. Appl. Mech.*, **Vol. 38**, pp. 615-622.

Wu, C.-H. (1979) Large finite strain membrane problems, *Quart. Appl. Math.*, **Vol. 36**, pp. 347-359.

Yang, W.H. (1967) Stress Concentration in a rubber sheet under axially symmetric stretching, *J. Appl. Mech.*, **Vol. 34**, pp. 942-946.

Yang, W. H. and Feng, W. W. (1970) On axisymmetrical deformations of non-linear membranes, *J. Appl. Mech.*, **Vol. 37**, pp. 1002-1011.

Yang, W.H. and Hsu, K.H. (1971) Indentation of a circular membrane, *J. Appl. Mech.*, **Vol. 38**, pp. 227-229.

Yang, W.H. and Lu, C.H. (1973) General deformations of Neo-Hookean membrane, *J. Appl. Mech.*, **Vol. 40**, pp. 9-12.

Yeoh, O.H. (1993) Some forms of the strain energy function for rubber, *Rubber Chem. Technol.*, **Vol. 66**, pp. 754-771.

Yoshida, H., Hozumi, H., Tanaka, N. (1996) Theoretical study on temperature distribution in a sanitary landfill, in: Kamon, M. (Eds.) *Proceedings of the Second International Congress on Environmental Geotechnics*, **Vol.1**, Osaka, pp. 323–328.

Yu, Q. and Selvadurai, A.P.S. (2005) Mechanical behaviour of a plasticized PVC subjected to ethanol exposure, *Polym. Degrad. Stab.*, **Vol. 89**, pp. 109-124.

Zehnder, A.J.B., Ingvorsen, K. and Marti, T. (1982) Microbiology of methane bacteria, in: Hughes, D.E. (Eds.), *Anaerobic Digestion*, Elsevier Biomedical Press, Amsterdam, The Netherlands.

Zhang, S.W. (1998) State-of-the-art of polymer tribology, *Tribol. Int.*, **Vol. 31**, pp. 49-60.